

**SYNTHESIS AND COORDINATION CHEMISTRY OF COMPLEXES
OF CHELATING PHOSPHINE-CARBENE LIGANDS**

By:

SULTAN M. H. AL-SAAD

Submitted in partial fulfilment of the requirements of the Degree of

Doctor of Philosophy

School of Chemistry

Cardiff University

Wales, UK

**This dissertation was carried out in the Department of Chemistry at the
University of Wales Cardiff under the supervision of Prof. Peter G.
Edwards and Dr. P. D. Newman.**

Declaration

This work has not previously been accepted in substance for any degree and is not being concurrently submitted in candidature for any degree.

Signed

Dated

Statement 1

This thesis is being submitted in partial fulfilment of the requirements for the degree of PhD.

Signed

Dated

Statement 2

This thesis is the result of my own investigations, except where otherwise stated. Other sources are acknowledged by footnotes giving explicit references. A bibliography is appended.

Signed

Dated

Statement 3

I hereby give consent for my thesis, if accepted, to be available for photocopying and for inter-library loan, and for the title and summary to be made available to outside organisations.

Signed

Dated

Contents

Acknowledgment

Abstract

Abbreviations

Chapter 1- Introduction

1.1 Introduction

1.2 General properties of phosphines

1.3 General properties of *N*-heterocyclic carbenes (NHCs)

1.4 Preparation of free *N*-heterocyclic carbenes (NHCs)

1.5 Coordination chemistry of bidentate (carbene-phosphine) systems

1.6 Coordination chemistry of phosphine-NHC complexes

1.7 *N*-Heterocyclic Carbene Ligands in Catalysis

1.7.1 Ruthenium metathesis

1.7.2: Carbon-carbon bond formation

1.7.3: Asymmetric catalysis

1.7.4: Hydrogenation

1.8 Coordination chemistry of phosphine-NHC complexes of Group 11, 10, Ir and Mn

1.9 Aims and objectives of this thesis

1.10 References

Chapter 2- Synthesis of an Imidazolium Precursor and Functionalised Phosphine-Imidazolium
Salt derivatives as Ligands for the Formation of Metal Complexes

2.1 Introduction

2.1.1: Imidazolium Salts

2.1.2: Phosphine-imidazolium ligands

2.1.3: Ligand Structure

- 2.2 Results and Discussion
 - 2.2.1: Synthesis and characterisation of Imidazolium salts (2.2)
 - 2.2.2: Synthesis and characterisation of functionalised alkyl phosphine-imidazolium salts (2.5)
 - 2.2.3: Synthesis and characterisation of functionalised alkyl phosphine-imidazolium salts (2.6)
 - 2.2.4: Synthesis and characterisation of functionalised alkyl phosphine-imidazolium salts (2.7)
- 2.3 Conclusion
- 2.4 Experimental
 - 2.4.1: General Comments and Materials:
 - 2.4.2: Preparation of Compounds:
 - Preparation of 1-(2-Fluorobenzene)imidazole (2.1)
 - (1-Fluorobenzene-3-methyl)imidazolium iodide (2.2)
 - (1-Fluorobenzene-3-methyl)imidazolium chloride (2.3)
 - Preparation of Lithium diisopropylphosphide [LiP(Prⁱ)₂] (2.4)
 - (1-Benzene-*o*-diisopropylphosphine-3-methyl)imidazolium iodide (2.5)
 - (1-Benzene-*o*-diisopropylphosphine-3-methyl)imidazolium chloride (2.6)
 - (1-Benzene-*o*-diphenylphosphine-2-(propan-2-ol)-3-methyl) imidazolium iodide (2.7)
- 2.5 References

Chapter 3- Synthesis of NHC-phosphine complexes of metals of Groups 11, 10, Ir and Mn

- 3.1 Introduction
- 3.2 Results and discussion of NHC-phosphine complexes of group 11 metals
 - 3.2.1: Au complex (3.1):
 - A. *Via* Free Carbene
 - 3.2.2: Ag complex (3.2):
 - 3.2.3: Cu Complex (3.3):
 - A. *Via* Free Carbene
 - B. *Via* Transmetallation
- 3.3 Results and discussion of NHC-phosphine complexes of group 10 metals
 - 3.3.1: Ni Complex (3.4):
 - Via* Free Carbene

- 3.3.2: Pd complex **(3.5)**:
 - A. *Via* Free Carbene
 - B. *Via* Transmetallation
- 3.3.3: Pt Complex
 - 3.3.3.1 Bis-(phosphine-NHC) Pt(II) complex **(3.6)**
 - Via* Free Carbene
 - 3.3.3.2: Mono-(phosphine-NHC) Pt(II) complex **(3.7)**
 - A. *Via* Free Carbene
 - B. *Via* Transmetallation
- 3.4 Results and discussion of NHC-phosphine complexes of Mn complex **(3.8)**
 - Via* Transmetallation
- 3.5 Results and discussion of NHC-phosphine complexes of Ir complex **(3.9)**
 - Via* Free Carbene
- 3.6 Conclusion
- 3.7 Experimental
 - 3.7.1: General Comments and Materials
 - 3.7.2: Preparation of Complexes:
 - Synthesis of mono-(phosphine-carbene) Au(I) complex **(3.1)**:
 - Via* Free Carbene
 - Synthesis of bis-(phosphine-carbene) Ag(I) complex **(3.2)**
 - Synthesis of bis-(phosphine-carbene) Cu (I) complex **(3.3)**:
 - Via* Free Carbene
 - Synthesis of bis-(phosphine-carbene) Ni(II) complex **(3.4)**:
 - Via* Free Carbene
 - Synthesis of bis-(phosphine-carbene) Pd(II) complex, using PdCl₂COD **(3.5)**:
 - Method # 1: *Via* Free Carbene:
 - Using **(2.5)**
 - Using **(2.6)**
 - Method # 2: *Via* Transmetallation
 - Synthesis of bis-(phosphine-carbene) Pd(II) complex using Pd(acetate)₂:
 - Via* Free Carbene **(3.5)**
 - Synthesis of bis-(phosphine-carbene) Pt(II) complex **(3.6)**:
 - Via* Free Carbene

Synthesis of mono-(phosphine-carbene) Pt(II) complex (**3.7**):

Method # 1: *Via* Free Carbene

Method # 2: *Via* Transmetallation

Synthesis of mono-(phosphine-carbene) Mn (I) complex (**3.8**):

Via Transmetallation

Synthesis of mono-(phosphine-carbene) Ir complex (**3.9**):

Via Free Carbene

3.8 References

Chapter 4- Other attempted complexations

Attempts for NHC-phosphine complexes synthesis of Groups 4, 6, 7, 8, 9 and 10 metals

Recommendation for future work

Appendix

Acknowledgements

Indeed, my deepest appreciation is due first to my supervisor, Professor Peter Edwards, for giving me the opportunity to have a lab space to work under his excellent supervision. His great insights, perspectives, guidance and sense of humour stamped in mind a charisma I wouldn't forget ever. Without his cooperation and persistent help throughout in all academic and financial matters this dissertation would not have been possible. Sincere Thanks to him to attend Spain, Belfast, Edinburgh, Bath, oxford, and leister conferences as well as many leisure trips especially the one on the Canal. Despite his many academic and professional commitments, his focus on the highest standards showed me a great individual whom inspired and motivated me.

"Thanks" wouldn't quench the thrust in my heart to our group's "Godfather", Dr. Paul Newman, Woody. He is a very powerful but quiet dynamo. I am really amazed how he could manage everyone's matters in very distinctive way of wisdom and patience. He has been very generous with his time and energy to engage ideas in improving this and others' work. Thanks for his warmth and understanding, for his help with the tone and discipline of my writing, and his effort for improving the quality of this dissertation. He is great assets to me and others at the department of chemistry. Woody sets a wonderful example of grace and humour. Without any doubt, his support made this work. I owe you a special debt.

I am very grateful for Dr. Abdul-Razzaq. He has been a wonderful source of advice, enthusiasm and encouragement at crucial decision-points along all these years. He played a significant role in helping me to achieve the first ligand precursor. Thanks extended to Dr. Angelo Amoroso, Dr. Nancy Dervisi, and Dr. Ian Fallis for his early stage guidance.

Thanks to the crystallography team: Dr. Kariuki for being patient, Dr. Liling, Dr. Stasch, James and Baz whom all showed great effort and kindness to find a valuable single crystal. And, Thanks to Fawaz for being very helpful with its software as well. To my dearest colleagues: Eli for her comments and supportive advices, Wenjian, Becky, Kate, Huw, Craig, Toz, Matt, Lenali, and finally my dude Chris for sharing conversations and debates in various topics and for being a good language exchange partner. I wish you a happy future.

Thanks are due to students Rhian and Huw who firstly started with this project strategy and which I have followed. They were very helpful.

I also gratefully thank Dr. Rob Jenkins for technical assistance in NMR spectroscopy and your good willing to help with a smile. My appreciation goes to the rest of the technical team at the department: Robin, JoBo, Gaz, Sham, Jamie, Alun, Dave and finally the nitrogen guy, Mal.

I want to thank the good friends that I have made in Cardiff: Khalid, Saeed, Zakarya, Abdullah, Sultan, and Salem in their support and entertainment throughout my time over there.

Thanks to Qaboos University for this scholarship and special thanks to Prof. M. Khan at the chemistry department who introduced me to Cardiff University and for his support and assistance with proof reading and comments of the draft thesis. I extend my thanks to Prof. Salma Al-Kindy, Dr. Muna Al-Mandhary, Dr. Usama, Dr. Haidar, and Prof. Majek Fatope. Thanks to the smiley face Dr. Serajul Haque Faizi for his last stage help at X-ray and NMR softwares.

Finally, my extreme gratitude goes to my parents whom their supplication never stopped even through the pain of my father's long illness. Thanks to my cousin Zakariya and my brother Nasser along with my sisters to stand on my behalf in such a crucial situation helping our father, so I had time to complete the writing of one of the greatest challenges I have ever had to face. To my wife who supported, encouraged and believed in me in all my endeavours, I do owe you special thanks. We have had fantastic beautiful memories especially with our kids as well in a very beautiful place, Cardiff, which was our honeymoon city.

Abstract

Results presented and discussed in this thesis are collected into 4 chapters. Chapter 1 is an introduction to the synthesis and properties of phosphine and *N*-heterocyclic carbene compounds and complexes. Related complexes of *N*-heterocyclic carbene-phosphine ligands are also reviewed in this chapter. The synthesis and characterisation of a new phosphine-functionalized *N*-heterocyclic carbene ligand precursor, **2.5**, is described in chapter 2. A synthetic route has been successfully established for this ligand which is designed with *N*-methyl group on one side of the imidazole core and a pendant PR_2 moiety on the other side, (where $\text{R} = \text{Pr}^i$). The ring between the phosphorus group and the imidazolium ring is bound directly to give the rigidity to the whole chelating ligand structure. The corresponding phosphine-NHC ligand was generated *in situ* and reacted with suitable metal precursors. In addition, the reactivity of the ligand under various conditions was shown to cause cleavage of THF with concomitant formation of an alcohol group attached to the carbene's carbon atom, **2.7**. Chapter 3 describes reactions with metal precursors in the presence of a base (*via* free carbene) or *via* silver transfer agents and afforded a number of new metal complexes of the phosphine-NHC ligand. These included complexes of groups 11, 10, 9 and 7: Au (**3.1**), Ag (**3.2**), Cu (**3.3**), Ni (**3.4**), Pd (**3.5**), Pt (**3.6**), Mn (**3.7**) and Ir (**3.8**). The synthesis of Ag(I) complex was achieved by the reaction of the ligand, phosphine-imidazolium salt (**2.5**) with Ag_2O . The synthesized phosphine *N*-heterocyclic carbene complexes were characterised by analytical and spectroscopic methods and in some cases by X-ray crystallography. Chapter 4 lists other attempted complexations which did not succeed to yield desired products.

Abbreviations

Ar	aryl group
COD	1, 5-cyclooctadiene
DCM	dichloromethane
DMSO	dimethylsulfoxide
ESI	electrospray ionisation
Et ₂ O	diethyl ether
Et	ethyl
GC	gas chromatography
<i>i</i> -Pr	<i>iso</i> -propyl
L	neutral, 2 electron donor ligand
M	metal
Me	methyl
MS	mass spectrum
<i>n</i> -Bu	<i>n</i> -Butyl
NHC	<i>N</i> -heterocyclic carbene
NMR	Nuclear Magnetic Resonance
	(s) singlet
	(d) doublet
	(t) triplet
	(m) multiplet
	(br) broad
Ph	phenyl
Pr	propyl
ppm	parts per million
R	generic alkyl
r.t.	room temperature
THF	tetrahydrofuran
UV	ultra violet
VT NMR	variable temperature NMR
X	anionic ligand e.g. halogen

Dedication:

**"To My Father;
May His Soul Be Granted To Rest In Eternal Peace! "**

Chapter 1

Introduction

1.1 Introduction:

N-Heterocyclic carbenes represent a growing class of ligands in transition-metal catalysis, which have several features such as stability to air and moisture, low toxicity, strong σ -donor and poor π -acceptor properties.¹⁻³ NHC complexes find potential use for their biological activities^{4,5} and for their applications which include extensive studies in homogeneous catalysis.⁶⁻⁸

As part of a longer study into the chemistry of mixed-donor type of ligands, we sought to synthesise carbene-phosphine ligands and their complexes and to explore some aspects of their coordination chemistry. Complexes of chelating carbene-phosphine ligands are well known.⁹⁻¹¹

The main interest of these *N*-heterocyclic carbene complexes, in comparison to phosphine complexes, resides in producing robust catalysts which will not undergo decomposition or deactivation. On the other hand, the incorporation of a weaker coordinating unit on the same ligand should ensure a good activity for catalytic applications.¹²

Phosphine and carbene ligands have played important roles as reactive intermediates in organometallic reactions. Since NHCs are much more stable at high temperature and pressure and can form stronger bonds to metals than phosphines, the tendency toward such type of complexes is on the rise. Basicity of NHC is even more than the most basic phosphine, and thus it influences the reactivity of the applied catalytic system. Synthesis and characterization of bidentate carbene-phosphine ligands in order to promote homogeneous catalytic reactions are of paramount importance.

1.2 General properties of phosphines

Phosphine ligands have been used efficiently in homogeneous catalysis for long time. Tertiary phosphines (PR_3) readily coordinate to a large number of transition metals. Their ability to act as both σ -bases as well as π -acids enhances the stabilisation of metals in low oxidation states. A phosphine-metal bond is characterised as ($\text{P} \rightarrow \text{M}$) σ donation of the phosphorus lone pair electrons to an empty p or d s-orbital of the metal, and the π -bond ($\text{M} \rightarrow \text{P}$) is derived from back-donation to the empty orbital on the phosphine from the filled metal d-orbital, Figure 1.¹³⁻¹⁶ The strength of the σ -bond depends mainly on the Lewis acidity of the metal; the more electropositive metals form stronger σ -bonds. A phosphine will

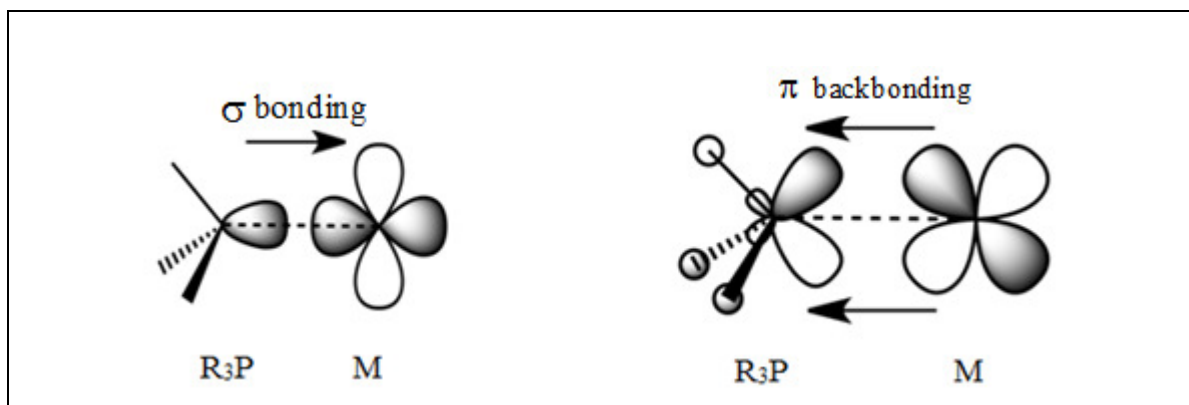


Figure 1: Phosphine donation and metal back donation

increase its π -acidity, and will thus be able to accept more π -donation from the metal's d-orbitals. Phosphines with more π -acceptor character will decrease (by competition) the amount of back donation that is possible to the other ligands bonded to the same metal.¹⁷ The nature of the "R" substituents on the phosphorus atoms may influence the degree of donor or acceptor ability of this phosphine ligand. In general, alkyl phosphines are less π -acidic than aryl phosphines due to the relatively lower withdrawing (greater electron donating) behaviour of alkyl substituents.¹⁸⁻²⁰

1.3 General properties of *N*-heterocyclic carbenes (NHCs)

Two types of carbenes, singlet (Fischer type²¹) and triplet (Schrock type²²), Figure 2, are observed. These are distinguished by the two possible arrangements (spin states) of the electrons available for donation to a metal ion when the carbene acts as a ligand. The triplet variant is the most stable type due to the preferred low energy configuration with one electron in each of the carbon σ - and p - π orbitals; the alternative singlet state has both electrons in the sp^2 orbital and requires spin pairing which causes this state to be slightly higher in energy.²³

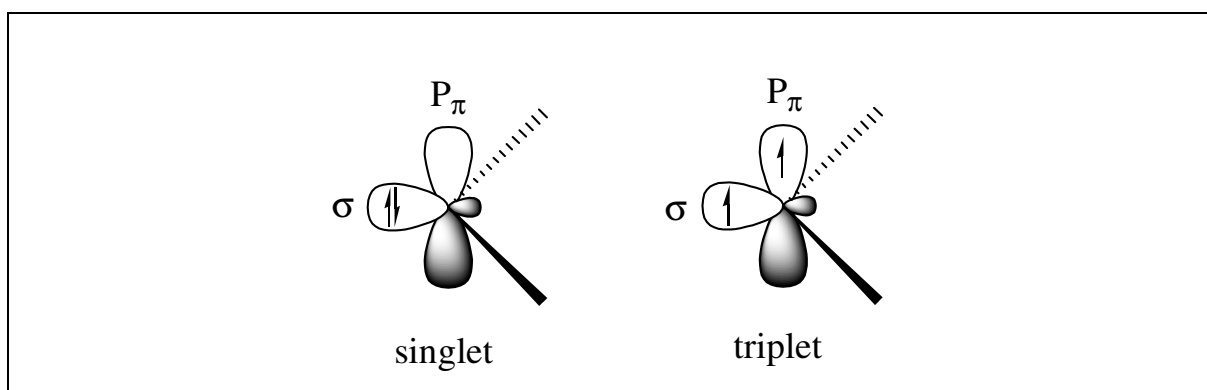


Figure 2: Schrock and Fischer types of carbene.

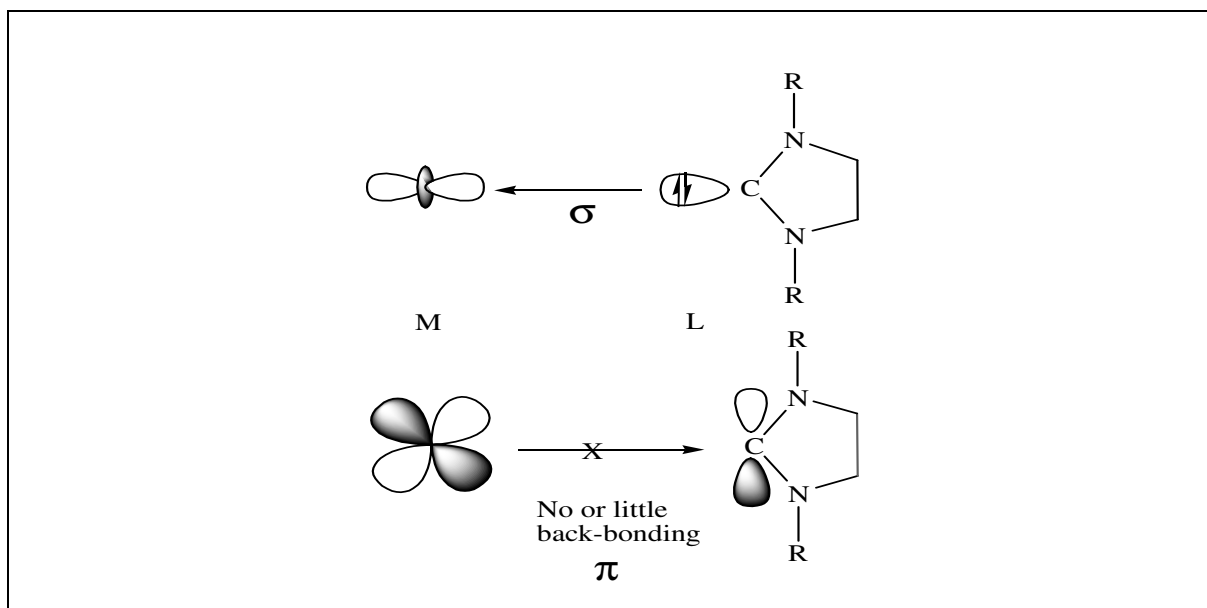


Fig. 3A: Contribution between NHC and metal

NHCs have a singlet configuration with two electrons in the carbon σ -orbital and coordinate to the metal by a predominantly σ -bond with little or no back-bonding, Figure 3A.²⁴ However, changing the substituents to σ -electron donating ones may favour the triplet state due to the small σ - $p\pi$ gap.

Donation (mesomeric effect) from the filled nitrogen $p\pi$ -orbitals into the empty sp^2 of the carbene carbon is mainly responsible for the stability of the NHC system.^{25,26} The σ electron density on the carbon centre is also pulled towards the more electronegative nitrogen atoms (inductive effect) which helps to stabilise the carbene lone pair, Figure 3B.²⁷ Carbenes flanked by substituent on the imidazolium ring will provide a steric protection which certainly

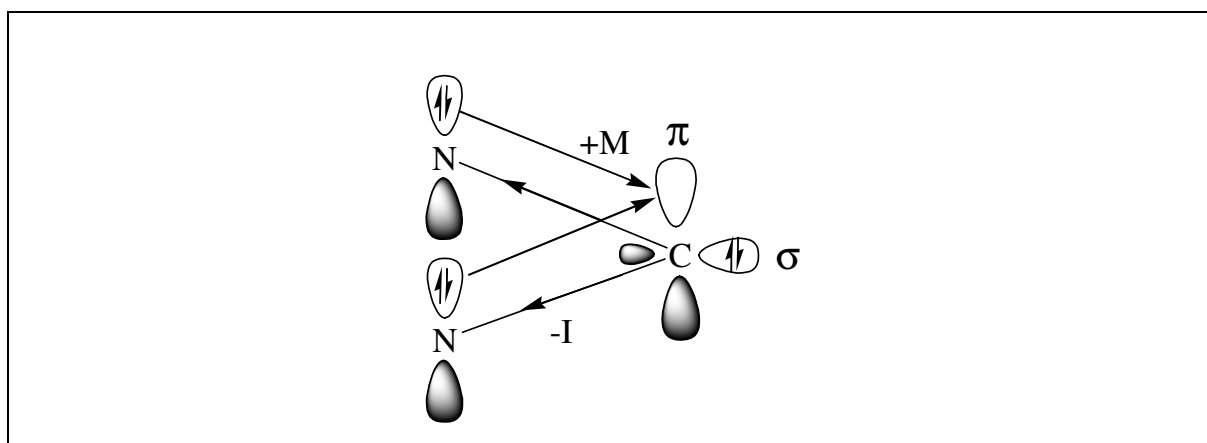


Figure 3B: Stabilisation of free carbene through mesomeric (M) and inductive effects (I).

enhances its stability.²⁸ Donating substituents on the carbene would add an electronic stabilising factor that may also reduce its susceptibility to nucleophilic attack.²⁹ Therefore, the mesomeric-push from the neighbouring nitrogen atoms, the inductive-pull by these nitrogen atoms, and the electronic-push of the substituents are dominant factors that influence the stability of NHCs.

The coordination chemistry of neutral NHCs is dominated by the ligands acting as 2-electron donors in a manner similar to tertiary phosphines,^{11,30-33} NHCs are, in general, even stronger σ -donors than phosphines.^{34,35} They are very weak π -acceptors but strong σ -bases which likely have a large *trans* influence. Thus NHCs bind to transition metals by σ -donation with minimal π -accepting ability.^{27,36,37} Even for electron-rich transition metals, the contribution from back-bonding is very small.^{31-33,38} As mentioned earlier, this is because the $p\pi$ -orbital of the carbene carbon is occupied by the donation of electron density by the neighbouring nitrogen atoms.²⁷ X-ray diffraction data has also shown that M-NHC bond lengths are typically similar to those of M-C single bonds.^{34,38,39} The most acidic proton in imidazolium salts is that at the C₂ carbon atom, therefore C₁-coordinated metal imidazol-2-ylidenes are referred to as normal carbenes, Figure 4. However, abnormal carbenes refers to when the coordination goes to the other carbons on the imidazolium ring, C₃ or C₄. One of the more useful physical properties is the diagnostic chemical shift of the carbenic carbon atom in the ¹³C-NMR spectrum, which, normally, is in the range between 200 and 300 ppm. Upon coordination to metal centres, the ¹³C carbene resonance usually shifts upfield. These properties have several advantages for selected metals in specific oxidation states such as: high thermal stability, resistance to ligand dissociation, robust binding to the metal.^{30,31,40,41} In addition, these ligands are not readily susceptible to any nucleophilic or electrophilic attack, and tend not to participate in rearrangements within the metal coordination sphere.^{10,40,42}

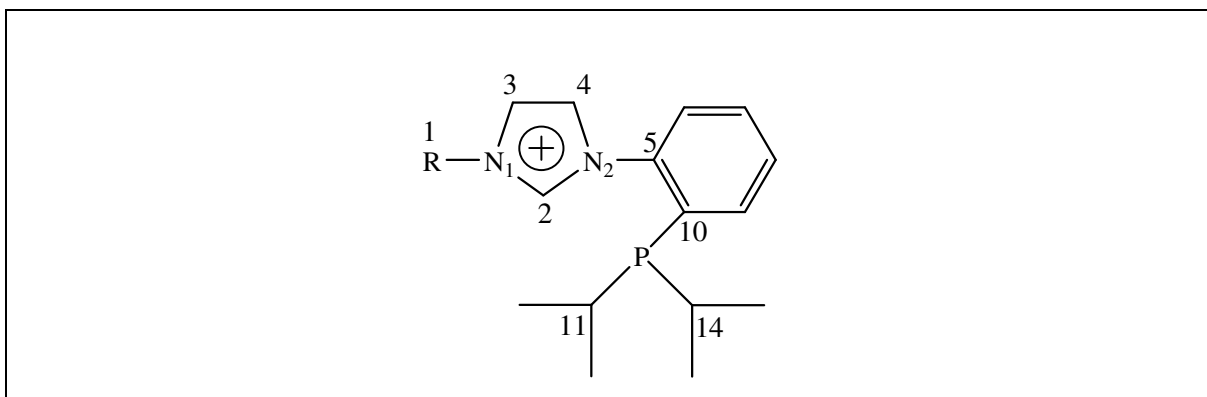
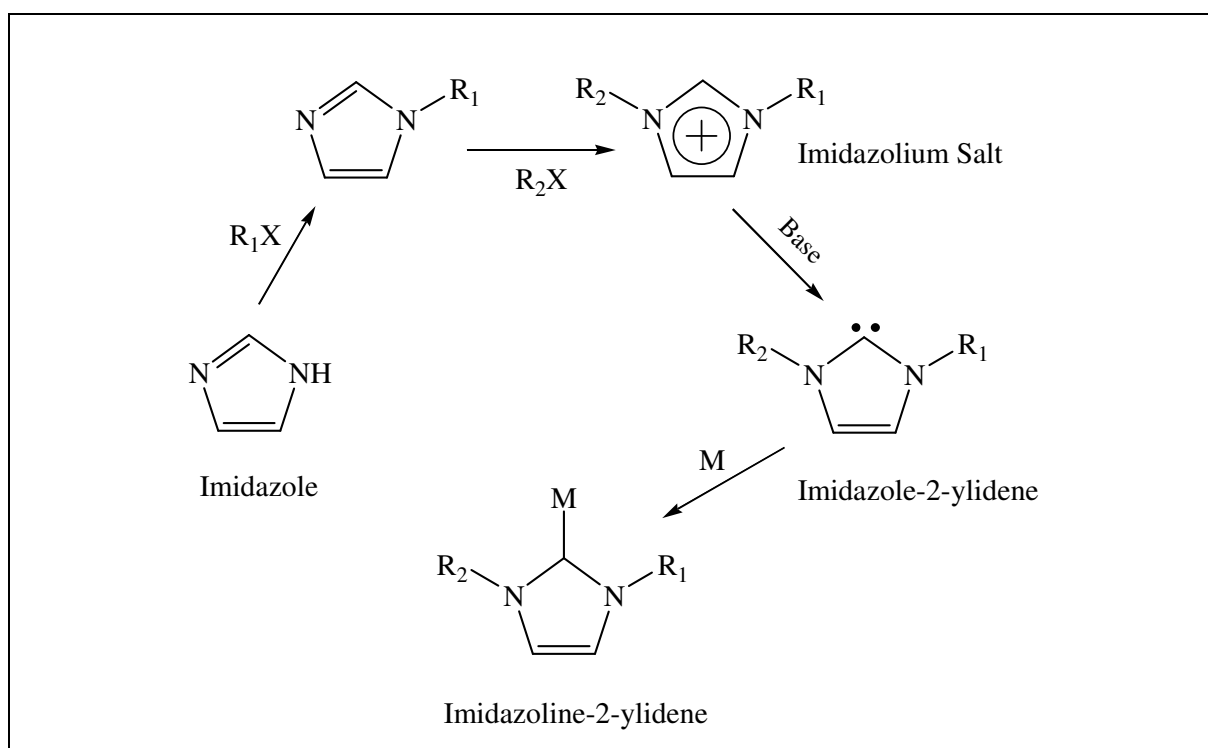


Figure 4: Numbering of a rigid chelating phosphine-carbene ligand

The nature of the carbene moiety assists the initiation and propagation of the catalytic reaction.³² We are interested in coordinating the C₂ carbon and phosphine to transition metals and exploiting the features of these bidentate carbene-phosphine complexes, i.e. stability of the carbene-metal bond and the activity (easy dissociation) of the phosphine.^{11,43} In contrast to metal phosphine complexes, they form metal complexes that have higher stability toward heat, moisture, and oxygen.⁴⁴

1.4 Preparation of free *N*-heterocyclic carbenes (NHCs)

The most frequently used method for the generation of a free carbene is based on the deprotonation of an imidazolium salt at the 2-position by a strong base. These reactions require Schlenk-line techniques due to their air/moisture sensitivity. Obviously this type of reaction must be performed under a dry, inert atmosphere in non-protic solvents or compounds of even moderate acidity. Arduengo's group used bases such as KOBu^t and NaH at room temperature.²⁹ Some functionalised groups on imidazolium salts cannot be reacted with such strong bases. Lithium alkyls, e.g. BuLi,^{33,45} are also effective reagents in the deprotonation of imidazolium salts, while milder reagents such as amides,^{9,42,43,43,46,47} e.g. K[N(SiMe₃)₂] and Li(N^tPr₂), have proven to be reliable. The nature and amount of base and



Scheme 1: Formation of imidazoline-2-ylidene

solvents are very important to optimise the reaction rates and overall yields. A range of imidazolium salts are available by consecutive alkylation of imidazole which in turn will react with organometallic or inorganic bases in nonprotic solvents (deprotonation step) to form the corresponding free carbenes (imidazole-2-ylidenes), Scheme 1.^{40,42}

Carbenes are highly air and moisture sensitive and can also be a problem with stability if the NHC functional groups have acidic protons. A method to avoid such problems involves forming the free NHC at low temperature with bases such as $\text{KN}(\text{SiMe}_3)_2$, followed by *in situ* reaction with the metal precursor.^{45,48,49} The deprotonation of imidazolium salts by the base $\text{KN}(\text{SiMe}_3)_2$ has proven to be highly effective. This is due to the fact that the deprotonation of a range of imidazolium salts by this base is very efficient with imidazolium salts that contain acidic protons when used at low temperature.^{47,48} $\text{HN}(\text{SiMe}_3)_2$ and KX as by-products of the reaction between the imidazolium salt and the base $\text{KN}(\text{SiMe}_3)_2$ are easily removed.

1.5 Coordination chemistry of bidentate (carbene-phosphine) system

Monodentate NHCs have been found to stabilise catalytic cycles and have advantages over the monodentate phosphorus ligand systems. Bidentate phosphine ligands have played a major role in homogeneous catalysis for a number of years. Later on, chemistry of bidentate carbene systems came into focus. However, this thesis will concentrate on carbene-phosphine bidentate ligands and their complexes.

The σ -donating phosphine group tethered to the NHCs would add some importance to the ligand design and its catalyst cycle. Firstly, the phosphine is expected to bind strongly to the transition metals. Secondly, the rigidity of the ring would fix the size of the chelating ring and highly promote ligand lability at the position *trans*. Thirdly, since carbene and phosphine are known as strong *trans* effect/influence ligands, so they would be able to activate/labillise groups coordinated in a position *trans* to them. Since tertiary phosphines (PR_3) and nucleophilic heterocyclic carbenes (NHC) each have many advantageous properties such as a large *trans* effect or influence respectively (but different donor/coordination properties),⁴³ combined functionalities should be effective in promoting migratory reactions of substrate molecules coordinated in *trans* positions, which make them desirable as novel ligands. There is also an interest in the bonding properties of ligands that must bind mutually *cis* sites since these would require remaining reactive sites to be mutually *cis* to each other (ideal for migration reactions) as well as simultaneously *trans* to the carbene's *trans*-influence or the phosphine's *trans*-effect.

A rigid bidentate carbene-phosphine coordination sphere is formed by covalently binding an imidazolium ring to a phenyl ring. With this aim, we have prepared a ligand with rigid *o*-phenylene backbone spacers and alkyl phosphine donors, Figure 5. For ligands based upon this class, chelate complexes may be expected where the ligand binds through the imidazole's carbene carbon (*N*-heterocyclic carbene) and phosphine donor. This, in turn, will force the coordination sphere metal-carbene to be co-planar. Chelating carbene-phosphine ligands bearing various aliphatic and aromatic substituents would be expected to have interesting properties of the resulting metal complexes. The rigid backbone may be expected to enhance the stability of complexes to a greater extent than the currently known related systems with aliphatic backbone. As well, bulkiness of functionalized groups and their steric effect may enhance the stability and reactivity. Complexes of this type of ligands might catalyse a range of organic reactions. They are expected to enhance reactivity. Whereas previous literatures were dominated by aryl phosphine, a further modification involves the substituent at the phosphorus moiety. So, we are interested in coordinating the C_2 -carbon and phosphine to some transition metals and exploiting the features of these bidentate carbene-phosphine complexes, i.e. the stability of the carbene-metal bond and the potential dissociation, of the phosphine.^{11,43}

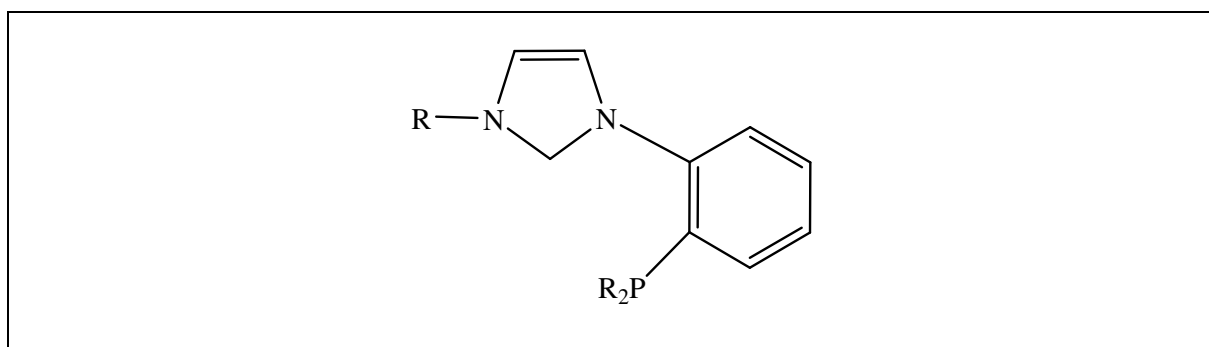


Figure 5: Proposed rigid bidentate functionalized carbene-phosphine

1.6 Coordination chemistry of phosphine-NHC complexes

This thesis describes synthetic procedures and characterization details of a ligand of NHC with alkyl phosphine derivatives and its complexes. Complexes of Cu, Ag, Au, Ni, Pd, Pt, Mn and Ir transition metals have been investigated and details of these will be presented. There is an abundance of such complexes in the literature. Since Wang and Lin proved the capability of Ag(I)-NHC complexes as carbene transfer agents, a large number of solid state

structures of Ag(I) compounds have been published due to its easy preparation.⁵⁰ Many potential applications were found for Au(I)-NHC ranging from homogeneous catalysts to their pharmaceutical use as anticancer, antiarthritic, and antibacterial agents.^{51,52} Au(I)-NHC complexes have been used as catalysts in many important reactions, for examples, nucleophilic additions, C–H activations, hydrogenations, and oxidations.^{50,53} The +II oxidation state is by far the most common for all three group 10 metals. The electronic configuration of these (Pt(II), Pd(II), and Ni(II)) complexes is d^8 and so the complexes are typically square planar.

Late transition metal imidazoline-2-ylidene complexes derived from imidazole (and its derivatives) have attracted bioinorganic chemist's recent attention^{10,30,40} due to their role in metal-based enzymes and proteins.⁴³ In contrast to metal phosphine complexes, metal *N*-heterocyclic carbene complexes have high stability towards moisture and oxygen.³⁶ In addition, the carbene ligands are hard to dissociate from the metal center. Moreover, metal *N*-heterocyclic carbene complexes possess high thermal stability in the solid state and in solution. Finally, syntheses of the carbene ligands are more convenient and inexpensive.⁵⁴ In 1991 in a landmark discovery by Arduengo *et al.*, a thermally stable *N*-heterocyclic carbenes (NHCs) were isolated in the free state and crystallographically characterised by deprotonation of the corresponding imidazolium salt with a base, KH.^{29,38,41,42} The crystalline free carbene was stable in the absence of oxygen and moisture. They attributed the stability of the carbene to both steric and electronic factors. The steric factors resulted from the presence of the two adamantyl groups, which shield the carbene center and thereby enhance kinetic stability. The electronic stability of the carbene was ascribed to the electron donation of the nitrogen filled *p*-orbitals into the vacant out-of-plane *p*-orbital of the carbene combined with the sigma-electronegativity effect of the nitrogen atoms.¹² However, in 1968, Wanzlick⁵⁵ and Öfele⁵⁶ reported independently the first stable NHC coordinated to a metal even though the carbenes were not isolated. In 1993, Lappert *et al.* synthesized the first (carbene-phosphine)-Mo complex.^{40b}

A number of groups have investigated (NHC/P)–M complexes. Some have introduced various functional groups at the imidazole ring and tested the differences with one NHC and one Phosphine, bis-NHC, and bis-phosphine. In general, the more bulky the functional group the more stable the compound. As well, once the complex has NHC moiety, the better the complex catalytic operation.^{11,31,43} Enhanced thermal stability is found with bulky carbene ligands.^{57,58} However, bulkiness is not always favourable as Nolan reported for the compound $Cp^*Ru(L)Cl$ where in some cases, alkyl is more favourable than aryl.³² He suggested that the

steric congestion around the carbene carbon inhibits the approach of the lone pair to overlap with the metal. Improved catalytic activity is observed in Suzuki-type coupling reactions, amination of aryl chlorides, olefin metathesis, and hydrogenation when a bulky electron-donating phosphine with an electron rich nucleophilic carbene coordinated to a metal centre.

Another essential way to form NHC complexes is by transmetallation with Ag reagents without the use of Schlenk techniques. Ag(NHC) complexes work as intermediates in the preparation of other transition metal-(NHC) complexes. In 1993, Arduengo first reported the straight forward preparation of Ag(NHC) complexes.^{59a} In 1998, Wang and Lin reported a major breakthrough in handling Ag as a transfer agent when 1,2-diethylbenzimidazolium bromide reacts with Ag₂O in DCM to give the corresponding [Ag(NHC)₂]⁺ complexes in good yield.^{59b} Ag₂O became a very useful reagent in the transfer from Ag(I) to a number of transition metals.

1.7 *N*-Heterocyclic Carbene Ligands in Catalysis

Due to their σ -donor ability and strong metal-carbon bond, NHC ligands have been applied as directing ligands in various catalytic transformations.⁶⁰ Since Arduengo's discovery of stable *N*-heterocyclic carbenes, extensive research efforts have focused on the design and application of carbenes as ligands in catalysis. In 1994, Herrmann developed the use of NHCs as spectator ligands in homogeneous catalysis. He reported Heck reaction yielding the coupling product in high yield with palladium *N*-heterocyclic carbene complexes. Thereafter, nucleophilic *N*-heterocyclic complexes attracted growing interest in other areas of catalysis. Significant advances in catalytic performances have been achieved with nucleophilic carbene ligands in various catalytic reactions such as:

1.7.1 Ruthenium metathesis: The first well-defined ruthenium catalyst for olefin metathesis was discovered in 1992^{62a}, Figure 6(A). This initial ruthenium catalyst was followed in 1995 by what is now known as the first generation Grubbs catalyst^{62b,c}, Figure 6(B), which is important as a precursor to all other Grubbs-type catalysts. A breakthrough in catalytic metathesis reactions was achieved when NHC ligands were used to replace one of the phosphines of complex 6(B). Herrmann *et al.* showed that having NHC moiety favours the dissociative substitution of the phosphine ligand with an olefinic substrate, showing excellent activities in the ring opening metathesis.^{61a,b} The first generation Grubbs catalyst was replaced by the second generation in the same year, 1999.^{63a} One of the great successes in the area of catalyst came from the modification of Grubbs^{63b} first generation catalyst, with more basic

NHC, Grubbs second generation catalyst as a new generation of ring closing metathesis catalysts, Figure 6(C). The very high *trans* effect *N*-heterocyclic carbene (NHC) labilizes the $\text{P}(\text{Cy})_3$ ligand, and the rates go up by a factor of 10^2 to 10^3 relative to the prior bis- PCy_3 complex. This second Grubbs type of catalyst is based on a saturated *N*-heterocyclic carbene (1,3-bis(2,4,6-trimethylphenyl) dihydroimidazole). It is in common use and doesn't require a co-catalyst because the carbene is already present and its activity is very high. This catalyst is stable toward moisture and air,^{63c} thus is easier to handle in the lab. Replacing the phosphine ligand with more labile pyridine ligands will produce the 3rd generation Grubbs' catalyst (Fast-Initiating Catalysts), Figure 6(D). By using 3-bromopyridine, the initiation rate is increased more than a million fold.⁶⁴ All Grubbs' catalysts have almost the same uses in organic synthesis, but generally with higher activity. These catalytic synthesis applications include: First metathesis, ring-opening metathesis polymerization (ROMP) of strained cyclic olefins, olefin cross metathesis (CM), ring closing metathesis (RCM) of terminal olefins under a variety of reactions conditions, and ethenolysis of internal olefins. Both the 1st and 2nd generation Grubbs' catalysts are commercially available, along with many derivatives of

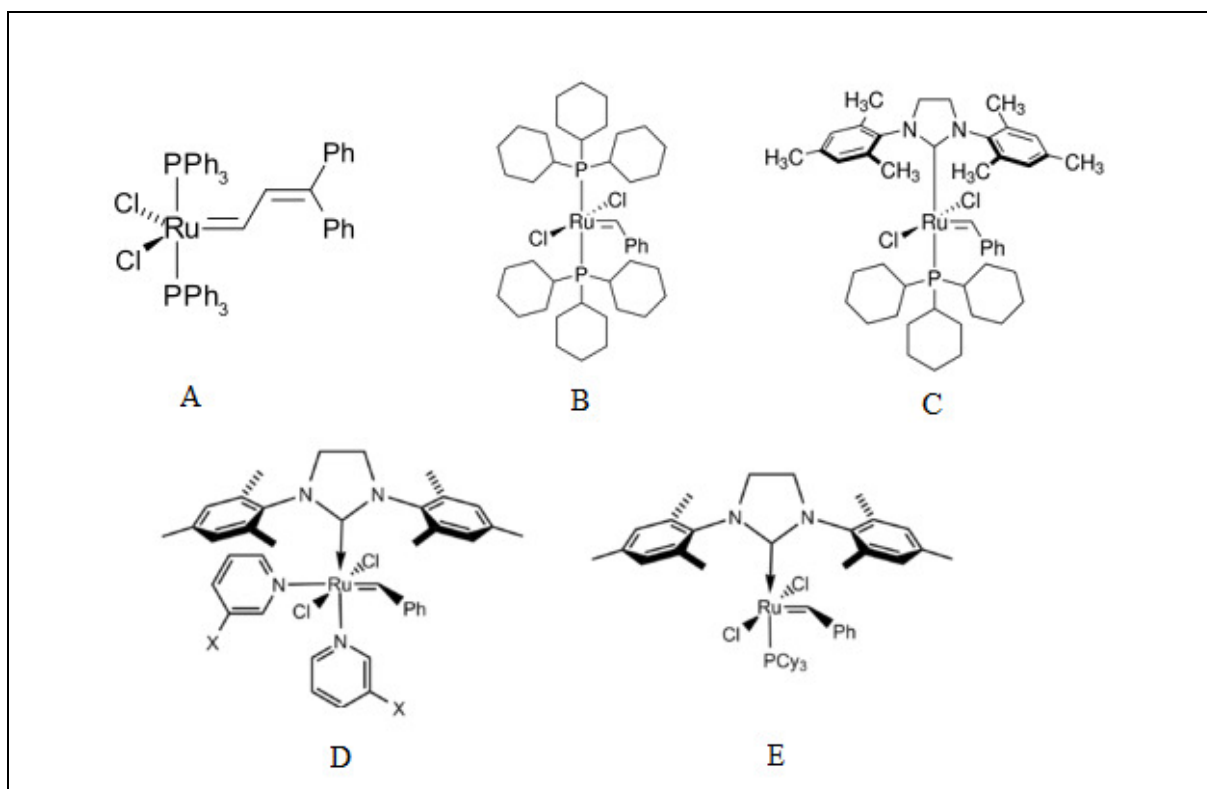


Figure 6: 1st, 2nd and 3rd generation Grubbs' catalysts

the 2nd generation catalyst. Shortly before the discovery of the Grubbs 2nd generation catalyst, a similar catalyst based on an unsaturated *N*-heterocyclic carbene (1,3-bis(2,4,6-trimethylphenyl)imidazole), Figure 6(E), was reported independently by Nolan^{65a} and Grubbs^{65b} in March 1999, and by Fürstner^{65c} in June of the same year.

In the same year, 1999, the 1st generation Hoveyda–Grubbs catalyst, Figure 7(A) was reported by the Hoveyda group,^{66a} and a year later, the 2nd generation Hoveyda–Grubbs catalyst, Figure 7(B) was described in nearly simultaneous publications by the Blechert^{66b} and Hoveyda.^{66c} The chelating oxygen atom replaces a phosphine ligand, which in the case of the 2nd generation catalyst, gives a completely phosphine-free structure. The Hoveyda–Grubbs catalysts are more expensive and slower to initiate than the Grubbs catalyst, but they are popular because of their improved stability.⁶⁷

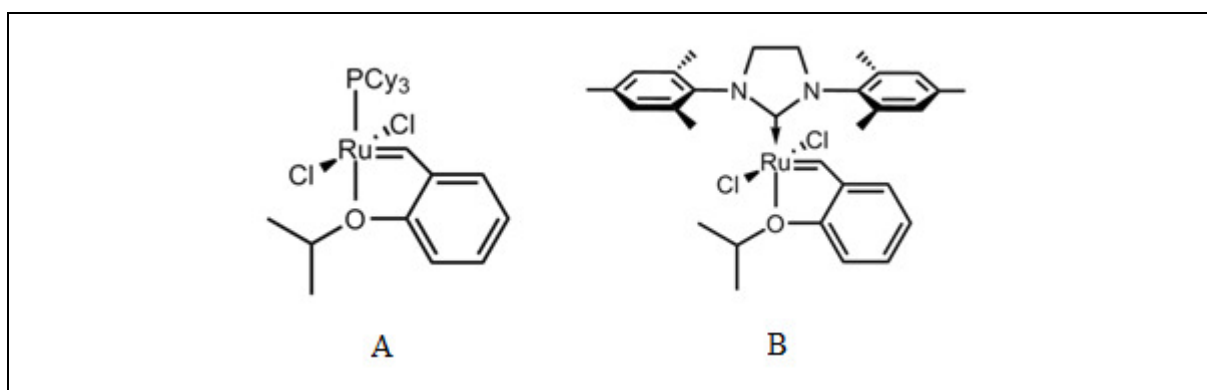


Figure 7: 1st and 2nd generation Hoveyda–Grubbs catalysts

1.7.2: Carbon-carbon bond formation: C-C bond forming reactions through cross-coupling plays an important role in synthetic organic chemistry. Huge interest has been focused on transition-metal catalyzed reactions of organometallic complexes. These reagents supply a source of nucleophilic carbon site which may react with an electrophilic carbon to form a new carbon-carbon bond. These type of coupling reactions are greatly involved in the synthesis of pharmaceuticals, fine chemicals, petrochemicals, agricultural chemicals, and polymers.^{20,68,69}

1.7.3: Asymmetric catalysis: Work of Enders⁷⁰ and Herrmann,³⁴ in 1997, was the first example of chiral carbenes used in asymmetric catalysis. Enders applied the NHC and their derivatives in carbene catalysed asymmetric nucleophilic acylation processes. Since then, the field has expanded on the use of NHCs in asymmetric homogeneous catalysis. Applications include: Rh-hydrosilylation of ketones,^{34,71,72} olefin metathesis,⁵⁶ Pd-oxindole reaction,^{61b,73}

Pd-allylic alkylation,⁷⁴ Rh(I)- and Ir(I)-transfer hydrogenation of ketones⁷⁵ Cu-catalysed addition of diethylzinc to cyclohexenones,^{76,77} Ni-hydroamination of acrylonitrile derivatives⁷⁸ and hydrogenation.

1.7.4: Hydrogenation: In 2001, Nolan and Burgess published two papers on iridium-catalysed hydrogenation with NHC ligands. Nolan initiated investigations into the field using achiral monodentate NHC iridium complex for the hydrogenation of cyclohexene and 1-methylcyclohexene.⁷⁹ They noticed that this Ir-catalyst and Crabtree's catalyst had comparable activity at room temperature, but are more robust and efficient at higher temperature. In 2002, Buriak showed that combining NHC with phosphine ligands led to efficient systems for the hydrogenation of simple olefins.³¹ The comparison of Buriak's complex with its analogue where pyridine ring replaces phosphine group, for the hydrogenation of 1-methylcyclohexene and 2,3-dimethyl-2-butene, proved its superiority of catalysis in terms of activity (time and conversion percentage).

1.8 Coordination chemistry of phosphine-NHC complexes of Group 11, 10, Ir and Mn

Herrmann *et al.*,^{80a} in 1997, prepared a square planar mixed carbene-phosphine complex of palladium, Figure 8. The phosphine group was found to be in a *cis* configuration to the carbene carbon. The P-Pd bond is, as expected, longer than C-Pd, and the Pd-X bond *trans* to the carbene is longer than that *trans* to the phosphine showing a greater trans influence for the NHC. It shows the donation difference between the two donors.

In 1999, a method of carbene transfer between metal ions was used by Liu *et al.*^{80b} in order to prepare other carbene species similar to Figure 8. This Pt complex of phosphine-substituted carbene was obtained from the corresponding CO-substituted carbene.

A similar complexation in 2009 and 2010, Lee *et al.*^{80c,d} prepared electron-rich palladium(II) complexes of mixed-donor *cis*-phosphine/carbene ligands which proved to be efficient as catalytic precursors in Suzuki Coupling. They found PCy₃/carbene complexes are more active than PPh₃/carbene complexes which may be attributed to the faster dissociation of labile PCy₃. In 2010, Liu and co-workers showed analogous complex of a bidentate Pd-NHC/PPh₃.^{80e}

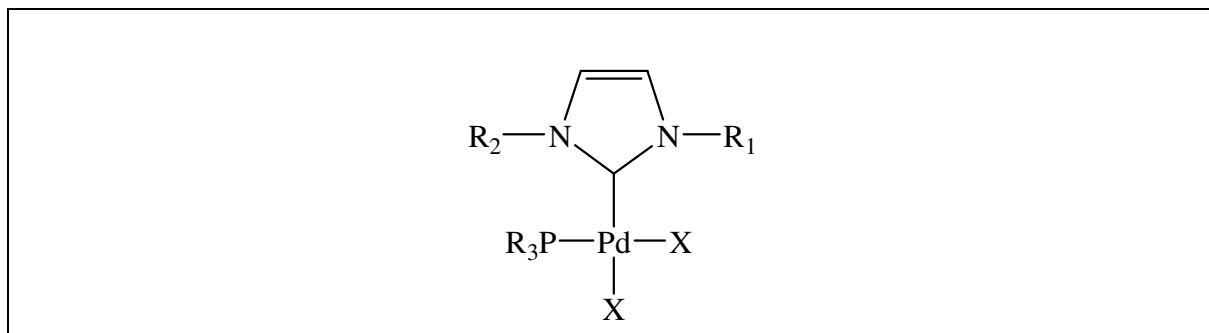


Figure 8: Pd-complexation of mixed carbene-phosphine, (PR₃= PPh₃, PCy₃)

In 1998, Leung synthesised the first stable bidentate chelating palladium carbene-phosphine complex *via* a metal template synthesis.⁴⁴ He proved that certain transition-metal phosphine complexes can serve as templates for the synthesis of chelating NHC ligands. Having a functional group within the template, such as phosphine moiety, is necessary to form chelating NHC, Figure 9.

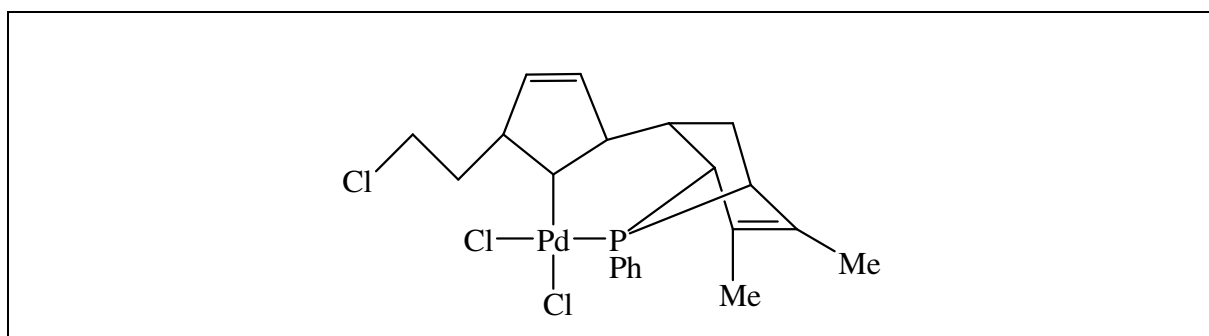


Figure 9: Bidentate chelating palladium carbene-phosphine complex, Leung⁴⁴

Cationic Ni(II) complexes of the chelating *N*-heterocyclic carbenes have been prepared and structurally characterized by Green/Danopoulos and co workers in 1999.⁸¹ This chelating di-*N*-heterocyclic carbene is the first example of methylene and ethylene-bridged dicarbene transition metal complex in this monocationic class of salts with a phosphorus group attached *trans* to one of the imidazolium ring, Figure 10.

A variety of mixed *trans*-NHC/phosphine complexes of palladium were prepared by the Herrmann group, 1999, in a similar result to his 1997's *cis*-NHC/P complex.¹¹ From bis-phosphine metal complexes, the replacement of one of the phosphine ligands by an NHC ligand will enhance the electron density at the metal.⁵⁷

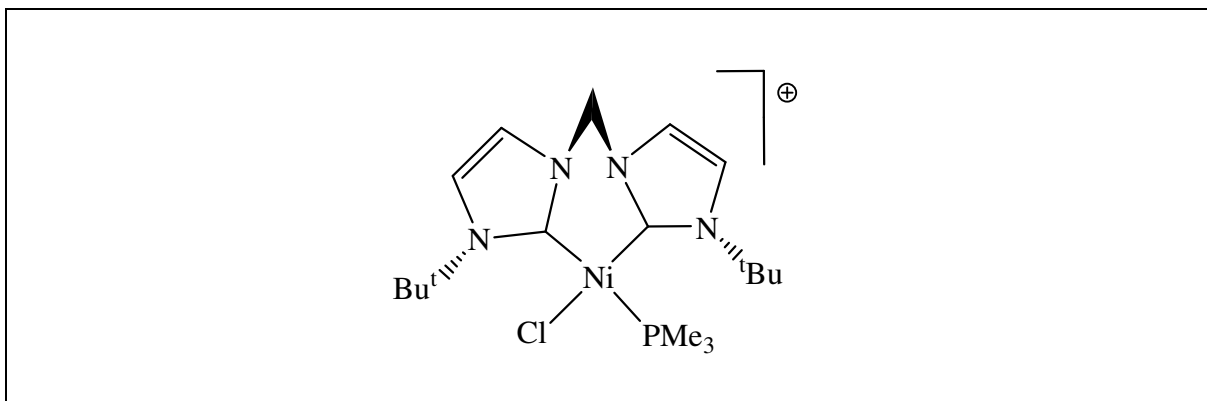


Figure 10: Ni(II) complexes of the chelating *N*-heterocyclic carbenes, Danopoulos⁸¹

This type of complexes, $[(\text{NHC})\text{Pd}(\text{PR}_3)_2\text{I}_2]$, with bulky *N*-heterocyclic carbenes (NHC), Figure 11, were found to be efficient catalysts for aryl coupling reactions such as the Suzuki and Stille cross-coupling reaction. It has a combination of the advantageous stability of carbene and the good activity of the phosphine. In general, one of the interesting characteristics of the palladium(II) complexes of *N*-heterocyclic carbenes is the extraordinary thermal stability and the high dissociation energies of the Pd-NHC bond.³⁷

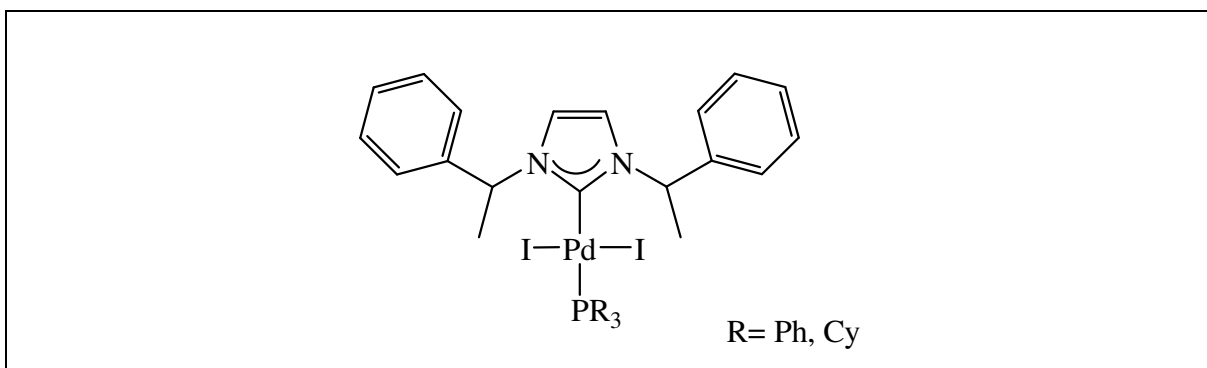


Figure 11: Mixed *trans*-NHC/phosphine complexes of palladium, Herrmann¹¹

In 2001, Nolan *et al.* prepared and examined the first mixed donor chelating phosphine-imidazolium ligand in which the phosphine was attached to the imidazolium ring by an aliphatic linker, Figure 12. This chelating bidentate phosphine-carbene ligand derived from the imidazolium salt would potentially form a more stable palladium catalyst which proved to work as a highly efficient catalytic system for Heck chemistry. A theoretical calculation study, in 1998, showed that a chelating ligand consisting of a carbene and a phosphine moiety had efficiency for the Pd-catalyzed Heck reaction.⁶² However, the aliphatic

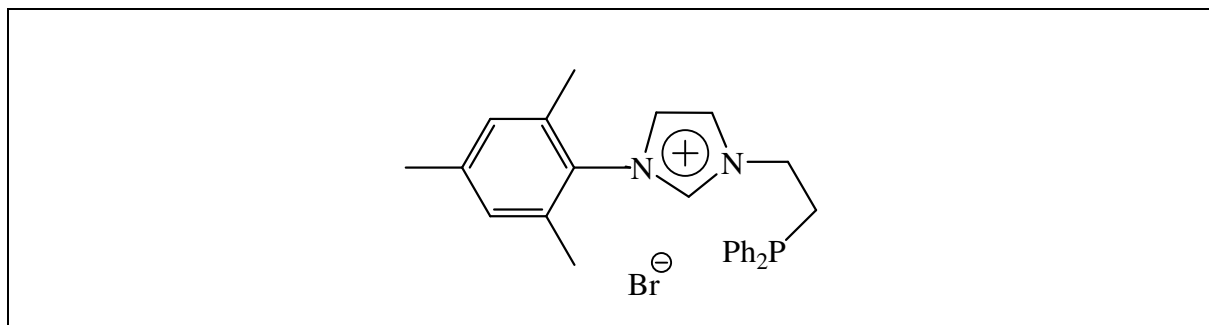


Figure 12: Phosphine-imidazolium salt of Nolan *et al.*³³

bridge may not provide a strong chelate of phosphine to metals and the ligand may be susceptible to reductive elimination due to its flexible geometry.³³ Thus, replacing the ethane bridge with a more planar rigid linker, as in our system, could help to form a ‘stronger’ bidentate chelating system.

In 2001, a number of new cationic mixed bis-phosphine-*cis*-methyl/NHC Pd(II) complexes, $[\text{Pd} \{ \text{cis-Me-(NHC)} \} \text{-P}_2]\text{BF}_4$, have been prepared and fully characterized and their reaction behaviour has been studied by Yates *et al.*⁸³ Another paper in the same year by Cavell *et al.*^{84a,b} confirmed, for the first time, that oxidative addition of different imidazolium cations to zerovalent group 10 metal precursors, Pd and Pt, can occur in order to afford mixed bis-phosphine/NHC complexes, Figure 13. Fürstner, in 2003, has also shown the same result that oxidative addition of imidazolium chlorides is a method for the preparation of mixed *cis*-mono-phosphine/NHC complexes of Pd.⁸⁵

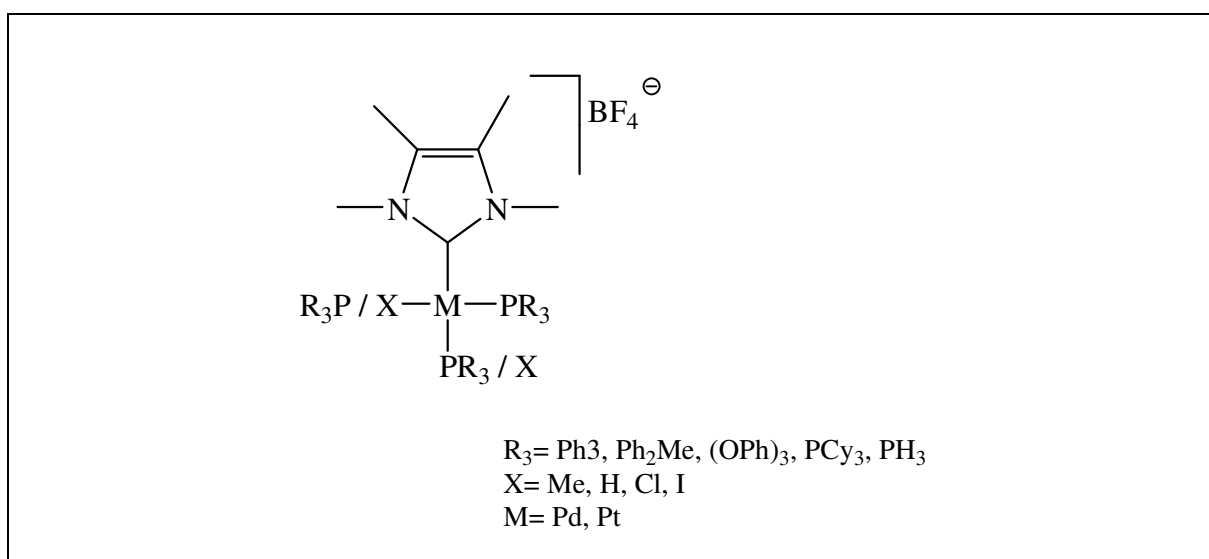


Figure13: Mixed bis-phosphine/NHC Pd(II) complexes, Yates⁸³

Analogous to Herrmann complexes reported in 1997, Welton and co-workers,⁸⁶ in 2001, have demonstrated the *in situ* formation of mixed *trans*-di-phosphine/NHC palladium complexes which can be formed from the reaction of ionic liquids with Pd(II) precursors under conditions similar to many ionic liquid mediated palladium-catalyzed coupling reactions, Figure 14.

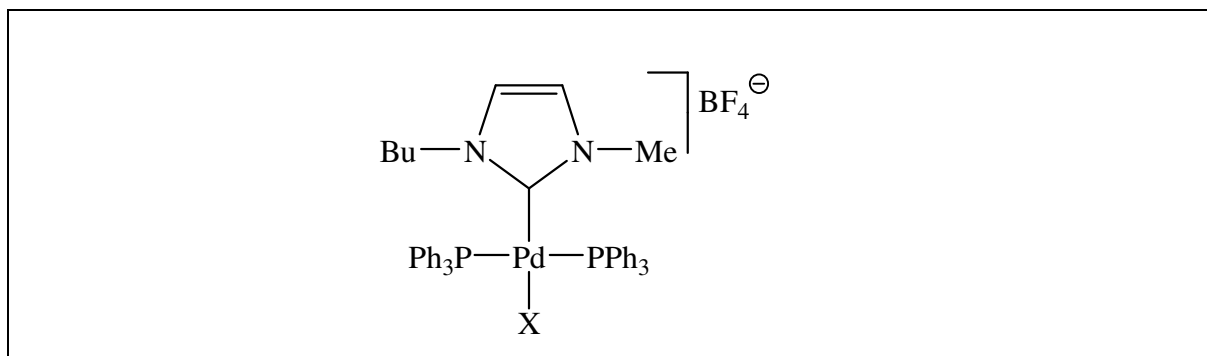


Figure 14, (X=Cl, Br): Mixed *trans*-di-phosphine/NHC palladium complexes, Welton⁸⁶

Caddick and co-workers,^{87a} in 2001, described the synthesis and ligand reactivity of mixed NHC and phosphine complexes of palladium, Figure 15. They examined the ability of these complexes to promote amination reactions which have indicated that these are extremely good catalysts.

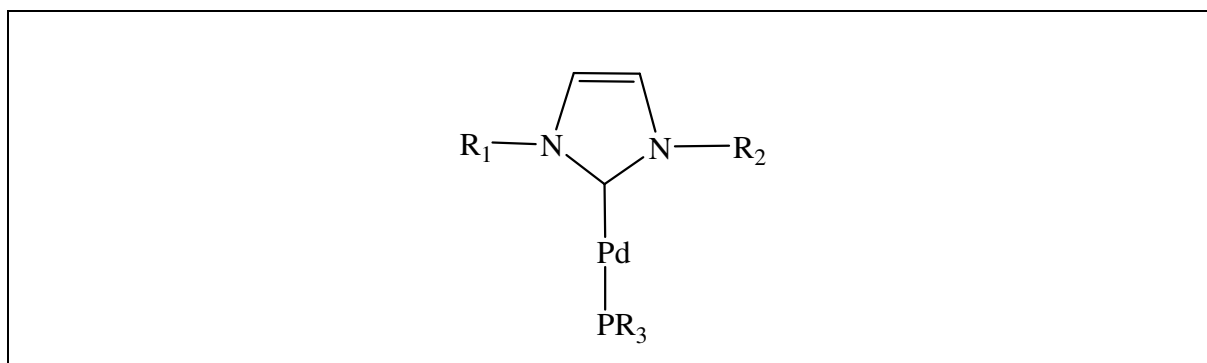


Figure 15, ($R_1 = \text{Bu}^t$, 2,6- Pr_2 ; $R_2 = \text{Cy}$, o-tolyl): Mixed NHC/phosphine complexes of Pd

For the first time, a monoanionic chelating dicarbene ligand was synthesized *in situ* by Fehlhammer *et al.* in 2001.^{87b} Palladium and platinum neutral complexes, Figure 15b, of this ligand as mixed dicarbene / phosphine compound was described in good yields.

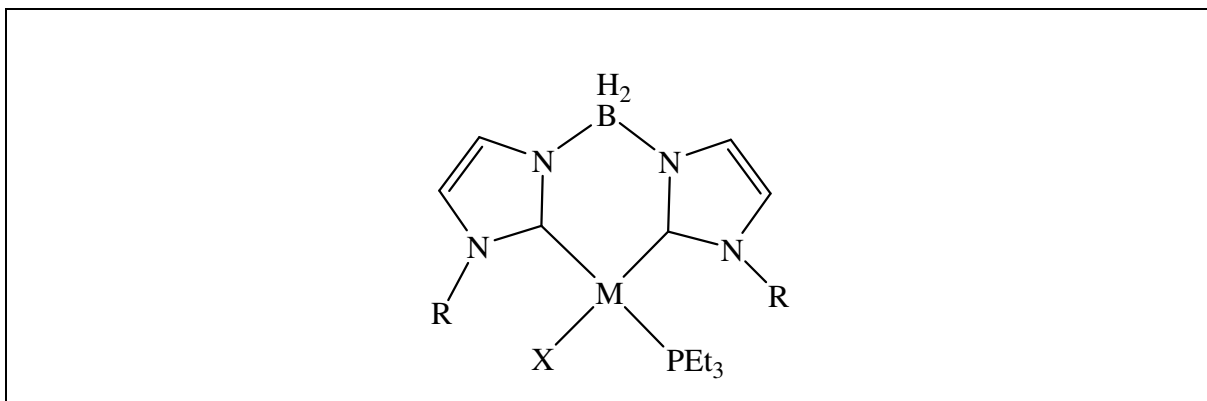


Figure 15b, (M= Pd, Pt): A monoanionic chelating dicarbene ligand, Fehlhammer^{87b}

In 2002, Grutzmacher and co-workers⁸⁸ synthesized and crystallized the first stable cationic mixed phosphine-carbene gold complex, NHC-Au-P, which expands the class of functionalised carbene complexes, Figure 16.

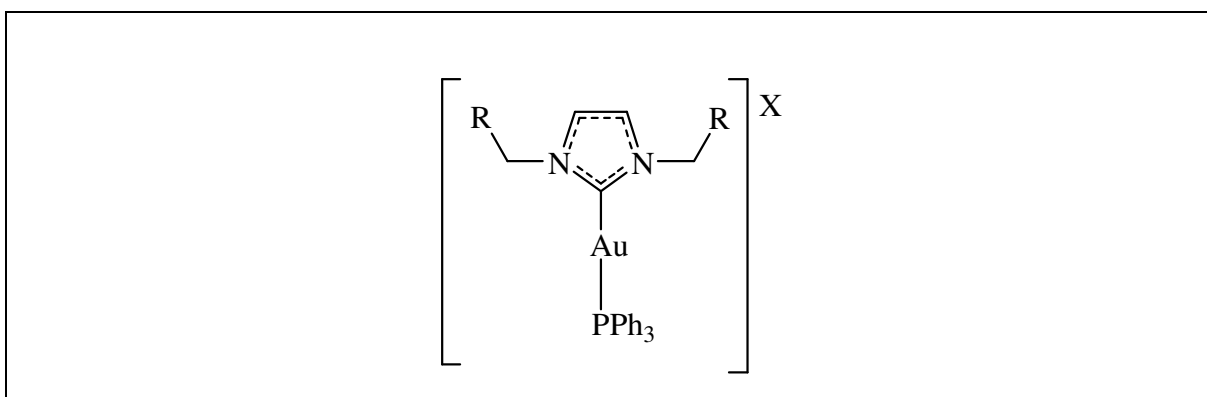
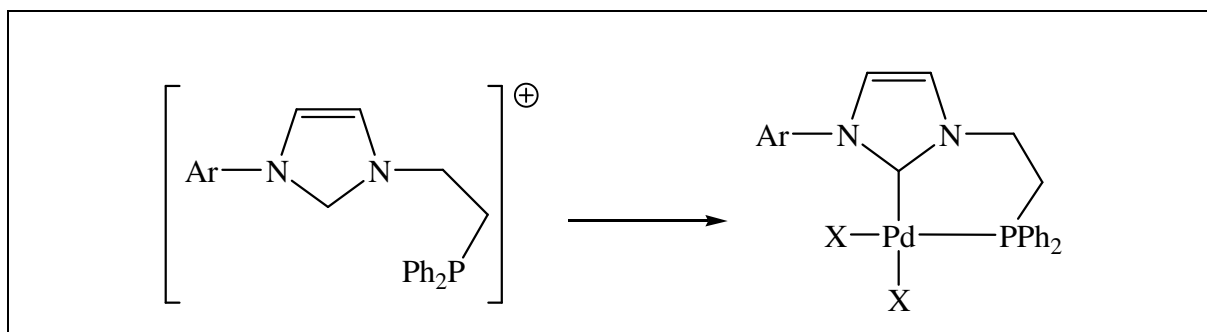


Figure 16: Cationic mixed phosphine-carbene Au complex, Grutzmacher⁸⁸

In 2002 and 2003, Danopoulos *et al.* published papers on the synthesis of similar ligands to those reported by Nolan, which included the formation of a series of thermally stable bidentate chelating phosphine-functionalized NHCs ligands and their complexation with Pd(II).⁸⁹ In these reports, Danopoulos prepared Nolan's ligand by a new method in higher yield. They described the formation of the diphenylphosphine-functionalised NHC complexes of palladium for their salt and Nolan's salt as well. The incorporation of functional groups like phosphine donors into the carbene ligand systems facilitates electronic tuning of the metal coordination sphere. Deprotonation of the imidazolium salt by the base $\text{KN}(\text{SiMe}_3)_2$ in THF at $-78\text{ }^\circ\text{C}$ was followed by *in situ* reaction with the metal precursor, Scheme 2.^{42,47} The diisopropyl-phenyl ligand was formed as a stable free carbene at room temperature due to the

two nitrogen bound functional groups.⁴² In 2004, Lee and co-workers reported another high yield synthetic route designed to make chelating phosphine-functionalized imidazolium salts illustrated in Scheme 2 (where X= Cl⁻ and Ar = mesityl, benzyl, F-benzyl, MeO-benzyl, naphthalen-1-ylmethyl).⁴⁶



Ar = mesityl, di-isopropyl phenyl; X= Me, Br

Scheme 2: Synthesis of bidentate phosphine-carbene complexes

Grushin and co-workers,^{90a} in 2003, synthesized and structurally characterized the first aryl-palladium complex containing the Prⁱ *N*-heterocyclic carbene ligand and chloro-Pd-aryl species, [(Prⁱ)Pd(PPh₃)(Ph)Cl], Figure 17a.

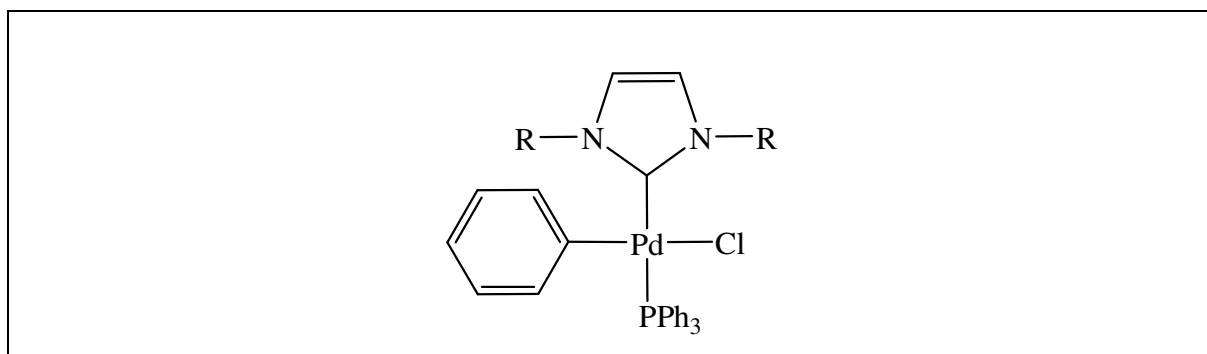


Figure 17a: Aryl-palladium complex of mixed P-NHC, Grushin^{90a}

The first example of a mixed carbene/phosphine hydridoplatinum complex had been obtained by Elsevier *et al.*^{90b} in 2003, Figure 17b. It was generated by using Whiteside's system that reacts selectively with C–H bonds in the 2-position of imidazolium salts. This method of C–H activation was found to be more effective and gave a very good yield.

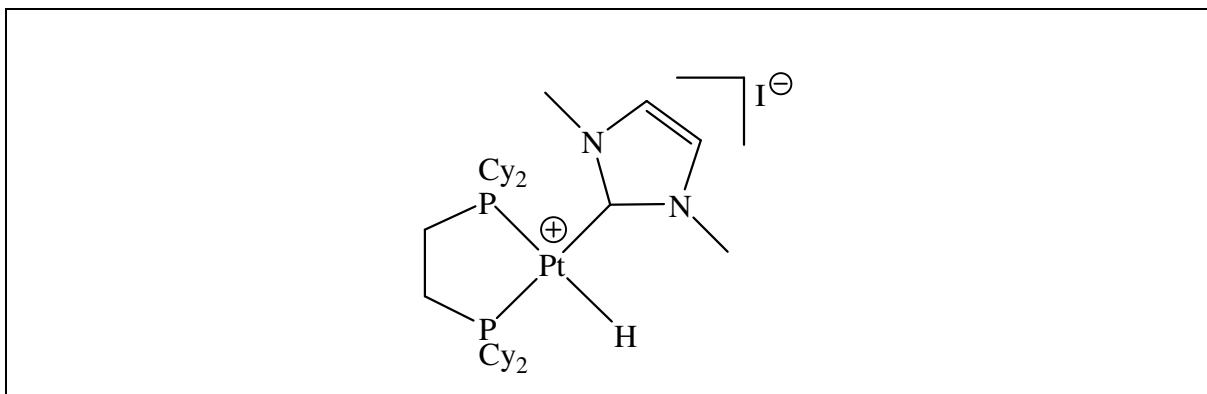


Figure 17b: Mixed carbene/phosphine hydridoplatinum complex, Elsevier^{90b}

A report of a new tridentate pincer phosphine-*N*-heterocyclic carbene ligand and the corresponding palladium, silver and ruthenium complexes came from Lee *et al.* in 2004 and 2005, Figure 18.^{91a,b,c} This 2P-NHC ligand with alkyl linkers to the imidazolium ring was prepared by transmetallation and direct addition of Pd precursor without the need of a base.

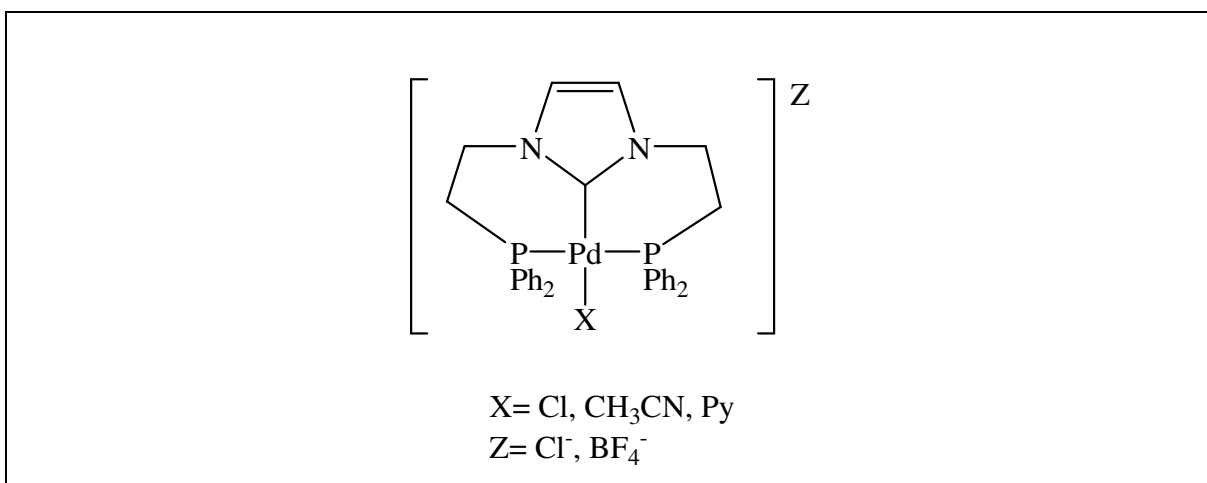


Figure 18: Tridentate pincer of P-NHC, Lee⁹¹

One of the possible ways to introduce chirality in the *N*-substituents of the NHCs is to use planar chiral ferrocenyl fragments. In the same year of 2004, a chiral C_2 -symmetric tridentate ligand, PCP, where an NHC is combined with two ferrocenyl phosphine units was prepared by Togni and Gischig in a good yield.^{92a,b} The synthesis and the X-ray crystal structure of a palladium complex of this chiral imidazolium salt was obtained, Figure 18b.

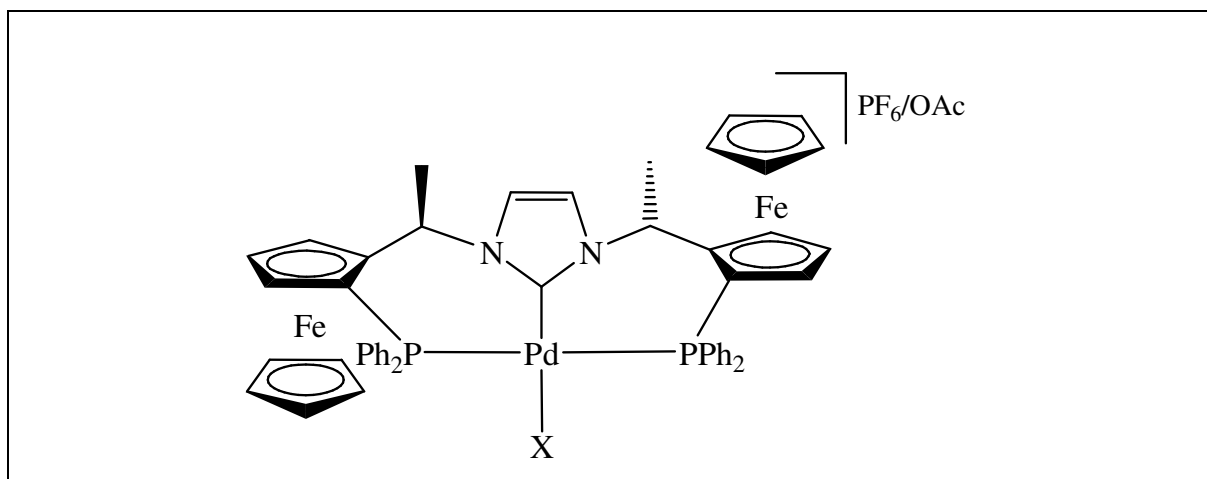


Figure 18b: Tridentate ligand, PCP, Togni⁹²

In 2005, Zhou and his group reported *in situ* production of palladium complexes of bidentate triaryl phosphine-functionalized NHC ligands, Figure 19.^{93a,b} Their application in palladium-catalyzed Heck reaction showed a high efficiency for the coupling of a wide range of aryl halides with acrylates and the coupling of aryl bromides with styrene derivatives. In these Heck reactions, the introduction of the bulky substituents on the *N*-phenyl ring was found to be beneficial in term of increasing the activity of the Pd catalyst.

Zhou's group was also able to synthesise a pincer chelating PCP ligand analogous to the above ligand but with two arms of diphenylphosphinobenzyl pendant function and without any metal complexation.

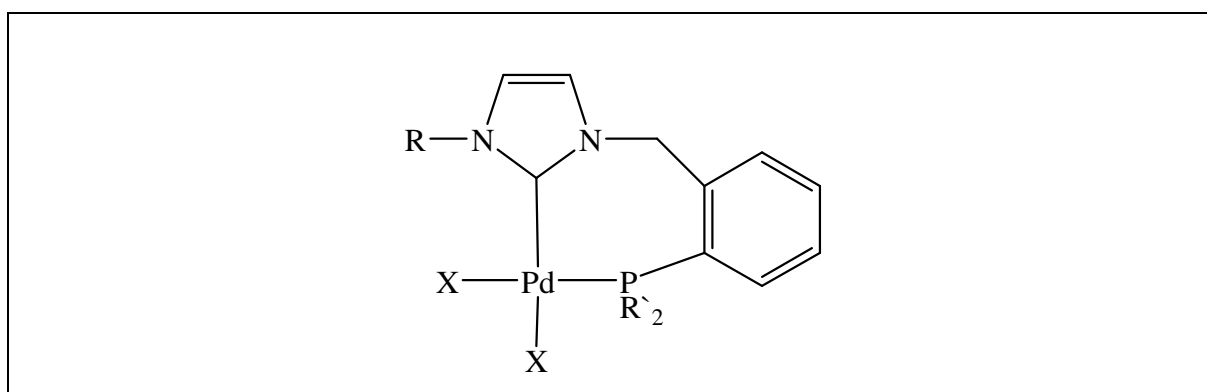


Figure 19: (Zhou's: R=Ar, $\text{PR}'_2=\text{PPh}_2$; Lee's: R=Me, $\text{PR}'_2=\text{PPh}_2$ or PCy_2)

A similar bidentate phosphine-functionalized *N*-heterocyclic carbene ligand with a combination of Pd(II)-metal precursor was reported by Lee *et al.*, in 2009.⁹⁴ They prepared

the first example of a hybrid NHC ligand containing a more electron donating PCy₂ moiety as well as a complex containing a PPh₂ moiety. A series of palladium complexes were synthesized, isolated and crystallized.

Baker *et al.*,⁹⁵ in 2005, obtained and crystallized bidentate (P-NHC) gold complex analogous to Grutzmacher's complex⁸⁸. It was isolated as the hexafluorophosphate salt (P-Au-NHC)⁺ PF₆⁻.

The group of Herrmann, in 2005, prepared and crystallized a cationic monocarbene diphosphine Ni(II) complex by oxidative substitution, Figure 20.⁹⁶

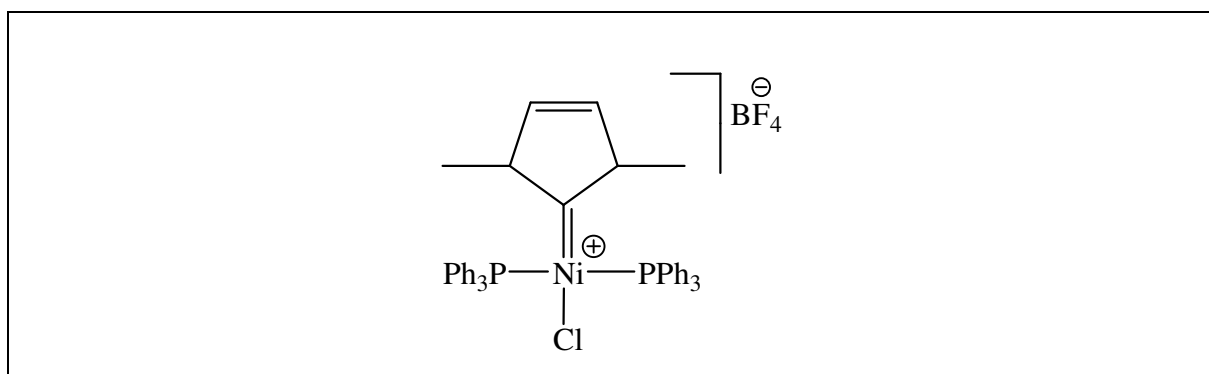


Figure 20: Cationic monocarbene diphosphine Ni(II) complex, Herrmann⁹⁶

Hahn *et al.*,⁹⁷ in 2006, succeeded in obtaining mono- and di-phosphine-functionalized benzo-carbene ligands as bidentate and pincer-type complexes. Pd and Pt complexes with diphosphine moieties were prepared by carbene transfer from the corresponding Ag-complex, *via* transmetallation, Figure 21.

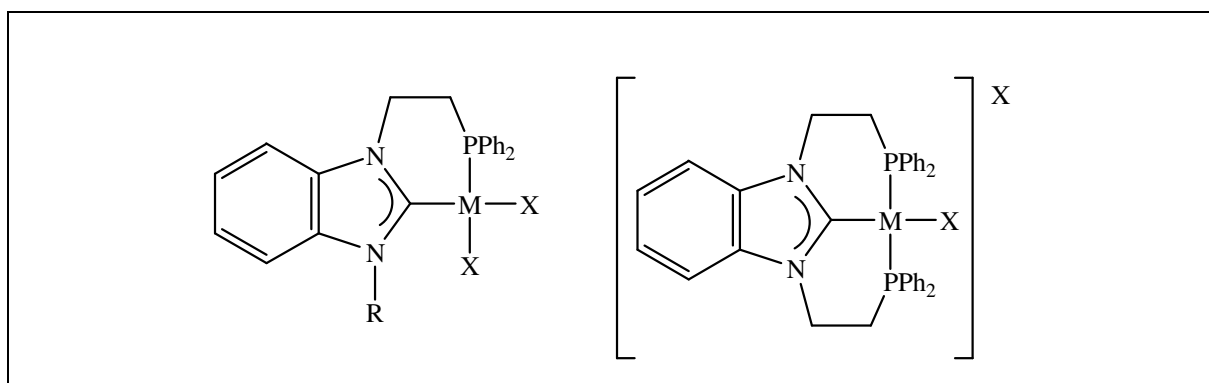


Figure 21: (M=Ag, Pd, Pt; X= Cl), Bidentate and pincer P-NHC, Hahn⁹⁷

Poli *et al.*, in 2006, described the preparation and characterisation of Ni(II) complexes bearing a chelating P-NHC ligand where the metal is bonded to a phosphine ligand that contains a pendant imidazolium moiety, Figure 22.^{12,98} However, their attempts to isolate a neutral phosphine-functionalized *N*-heterocyclic carbene complex of nickel(II) were not successful, even though observations agreed with the generation of such carbon-bonded species.

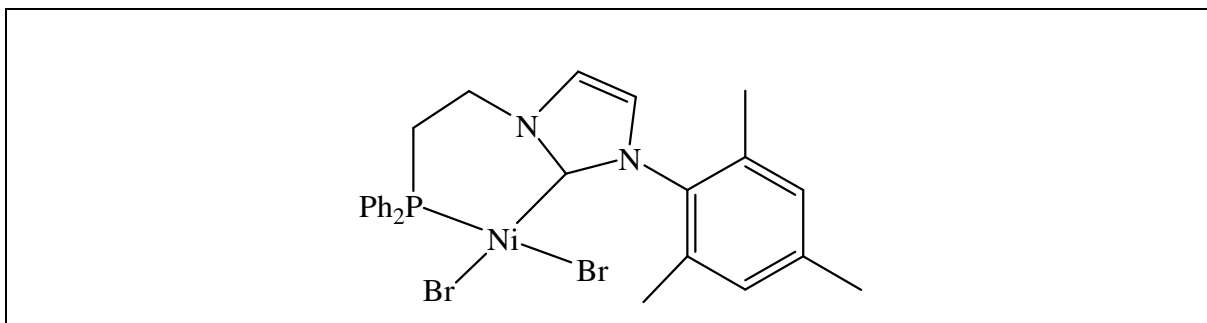


Figure 22: Ni complex of Chelating P-NHC, Poli⁹⁸

In 2007, Lee and co workers⁹⁹ prepared and structurally characterized Ni(II) complexes of two bidentate phosphine/NHC ligands, Figure 23. The nickel bonded with two arms of phosphine moieties as well as the two carbenic carbons which proved to be highly robust in air, which is a desirable property of a catalyst precursor. This Ni complex was found to be a highly effective catalyst for Suzuki cross-coupling.

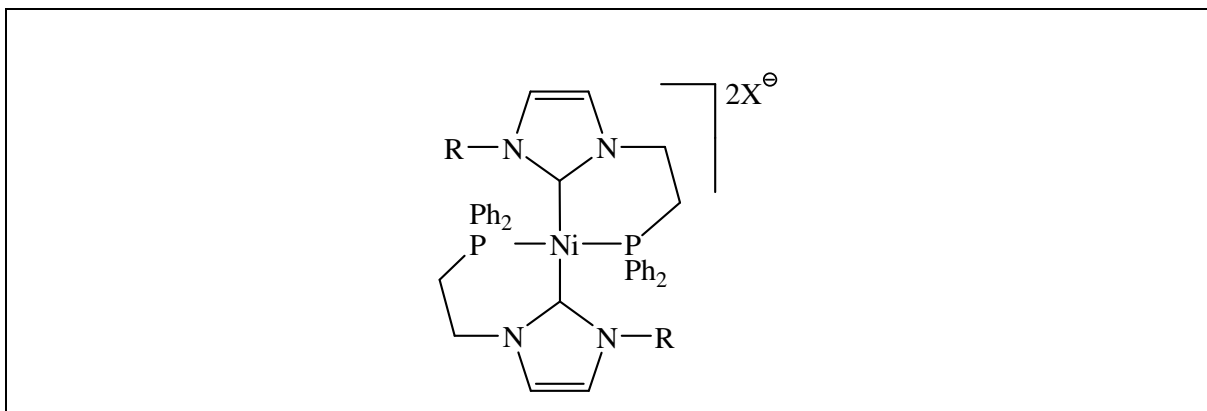


Figure 23: Ni(II) complexes of two bidentate phosphine/NHC, Lee⁹⁹

In a similar manner to that of Bappert and Helmchen,⁸⁹ Huw Roberts, in 2007, synthesized phosphine-substituted imidazole ligands, Figure 24, and their Ni, Pd and Pt complexes in moderate yields.¹⁰⁰

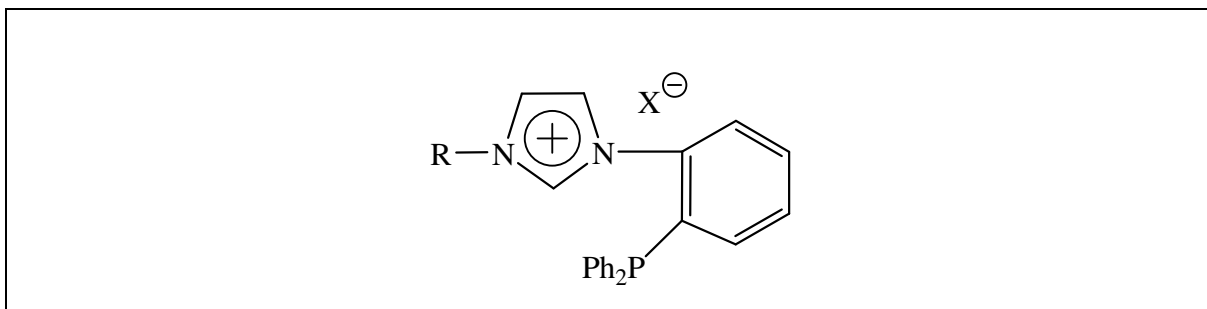
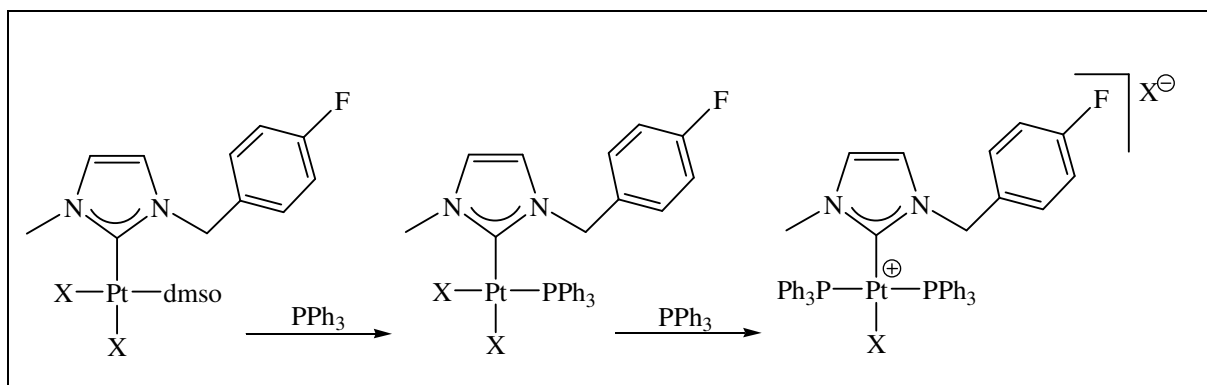


Fig 24, (R=Me, Benzyl): Group 10 complexes of bidentate P-NHC, Huw¹⁰⁰

A (NHC)AgX complex was used as a transmetallating agent to introduce the NHC to a platinum centre in order to form a Pt-complex of this NHC ligand. A complex bearing a coordinated DMSO ligand was formed which was easily replaced by other ligands such as phosphines to give mixed *cis*-NHC/phosphine and *cis*-NHC/bis-phosphine complexes.¹⁰¹ Rourke and co-workers found, in 2007, that the *cis*-[(NHC)(DMSO)PtCl₂] complex was useful in synthesising mixed ligand complexes. A reaction of triphenyl phosphine, PPh₃, with such a complex resulted in the generation of a *cis*-[(NHC)(PPh₃)PtCl₂] complex. The reaction of a second equivalent of triphenyl phosphine with the *cis*-[(NHC)(PPh₃)PtCl₂] complex resulted in the formation of a cationic mixed [*cis*-(NHC)(PPh₃)₂PtCl]⁺ complex, Scheme 3.



Scheme 3: Pt complex of mixed P/NHC, Rourke¹⁰¹

A new synthetic strategy by Marinetti *et al.*,^{102a,b} in 2007, allows access to an axially chiral square-planar platinum(II) complexes by combining diphosphine, dppe, and NHC ligand. The reaction was also carried out with chiral bidentate phosphines and achiral NHC ligands in order to generate the corresponding mixed NHC/diphosphine platinum complexes as diastereomeric pairs, Figure 25.

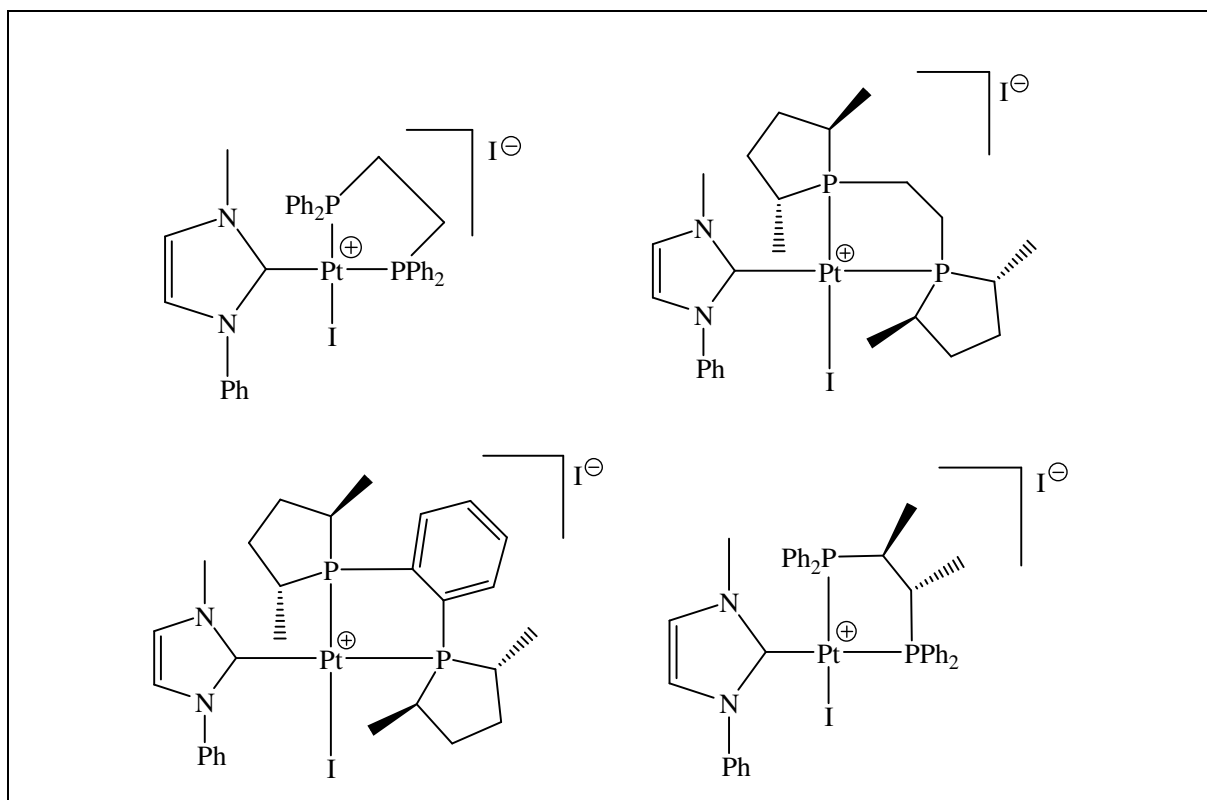


Figure 25: Pt complex of mixed di-P/NHC, Marinetti¹⁰²

Pd complexes of diphenylferrocenylphosphine-functionalized imidazolium salt was prepared in moderate yield by Shi and co-workers in 2008, Figure 26.¹⁰³ This ligand was evaluated and found to be efficient in the palladium-catalyzed amination of aryl halides with a variety of primary and secondary cyclic and acyclic alkyl amines.

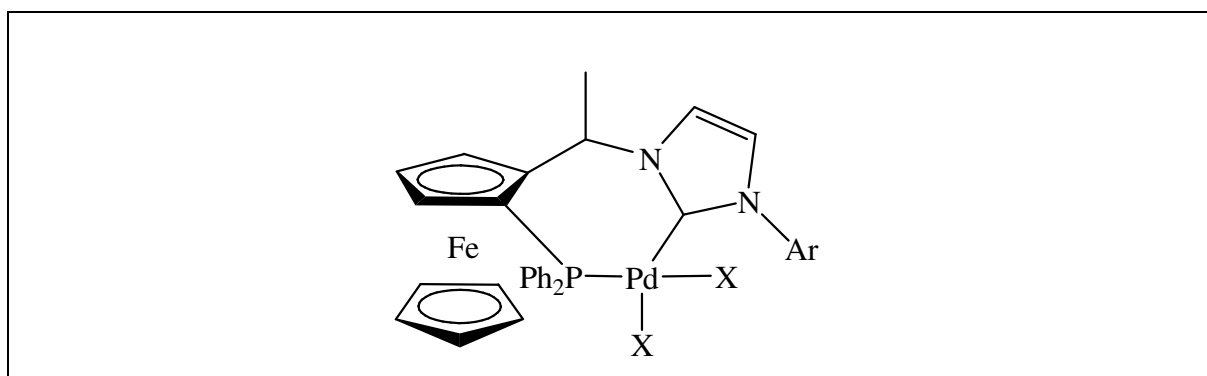


Figure 26: Pd complex of bidentate P-NHC, Shi¹⁰³

Fryzuk *et al.*, in 2009, synthesized and structurally characterized a new type of neutral pincer ligand of the PCP type wherein the central carbon donor is a saturated NHC.¹⁰⁴ The

imidazolium unit is flanked by two phosphine moieties and has *o*-phenylene linkers between the NHC and the phosphine donors. Subsequent reaction with Group 10 metal precursors, (Ni, Pd, Pt), produced the corresponding metal hydride complexes as PF_6^- salts, $[(\text{PCP})\text{MH}]\text{PF}_6$, in high yields. The incorporation of group 10 metals with the di-*o*-phenylene-bridged tridentate ligand, PCP, proceeds smoothly to generate a stable square-planar complex, Figure 27.

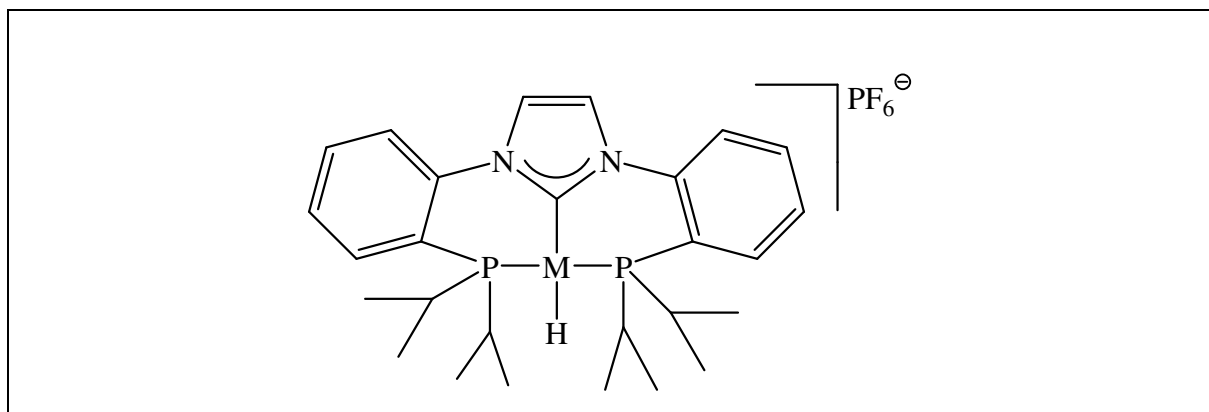
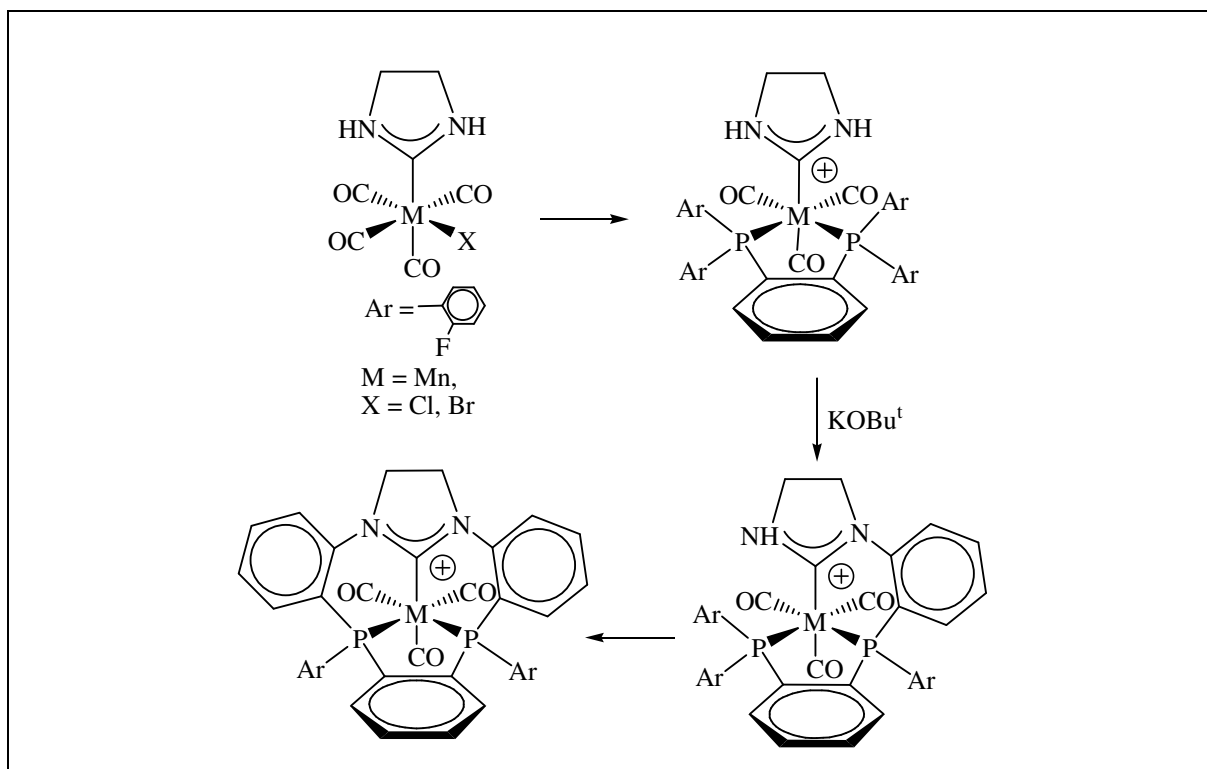


Figure 27, (M= Ni, Pd, Pt): PCP, Fryzuk¹⁰⁴

Using more direct method compared to Fryzuk system, Edwards and co-workers, in early 2009, prepared complexes with a facially coordinated macrocyclic 2P/NHC ligand, the first macrocycle containing carbene and phosphorus donors.^{105a} This tridentate *N*-heterocyclic carbene-diphosphine macrocycle ligand was produced by the template controlled linkage of a coordinated diphosphine to a NHC ligand at Mn *via* nucleophilic displacement of fluoride in 2-fluoroaryl phosphines, Scheme 4. The resultant complex contains two phosphine-phenyl groups and one NHC donor group coordinated to Mn(I) and Re(I). The facial incorporation of a tridentate macrocyclic ligand into a metal complex, such as $\text{NHC-Mn}(\text{CO})_4\text{Br}$,^{105b} may impart interesting properties to a given metal complex since this PCP donor set is restricted to bind in a facial mode (due to the *o*-phenylene linkers restricting the ligand ring size), and thus forcing the remaining coordination sites into mutually *cis* positions; a configuration required for catalytic applications.



Scheme 4: Mn complex of macrocyclic 2P/NHC, Edwards¹⁰⁵

Macrocyclic ligands containing both NHC and phosphine donor groups remain very rare. Subsequent to the report of Edwards *et. al.*, Hahn *et al.*,¹⁰⁶ in 2010, described mixed bis-carbene/bisphosphine platinum complexes and the template-controlled preparation of platinum macrocyclic complexes. Their syntheses led to platinum complexes with two *trans*-phosphine groups and two *trans*-coordinated NHC carbene ligands, Figure 28.

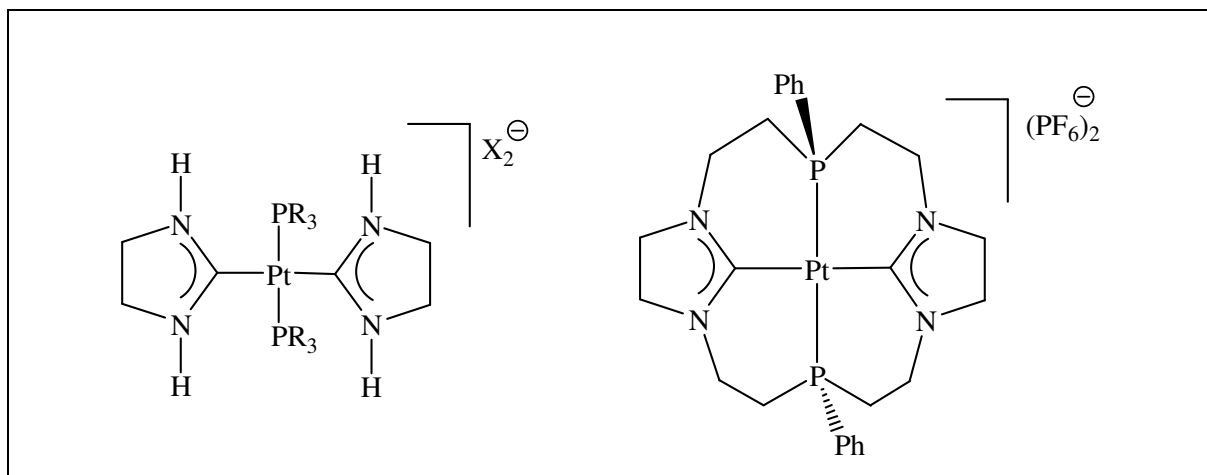


Figure 28: Pt complexes of mixed P/NHC and macrocyclic ligands, Hahn¹⁰⁶

These latter complexes reacted with phosphine ligand, which is capable of bridging to the NH,NH-stabilized carbene ligands, followed by an intramolecular hydroamination reaction to produce the tetradentate 2NHC/2P macrocyclic platinum complexes, Figure 28. This template-controlled preparation and crystallization of cationic platinum complexes constitutes the first example of a complex bearing a tetradentate bis-NHC/bis-phosphine macrocycle.

In 2011, Hahn *et al.*^{107a} synthesized and crystallized monodentate NHC-M complexes *via* an oxidative addition method of the C₁-Cl bond of a benzimidazolium derivative followed by protonation of the unsubstituted nitrogen atom with an acid, NH₄BF₄. This development of a one-pot synthesis for such complexes was used for the coordination of zero-valent Pd and Pt metal precursors having PPh₃ ligands. For the Pd complex, NHC-*trans*-X was obtained, while the oxidative addition for Pt yielded a mixture of *cis* (major) and *trans* (minor). Huynh and coworkers achieved a similar result for Pt complex of mixed NHC/mono-phosphine/2-halide, in 2007.^{107b}

Based on benzimidazolium backbone such as in Figure 29, Sakaguchi and Kamisue, in 2011,¹⁰⁸ designed and synthesized amide-functionalized *N*-heterocyclic carbene (NHC) precursors. By *in situ* Ag-transmetallation method, they afforded and crystallized mixed NHC/phosphine complexes with Pd such as [(NHC)(PPh₃)PdCl₂] together with a cationic [(NHC) (PPh₃)₂PdCl]⁺ Cl⁻ complex. This one-pot procedure, without purification of the NHC-Ag intermediates, resulted a high yield complexation which expanded the collection of NHC-Pd(II) complexes bearing amide functionalities.

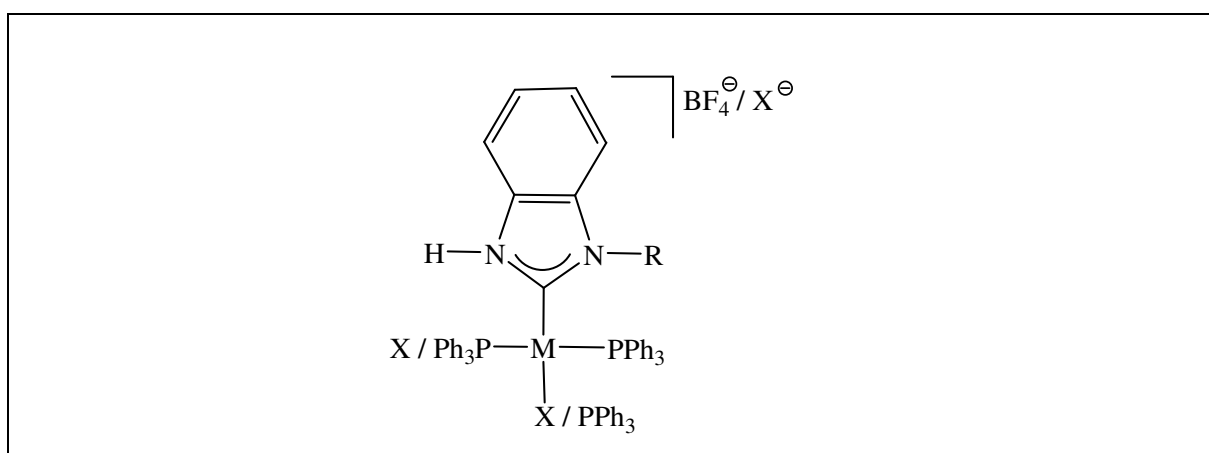


Figure 29: Pd complex of mixed 2P/NHC, Kamisue¹⁰⁸

Manganese complexes of NHC/phosphine ligands are less common and most of these complexes bear unsaturated imidazolin-2-ylidene ligands.¹⁰⁹ Attempts by Hahn *et al.*,¹¹⁰ in 2011, to synthesise a facial mixed NHC/diphosphine manganese complex were unsuccessful as the NH,NH-substituted saturated cyclic diaminocarbene and the diphosphine ligands could not be coordinated in the required facial geometry, as was previously observed with other metals, but instead featuring a meridional arrangement of the diphosphine and the NHC ligand, Figure 30.

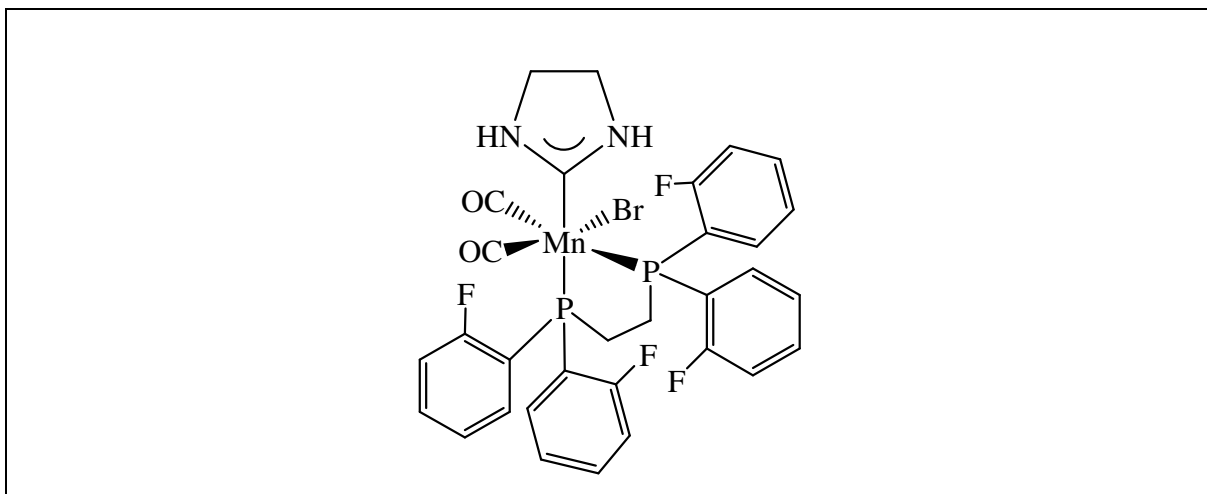


Figure 30: Mn complex of mixed 2P/NHC, Hahn¹¹⁰

In 2012, Xu *et al.*¹¹¹ synthesised and crystallized two mixed donor NHC/phosphine palladium complexes, Figure 31. These two *trans* and *cis* NHC/phosphine palladium(II) complexes have been prepared from the reaction of the corresponding NHC-(dimethoxyphenyl). Single-crystal X-ray analysis confirms there are intermolecular C-H \cdots X and C-H \cdots O hydrogen bonds in such complexes. These complexes were found to be efficient catalysts for the Suzuki reaction of aryl bromides.

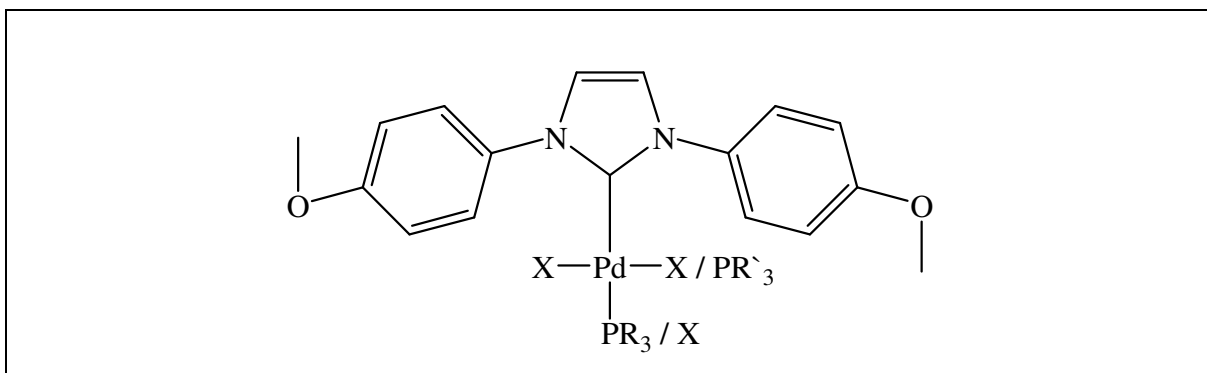
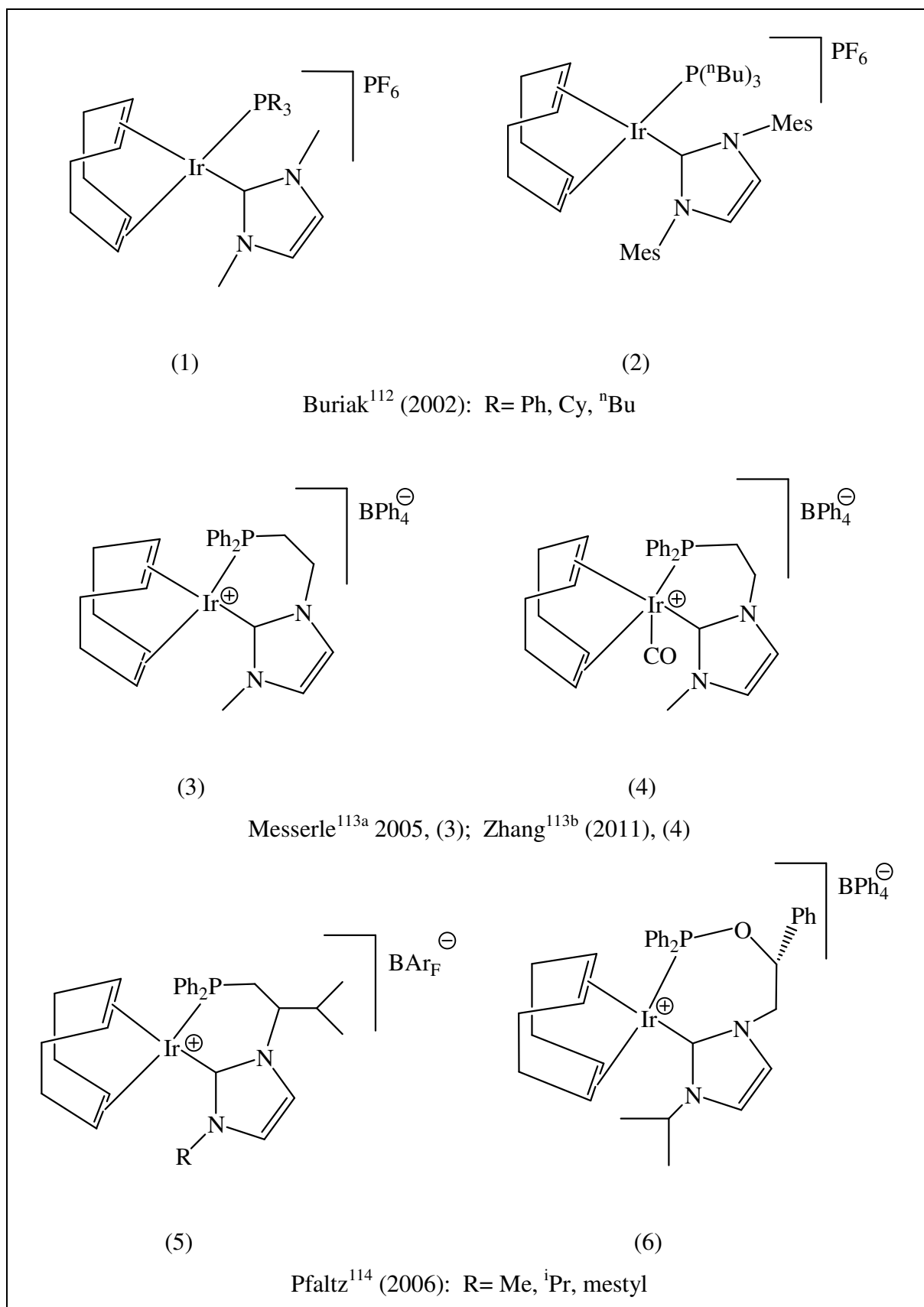
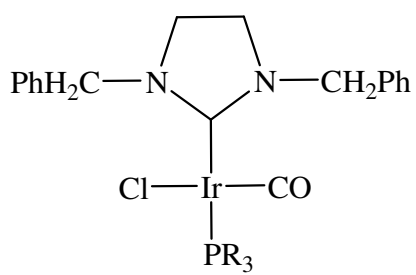


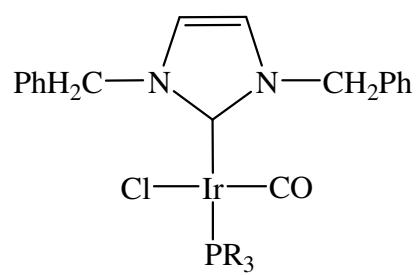
Figure 31: (R= Ph₃, R' = (C₆H₄-p-Me)₃, Pd complex of mixed P/NHC, Xu¹¹¹

Other related iridium complexes of mixed dentate NHC/P are depicted below in Figure 32.



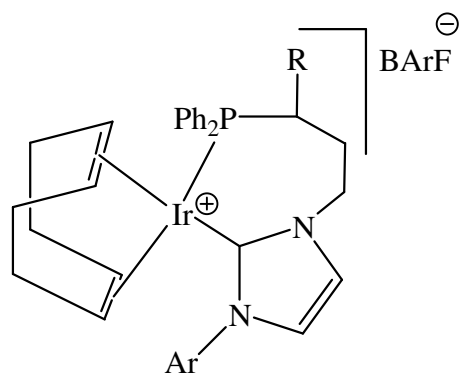


(7)



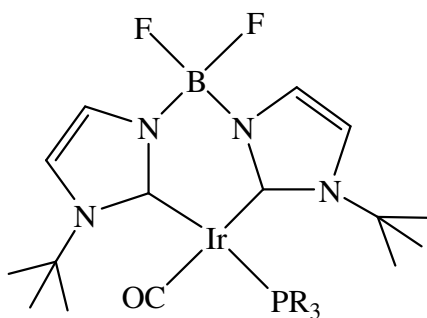
(8)

Liu¹¹⁵ (2009): R= Ph, Cy



(9)

Jubault¹¹⁶ (2011): R= Me, Et, ⁱPr; Ar= Mes, dipp



(10)

Chen¹¹⁷ (2012): R= Ph, Cy

Figure 32

1.9: Aims and objectives of this thesis

Transition metal NHC complexes have been applied as homogeneous and heterogeneous catalysts with good results. *N*-heterocyclic carbene/phosphine complexes have been explored by many research groups and have played a role in organometallic chemistry. This special attention was due to their high thermal and chemical stability and high dissociation energies.

To date, research has mainly focused on chelating *N*-heterocyclic carbene/phosphine ligands with aliphatic backbone functions, leaving chelating *N*-heterocyclic carbene/phosphine ligands with rigid *o*-phenylene backbone spacers and aryl phosphine donors relatively unexplored. The work presented in this thesis will focus on the synthesis and characterisation of rigid chelating *N*-heterocyclic carbene/phosphine ligands bearing various aliphatic and aromatic substituents and their complexes.

There is an interest in the contribution of bonding properties in a ligand that must bind to mutually *cis* sites requiring reactive sites to be mutually *trans* to the carbene's trans-influence or the phosphine's trans-effect. Rigid chelating ligands are favoured in order to minimise side reactions resulting from spectator ligand dissociation. With this aim, I have prepared a series of ligands with rigid *o*-phenylene backbone spacers and aryl phosphine donors. In this thesis, I describe alkyl phosphine derivatives and synthetic details of this study. Once this ligand synthesis is achieved, the coordination chemistry of the ligand with metals of Group 7, 9, 10 and 11 have been investigated and details of these will be presented. Complexes of this type of ligands are likely to have interesting properties and catalyse a wide range of organic reactions. The design and synthesis of such type of complexes are, therefore, an appealing enterprise. However, the available synthetic methods for such rigid chelating NHC/phosphine ligands and their complexes are low yielding. Consequently, new synthetic methodologies with good yields need to be developed.

Finally, the catalytic properties of such complexes should be investigated in separate study. Also NHC ligands bearing other aliphatic functionalized phosphine groups should be developed and investigated.

References:

- [1] J. Yang, R. Zhang, W. Wang, Z. Zhang, M. Shi, *Tetrahedron: Asymmetry*, **2011**, 22, 2029.
- [2] S. P. Nolan, *N-Heterocyclic Carbenes in Synthesis*; 1st ed.; Wiley-VCH: Weinheim, Germany, **2006**.
- [3] S. Diez-Gonzalez, S. P. Nolan, *Coord. Chem. Rev.* **2007**, 251, 874.
- [4] A. K. Nebioglu, M. J. Panzner, C.A. Tessier, C. L. Cannon, W. J. Youngs, *Coord. Chem. Rev.*, **2007**, 251, 884.
- [5] M. L. Teyssot, A. S. Jarrousse, M. Manin, A. Chevy, S. Roche, F. Norre, C. Beaudoin, L. Morel, D. Boyer, R. Mahiou, A. Gautier, *Dalton Trans.*, **2009**, 6894.
- [6] S. Diez-Gonzalez, N. Marion, S. P. Nolan, *Chem. Rev.* **2009**, 109, 3612.
- [7] I.I.F. Boogaerts, S. P. Nolan, *Chem. Commun.*, **2011**, 47, 3021.
- [8] W. Henderson, A. G. Oliver, *Inorg. Chim. Acta*, **2011**, 378, 121.
- [9] N. Tsoureas, A. A. Danopoulos, A. A. D. Tulloch, M. E. Light, *Organometallics*, **2003**, 22, 4750.
- [10] S. P. Nolan, G. A. Grasa, M. S. Viciu, J. Huang, *J. Org. Chem.*, **2001**, 66, 7729.
- [11] W. A. Herrmann, V. P. Bohm, C. W. Gstottmayr, M. Grosche, C. P. Reisinger, T. Weskamp, *J. Organomet. Chem.*, **2001**, 617, 616.
- [12] J. Wolf, A. Labande, D. Jean-Claude, R. Poli, *J. Organomet. Chem.*, **2006**, 691, 433.
- [13] S. X. Xiao, W. C. Trogler, Z. Y. W. C. Ellis, *J. Am. Chem. Soc.*, **1983**, 105, 7033.
- [14] D. S. Marynick, *J. Am. Chem. Soc.*, **1984**, 106, 4064.
- [15] M. Braga, *Inorg. Chem.*, **1985**, 24, 2702.
- [16] N. G. Connelly, A. G. Orpen, *J. Chem. Soc. Chem. Commun.*, **1985**, 1310.
- [17] C. A. Tolman, *J. Am. Chem. Soc.*, **1970**, 92, 2952.
- [18] J. P. Collman, L. S. Hegedus, J. R. Norton, R. G. Finke, *Principles and applications of organotransition metal chemistry*, 2nd. ed., University Science Books, Mill Valley, California, **1987**.
- [19] A. F. Hill, *Organotransition Metal Chemistry*, The Royal Society of Chemistry, Cambridge, **2002**.
- [20] R. H. Crabtree, *The Organometallic Chemistry of the Transition Metals*, 3rd ed., John Wiley & Son, New York, **2001**.
- [21] E. O. Fischer, *Adv. Organomet. Chem.*, **1976**, 14, 1.

- [22] R. R. Schrock, *Acc. Chem. Res.*, **1979**, *12*, 98.
- [23] J. Clayden, N. Greeves, S. Warren, P. Wothers, *Organic Chem.*, **2001**, 1060.
- [24] C. Boehme, G. Frenking, *Organometallics*, **1999**, *17*, 5801.
- [25] H. W. Wanzlick, *Angew. Chem. Int. Ed. Engl.*, **1962**, *1*, 75.
- [26] L. Jafarpour, S. P. Nolan, *Adv. Organomet. Chem.*, **2001**, *46*, 181.
- [27] W. A. Herrmann, T. Weskamp, V. P. W. Böhm, *Adv. Organomet. Chem.*, **2001**, *48*, 1.
- [28] A. J. Arduengo III, H. V. R. Dias, , R. L. Harlow, M. A. Kline, *J. Am. Chem. Soc.* **1992**, *114*, 5530.
- [29] A. J. Arduengo III, R. L. Harlow, M. A. Kline, *J. Am. Chem. Soc.* **1991**, *113*, 361
- [30] A. A. D. Tulloch, A. A. Danopoulos, S. Kleinhenz, M. E. Light, M. B. Hursthouse, G. Eastham, *Organometallics*, **2001**, *20*, 2027.
- [31] L. D. Vazquez-Serrano, B. T. Owens, J. M. Buriak, *Chem. Comm.* **2002**, 2518.
- [32] L. Jafarpour, S. P. Nolan, *J. Organomet. Chem.*, **2001**, *617*, 17.
- [33] Ch. Yang, H. M. Lee, S. P. Nolan, *Org. Lett.*, **2001**, *3*, 1511.
- [34] W. A. Herrmann, L. J. Goossen, C. Koecher, G. R. J. Artus, *Angew. Chem., Int. Ed.* **1997**, *35*, 2805.
- [35] K. Öfele, W. A. Herrmann, D. Mihalios, M. Elison, E. Herdtweck, W. Scherer, J. Mink, *J. Organomet. Chem.*, **1993**, *459*, 177.
- [36] J. Huang, H.J. Schanz, E. D. Stevens, S. P. Nolan, *Organometallics*, **1999**, *18*, 2370.
- [37] J. Schwarz, V. P. W. Böhm, M. G. Gardiner, M. Groshe, W. A. Herrmann, W. Hieringer, G. Raudaschl-Sieber, *Chem. Eur. J.*, **2000**, *6*, 1773.
- [38] A. A. Danopoulo, D. M. Hankin, G. Wilkinson, S. M. Cafferkey, T. K.N. Sweet, M. B. Hursthouse, *Polyhedron*, **1997**, *16*, 3879.
- [39] D. Bourissou, O. Guerrent, F. Gabbaï, G. Bertand, *Chem. Rev.*, **2000**, *100*, 39.
- [40] (a) W. A. Herrmann, L. J. Gooben, M. Spiegler, *J. Organomet. Chem.*, **1997**, *547*, 357.
(b) J. A. Chamizo, P. B. Hitchcock, H. A. Jasim, M. F. Lappert, *J. Organomet. Chem.*, **1993**, *451*, 89.
- [41] M. J. Green, K. J. Cavell, B. W. Skelton, A. H. White, *J. Organomet. Chem.*, **1998**, *554*, 175.
- [42] A. A. D. Tulloch, A. A. Danopoulos, G. J. Tizzard, S. J. Close, M. B. Hursthouse, R. S. Hay-Motherwell, W. B. Motherwell, *Chem. Commun.*, **2001**, *14*, 1270.
- [43] A. A. Danopoulos, S. Winston, T. Gelbrich, M. B. Hursthouse, R. P. Tooze, *Chem. Commun.*, **2002**, *5*, 482.

- [44] H. Lang, J. J. Vittal, P.-H. Leung, *J. Chem. Soc., Dalton Trans.*, **1998**, 2109.
- [45] V. P. W. Böhm, C. W. K. Gstöttmayr, T. Weskamp, W. A. Herrmann, *J. Organomet. Chem.*, **2000**, 595, 186.
- [46] H. M. Lee, P. L. Chiu, J. Y. Zeng, *Inorg. Chim. Acta*, **2004**, 357, 4313.
- [47] A. D. Tulloch, S. Winston, A. A. Danopoulos, G. Eastham, M. B. Hursthouse, *J. Chem. Soc., Dalton Trans.*, **2003**, 699.
- [48] A. W. Waltham, R. H. Grubbs, *Organometallics*, **2004**, 23, 3105.
- [49] A. D. Tulloch, A. A. Danopoulos, R. P. Tooze, S. M. Cafferkey, S. Kleinhenz, M. B. Hursthouse, *Chem. Commun.*, **2000**, 1247.
- [50] Ch. Topf, Ch. Hirtenlehner, U. Monkowius, *J. Organomet. Chem.*, **2011**, 696, 3274.
- [51] P. de Frémont, N. Marion, S. P. Nolan, *J. Organomet. Chem.*, **2009**, 694, 551.
- [52] J. Lemke, A. Pinto, P. Niehoff, V. Vasylyeva, N. Metzler-Nolte, *Dalton Trans.*, **2009**, 7063.
- [53] S. P. Nolan, *Acc. Chem. Res.* **2011**, 44, 91.
- [54] N. J. Whitcombe, K. K. Hii, S. E. Gibson, *Tetrahedron* **2001**, 57, 7449-7476.
- [55] H. W. Wanzlick, H. J. Schönherr, *Angew. Chem., Int. Ed. Engl.* **1968**, 7, 141.
- [56] (a) K. Öfele, *J. Organomet. Chem.* **1968**, 12, 42.
 (b) K. Öfele, *Angew. Chem., Int. Ed. Engl.* **1970**, 9, 739.
 (c) K. Öfele, *J. Organomet. Chem.*, **1970**, 22, C9.
- [57] Th. Weskamp, V. P. W. Böhm, W. A. Herrmann, *J. Organomet. Chem.*, **1999**, 585, 348.
- [58] G. A. Grasa, Z. Moore, K. L. Martin, E. D. Stevens, S. P. Nolan, V. Paquet, H. Lebel, *J. Organomet. Chem.*, **2002**, 658, 126.
- [59] (a) A. J. Arduengo III; H. V. R. Dias, J. C. Calabrese, F. Davidson, *Organometallics*, **1993**, 12, 3405.
 (b) H. M. J. Wang, I. J. B. Lin, *Organometallics*, **1998**, 17, 972.
- (60) W. A. Herrmann, *Angew. Chem., Int. Ed.* **2002**, 41, 1290.
- (61) (a) M. S. Sanford, J. A. Love, R. H. Grubbs, *J. Am. Chem. Soc.* **2001**, 123, 6543.
 (b) S. Lee, J. F. Hartwig, *J. Org. Chem.* **2001**, 66, 3402.
- [62] (a) S. T. Nguyen, L. K. Johnson, R. H. Grubbs, J. W. Ziller, *J. Am. Chem. Soc.*, **1992**, 114, 3974.
 (b) P. Schwab, M. B. France, J. W. Ziller, R. H. Grubbs, *Angew. Chem.*, **1995**, 34, 2039.

- (c) P. Schwab, R. H. Grubbs, J. W. Ziller, *J. Am. Chem. Soc.*, **1996**, *118*, 100.
- [63] (a) M. Scholl, S. Ding, C. W. Lee, R. H. Grubbs, *Org. Lett.*, **1999**, *1*, 953.
 (b) T. M. Trnka, R. H. Grubbs, *Acc. Chem. Res.*, **2000**, *34*, 18.
 (c) E. Peris, J. A. Loch, J. Mata, and R. H. Crabtree, *Chem. Comm.*, **2001**, *2*, 201.; J. A. Loch, M. Albrecht, E. Peris, J. Mata, J. W. Faller, and R. H. Crabtree, *Organometallics*, **2002**, *21*, 700.
- [64] J. A. Love, J. P. Morgan, T. M. Trnka, R. H. Grubbs, *Angew. Chem.*, **2002**, *41*, 4035.
- [65] (a) J. K. Huang, E. D. Stevens, S. P. Nolan, J. L. Petersen, *J. Am. Chem. Soc.*, **1999**, *121*, 2674.
 (b) M. Scholl, T. M. Trnka, J. P. Morgan, R. H. Grubbs, *Tetrahedron Lett.*, **1999**, *40*, 2247.
 (c) L. Ackermann, A. Fürstner, T. Weskamp, F. J. Kohl, W. A. Herrmann, *Tetrahedron Lett.*, **1999**, *40*, 4787.
- [66] (a) J. S. Kingsbury, J. P. A. Harrity, P. J. Bonitatebus, A. H. Hoveyda, *J. Am. Chem. Soc.*, **1999**, *121*, 791.
 (b) S. Gessler, S. Randl, S. Blechert, *Tetrahedron Lett.*, **2000**, *41*, 9973.
 (c) S. B. Garber, J. S. Kingsbury, B. L. Gray, A. H. Hoveyda, *J. Am. Chem. Soc.*, **2000**, *122*, 8168.
- [67] G. C. Vougioukalakis, R. H. Grubbs, *Chem. Rev.*, **2010**, *110*, 1746.
- [68] J. R. Anderson, M. Boudart, *Catalysis: Science and Technology*; Springer,-Verlag, **1997**.
- [69] F. J. McQuillin, D. G. Parker, G. R. Stephenson, *Transition Metal Organometallics for Organic Synthesis*, Cambridge Press, New York, **1991**.
- [70] D. Enders, H. Gielen, K. Breuer, *Tetrahedron: Asymmetry* **1997**, *8*, 3571.
- [71] L. H. Gade, V. Cesar, S. Bellemin-Laponnaz, *Angew. Chem., Int. Ed.*, **2004**, *43*, 1014.
- [72] W. L. Duan, M. Shi, G-B. Rong, *Chem. Comm.* **2003**, 2916.
- [73] F. Glorius, G. Altenhoff, R. Goddard, C. Lehmann, *Chem. Comm.* **2002**, 2704.
- [74] L. G. Bonnet, R. E. Douthwaite, B. M. Kariuki, *Organometallics* **2003**, *22*, 4187.
- [75] H. Seo, B. Y. Kim, J. H. Lee, H.-J. Park, S. U. Son, Y. K. Chung, *Organometallics*, **2003**, *22*, 4783.
- [76] F. Guillen, C. L. Winn, A. Alexakis, *Tetrahedron: Asymmetry* **2001**, *12*, 2083.

- [77] A. Alexakis, C. L. Winn, F. Guillen, J. Pytkowicz, S. Roland, P. Mangeney, *Adv. Synth. Catal.* **2003**, 345, 345.
- [78] L. Fadini, A. Togni, *Chem. Comm.* **2003**, 30.
- [79] H. M. Lee, T. Jiang, E. D. Stevens, S. P. Nolan, *Organometallics* **2001**, 20, 1255.
- [80] (a) W. A. Herrmann, L. J. Goossen, M. Spiegler, *J. Organomet Chem.*, **1997**, 547, 357.
 (b) R. Z. Ku, J. Ch. Huang, J. Y. Cho, F. M. Kiang, K. R. Reddy, Y. Ch. Chen, K. J. Lee, J. H. Lee, G. H. Lee, Sh. M. Peng, Sh. T. Liu, *Organometallics*, **1999**, 18, 2145.
 (c) Ch. Y. Liao, K. T. Chan, Ch. Y. Tu, Y. W. Chang, Ch. H. Hu, H. M. Lee, *Chem. Eur. J.* **2009**, 15, 405.
 (d) K. T. Chan, Y. H. Tsai, W. Sh. Lin, J. R. Wu, Sh. J. Chen, F. X. Liao, Ch. H. Hu, H. M. Lee, *Organometallics*, **2010**, 29, 463.
 (e) Ch. F. Fu, Y. H. Liu, Sh. M. Peng, Sh. T. Liu, *Tetrahedron*, **2010**, 66, 2119.
- [81] R. E. Douthwaite, D. Haüssinger, M. L. H. Green, P. J. Silcock, P. T. Gomes, A. M. Martins, A. A. Danopoulos, *Organometallics*, **1999**, 18, 4584.
- [82] K. Albert, P. Gisdakis, N. Rou'sch, *Organometallics*, **1998**, 17, 160, 8511.
- [83] D. S. McGuinness, N. Saendig, B. F. Yates, K. J. Cavell, *J. Am. Chem. Soc.* **2001**, 123, 4029.
- [84] (a) D. S. McGuinness, K. J. Cavell, B. F. Yates, B. W. Skelton, A. H. White, *J. Am. Chem. Soc.* **2001**, 123, 8317.
 (b) A. M. Magill, B. F. Yates, K. J. Cavell, B. W. Skelton, A. H. White, *Dalton Trans.*, **2007**, 3398.
- [85] A. Fürstner, G. Seidel, D. Kremzow, C. W. Lehmann, *Organometallics*, **2003**, 22, 907.
- [86] C. J. Mathews, P. J. Smith, T. Welton, A. J. P. White, D. J. Williams, *Organometallics*, **2001**, 20, 3848.
- [87] (a) L. R. Titcomb, S. Caddick, F. Geoffrey, N. Cloke, D. J. Wilson, D. McKerrecher, *Chem. Commun.*, **2001**, 1388.
 (b) R. Fränkel, J. Kniczek, W. Ponikwar, H. Nöth, K. Polborn, W. P. Fehlhammer, *Inorg. Chim. Acta*, **2001**, 312, 23.
- [88] C. Böhrer, D. Stein, N. Donati, H. Grützmacher, *New J. Chem.*, **2002**, 26, 1291.
- [89] E. Bappert, G. Helmchen, *Syn. Lett.*, **2004**, 10, 1789.
- [90] (a) W. J. Marshall, V. V. Grushin, *Organometallics* **2003**, 22, 1591.
 (b) M. A. Duin, N. D. Clement, K. J. Cavell, C. J. Elsevier, *Chem. Commun.*, **2003**, 400.

- [91] (a) H. M. Lee, J. Y. Zeng, C. H. Hu, M. T. Lee, *Inorg. Chem.* **2004**, *43*, 21, 6822.
 (b) H. M. Lee, P. L. Chiu, J. Y. Zeng, *Inorg. Chim. Acta*, **2004**, *357*, 4313.
 (c) P. L. Chiu, H. M. Lee, *Organometallics*, **2005**, *24*, 1692.
- [92] (a) S. Gischig, A. Togni, *Organometallics*, **2004**, *23*, 2479.
 (b) F. Wanga, Lian-jun Liua, W. Wanga, L. A. Shengke, Min Shi, *Coord. Chem. Rev.*, **2012**, *256*, 804.
- [93] (a) Wang, A-E; Zhong, J; Xie, J-H.; Li, K, Zhou, Q-L. *Adv. Synth. Catal., Communications*, **2004**, *346*, 595.
 (b) A. E. Wang, J. H. Xie, L. X. Wang, Q. L. Zhou, *Tetrahedron*, **2005**, *61*, 259.
- [94] Ch. Ch. Ho, S. Chatterjee, T. L. Wu, K. T. Chan, Y. W. Chang, T. H. Hsiao, H. M. Lee, *Organometallics*, **2009**, *28*, 2837.
- [95] M. V. Baker, P. J. Barnard, S. J. Berners-Price, S. K. Brayshaw, J. L. Hickey, B. W. Skelton, A. H. White, *J. Organomet. Chem.*, **2005**, *690*, 5625.
- [96] S. K. Schneider, G. R. Julius, Ch. Loschen, H. G. Raubenheimer, G. Frenking, W. A. Herrmann, *Dalton Trans.*, **2006**, 1226.
- [97] F. E. Hahn, M. C. Jahnke, T. Pape, *Organometallics*, **2006**, *25*, 5927.
- [98] J. Wolf, A. Labande, M. Natella, J.-Claude Daran, R. Poli, *J. Mol. Catal. A: Chem.*, **2006**, *259*, 205.
- [99] Ch. Ch. Lee, W. Ch. Ke, K. T. Chan, Ch. L. Lai, Ch. H. Hu, H. M. Lee, *Chem. Eur. J.* **2007**, *13*, 582.
- [100] H. J. Roberts, PhD Thesis, Cardiff University, **2007**, 76.
- [101] Ch. P. Newman, R. J. Deeth, G. J. Clarkson, J. P. Rourke, *Organometallics*, **2007**, *26*, 6226.
- [102] (a) D. Brissy, M. Skander, P. Retailleau, A. Marinetti, *Organometallics*, **2007**, *26*, 5782.
 (b) D. Brissy, M. Skander, P. Retailleau, G. Frison, A. Marinetti, *Organometallics*, **2009**, *28*, 140.
- [103] J. Ch. Shi, P. Yang, Q. Tong, L. Jia, *Dalton Trans.*, **2008**, 938.
- [104] T. Steinke, B. K. Shaw, H. Jong, B. O. Patrick, M. D. Fryzuk, *Organometallics*, **2009**, *28*, 2830.
- [105] (a) O. Kaufhold, A. Stasch, P. G. Edwards, F. E. Hahn, *Chem. Commun.*, **2007**, 1822.
 (b) O. Kaufhold, A. Stasch, T. Pape, A. Hepp, P. G. Edwards, P. D. Newman, F. E. Hahn, *J. Am. Chem. Soc.*, **2009**, *131*, 306.
- [106] A. F. Figueroa, T. Pape, K. O. Feldmann, F. E. Hahn, *Chem. Commun.*, **2010**, *46*, 324.

- [107] (a) T. Kösterke, T. Pape, F.E. Hahn, *J. Am. Chem. Soc.*, **2011**, *133*, 2112.
 (b) Y. Han, H. V. Huynh, G. K. Tan, *Organometallics*, **2007**, *26*, 4612.
- [108] R. Kamisue, S. Sakaguchi, *J. Organomet. Chem.*, **2011**, *696*, 1910.
- [109] J. Ruiz, B. F. Perandones, *J. Am. Chem. Soc.* **2007**, *129*, 9298.
- [110] V. Blase, T. Pape, F. E. Hahn, *J. Organomet. Chem.*, **2011**, *696*, 3337.
- [111] Ch. Xu, X. Q. Hao, Z. Li, X. M. Dong, L. M. Duan, Z. Q. Wang, B. M. Ji, M. P. Song, *Inorg. Chem. Commun.*, **2012**, *17*, 34.
- [92] L. D. Vázquez-Serrano, B. T. Owens, J. M. Buriak, *Chem. Commun.*, **2002**, 2518.
- [113] (a) L. D. Field, B. A. Messerle, K. Q. Vuong, P. Turner, *Organometallics* **2005**, *24*, 4241.
 (b) X. Gong, H. Zhang, X. Li, *Tetrahedron Lett.*, **2011**, *52*, 5596.
- [114] S. Nanchen, A. Pfaltz, *Chim. Acta* **2006**, *89*, 1560.
- [115] Y. H. Chang, Ch. F. Fu, Y. H. Liu, Sh. M. Peng, J. T. Chen, Sh. T. Liu, *Dalton Trans.*, **2009**, 861.
- [116] J. Passays, T. Ayad, V. R. Vidal, A. C. Gaumont, Ph. Jubault, E. Leclerc, *Tetrahedron: Asymmetry*, **2011**, *22*, 562.
- [117] F. Chen, G. F. Wang, Y. Z. Li, X. T. Chen, Z. L. Xue, *J. Organomet. Chem.*, **2012**, *710*, 36.

Chapter 2

Synthesis of an Imidazolium Precursor and Functionalised Phosphine-Imidazolium Salt derivatives as Ligands for the Formation of Metal Complexes

2.1: Introduction

2.1.1: Imidazolium Salts

This thesis focuses exclusively on a single NHC precursor and the synthesis of its imidazolium salt and complexes. The approach to the synthesis of phosphine-imidazolium salts, (**1**, Figure 2.1), involves an *in situ* coupling reaction of alkyl halides with imidazole.

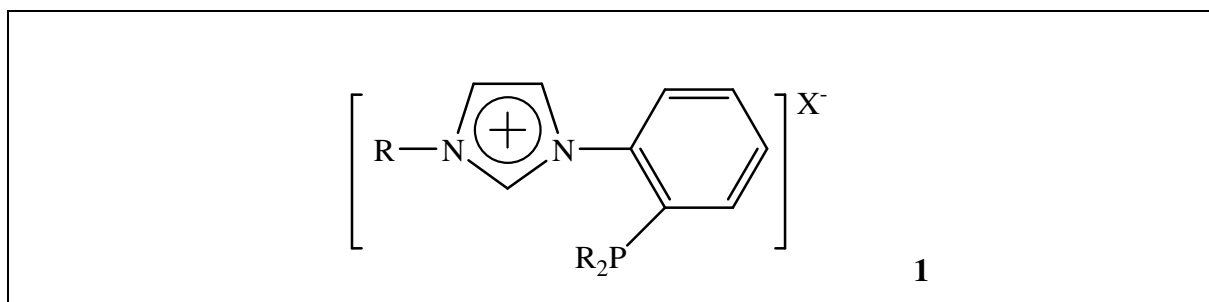


Figure 2.1: Phosphine-imidazolium salt

Related catalytic amination reactions of aryl halides have been reported by Buchwald^{1,2} and Hartwig.³ Palladium and copper have been employed as the catalyst sources in these syntheses. In the synthesis of **1**, we have utilised all three methodologies. These have been studied as a function of a variety of variables such as temperature, time of reaction, base, ligand, catalyst loading, etc. The copper-catalysed system of Buchwald *et al.*¹ was by far the most successful method of the three for the cross-coupling reactions attempted. However, yields were still poor with 34% maximum isolated yield.

Imidazolium salts can be prepared by reacting the potassium salt of imidazole with one equivalent of primary alkyl halide in a non-polar solvent, to prevent any elimination.⁵ Another equivalent of a different alkyl halide may then be reacted with the resulting *N*-alkylated imidazole in a polar solvent.

The route to synthesise *N*-substituted imidazoles was adapted from Gridnev and Arduengo from the literature method.^{6,7} It sought to build the imidazole ring from the corresponding amine, which proved to be a much more effective method. So, imidazolium salts were formed by converting primary amines to di-imines.^{6,7} Grubbs *et al.* reported the synthesis of unsymmetrical *N,N*-diaryl imidazolium salts.⁸ Thus, these studies support the indication that it should be possible to synthesise classes of ligands having different alkyl and/or aryl groups at the N₁ and N₂ positions, and with similar or different functionalities.

The imidazolium salt in this thesis is derived from *N*-substituted imidazole.⁹ This substituted imidazole **2.1** is prepared by the reaction of primary amines, glyoxal and formaldehyde in acidic conditions, Scheme 2.2.

2.1.2: Phosphine-imidazolium ligands

In the case of monodentate carbenes, a reductive elimination may occur with *cis*-orientated (to the carbene-carbon) alkyl groups. This decomposition is suggested to be facilitated by distortions (compression) of inter-ligand bond angles and because orbitals of the carbene-carbon and these alkyl groups can overlap easily.¹⁰ NHC-phosphine complexes have been found to increase the catalytic activity in many reactions such as hydrogenation, carbonylation, hydroformylation, and ring-opening metathesis.¹¹

To limit such reductive eliminations, chelating bidentate ligands, especially those bearing rigid linkers forming 6-membered chelating rings with the metal, would be expected to be less susceptible to reductive elimination than related flexible aliphatic linkers. Thus rigid aryl linker rings would be expected to enhance the complex stability by limiting the linker free movements around the metal centre. Previous work of Nolan and Danopoulos has showed substituted imidazolium ligands with phosphine-alkyl linkers^{12a-b,13} with and without aryl interspersed in the alkyl linker chains.^{14,15,16} These have been shown to have moderate activity in C-C coupling reactions albeit with some decomposition in chlorinated solvents.¹³ The reported bidentate P-NHC ligands with a linker between the imidazolium ring and the phosphine moiety were found to be unfavourable flexible bridge, which prompted the Edwards-Cavell group to design a rigid linker such as a phenyl ring between the two functional groups so that the chelating ligand will be unable to rotate freely. Correspondingly, this thesis is focused in synthesising a ligand that has a rigid aryl linker and which forms a 6-membered chelate ring upon coordination with a transition metal.

A rigid bidentate carbene-phosphine coordination mode would be formed by directly connecting an *o*-phenylene (1,2-benzdiyl) ring spacer between the imidazolium core and the phosphine donor. This, in turn, will force the coordinated carbene to tend towards co-planarity (with the chelate ring and coordination plane) instead of being at $\sim 65^\circ$ to the coordination plane as is commonly observed.¹⁷ In this context, the study of complexes of these bidentate carbene-phosphines, i.e. the stability of the carbene-metal bond and ease of dissociation of the phosphine will be of interest.^{18,19}

Complexes of chelating carbene-phosphine ligands are known.^{13,19,20} The ligands studied to date are predominantly flexible with aliphatic backbone functions. Phosphine-

imidazolium salts with an aryl linker which forms 7-membered chelate rings have been studied in our group,^{4,21} Figure 2.2, A. Other mixed phosphine-imidazolium salts with alkyl linkers forming 6-membered chelate ring with a metal were synthesised in 2001 by Nolan *et al.*,¹² Figure 2.2, B.

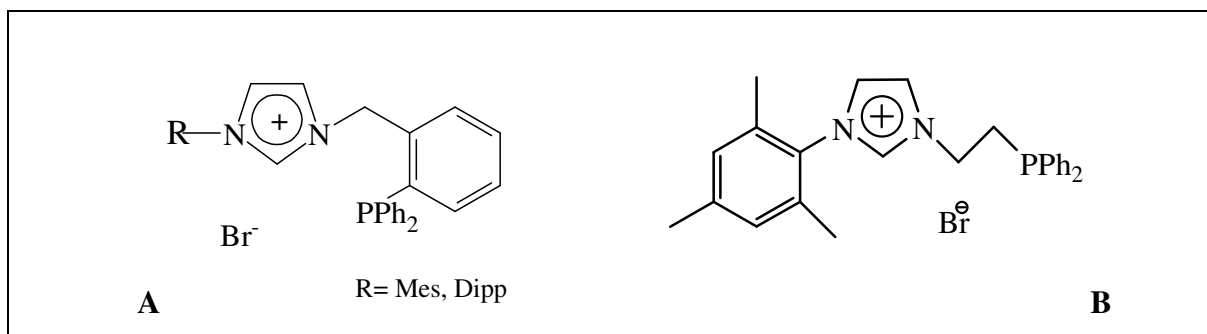
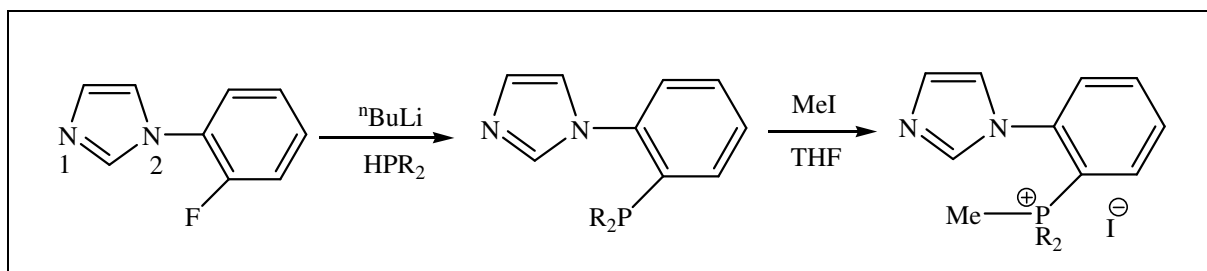


Figure 2.2

Incorporation of phosphorus donors into aromatic systems by nucleophilic substitution of fluoride in aryl-fluorides has been developed by Edwards *et al.* in the synthesis of P-macrocycles.^{21b} In this reaction, fluoride is an effective leaving group, especially when the 2-fluoroaryl function is adjacent to an electron withdrawing centre (e.g. a metal cation or imidazolium core). We have shown that this method does work for imidazole functionalised fluoroarenes although in these earlier attempts in our laboratories to prepare a benzo bridged chelating carbene-phosphine imidazolium salt precursor, phosphonium salts were preferentially formed Scheme 2.1.²¹ An alternative method was adopted in this thesis to synthesise the target where the imidazole ring would be substituted with an alkyl group at the N₁ position before nucleophilic substitution of aromatic fluoride with the relevant phosphide nucleophile.



Scheme 2.1: R= cyclohexyl, ⁱBu

This thesis describes work towards rigid chelating ligands designed to minimise side reactions resulting from spectator ligand dissociation. With this aim, we have prepared a ligand with a rigid *o*-phenylene backbone spacer and alkyl phosphine donors. The work described in this thesis establishes the synthetic methodology and the structure of a number of novel donor phosphine-NHC ligands and complexes. In particular, chelating phosphine-NHC ligands bearing diisopropyl substituents will be focussed upon for the synthesis of metal complexes. A number of chelating phosphine-carbene ligands and their complexes have been synthesised. However, this field is still relatively new and the ligand design and its catalytic aspects have not yet reached full potential. Mixed phosphine-NHC ligand and its complexes were synthesised for study in this thesis.

2.1.3: Ligand Structure:

In principle, attaching an aryl ring directly to the imidazole ring will form a rigid chelating phosphine-carbene ligand, as illustrated in Figure 2.3, (A). In these structures, carbene and phosphine donors should work together in a bidentate fashion chelating the metal and forming a 6-membered chelate ring.

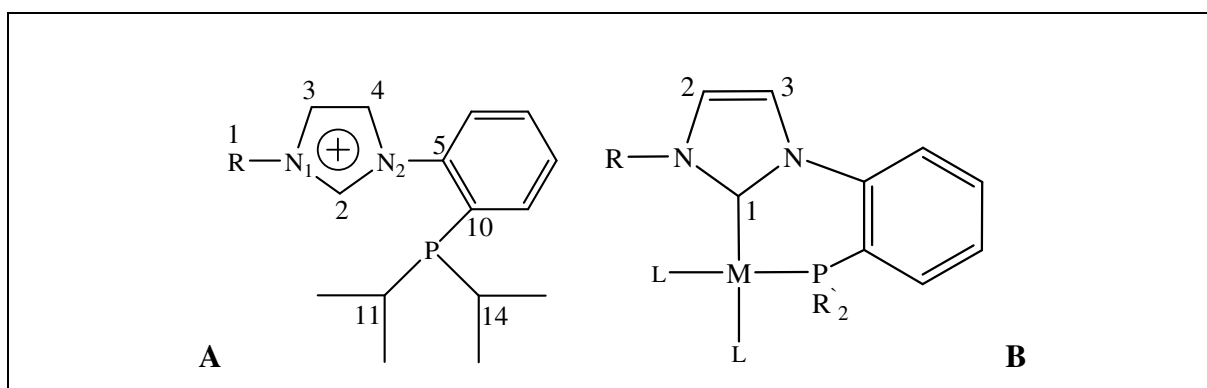


Figure 2.3: Illustration of a rigid chelating phosphine-carbene ligand and complex

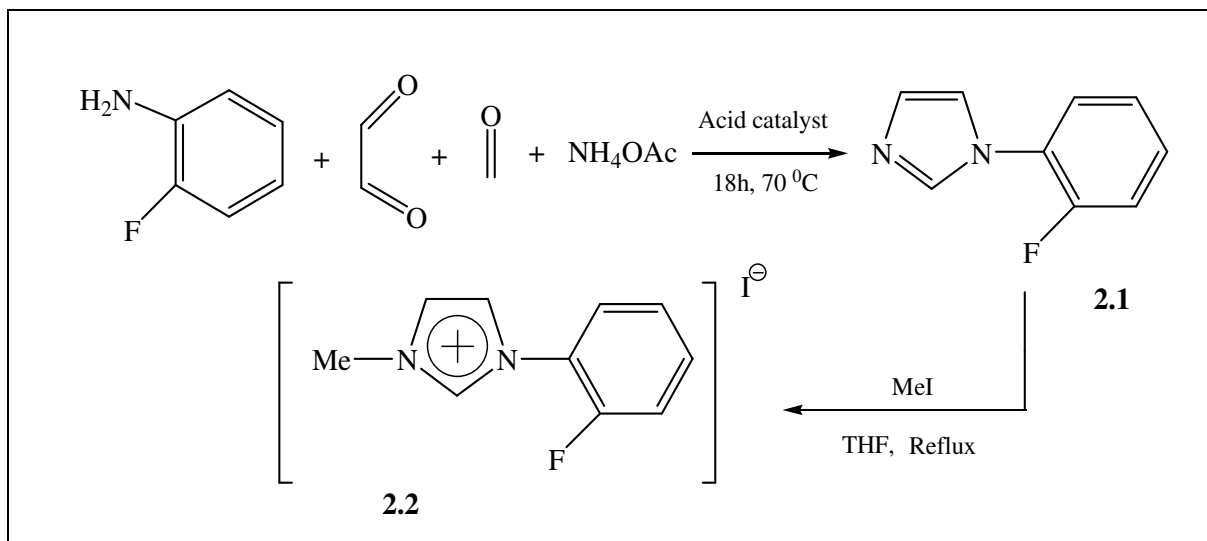
A prefix "*im*" is an abbreviation to denote the substituent's positions on the imidazole ring. As an example, (*im*C₂) refers to the carbon atom at the 2-position and *im*C₂-H to the hydrogen on that carbon atom of the imidazole ring. The letter "L" refers to the free ligand which is a phosphine-*N*-heterocyclic carbene (P-NHC) salt. In the crystal structures described herein, the labelling of C₂ will be for the carbene's carbon on ligand "L" and C₁ for the carbene's carbon of complexes of that ligand, the numbering Scheme adopted for the ligand and complexes are illustrated in Figures 2.3.

2.2: Results and discussion

2.2.1 Synthesis and characterisation of imidazolium salts (2.2)

The compound **2.1** was synthesised in moderate yields by using the acid catalysed reaction of 2-fluoroaniline, ammonium acetate, glyoxal and formaldehyde Scheme 2.2. The crude solid was washed with water and extracted into diethyl ether or hot hexane to produce the fluorinated-phenyl imidazole as a light brown oil, **2.1**.

The desired imidazolium salts, could be prepared by reacting the *N*-substituted 1-(2-fluorobenzene)imidazole with an appropriate alkyl halide. For this study, the *N*-substituted 1-(2-fluorobenzene)imidazole was reacted with methyl iodide and refluxed overnight in THF to give the corresponding imidazolium salt (1-fluorophenyl-3-methyl)imidazolium iodide, **2.2**, in almost quantitative yields. **2.2** was obtained as a tan solid which was moderately soluble in dichloromethane, but poorly soluble in ethers and hydrocarbons. Literature precedence indicates that alkylation with bulkier groups would also be possible enabling a more general synthetic route to be established.^{22a,b}



Scheme 2.2: Synthesis of compounds; imidazole **2.1** and imidazolium salt **2.2**

The imidazole ¹H NMR spectrum shows a resonance attributable to the _{im}C₂-H proton at 7.71 ppm. In the imidazolium salt **2.2** (carrying the *N*-methyl group), the ¹H NMR spectrum for the _{im}C₂-H proton is shifted downfield to 10.14 ppm. The protons of the *N*-methyl group appear as a singlet at 4.24 ppm. In the ¹³C{¹H} NMR spectrum, the _{im}C₂ carbon

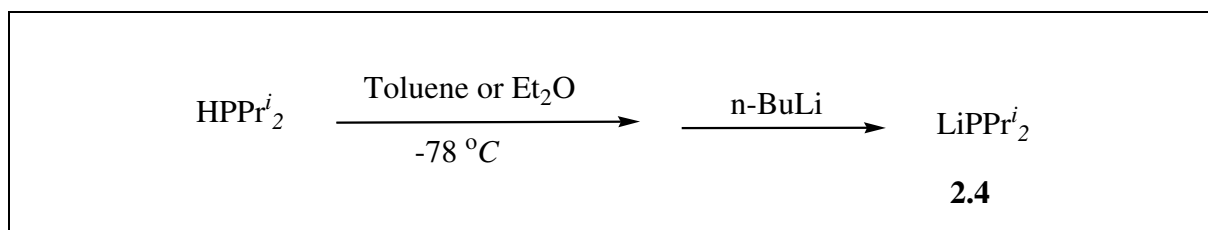
resonance appears at 137.0 ppm. The fluoride atom gives rise to a resonance at approximately -124 ppm in both ligands **2.1** and **2.2** in their $^{19}\text{F}\{^1\text{H}\}$ NMR spectra.

A halide exchange resin column was used to exchange the counter ion from iodide (I^-), of compound **2.2**, to chloride (Cl^-), compound **2.3**. A halogen test confirmed a complete exchange to the chloride counter ion.

2.2.2: Synthesis and characterisation of functionalised alkyl phosphine-imidazolium salt (2.5)

At the onset of this work, attempts to synthesise imidazole precursors and salts such as (**2.1**), and (**2.2**) had been unsuccessful. A key approach was based upon early observations in the nucleophilic displacement of fluoride from aryl-fluoro compounds by Edwards *et al.*,⁴ the fluoro-aryl moiety rather than other halide due to the fact that the fluorine-aryl bond is known to react more readily with potassium diarylphosphide than the bromine-aryl bond,^{23,24,25}

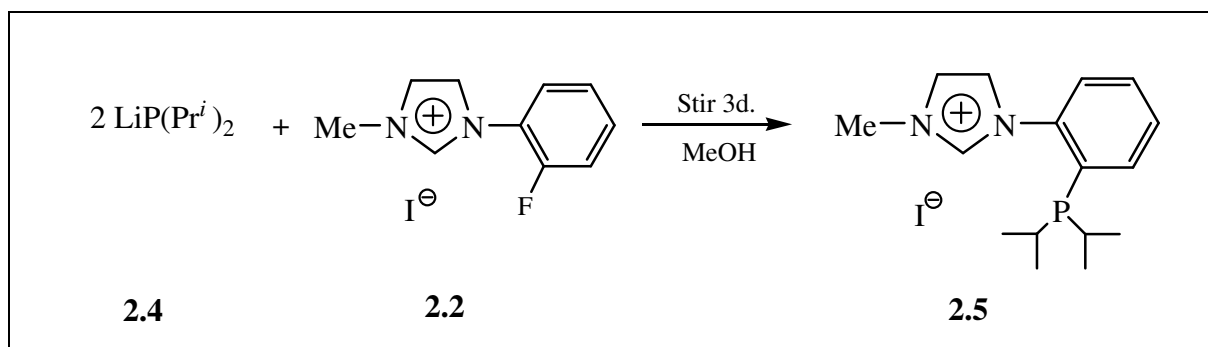
In order to substitute the fluoride with alkylphosphide, the latter moiety should undergo a lithiation step. To a solution of LiAlH_4 , chloro-diisopropylphosphine (ClPPr^i_2), was added drop-wise at room temperature to be left stirring overnight. The work-up was modified from literature¹⁷ such that addition of distilled water, quenching LiAlH_4 by NaOH , and stirring with drying agent. The corresponding diisopropylphosphine, HPPr^i_2 , was collected by distillation at boiling point at $118\text{ }^\circ\text{C}$ showing ^{31}P NMR at -15.3 ppm . HPPr^i_2 was then reacted with a strong base, $n\text{-BuLi}$, in order to form lithium diisopropylphosphide, LiPPr^i_2 , a better liberated cation to react with the fluoride in the fluorinated phenyl-imidazolium salt, **2.2** or **2.3**. The reaction was carried out in toluene and stirred for about 3-4 days. A white precipitate **2.4**, Scheme 2.3, formed which was very air sensitive. Its ^{31}P NMR spectrum shows the absence of P-H coupling and a resonance at -1.5 ppm (in toluene) or at -18.4 ppm (in Et_2O).



Scheme 2.3: Preparation of lithium diisopropylphosphide **2.4**

This lithiated diisopropylphosphide **2.4** in toluene was added to a solution of the fluorinated phenyl-imidazolium salt **2.2** or **2.3** at $0\text{ }^\circ\text{C}$. During the course of 3 days reaction between **2.2**

or **2.3** and lithium diisopropylphosphide, the reaction changed from orange to light brown colour, as the lithium diisopropylphosphide was consumed. The solvent was removed under vacuum and MeOH added to quench any unreacted LiPPr^i_2 . HPPr^i_2 and any excess of MeOH was then removed under vacuum. Degassed water was added to the crude mixture to dissolve the alkyl phosphinated imidazolium salt which was then extracted into dichloromethane. The volume of DCM extract was reduced under vacuum. Diethyl ether was added to give a precipitate that was washed with a large volume of Et_2O to give the desired phosphine-imidazolium salt **2.5** or **2.6** as a pale brown solid, Scheme 2.4. The reaction was first carried out in different solvents such as THF, Et_2O , DME, and liquid NH_3 in the same way described for the synthesis of lithium diisopropylphosphide and ligand **2.5** or **2.6**. However, it was found that a higher isolated yield with less impurity was obtained when toluene was used as the solvent. This may be due to the fact that toluene is behaving as a poorer solvent for the lithium salt metathesis product, as well as being less reactive to the lithium phosphide precursor than other solvents. Regardless of the rationalisation, the work-up is cleaner and simpler.



Scheme 2.4: Synthesis of diisopropylphosphine imidazolium salt **2.5**

The product was fully characterised by ^1H , $^{13}\text{C}\{^1\text{H}\}$, $^{31}\text{P}\{^1\text{H}\}$ NMR spectroscopy, high resolution mass spectrometry, and elemental analysis. In the ^1H NMR spectrum, in CDCl_3 , the $_{\text{im}}\text{C}_2\text{-H}$ proton was observed at 9.62 ppm, the $_{\text{im}}\text{N}_1\text{-CH}_3$ protons appeared at 4.25 ppm and protons of diisopropyl appears at 0.84 ppm as doublet-of-doublets, Figure 2.4. Protons of the aromatic groups, phenyl and imidazolium rings appear in the range of 7.84-7.27 ppm.

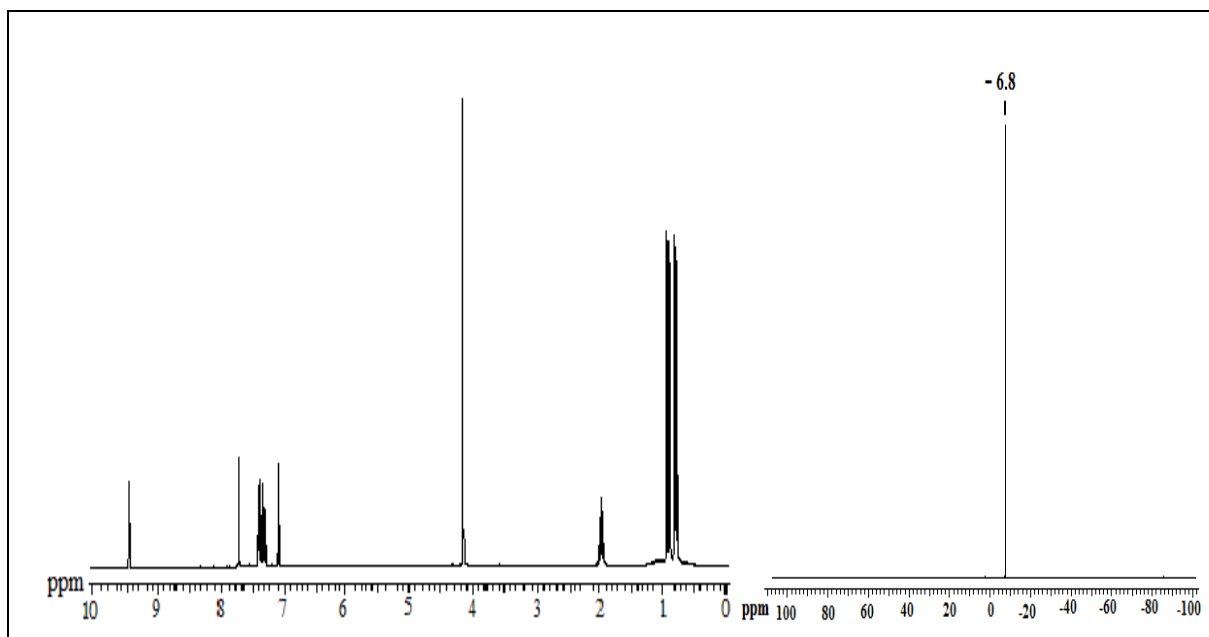


Figure 2.4: ^1H -NMR and $^{31}\text{P}\{^1\text{H}\}$ -NMR spectra, in CDCl_3 , of ligand **2.5**

A singlet resonance peak was observed in the $^{31}\text{P}\{^1\text{H}\}$ -NMR spectrum at -6.8 ppm, in CDCl_3 , which corresponds to the free phosphine ligand, Figure 2.5. This chemical shift value is up-field of that of PPr^i_3 ($\delta = 21$ ppm) and somewhat down-field of that of LiPr^i_2 ($\delta = -18.4$ ppm). Recent related compounds with *ortho*-substituents to the phosphine reported by Fryzuk *et al.*²⁶ show a shift value at (-6.4 ppm) in their ^{31}P -NMR spectra compared to compound **2.5**.

The imC_2 carbon appeared as singlet at 137.4 ppm in the ^{13}C -NMR spectrum, in CDCl_3 . A mass of 402.3 in the mass spectrum corresponds to the molecular ion and elemental analysis of the ligand is consistent with calculated values validating the formulation.

Crystals suitable for a single crystal X-ray crystallographic determination were obtained upon concentrating a solution of **2.5** in DCM at 5 °C. The crystal structure and labelling Scheme for **2.5** is shown in Figure 2.5 (Appendix: Data set 1). The imidazolium proton is orientated in a different direction to the phosphine lone pair with a distance of 3.343(3) Å, probably because of electrostatic repulsion in that region. The imC_2 -H proton does not interact with the iodine ion, $\text{H}(2)\text{-I} = 2.911(5)$ Å, or with any other atom. The average P-C bond length (1.866 Å) is of a similar average value compared to triisopropylphosphine²⁷ (1.862(9) Å) and differs slightly in comparison to the related ligand bearing two P-phenyl groups (which is (1.833 Å)⁴ rather than P-diisopropyl groups in our ligand, **2.5**. The average C-P-C bond angle in **2.5** (100.6(6)°) shows small differences (of about 3 degrees) from that in triisopropylphosphine²⁷ and (1.5 degrees) than in the diphenylphosphine imidazolium salt.⁴

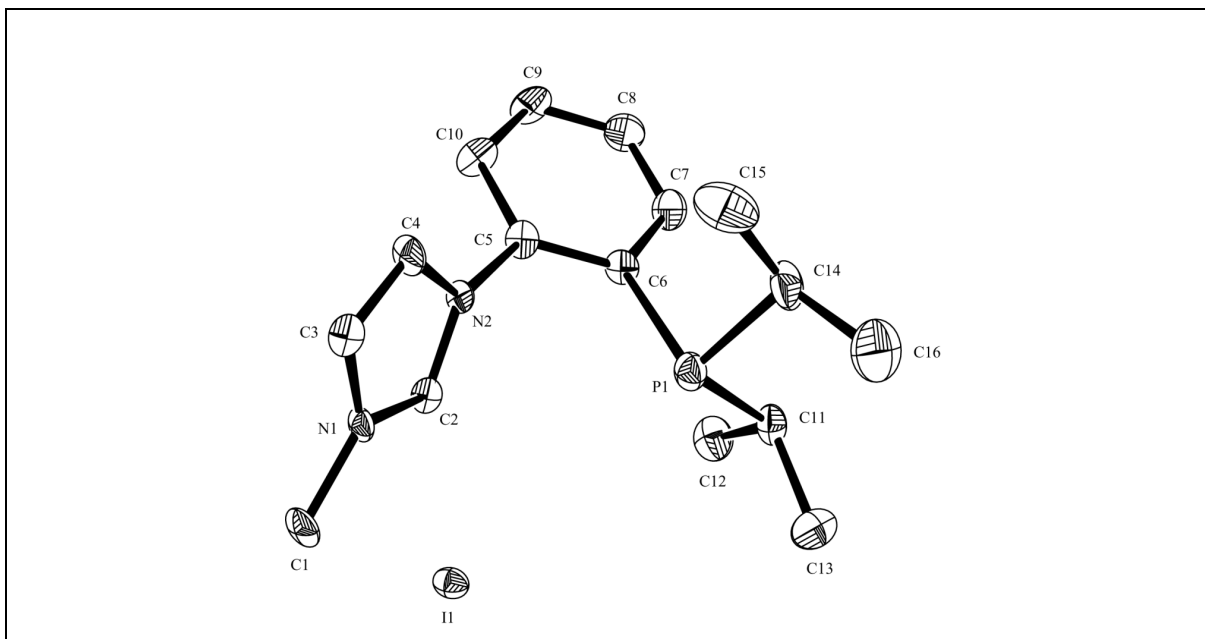


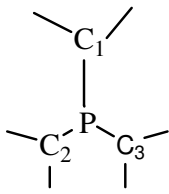
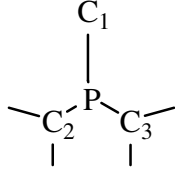
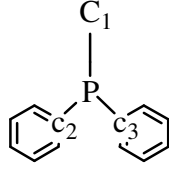
Figure 2.5: Molecular structure of compound **2.5**, ORTEP projection, 40% probability ellipsoids, in CD_2Cl_2 , hydrogen atoms are omitted for clarity. (Appendix: Data Set 1)

Table 2.1: Some selected bond lengths (\AA) and angles (degrees) for imidazolium salt **2.5**.

Bond Lengths(\AA)				Bond Angles ($^\circ$)	
C(2)-N(1)	1.313(7)	C(5)-N(2)	1.428(7)	N(1)-C(2)-N(2)	109.6(5)
C(2)-N(2)	1.341(7)	C(1)-N(1)	1.460(7)	C(2)-N(2)-C(5)	126.7(5)
C(3)-N(1)	1.388(8)	C(10)-P(1)	1.862(6)	C(2)-N(1)-C(1)	125.3(5)
C(4)-N(2)	1.387(7)	C(11)-P(1)	1.871(7)	C(10)-P(1)-C(11)	102.7(3)
C(3)-C(4)	1.334(8)	C(14)-P(1)	1.863(7)	C(10)-P(1)-C(14)	97.1(3)
				C(11)-P(1)-C(14)	102.1(3)

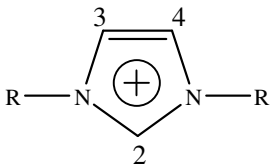
Some selected bond lengths and angles are collected in Table 2.1. Table 2.2 lists a comparison of bond lengths and angles between the diisopropylphosphine imidazolium salt **2.5**., its diphenylphosphine imidazolium salt analogue⁴ and triisopropylphosphine.²⁷

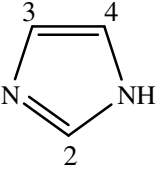
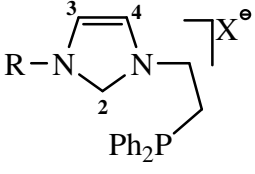
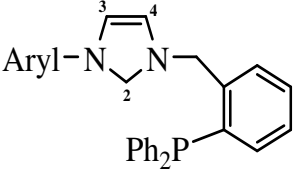
Table 2.2: Comparison of bonds and angles

Bond Lengths & Angles			
C ₁ -P	1.856(3)	1.862(6)	1.841(3)
C ₂ -P	1.860(3)	1.863(7)	1.835(3)
C ₃ -P	1.872(3)	1.871(7)	1.823(4)
C ₁ -P-C ₂	102.0(1)	97.1(3)	99.43(15)
C ₁ -P-C ₃	102.9(1)	102.7(3)	102.52(15)
C ₂ -P-C ₃	104.7(1)	102.1(3)	104.62(16)

Crystallography data shows that C₂-N₁ (1.313(7)) is shorter than C₂-N₂ (1.341(7)), which indicates lack of charge delocalization. One N_{imidazole} atom is positively charged and the carbene proton (C₂-H) is highly deshielded as shown in ¹H-NMR. A comparison of ¹H chemical shift of the ligand **2.5** with those of other related compounds is listed in Table 2.3.

Table 2.3: Comparison of ¹H-NMR of **2.5** and other compounds

NMR-Peaks, ppm Structure	C ₂ -H	C ₃ -H	C ₄ -H
 2.5	9.62	7.58	7.27

 Abraham ²⁹	7.74	7.13	7.13
 Lee ³⁰	9.60	8.19	7.92
 Zhou ¹⁵	10.88	8.11	7.46

2.2.3: Synthesis and characterisation of functionalised alkyl phosphine-imidazolium salt (2.6)

For the ligand **2.6**, Figure 2.6, an analogous procedure to that described for the synthesis of **2.5** above was followed for the synthesis of phosphine-imidazolium salt **2.6**, except that **2.3** was used where the counter ion of the fluorinated phenyl-imidazolium salt is chloride (Cl^-) instead of iodide as in **2.2**. The ligand was isolated as a pale brown solid. The product was fully characterised including MS and elemental analysis. The characteristic NMR peaks in CDCl_3 were observed at the same positions as in **2.5**.

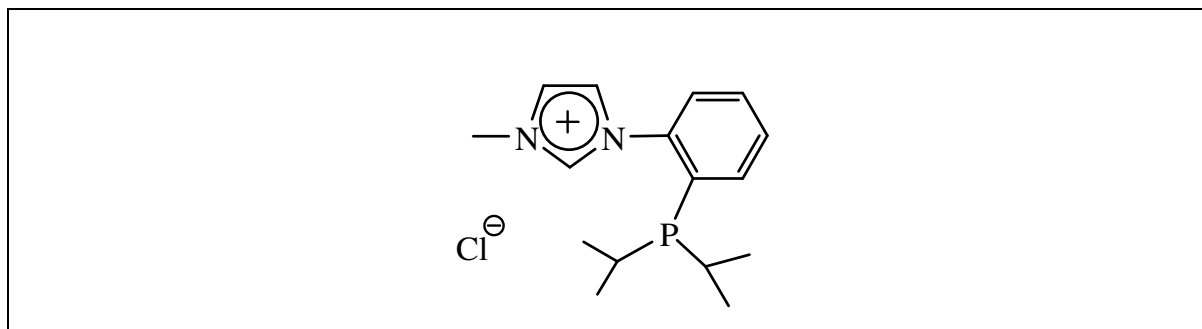


Figure 2.6: Ligand of **2.6**

2.2.4: Synthesis and characterisation of functionalised alkyl phosphine-imidazolium salt (2.7)

Initial trials to synthesise the salt **2.5** using THF as a solvent led to the synthesis and crystallization process of phosphine-imidazolium salt **2.7**, Figure 2.7. An analogous process to that described for the synthesis of **2.5** above was followed until the 18h stirring finished. The supernatant was transferred to another Schlenk and the solvent was concentrated. Drops of Et₂O were added to the solution and kept in freezer for crystallization at -35 °C. In the presence of a base during extended reaction times, a by-product was identified and characterised spectroscopically and by X-ray crystallography. A 2-hydroxyethyl substituent has been incorporated into the imidazole ring. Although its formation is currently speculative, this material in which the unique imidazole carbon has been alkylated is probably formed by the attack of the free carbene on THF. The ligand was isolated in poor yield as a pale brown solid. The product was again characterised by ¹H- and ³¹P{¹H} NMR spectroscopy, high resolution mass spectrometry, and X-ray crystallography.

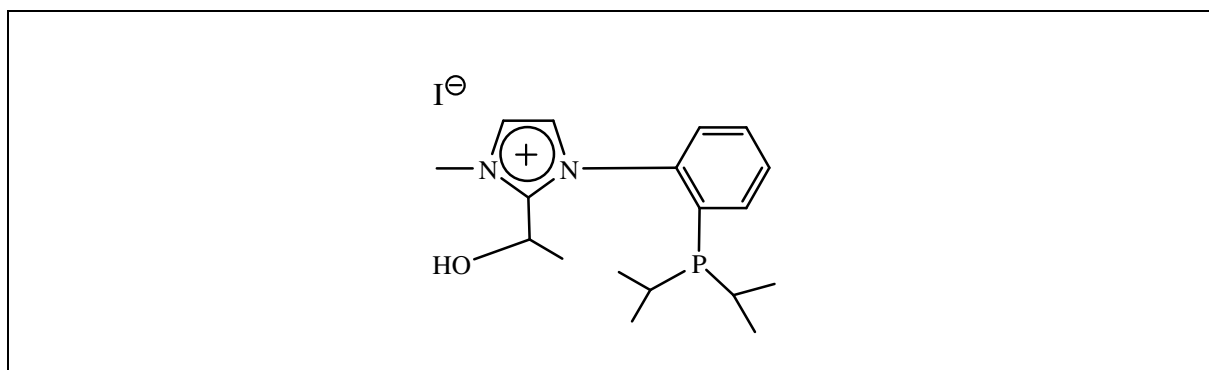


Figure 2.7: Ligand of **2.7**

The characteristic peak of the imidazolium-carbene proton in CDCl₃ was not observed in the ¹H-NMR spectrum indicating its absence in **2.7**. X-ray crystallography confirmed the presence of an alcohol group in this position in its place, Figure 2.8. A resonance at 5.35 ppm in the ¹H-NMR spectrum may be assigned to the alcohol proton, the _{im}N₁-CH₃ protons appeared at 4.25 ppm and protons of the isopropyl groups appear at 0.96 and 0.84 ppm as a doublet-of-doublets. A singlet was observed in the ³¹P{¹H}-NMR spectrum at -9.4 ppm in CDCl₃, which corresponds to the uncoordinated phosphine, Figure 2.8. This chemical shift is closer to that of ligand **2.5** as would be expected. A mass of 318.3 in the mass spectrum corresponds to the molecular ion and validates the formulation.

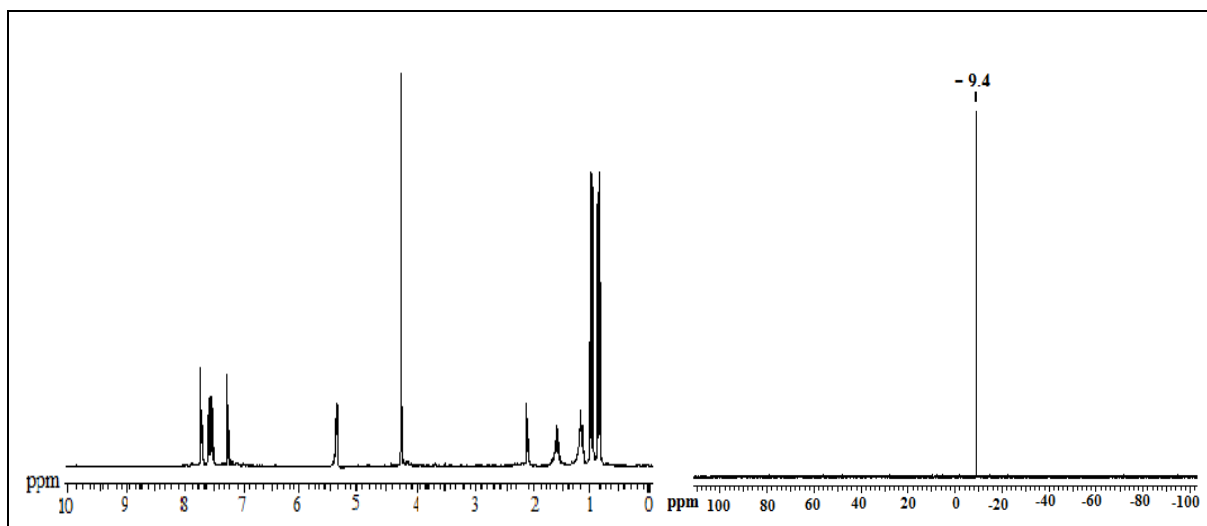


Figure 2.8: ^1H -NMR and $^{31}\text{P}\{^1\text{H}\}$ -NMR spectra, in CDCl_3 , of ligand **2.7**

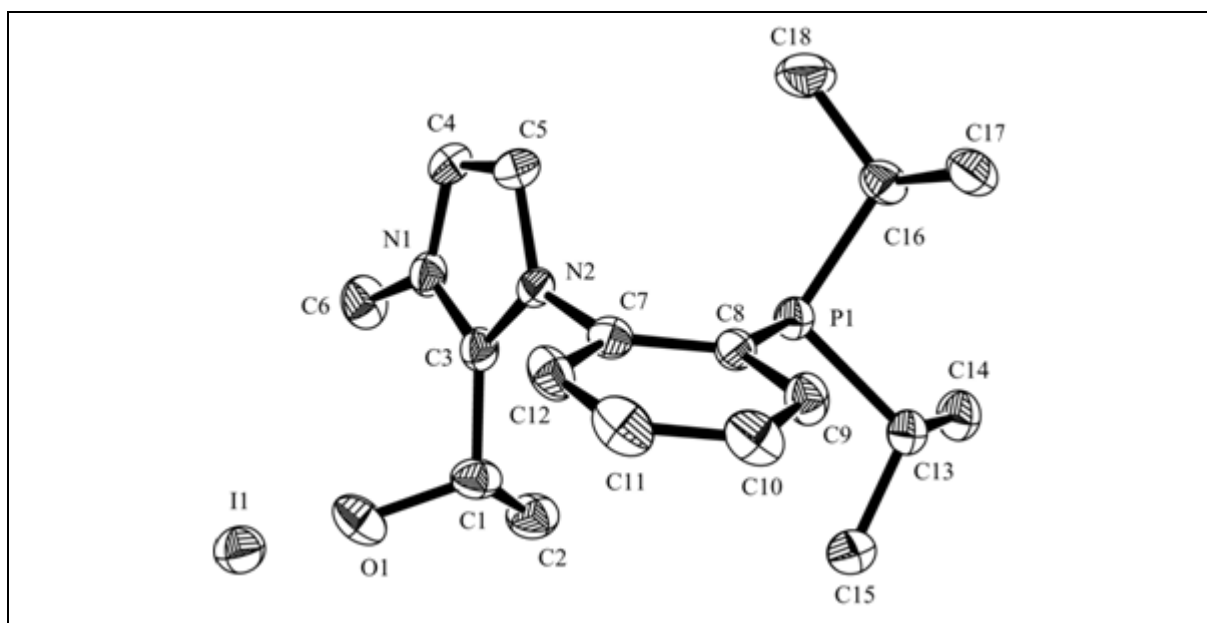


Figure 2.9: ORTEP projection of compound **2.7**, in CDCl_3 . Hydrogen atoms are omitted for clarity (Appendix: Data Set 2)

Crystals suitable for a single crystal X-ray crystallographic determination were obtained upon concentrating a solution of **2.7** by layering THF / Et_2O at $-35\text{ }^\circ\text{C}$. The crystal structure and labelling Scheme for **2.7** is shown in Figure 2.9, which shows a view through the plane of the central benzene ring. It appears that the oxygen of the alcohol group on the imidazole ring is orientated in a different direction to the phosphine lone pair with a distance

of 5.523(0) Å, probably because of the electrostatic repulsion between the two lone pairs of both atoms. Selected bond lengths and angles are collected in Table 2.4 (Appendix: Data 2).

Table 2.4: Some selected bond lengths (Å) and angles (degrees) for imidazolium salt **2.5**

Bond Lengths(Å)				Bond Angles (°)	
C(3)-N(1)	1.342(4)	O(1)-C(1)	1.426(4)	N(1)-C(3)-N(2)	107.5(3)
C(3)-N(2)	1.343(4)	C(6)-N(1)	1.470(4)	N(1)-C(3)-C(1)	127.4(3)
C(3)-C(1)	1.499(5)	C(8)-P(1)	1.839(3)	N(2)-C(3)-C(1)	125.1(3)
C(4)-N(1)	1.374(4)	C(13)-P(1)	1.863(3)	C(8)-P(1)-C(13)	101.8(4)
C(5)-N(2)	1.380(4)	C(16)-P(1)	1.869(4)	C(8)-P(1)-C(16)	104.1(3)
				C(13)-P(1)-C(16)	102.4(7)

The study of the coordination and reaction chemistry of the phosphine-imidazolium salts **2.5** or **2.6** with metal precursors, and the assessment of their complexes is a primary purpose of this research.

2.3 Conclusion

An imidazolium salt which combines an imidazolium moiety with an *N*-methyl group and an *N*-functional group side arm, have been synthesised and characterised as a precursor to the corresponding phosphine-NHC ligands. Phosphine-imidazolium derivatives have been formed (**2.5**) as well as another analogous salt with an alcohol group attached to the carbene position (**2.7**). The precursor **2.5** has its donor atoms organised in a manner suitable for complex formation with metal precursors and bidentate binding by carbene and phosphine sigma donors. All compounds were characterised by spectroscopic means, including ¹H, ¹³C and ³¹P-NMR spectroscopies, mass spectrometry and in some cases elemental analysis. Crystallographic determinations were obtained for the phosphine-imidazolium salts, **2.5** and **2.7**.

2.4: Experimental

2.4.1: General comments and materials:

All reactions and subsequent manipulations were carried out using standard Schlenk techniques under an atmosphere of dry argon or nitrogen. Solvents such as tetrahydrofuran (THF), diethyl ether (Et₂O), and *n*-hexane were dried and degassed by refluxing under nitrogen over sodium benzophenone ketyl. Dichloromethane (DCM), ethanol (EtOH), and methanol (MeOH) were pre-dried over 3Å molecular sieves and subsequently refluxed over calcium hydride under nitrogen. Dimethoxyethane (DME) and toluene were initially refluxed over sodium and distilled under nitrogen before use. All other anhydrous solvents were obtained by distillation from the appropriate drying agents under nitrogen. Deoxygenation of solvents and reagents was carried out by routine air-free techniques (freeze- thaw cycles). Water was deoxygenated by boiling under a purge of nitrogen and cooling to room temperature under nitrogen. Deuterated NMR solvents (CDCl₃) were purchased from Aldrich or Fisher. All reagents were purchased from commercial sources and used without further purification, unless otherwise stated. Air sensitive compounds and deuterated solvents were degassed or dried (3Å molecular sieves) then stored in Young's Schlenks. Glassware and transfer tubes, cannula etc. were stored at 120 °C prior to use. HPPr₂^{*i* 28a,b} and LiPPr₂^{*i* 17} were prepared as detailed in the literature.

All ¹H, ¹³C and ³¹P NMR data are given in δ / ppm. The ³¹P-NMR spectra (referenced to external 85% H₃PO₄, δ = 0 ppm) were measured on a Jeol Lamda Eclipse 300 MHz and a Bruker DPX500 spectrometer operating at 121.7 and 202.5 MHz respectively. ¹⁹F chemical shifts were recorded on Jeol Lamda Eclipse 300 at 282.78 MHz. ¹H and ¹³C spectra (referenced to residual solvent resonances) were recorded on a Bruker DPX400 Avance (operating at 400.8 MHz(¹H) and 100 MHz (¹³C)) and a Bruker DPX500 (operating at 500.13 MHz (¹H) and 125.75 MHz (¹³C)) spectrometers referenced to SiMe₄ (δ = 0 ppm). *J* values were measured in Hz and peak multiplicities are expressed by the usual conventions (s=singlet, d=doublet, t=triplet, m=multiplet, br=broad). Electrospray mass spectrometry (ESMS) was performed on a Waters LCT Premier XE or Waters micromass ZQ instrument. Elemental analyses were performed by MEDAC LTD, UK. Infrared spectra were measured either in solution or in KBr disks on Nicolet 510 FT-IR and JASCO 660 FT-IR spectrophotometers. A glove-box was used for transferring and weighing air sensitive reagents and compounds. Crystal data were obtained on a Bruker Nonius Kappa CCD

diffractometer using graphite monochromatised MoK α radiation, $\lambda = 0.71073\text{\AA}$ equipped with an Oxford Cryostream cooling apparatus.

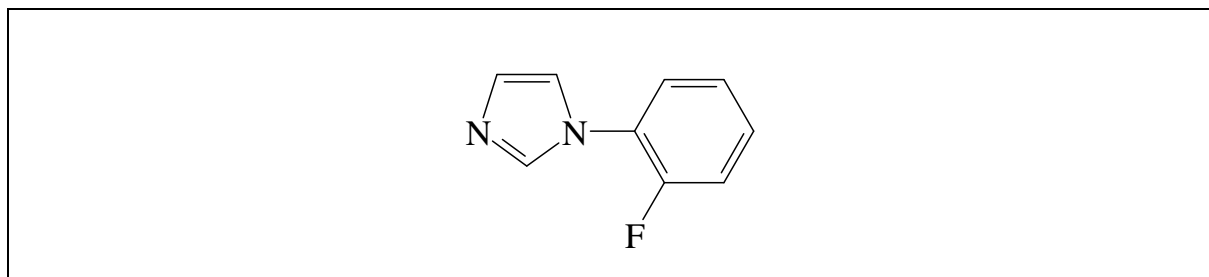
2.4.2 Preparation of compounds:

The following compounds were prepared by modification of a literature recipe:

1-(2-Fluorobenzene)imidazole (**2.1**)^{4,21}

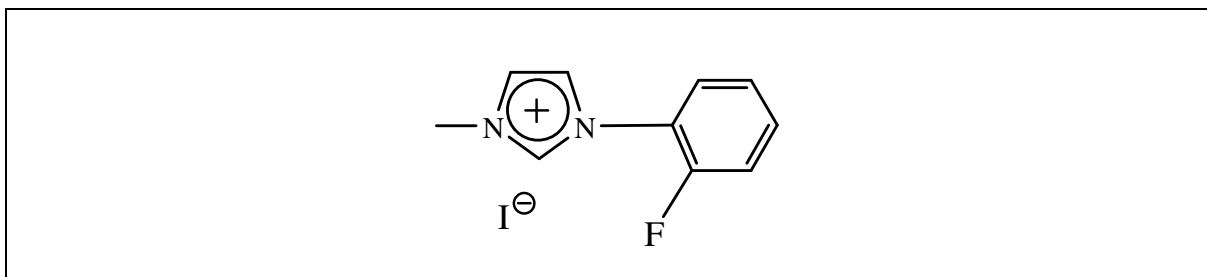
(1-Fluorobenzene-3-methyl)imidazolium iodide (**2.2**)^{4,21}

Preparation of 1-(2-fluorobenzene)imidazole (**2.1**):



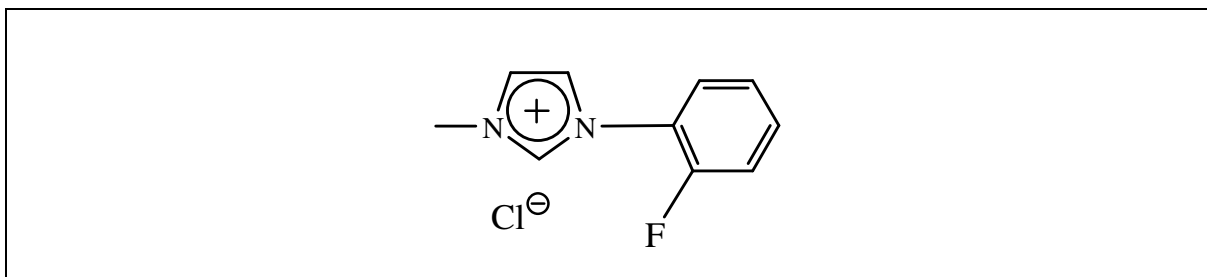
A mixture of formaldehyde (10.7 ml of 37 % solⁿ, 0.143 mol), glyoxal (16.4 ml of 40 % solⁿ, 0.143 mol) and glacial acetic acid (35 ml) was heated to 70 °C. To the hot solution was added drop-wise, with stirring, over a period of 3 h. a solution of NH₄OAc (11.0 g, 0.143 mol) and 2-fluoroaniline (13.8 ml, 0.143 mmol) in H₂O (6 ml) and glacial acetic acid (30 ml). The solution, which rapidly became orange/red, was stirred for 12 h. The solution was cooled to ambient temperature, then added drop-wise with stirring to a suspension of NaHCO₃ (151.00 g, 1.80 mol in H₂O (1 L). The solution was made alkaline to pH 9 with NaOH, and the resultant solid was then filtered off on a Buchner funnel and washed with H₂O (3 x 50 ml) before being dried by suction on the frit. The dry solid was extracted with hot hexane (6 x 200 ml) and filtered. The solvent was removed under vacuum to give the product as a yellow oil. Yield (9.11 g, 40 %). ¹H NMR (400.13 MHz, CDCl₃): 7.71 (s, 1H, _{im}H₁), 7.20 (s, 1H, _{im}H₂), 7.13 (s, 1H, _{im}H₃), 7.33-7.12 (m, 4H, _{Ar}H).

(1-fluorobenzene-3-methyl)imidazolium iodide (2.2):



A mixture of 1-(2-fluorobenzene)imidazole (**2.1**) (4.50 g, 27.7 mmol) and iodomethane (11.8 g, 83.3 mmol) in THF (40 ml) was gently refluxed for 12h. During the reaction a pale yellow solid was formed. The solid was collected by filtration, washed with several portions of THF, and dried under vacuum to give the product as an off-white solid. Yield (8.18 g, 97%). ¹H NMR (400.13 MHz, CDCl₃, δ): 10.14 (s, 1H, _{im}H₁), 7.95 (s, 1H, _{im}H_{2/3}), 7.90 (t, J = 7.8 Hz, 1H, _{Ar}H), 7.62 (s, 1H, _{im}H_{2/3}), 7.50 (m, 1H, _{Ar}H), 7.35-7.22 (m, 2H, _{Ar}H), 4.24 (s, 3H, Me). ¹³C NMR (100 MHz, CDCl₃, δ): 155.82 (s, C), 153.3 (s, C), 137.0 (s, CH), 132.4 (d, J=8, CH), 126.2 (d, J=5, CH), 124.7 (s, CH), 122.7 (d, J=4, CH), 122.3 (d, J=11, CH), 117.6 (d, J=19, CH), 37.9 (s, Me). MS (ES+), M/z: 177.1 [M]⁺. ¹⁹F NMR (282.78 MHz, CDCl₃, δ): -124

(1-fluorobenzene-3-methyl)imidazolium chloride (2.3):



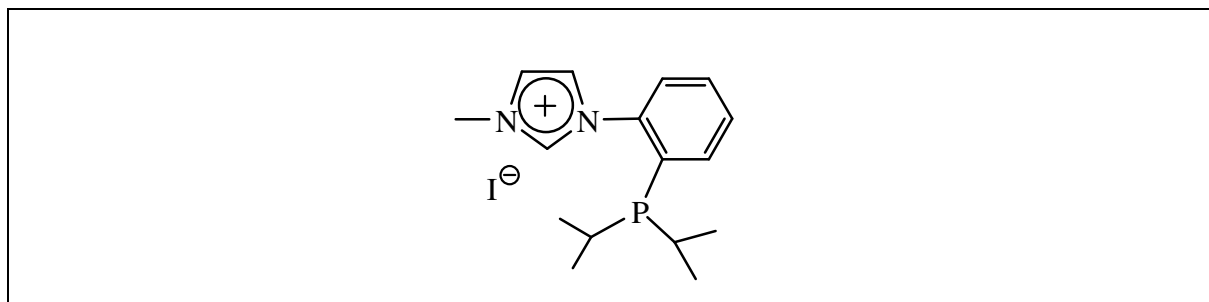
Dissolving the off-white (1-Fluorobenzene-3-methyl)imidazolium iodide (**2.2**) in MeOH and then passing it once through a Cl⁻-exchange resin column to ensure complete conversion of the counter ion from iodide to chloride.

Preparation of Lithium diisopropylphosphide [LiP(Prⁱ)₂] (2.4):

Diisopropylphosphine HPPr₂ⁱ (0.48 g, 4.04 mmol) was deprotonated by *n*-BuLi

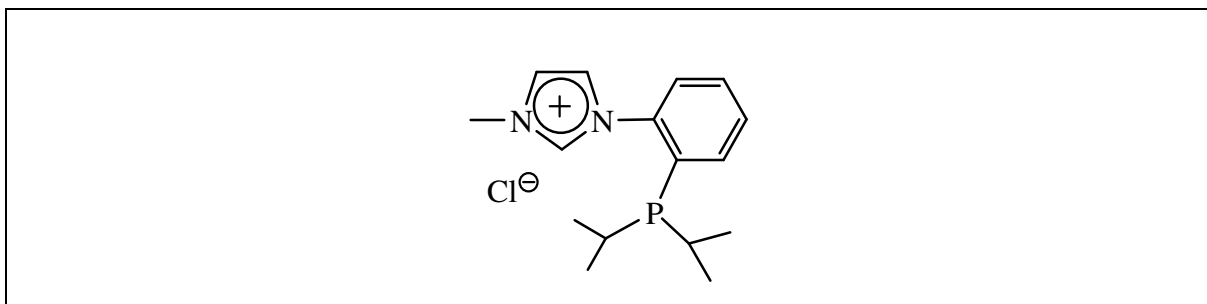
(1.93M, 2.11 ml, 4.04 mmol) in toluene or diethylether (40 ml) at -78 °C and stirring for about 3-4 days would give a white precipitate. Solvent then decanted and the solid was washed twice by toluene. It resulted in a high yield air sensitive white compound which was kept in a Schlenk in a glove box. A ^{31}P -NMR peak shows at -18.4 (in Et_2O).

1-Benzene-o-diisopropylphosphine-3-methylimidazolium iodide (2.5):



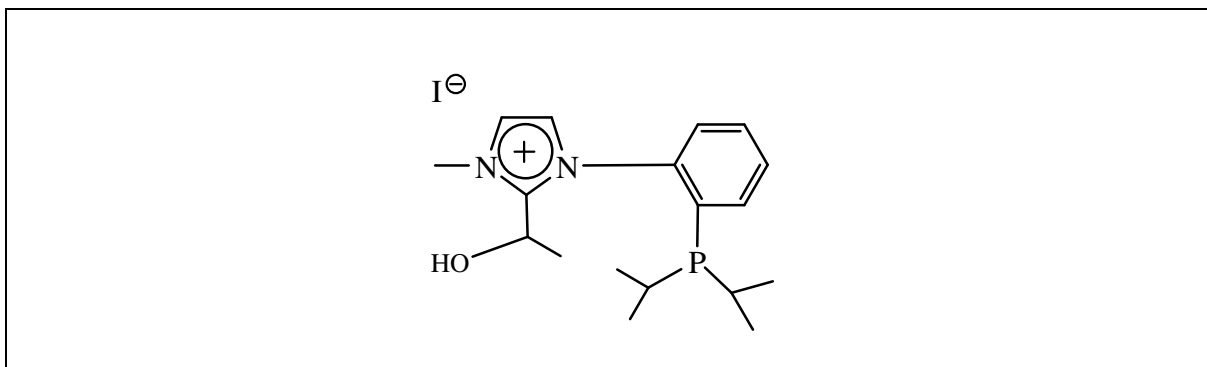
To (1-fluorobenzene-3-methyl)imidazolium iodide (**2.2**) (1.23 g, 4.04 mmol) in toluene (40 ml) at 0 °C, as a ratio of 1:1, was added 1mol equivalent of $\text{LiP}(\text{Pr}^i)_2$, and allowed to stir for 2-3 days at room temperature. The solution gave a graduate change in colour from tan to orange. The solvent was then decanted and removed under vacuum to give a light brown solid. Methanol (2 ml) was added to quench excess phosphide [$\text{LiP}(\text{Pr}^i)_2$]; the methanol and any excess $\text{HP}(\text{Pr}^i)_2$ were then removed under vacuum. Degassed water was added to the residue and the free ligand extracted into DCM (3 x 10ml). The volume of the DCM was removed *in vacuo* to give the product as an orange-brown precipitate. The solid was washed with Et_2O (3 x 10ml) and then EtOH was added to assist in the removal of water traces leaving the product as a pale brown solid. Single crystals were obtained upon concentrating a solution of **2.5** in DCM at 5 °C. Yield (0.1 g, 5%). ^1H NMR (500 MHz, CDCl_3 , δ): 9.62 (s, 1H, imH_2), 7.84 (s, 1H, $\text{imH}_{3/4}$), 7.58 (m, 4H, H_{Ar}), 7.27 (s, 1H, $\text{imH}_{3/4}$), 4.25 (s, 3H, Me), 2.01 (m, 2H, $\text{H}_{11/14}$), 0.96 (dd, 6H, $J=7.0, 16.0$ Hz, CH_3), 0.84 (dd, 6H, $J=7.0, 12.4$ Hz, CH_3). ^{13}C NMR (125.75 MHz, CDCl_3 , δ): 140.4 (d, $J=23.75$, C), 137.4 (s, CH), 134.0 (d, $J=3.75$, CH), 133.5 (d, $J=28.75$, C), 130.9 (d, $J=41.25$, CH), 127.2 (d, $J=2.5$, CH), 124.4 (d, $J=3.75$, CH), 123.8 (s, CH), 37.8 (s, Me), 24.2 (d, $J=11.25$, CH), 20.1 (d, $J=18.75$, CH_3), 19.9 (d, $J=8.75$, CH_3). ^{31}P NMR (121.7 MHz, CDCl_3 , δ): -6.8. MS (ES+), M/z : 274.3 $[\text{M}]^+$. Elemental Analysis: $\text{C}_{16}\text{H}_{24}\text{N}_2\text{PI}$, Calculated: C: 47.77; H: 6.01; N: 6.96; Found: C: 47.3; H: 6.0; N, 6.8.

(1-Benzene-*o*-diisopropylphosphine-3-methyl)imidazolium chloride (2.6):



2.6 was prepared following the same procedure used for the preparation of compound **(2.5)** except that the precursor (1-fluorobenzene-3-methyl)imidazolium chloride **(2.3)** was used instead of (1-fluorobenzene-3-methyl)imidazolium iodide **(2.2)**.

(1-Benzene-*o*-diphenylphosphine-2-(propan-2-ol)-3-methyl) imidazolium iodide (2.7):



2.7 was prepared following the same procedure as for **2.5**, except that THF was used as the reaction solvent and for crystallization. After 18h stirring, the supernatant was filtered and concentrated *in vacuo*. Drops of Et₂O were added by slow diffusion to the tetrahydrofuran (THF) solution to achieve saturation, and the resulting solution was cooled (- 35 °C) to give **2.7** which was isolated in poor yield as a pale brown crystalline solid. ¹H NMR (400 MHz, CDCl₃, δ): 7.84 (s, 1H, _{im}H_{4/5}), 7.58 (m, 4H, H_{Ar}), 7.27 (s, 1H, _{im}H_{4/5}), 5.35 (s, 1H, OH), 4.25 (s, 3H, Me), 2.01 (m, 2H, H_{13/16}), 1.55 (m, 1H, H₁), 1.10 (m, 3H, CH₃), 0.96 (dd, 6H, J=7.0, 16.0 Hz, CH₃), 0.84 (dd, 6H, J=7.0, 12.4 Hz, CH₃). ³¹P-NMR (121.7 MHz, CDCl₃, δ): -9.4. MS (ES+), M/z: 318.3 [M]⁺.

References

- [1] A. Kiyomori, J. F. Marcoux, S. L. Buchwald, *Tetrahedron Lett.*, **1999**, 40, 2657.
- [2] J. Åhman, S. L. Buchwald, *Tetrahedron Lett.*, **1997**, 38, 6363.
- [3] G. Mann, J. F. Hartwig, M. S. Driver, C. Fernández-Rivas, *J. Am. Chem. Soc.*, **1998**, 122, 827.
- [4] R. Lane, *PhD Thesis*, University of Wales- Cardiff, **2005**
- [5] P. Fournari, P. deCointet, E. Laviron, *Bull. Soc. Chim. Fr.*, **1968**, 2438.
- [6] A. A. Gridnev, I. M. Mihaltseia, *Synth. Commun.*, **1994**, 24, 1547.
- [7] A. J. Arduengo III, F. P. Gentry, P. K. Taverkine, H. E. Simmons, US Pat. 6177575, **2001**.
- [8] A. W. Waltman, R. H. Grubbs, *Organometallics*, **2004**, 23, 3105.
- [9] W. A. Herrmann, C. Köcher, L. J. Gooßen, G. R. J. Artus, *Chem. Eur. J.*, **1996**, 2, 12.
- [10] D. S. McGuiness, N. Saendif, B. Yates, K. J. Cavell, *J. Am. Chem. Soc.* **2001**, 123, 4029.
- [11] A. Pidcock, R. E. Richards, L. M. Venanzi, *J. Chem. Soc. A.* **1966**, 1707.
- [12] a. C. Yang, H. M. Lee, S. P. Nolan, *Org. Lett.*, **2001**, 3, 1511.
b. A. A. D. Tulloch, A. A. Danopoulos, J. G. Tizzard, S. J. Close, M. B. Hursthouse, R. S. Hay-Motherwell, W. B. Motherwell, *Chem. Commun.*, **2001**, 14, 1270.
- [13] N. Tsoureas, A. A. Danopoulos, A. A. D. Tulloch, M. E. Light, *Organometallics*, **2003**, 22, 4750.
- [14] E. Bappert, G. Helmchen, Synlett **2004**, 10, 1789.
- [15] A. E. Wang, J. Zhonz, J. H. Xie, K. Li, Q. L. Zhou, *Adv. Synth. Catal.*, **2004**, 346, 595.
- [16] A. E. Wang, J. H. Xie, L. X. Wang, Q. L. Zhou, *Tetrahedron Lett.*, **2005**, 61, 259.
- [17] K. Issleib, F. Krech, *J. Organomet. Chem.*, **1968**, 12, 283.
- [18] H. Lang, J. J. Vittal, P. H. Leung, *J. Chem. Soc., Dalton Trans.* **1998**, 2109.
- [19] W. A. Herrmann, V. P. Bohm, C. W. Gstottmayr, M. Grosche, C. P. Reisinger, T. Weskamp, *J. Organomet. Chem.*, **2001**, 617, 616.
- [20] S. P. Nolan, G. A. Grasa, M. S. Viciu, J. Huang, *J. Org. Chem.* **2001**, 66, 7729.
- [21] (a) H. Roberts, *PhD Thesis*, University of Wales- Cardiff, **2007**;
(b) T. Albers, P. G. Edwards, *Chem Comm*, **2007**, 858.

- [22] (a) D. J. Nielsen, *Functionalised nucleophilic heterocyclic carbene (NHC) complexes of silver(I) and palladium(II): chemistry, structure, and catalysis*, University of Tasmania, **2004**.
 (b) D. J. Nielsen, K. J. Cavell, B. W. Skeltra, A. H. White, *Inorg. Chim. Acta*, **2002**, 327, 116.
- [23] F. Bitterer, O. Herd, A. Hessler, M. Kühnel, K. Rettig, O. Stelzer, W. S. Sheldrick, S. Nagel, N. Rösch, *Inorg. Chem.*, **1996**, 35, 4103.
- [24] D. J. Brauer, K. W. Kottsieper, C. Liek, O. Stelzer, H. Waffenschmidt, P. Wasserscheid, *J. Organomet. Chem.*, **2001**, 630, 177.
- [25] D. J. Brauer, M. Hingst, K. W. Kottsieper, C. Liek, T. Nickel, M. Tepper, O. Stelzer, W. S. Sheldrick, *J. Organomet. Chem.*, **2002**, 645, 14.
- [26] T. Steinke, B. K. Shaw, H. Jong, B. O. Patrick, M. D. Fryzuk, *Organometallics*, **2009**, 28, 2830.
- [27] J. Bruckmann, C. Kruger, *Acta Crystallogr., Crystal Struct. Commun.*, **1996**, C52, 1733.
- [28] a. W. Voskuil, J. F. Arens, *Recl. Trav. Chim. Pays-Bas*, **1963**, 82, 302.
 b. Z. Keming, P. D. Achord; X. Zhang, K. Krogh-Jespersen, A. S. Goldman, *J. Am. Chem. Soc.*, **2004**, 126, 13053
- [29] R. J. Abraham, M. Reid, *J. Chem. Soc., Perkin Trans. 2*, **2002**, 1081.
- [30] Ch. Ch. Lee, W. Ch. Ke, K. T. Chan, Ch. L. Lai, Ch. H. Hu, H. M. Lee, *Chem. Eur. J.* **2007**, 13, 582.

Chapter 3

Synthesis of NHC-Phosphine Complexes of Metals of Groups 11, 10, Ir and Mn

3.1: Introduction

There are many methods for the preparation of metal complexes of *N*-heterocyclic carbenes including *in situ* deprotonation of ligand precursors and transmetallation which have both proved successful in the formation of carbene complexes. The imidazolium salt used in these reactions will not form isolable ‘stable’ carbenes in order to react directly with metal precursors. However a suitable base (such as potassium bis(trimethylsilyl)amide) can be used to form the NHC *in situ* with the appropriate metal precursors without isolating the free carbene. In this chapter, all phosphine-NHC complexes are formed either by *in situ* deprotonation or transmetallation.

NHC complexes are known to support catalysis due to the strong metal-carbon bonds which for some metals may be more robust (less labile) than the more widely used phosphines. The strength of the metal-carbon sigma bond in NHC carbene complexes leads to carbenes having a strong trans influence, whereas phosphines are known to have a strong trans effect (especially for good π -acceptor phosphines). A good *trans* effect from the ‘spectator ligand’ is helpful in catalysis since it helps labilise ligands in the active site, whereas the robustness of carbenes may help to enhance the stability of the catalyst. A combination of both carbene and phosphine in one skeleton may enhance these catalytic activities and introduce new properties of interest. This chapter is mainly concerned with complexation of the new chelating carbene-phosphine ligand discussed in chapter 2 with the following metals of Groups 7, 10 and 11: (Au(I), Ag(I), Cu(I)), (Ni(II), Pd(II), Pt(II)), Mn(I) and Ir(I).*

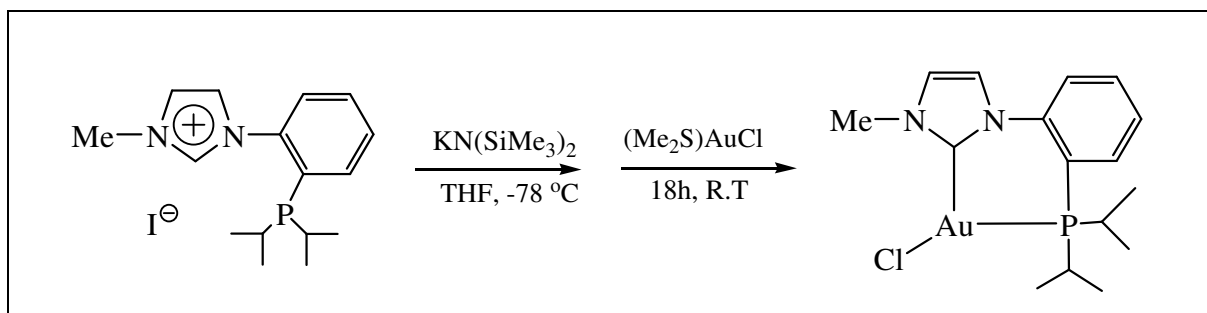
3.2: Results and discussion of NHC-phosphine complexes of group 11:

3.2.1: Au Complex

Via Free Carbene:

Au(I) complex was prepared from (Me₂S)AuCl, by reaction with the free carbene formed by addition of base to the phosphine-imidazolium salt, **2.5**, and was isolated as a light brown solid, as the mono-(phosphine-NHC) Au(I) complex, **3.1**, Scheme 3.1.

* Note: in all new crystal structures reported in this chapter, the carbene's carbon attached to the metal is denoted as C₁ in the numbering scheme.



Scheme 3.1: Formation of Au(I)-complex, **3.1**, *via* free carbene

Characteristic changes were observed in both the ^1H and ^{31}P -NMR spectra, Figure 3.1, along with satisfactory accurate mass spectrometry data, the spectroscopic data confirmed the formation of the mono-ligand complex **3.1**. The coordinated phosphine resonance appeared in the ^{31}P -NMR spectrum, in CDCl_3 , as a singlet at 47.8 ppm, displaying a considerable downfield coordination shift from the corresponding free ligand peak (which appears at -6.8 ppm). The chemical shift value of the coordinated phosphine was in the same range as that of related complexes.^{1,2} The spectrum showed no sign of un-coordinated phosphorus atoms indicating that the carbene-phosphine ligand binds the metal centre as a chelate, as well as, the absence of imidazolium proton peak at -9.6 ppm.

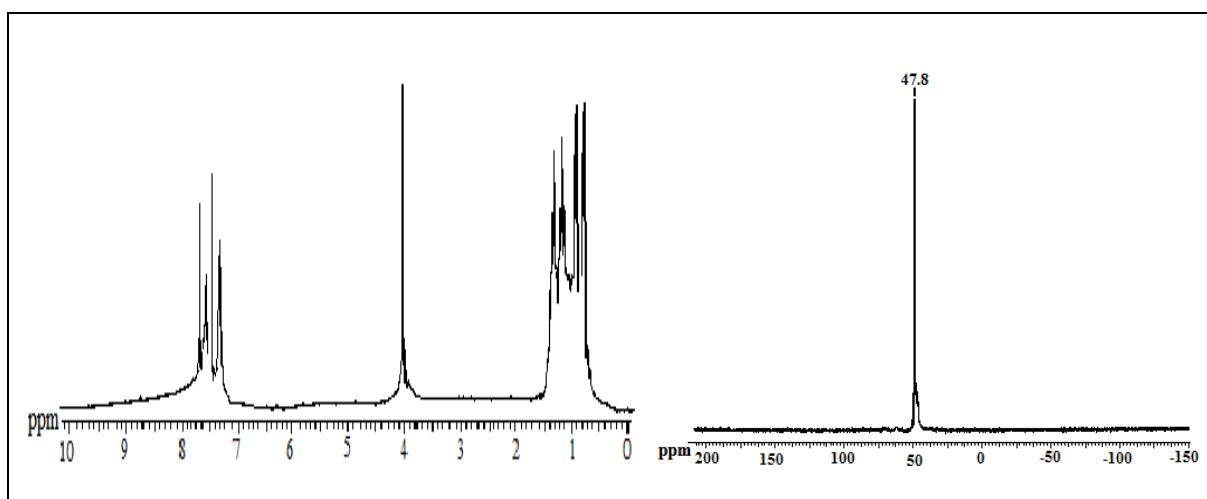
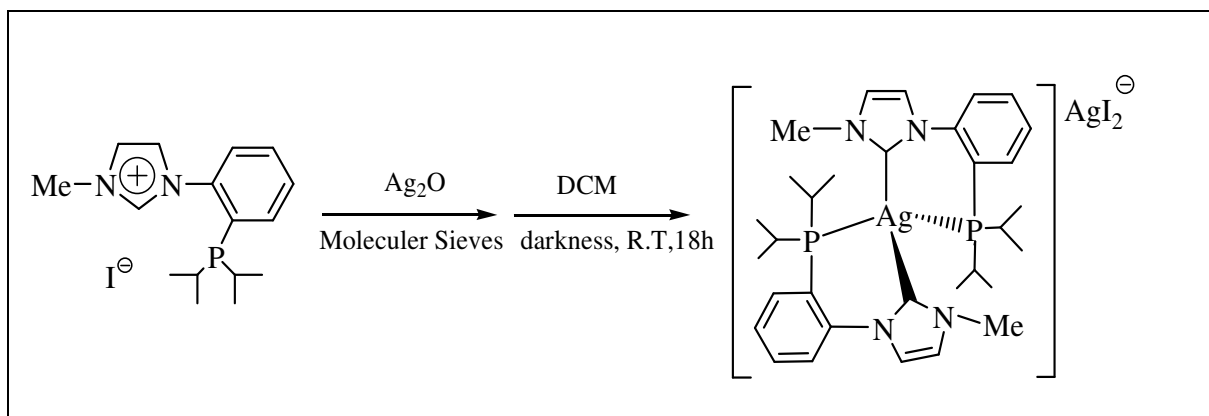


Figure 3.1: ^1H -NMR and $^{31}\text{P}\{^1\text{H}\}$ -NMR spectra, in CDCl_3 , of Au-complex, **3.1**

In the mass spectrum, the highest fragment peak was observed at 745.29 and corresponds to the molecular ion, $[\text{M}]$, of the mono-(phosphine-NHC) Au(I) chloro complex.

3.2.2: Ag complex

The synthesis of Ag(I) complex, **3.2**, was achieved *via* the reaction of a half molar equivalent of silver oxide, Ag₂O, with one equivalent (i.e. a 1:1 Ag:ligand ratio) of the corresponding phosphine-imidazolium salt, **2.5**, in the presence of degassed 4Å molecular sieves, following the method of Wang and Lin.³ Half the equivalent of Ag₂O with the salt was enough to cause disappearance of the *im*C₁-H proton peak in the ¹H-NMR spectrum, as the observations reported by Cavell⁴ and Helmschen *et al.*⁵ The isolation of the Ag(I) complex was achieved by work-up with DCM and the bis-(phosphine-NHC) Ag(I) complex, **3.1**, was isolated as a light brown solid in yield of 80%, Scheme 3.2.



Scheme 3.2: Formation of Ag-complex, **3.2**,

The product, Ag(I) complex **3.2**, was characterised by ¹H, ¹³C, ³¹P NMR spectroscopies and high resolution mass spectrometry. The ¹H-NMR spectrum of **3.2**, in CDCl₃, clearly indicates the coordination of the carbene to the silver by the absence of the distinctive carbene proton, *im*C₁-H, which appears at 9.62 ppm in the precursor, phosphine-imidazolium salt, **2.5**, Figure 3.2A. In the ¹³C-NMR spectrum, a singlet peak for the carbene's carbon, *im*C₁, was observed at 181.45 ppm, which is consistent with this type of carbon atom. A characteristic singlet resonance was observed at 5.4 ppm in the ³¹P{¹H}-NMR spectrum, in CDCl₃, Figure 3.2A. This chemical shift in the bis-(phosphine-NHC) Ag(I) complex is shifted downfield compared to the corresponding free ligand (which appears at -6.8 ppm) but is close to the value observed in a similar complex synthesised by Helmschen *et al.*⁵

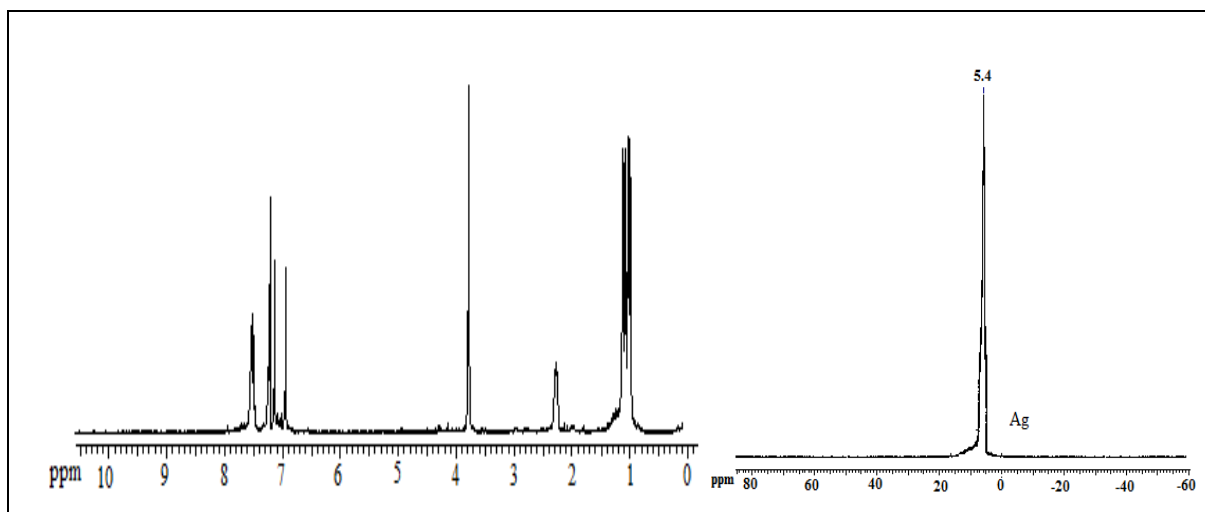
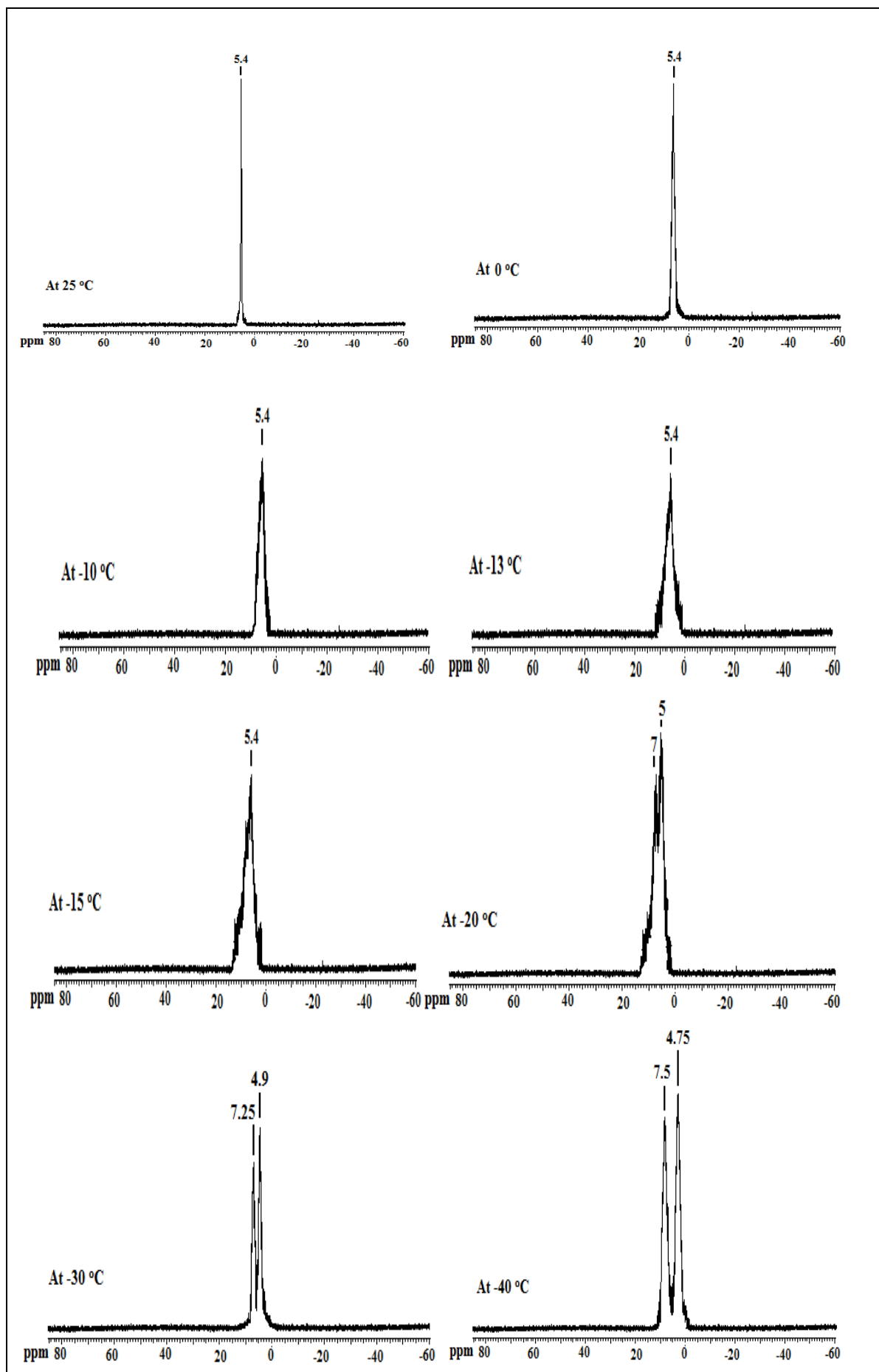


Figure 3.2A: ^1H -NMR and $^{31}\text{P}\{^1\text{H}\}$ -NMR spectra, in CDCl_3 , of Ag-complex, **3.2**

The spectrum showed no sign of free, un-coordinated phosphorus atoms indicating that both carbene and phosphorus donors are coordinated to the metal centre in a chelating configuration. At low temperatures, the ^{31}P -NMR spectrum of the Ag complex exhibits coupling to both ^{109}Ag and ^{107}Ag isotopes; $^1J(^{109}\text{Ag}, ^{31}\text{P}) = 259 \text{ Hz}$ and $^1J(^{107}\text{Ag}, ^{31}\text{P}) = 227 \text{ Hz}$ indicating that the complex is not labile on the NMR timescale, Figure 3.2B. A coupling pattern to ^{109}Ag or ^{107}Ag was not observed at room temperature. At room temperature, in CDCl_3 , there was only one fairly sharp signal. At -40°C , the ^{31}P signal of **3.2** clearly splits into two broad signals which was interpreted as two doublets due to the coupling to both silver isotopes, $^1J(^{31}\text{P}, ^{109}\text{Ag})$ and $^1J(^{31}\text{P}, ^{107}\text{Ag})$, both of which have a spin of $1/2$ and are therefore NMR receptive.^{6a,b} From the measured values of the coupling constants (259 and 227 Hz), the magnetogyric ratio is $259/227=1.14$ which matches almost exactly the relation of the magnetogyric ratio of the two silver isotopes: $\gamma(^{109}\text{Ag}) / \gamma(^{107}\text{Ag}) = 1.15$.^{7a,b} At low temperatures, it was possible to see the coupling between silver and phosphorus. This is a good indication that the splitting results from the 1J coupling of phosphorus to the silver isotopes.^{6a,b} The mass spectrometry data showed a peak, 655.2 $[\text{M}-\text{H}]^+$, corresponding to the bis-ligand-silver complex. Another molecular mass fragment (671.2 amu attributed to $[\text{M}+\text{O}]^+$) indicates that the complex is sensitive to oxidation. A fragment peak observed at 360.6 amu may be attributed to the counter ion of the complex, AgI_2^- . However, the structures drawn in Scheme 3.2 does not confirm that is the actual structure for the silver complex as it is difficult to ascertain the precise formula of such complexes without X-ray crystallography.



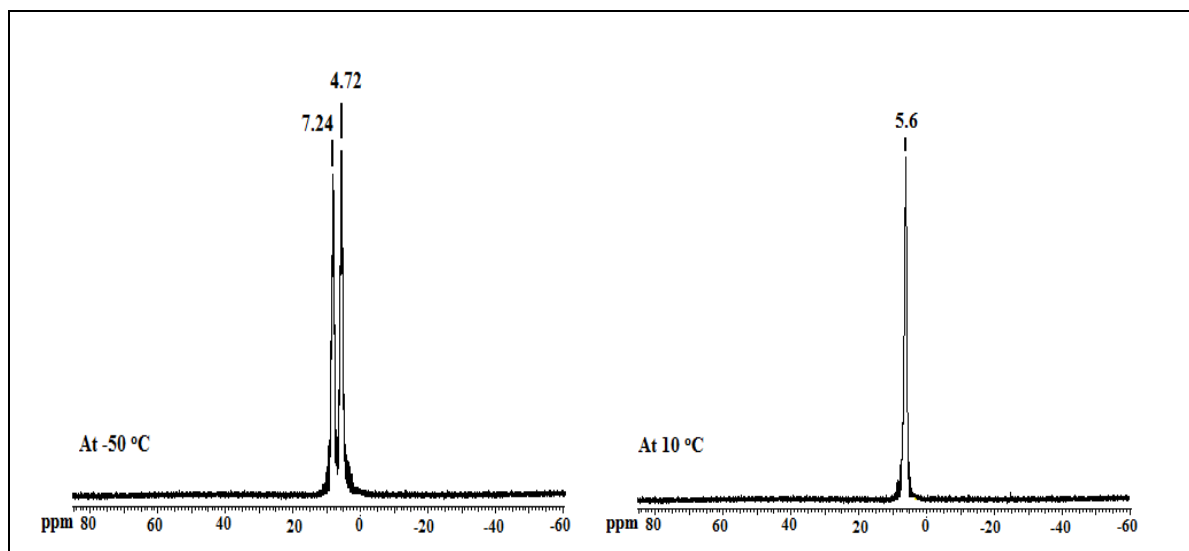
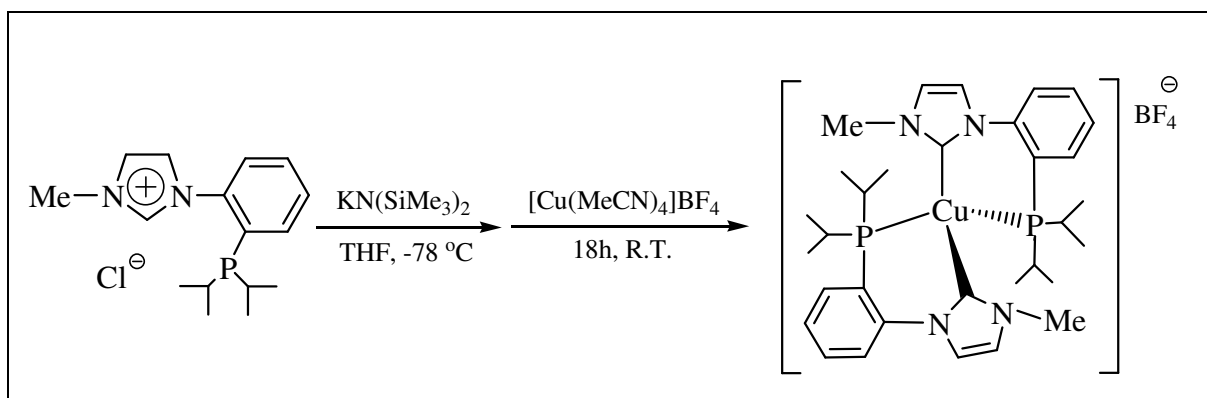


Figure 3.2B: $^{31}\text{P}\{^1\text{H}\}$ -NMR spectra, in CDCl_3 , of Ag-coupling for complex **3.2**

3.2.3: Cu complex

A. *Via Free Carbene:*

The chelating phosphine-NHC Cu(I) complex was synthesised in an analogous manner to other group 10 complexes *via* the formation of the free carbene. The free carbene was generated *in situ* by the equimolar reaction of the phosphine-imidazolium salt, **2.5**, with the base, $\text{KN}(\text{SiMe}_3)_2$ immediately before being transferred into a solution containing one equivalent of the copper precursor, $[\text{Cu}(\text{MeCN})_4]\text{BF}_4$, in a THF. The bis-(phosphine-NHC) Cu(I) complex, **3.3**, was isolated by extraction into dichloromethane as an off--white solid, Scheme 3.3.



Scheme 3.3: Formation of Cu-complex, **3.3**, *via* free carbene

The Cu(I) Complex, **3.3** was characterised by ^1H , ^{13}C and ^{31}P -NMR spectroscopies and high resolution mass spectrometry. The absence of the $\text{imC}_1\text{-H}$ proton from the ^1H -NMR spectrum, in CDCl_3 , indicated the formation of the carbene-copper bond, Figure 3.3. In the ^{13}C -NMR spectrum, in CDCl_3 , a singlet peak for the carbene carbon, imC_1 , was observed at 189.14 ppm, consistent with related NHC carbene complexes. The ^{31}P -NMR spectrum of **3.3**, in CDCl_3 , showed a downfield shift from -6.8 ppm in the phosphine-imidazolium salts to 3.8 ppm, indicating that the phosphine was coordinated to the metal centre, Figure 3.3, and that the ligand is in a chelating configuration. The mass spectrometry data for **3.3** only shows one peak at a molecular mass of 611.1 corresponding to the ion, M^+-H^+ for the bisligand-copper complex. The observed elemental analytical data is consistent with the formulation.

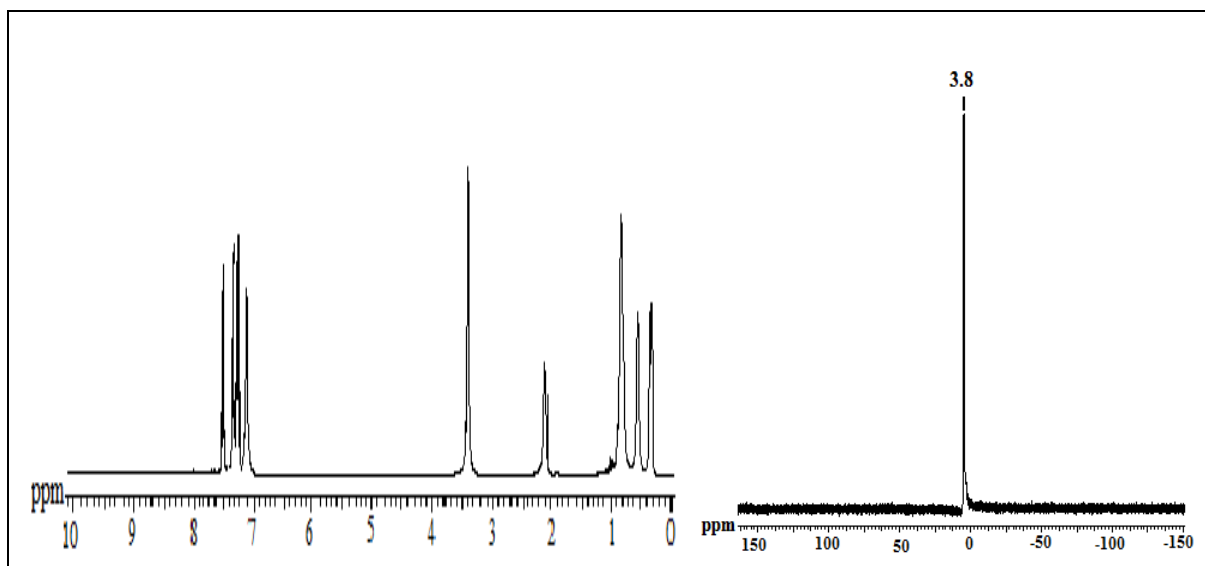
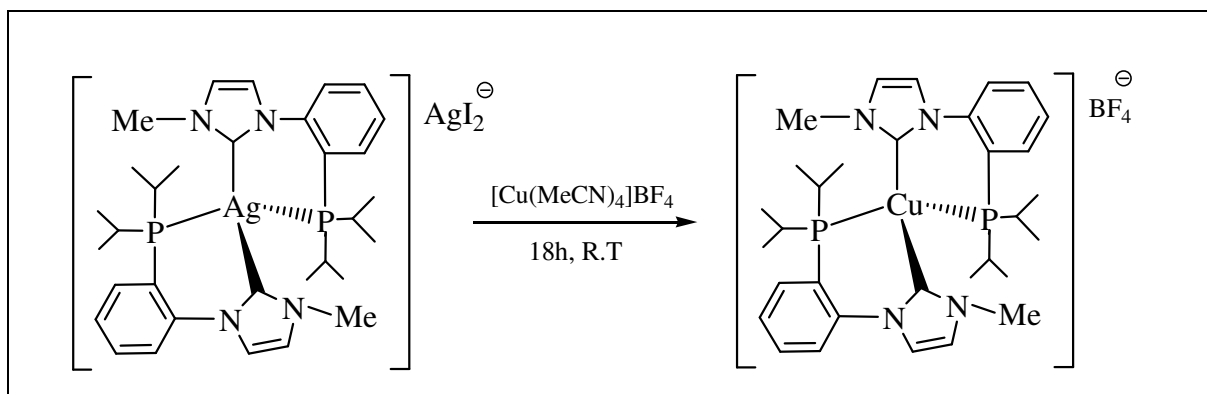


Figure 3.3: ^1H -NMR and $^{31}\text{P}\{^1\text{H}\}$ -NMR spectra, in CDCl_3 , of Cu-complex, **3.3**

B. Via Transmetallation:

The synthesis of the phosphorus-NHC copper(I) complex **3.3** was also achieved *via* transmetallation from the corresponding silver(I) complex **3.2** by reaction with the copper metal precursor, $[\text{Cu}(\text{MeCN})_4]\text{BF}_4$ in dichloromethane. Silver iodide precipitated during the reaction indicating that transmetallation reaction had occurred and the copper complex product (**3.3**) was isolated as a tan solid, Scheme 3.4.

Again, this product was characterised by ^1H , ^{13}C , ^{31}P -NMR spectroscopies and high resolution mass spectrometry which confirmed the formation of **3.3**. Attempts to grow crystals suitable for X-ray crystallography were unsuccessful.



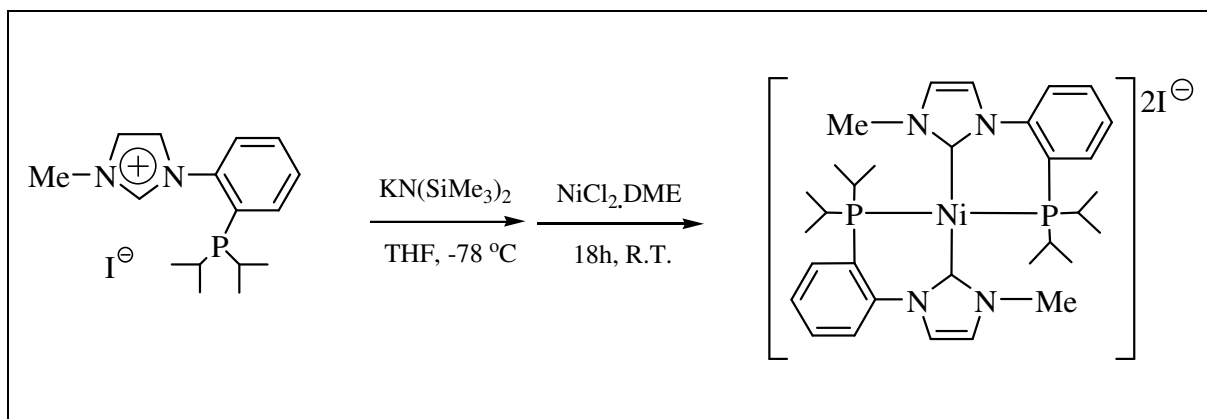
Scheme 3.4: Formation of Cu-complex, **3.3**, *via* transmetalation

3.3: Results and discussion of NHC-phosphine complexes of group 10:

3.3.1: Ni Complex

Via Free Carbene:

The synthesis of a phosphine-NHC nickel complex was achieved *via* the formation of the free carbene generated *in situ* by adding a base to the phosphine-imidazolium salt. The free chelating carbene ligand was then trapped with a suitable nickel precursor (NiCl₂.DME) to form the product complex, bis-(phosphine-NHC) Ni(II), **3.4**, which was isolated and recrystallized from EtOH as a yellow solid in 32% yield, Scheme 3.5. Using KN(SiMe₃)₂ as a base in the deprotonation of imidazolium salt was very effective due to the fact that this base is strong enough to deprotonate a range of imidazolium salts cleanly.^{8,9}



Scheme 3.5: Formation of Ni-complex, **3.4**, *via* free carbene

The product was fully characterised by ^1H , ^{13}C , ^{31}P -NMR spectroscopies, high resolution mass spectrometry, and by an X-ray crystallographic determination. In the ^1H -NMR spectrum, in CD_3CN , **3.4** shows an absence of the $\text{imC}_1\text{-H}$ proton indicating the coordination of the carbene to the nickel metal centre. A more pronounced (than in the group 11 metal complexes) coordination chemical shift was observed in the $^{31}\text{P}\{^1\text{H}\}$ -NMR spectrum, in CD_3CN , which appeared as a singlet at 36.9 ppm, Figure 3.4. The spectrum showed no sign of free phosphorus atoms again indicating complete coordination of the ligand to the metal centre in a chelating fashion. Since the nickel complex is doubly charged, a molecular mass of 303.13 in the mass spectrum corresponds to the molecular ion validating the formulation. Other peaks also occur at mass values consistent with this formulation.

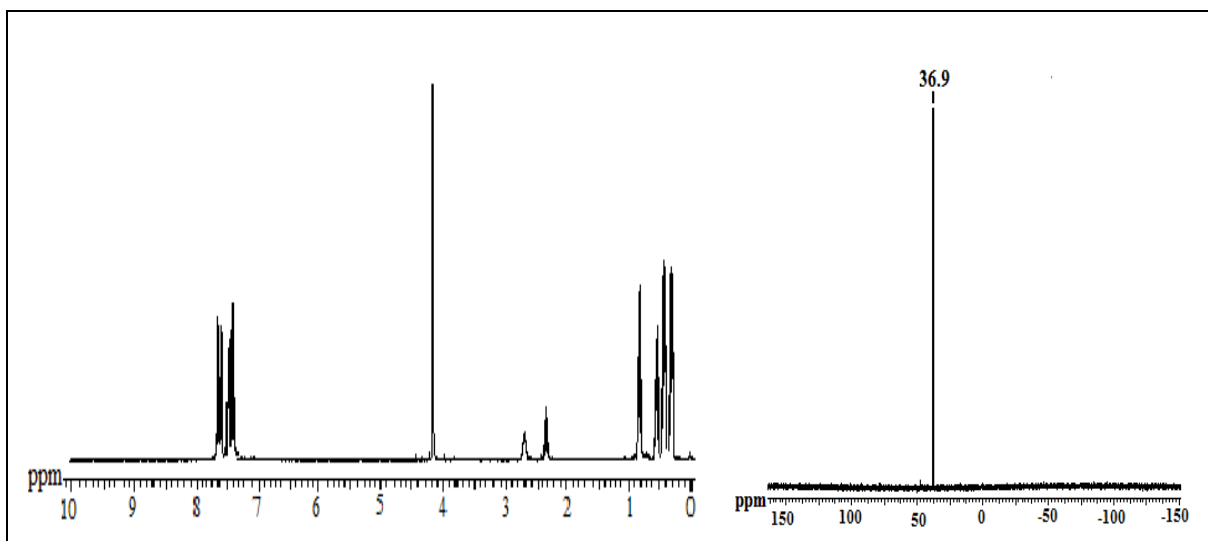


Figure 3.4: ^1H -NMR and $^{31}\text{P}\{^1\text{H}\}$ -NMR spectra, in CD_3CN , of Ni-complex, **3.4**

Crystals suitable for a single crystal X-ray crystallographic determination were obtained upon saturating a solution of nickel complex **3.4** in EtOH at 5 °C. The crystal structure and labelling Scheme for **3.4** is shown in Figure 3.5. Complex **3.4** exhibits a square-planar geometry where carbene is *trans* to carbene and phosphorus is *trans* to phosphorus. The square plane is distorted around the nickel metal centre, the distortion being manifested by a significant deviation of the C-Ni-C angle, (162.9°), and by the P-Ni-P angle, (150.5°), from the ideal angle of 180°; the C-Ni-C angle is closer to linearity than is the P-Ni-P angle. In **3.4**, the Ni-C(1), Ni-C(17), Ni-P(1) and Ni-P(2) bond lengths are 1.880(7) Å, 1.908(7) Å, 2.222(0) Å, and 2.221(6) Å respectively, and are close to related complexes.^{12,13}

The six-membered rings of the two chelating ligands with the metal centre are twisted; the metrical parameters of this Ni-complex, Table 3.1, are similar to those of related Ni-P-NHC complex structures, Figure 3.6 (A & B) reported by Man Lee¹⁰ and subsequently by Fryzuk¹¹.

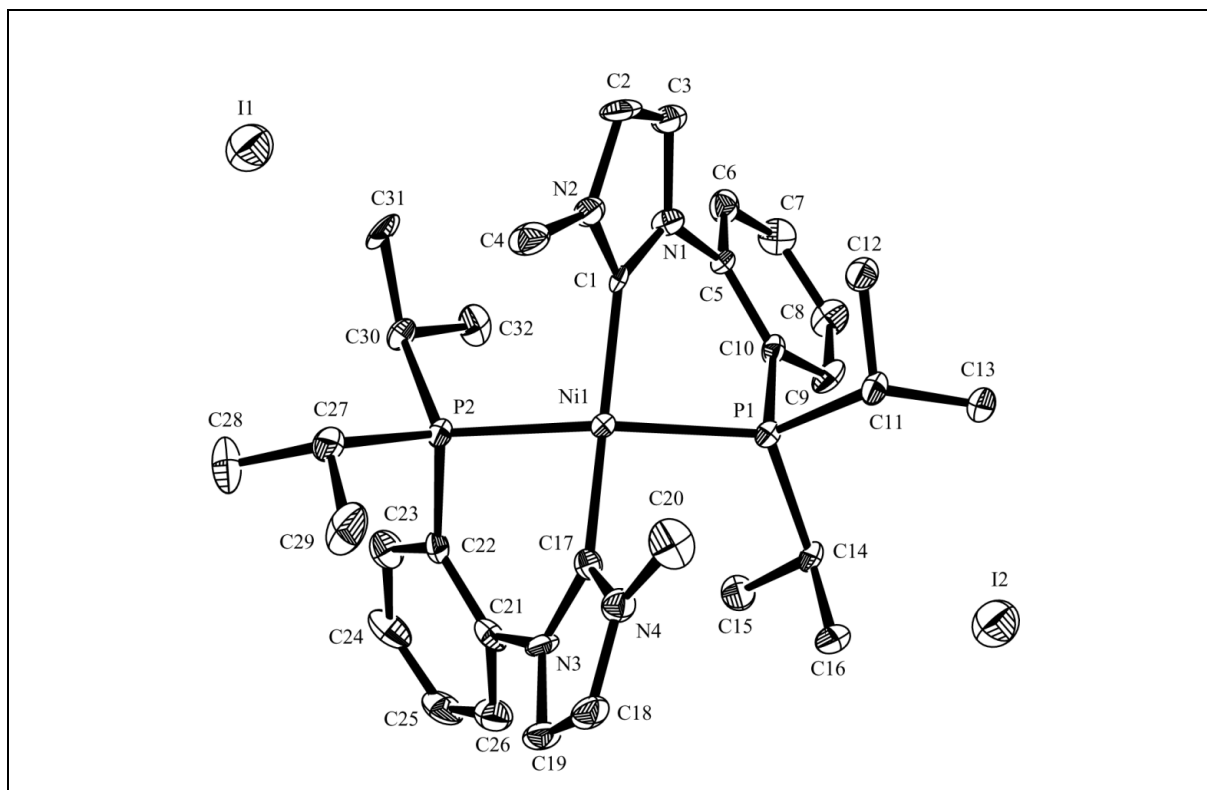


Figure 3.5: Molecular structure of Ni-complex (ORTEP projection of compound **3.4**, in C₂D₅OD, 40% probability ellipsoids, hydrogen atoms are omitted for clarity) (Appendix: Data Set 3)

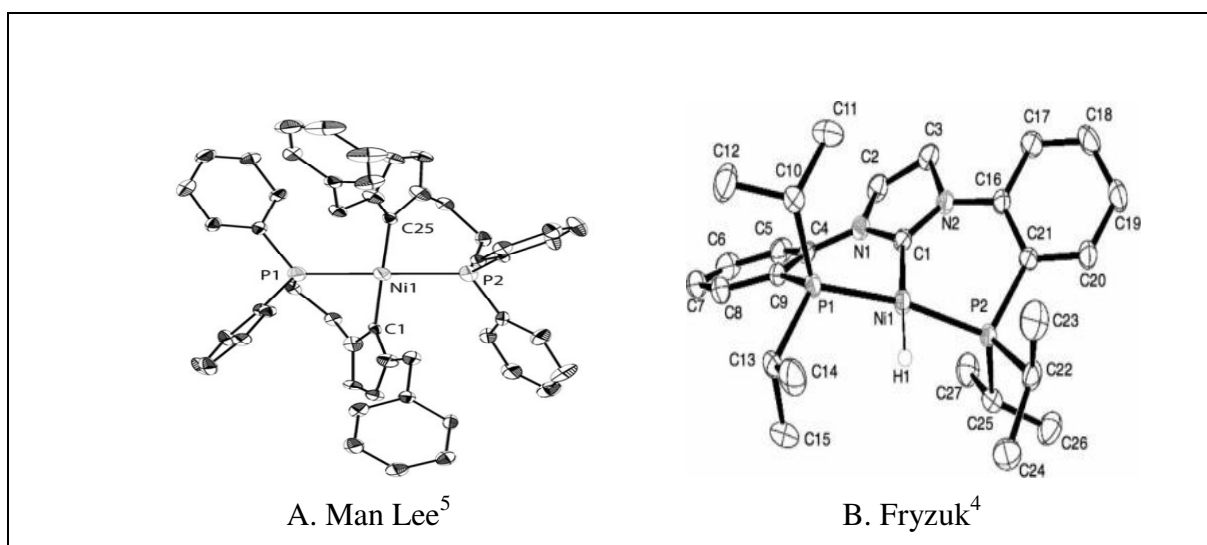


Figure 3.6

From the crystal data, the Ni-C bonds are shorter than the Ni-P bonds. This may indicate the smaller covalent radius of carbon but also may reflect that NHC ligands stronger σ -donors than trialkylphosphines.² Angles within the imidazole rings, N(1)-C(1)-N(2), 104.1(6)°, and N(3)-C(17)-N(4), 105.7(6)°, are within the expected range of 101° -106°.¹⁴ Selected bond lengths and angles are presented in Table 3.2.

Table 3.1: Comparison of angles and lengths of complex **3.4** with Lee's and Fryzuk's complexes.

	Complex 3.4	Man Lee	Fryzuk
C-Ni-C (°)	162.9(3)	179.15(18)	-
P-Ni-P (°)	150.56(7)	163.64(5)	169.03(2)
C-Ni-P (°)	86.7(2)	82.825(12)	94.70(6) 95.90(6)
	86.7(2)	85.29(13)	
	97.1(2)	94.21(12)	
	98.3(2)	97.85(13)	
C-Ni (Å°)	1.880(7)	1.971(4)	1.8629(19)
	1.908(7)	1.985(4)	
P-Ni(Å°)	2.2216(19)	2.1025(13)	2.1080(8)
	2.2220(19)	2.1074(13)	2.1129(9)

Table 3.2: Some selected bond lengths and angles for P-NHC nickel complex, **3.4**.

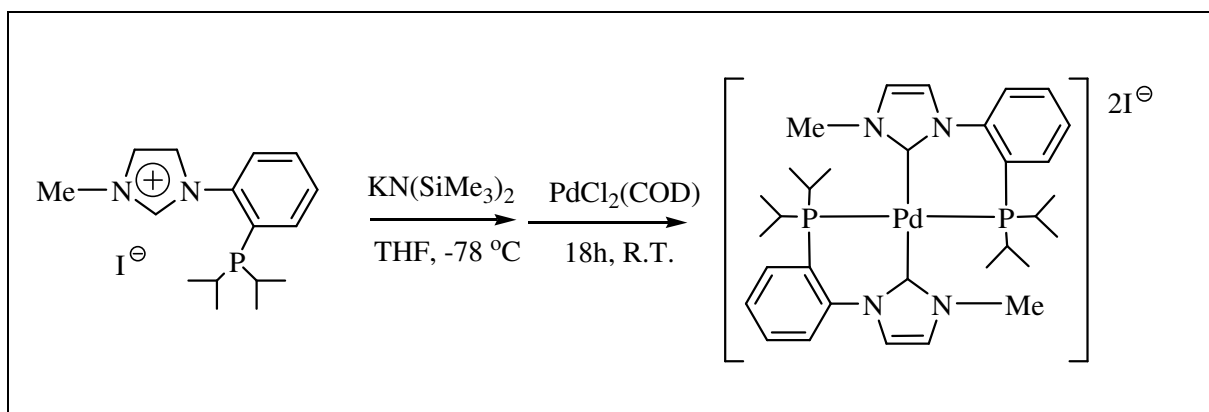
Bond Lengths(Å)				Bond Angles (°)	
P(1)-Ni(1)	2.2220(19)	C(10)-P(1)	1.817(7)	C(1)-Ni(1)-P(1)	86.7(2)
P(2)-Ni(1)	2.2216(19)	C(11)-P(1)	1.857(7)	C(17)-Ni(1)-P(2)	86.7(2)
C(1)-Ni(1)	1.880(7)	C(14)-P(1)	1.856(7)	C(1)-Ni(1)-P(2)	97.1(2)
C(17)-Ni(1)	1.908(7)	C(22)-P(2)	1.837(7)	C(17)-Ni(1)-P(1)	98.3(2)
C(1)-N(1)	1.356(9)	C(27)-P(2)	1.849(7)	C(1)-Ni(1)-C(17)	162.9(3)
C(1)-N(2)	1.368(9)	C(30)-P(2)	1.852(7)	P(1)-Ni(1)-P(2)	150.5(6)
C(17)-N(3)	1.343(8)			N(1)-C(1)-N(2)	104.1(6)
C(17)-N(4)	1.354(9)			N(3)-C(17)-N(4)	105.7(6)

3.3.2: Pd complex:

The synthesis of the phosphorus-NHC palladium complex was achieved from the palladium precursors, $[\text{PdCl}_2(\text{COD})]$ or $[\text{Pd}(\text{OAc})_2]$ by transmetallation and also by reaction with the free carbene following the same synthetic approach used in the synthesis of the Ni-complex **3.4**. Ligand **2.5** is used with $[\text{PdCl}_2(\text{COD})]$ and ligand **2.6** used with $[\text{PdCl}_2(\text{COD})]$ or $[\text{Pd}(\text{OAc})_2]$ to form the same Pd-complex. The Ag-complexes reacted smoothly with Pd precursors such as $[\text{PdCl}_2(\text{MeCN})_2]$, $[\text{PdMeCl}(\text{COD})]$, $[\text{PdCl}_2(\text{COD})]$ to give the carbene-phosphine complexes *via* transmetallation.¹⁵

A. Via Free Carbene:

The chelating phosphine-NHC Pd(II) complex was prepared by an analogous method to the Ni complex *via* the formation of the free carbene which was generated *in situ* by adding the phosphine-imidazolium salt, **2.5**, to the base, $\text{KN}(\text{SiMe}_3)_2$. Addition of one or two equivalents of the free carbene to the palladium metal precursor, $[\text{PdCl}_2(\text{COD})]$, in THF followed by workup with CH_3CN , gave the bis-(phosphine-NHC) Pd(II) complex as a pale brown solid, Scheme 3.6.



Scheme 3.6: Formation of Pd-complex, **3.5**, *via* free carbene

The product was characterised by ^1H , ^{13}C , ^{31}P -NMR, and high resolution mass spectroscopies, crystals suitable for a crystallographic determination could not be obtained. The ^1H -NMR spectrum of **3.5** shows the coordination of the carbene to the palladium metal centre by the absence of the distinctive protonated carbene proton, $\text{imC}_1\text{-H}$, Figure 3.7, which appears at 9.62 ppm in the corresponding phosphine-imidazolium salt. The aliphatic region of

the spectrum is more clearly observed in CD₃CN, Figure 3.7(A). However the aromatic region is more clearly displayed in CDCl₃ solvent, Figure 3.7 (B). A singlet resonance attributable to the palladium coordinated phosphorus atom was observed in the ³¹P{¹H}-NMR spectrum at 37.5 ppm in CD₃CN, shifted downfield from the corresponding peak of the imidazolium precursor which appears at -6.8 ppm (in CDCl₃), Figure 3.8. The disappearance of the latter phosphorus peak in the spectra indicates complete coordination of the ligand to the palladium metal atom in a chelating manner. A mass peak at 327.1 amu is observed in the mass spectrum. This corresponds to half molecular mass since the palladium complex is doubly charged and validates the formulation; other peaks in the mass spectrum are also consistent with the formulation.

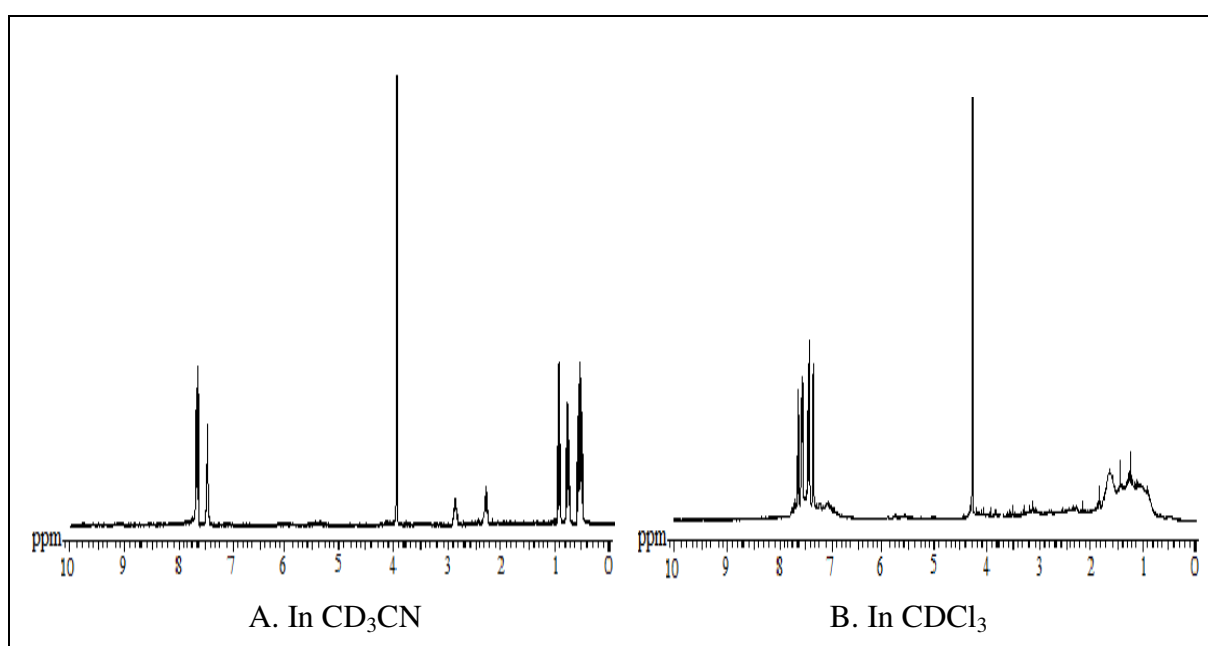


Figure 3.7: ¹H-NMR spectra of Pd-complex, **3.5**

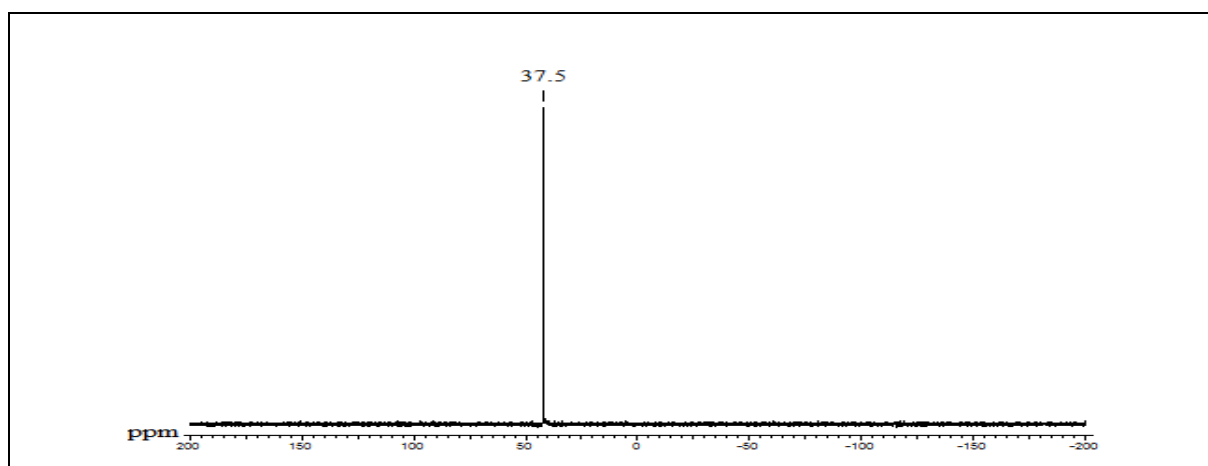
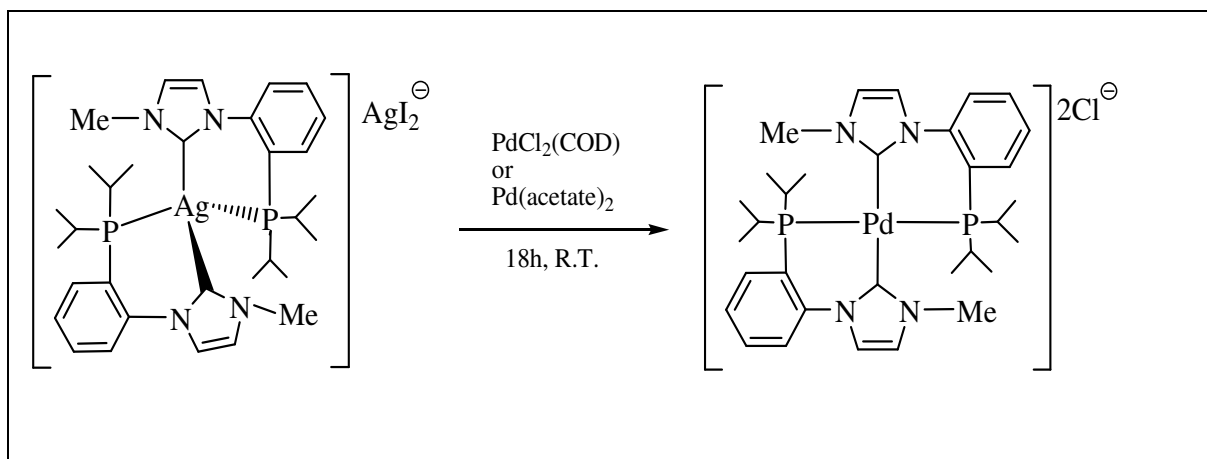


Figure 3.8: ³¹P{¹H}-NMR spectrum of Pd-complex, in CD₃CN, **3.5**

B. Via Transmetallation:

The synthesis of phosphorus-NHC palladium(II) complex **3.5** was achieved *via* transmetallation from the corresponding silver(I) complex **3.2**. Half a molar quantity of complex **3.2** and the palladium precursor, [PdCl₂(COD)] or [Pd(OAc)₂], was stirred together in dichloromethane at room temperature until precipitation of silver iodide ceased (as an indication that the transmetallation reaction had occurred and was complete). The resulting pale brown bis-(phosphine-NHC) Pd(II) complex was isolated by precipitation from dichloromethane upon addition of diethyl ether, Scheme 3.7.

The product was characterised by ¹H, ¹³C, ³¹P-NMR and high resolution mass spectroscopies, which confirmed that the same product (complex **3.5**) had been formed as obtained from the free carbene. Attempts to obtain crystals suitable for X-ray crystallography were unsuccessful.



Scheme 3.7: Formation of Pd-complex, **3.5**, *via* transmetallation

3.3.3: Pt Complex

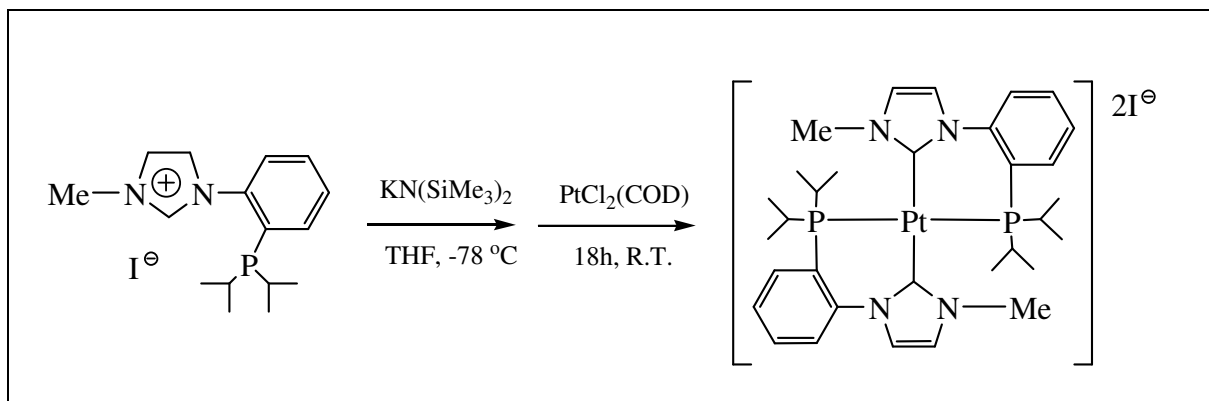
In trials for platinum complexation with phosphine-imidazolium salts, **2.5** and **2.6**, *via* free carbene and by transmetallation methods, two complexes were obtained, the bis-(phosphine-NHC) Pt(II) complex, **3.6**, and the mono-(phosphine-NHC) Pt(II) complex, **3.7**.

3.3.3.1: Bis-(phosphine-NHC) Pt complex, **3.6**

Via Free Carbene:

Following the same synthetic procedure outlined above for Ni(II) and Pd(II) complexes, the bis-chelate bis-(phosphine-NHC) platinum(II) complex, **3.6**, was prepared

from the free carbene. Solution of the free carbene in THF was reacted with one equivalent of the platinum precursor, $[\text{PtCl}_2(\text{COD})]$, to give an orange solution from which a yellow solid was isolated and identified as the bis-(phosphine-NHC) Pt(II) complex, in 40% yield, Scheme 3.8. Crystals of **3.6** suitable for X-ray crystallography were obtained from saturated MeOH or DCM solutions upon cooling (at 5 °C).



Scheme 3.8: Formation of Pt-complex, **3.6**, *via* free carbene

The product was fully characterised by ^1H , ^{13}C , ^{31}P -NMR and high resolution mass spectroscopies as well as by an X-ray crystallographic determination. The ^1H -NMR spectrum of **3.6**, in CD_3OD , shows the coordination of the carbene to the platinum by the absence of the distinctive protonated carbene proton, $_{\text{im}}\text{C}_1\text{-H}$, Figure 3.9.

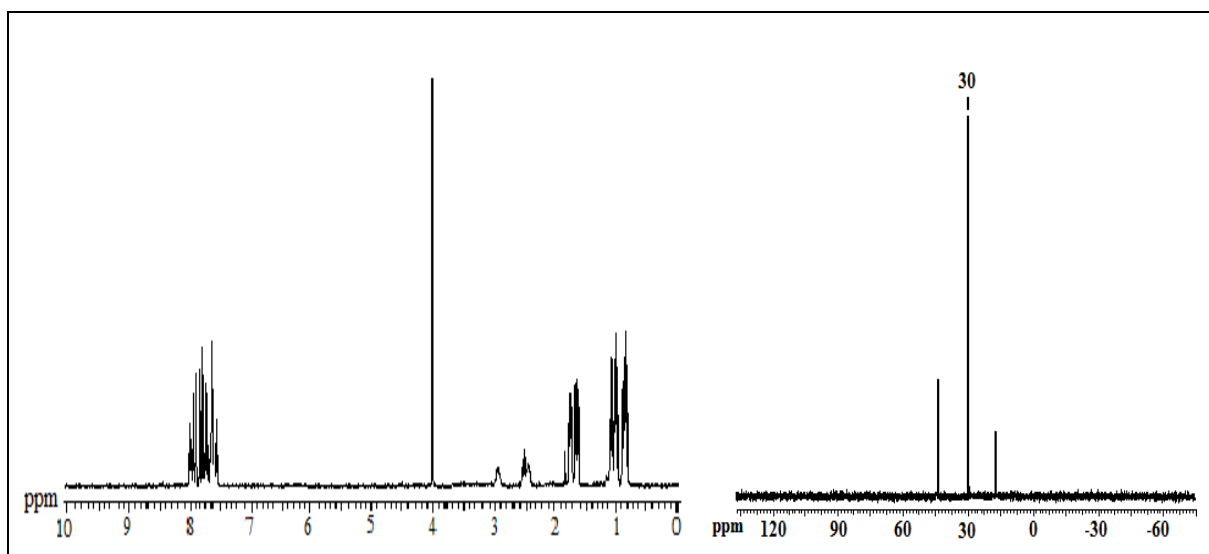


Figure 3.9: ^1H -NMR and $^{31}\text{P}\{^1\text{H}\}$ -NMR spectra of Pt-complex, in CD_3OD , **3.6**

A characteristic singlet was observed in the ^{31}P -NMR spectrum, Figure 3.9, which indicates that only one product was formed from this reaction. In CD_3OD , a chemical shift value for the coordinated phosphine to the platinum metal in the bis-(phosphine-NHC) Pt(II) complex is observed at 30 ppm. This peak has two platinum satellites ($^1J_{\text{Pt-P}} = 2790 \text{ Hz}$). The presence of Pt satellites indicates that the phosphine is not labile under the conditions (on the NMR timescale). The phosphine resonance is shifted downfield compared to the corresponding free ligand to a similar extent as in the Pd analogue. Again, the spectrum showed the absence of free phosphine indicating complete coordination of the ligand to the metal centre and consistent with a chelating bonding mode. A peak in the mass spectrum with a molecular mass of 371.7 amu corresponds to the half molecular ion and since the platinum complex is doubly charged, validates the formulation; other mass peaks are also consistent. The crystal structure and labelling Scheme for **3.6**, in CD_3OD , is shown in Figure 3.10. Complex **3.6** exhibits a square planar geometry, which is distorted around the platinum where each chelating arm of the ligand occupies *trans*-positions to the corresponding one, where

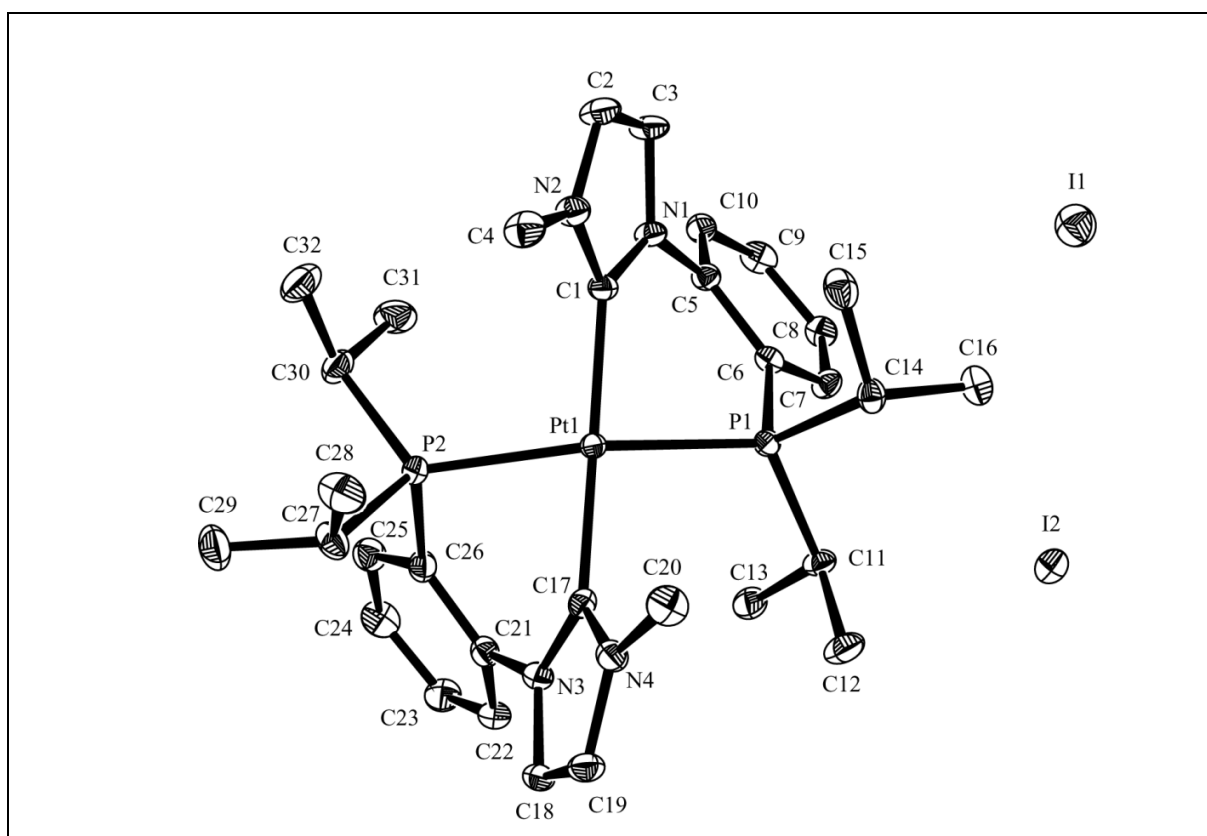


Figure 3.10: Molecular structure of Pt-complex (Ortep projection of compound **3.6**, in CD_3OD , 40% probability ellipsoids, Hydrogen atoms are omitted for clarity) (Appendix: Data Set 4)

carbene is *trans* to carbene and phosphorus is *trans* to phosphorus. This distortion is confirmed by the significant deviation of the C-Pt-C angle (170.6°) and the P-Pt-P angle (157.9°) from the ideal 180°. The C-Pt-C angle is closer to linearity than the P-Ni-P angle (157.9°) from the ideal 180°. The C-Pt-C angle is closer to linearity than the P-Ni-P angle resembling that of Ni-complex **3.4**. This six-membered ring formed by the chelating phosphine and carbene donors to the metal centre is twisted.

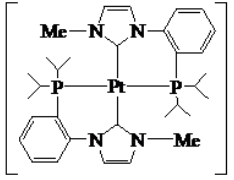
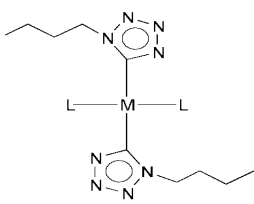
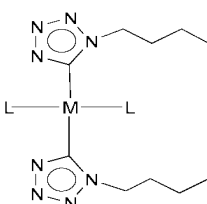
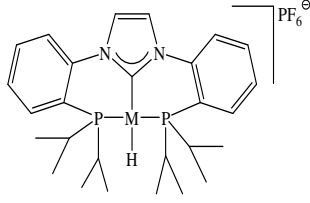
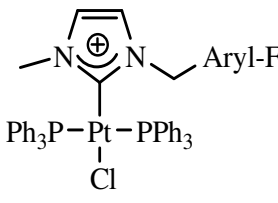
The Pt-C(1), Pt-C(17), Pt-P(1) and Pt-P(2) bond lengths in complex **3.6** are 2.033(5) Å, 2.026(4) Å, 2.3187(12) Å, and 2.3137(12) Å respectively. These are close to reported values in related complexes; selected values are listed in table 3.3. Most notably, due to the metal size, Pt-C and Pt-P bond lengths in platinum complex, **3.6** are longer than the corresponding nickel complex, **3.4**. The Pt-C bonds are shorter than the Pt-P bonds which is consistent with the relative magnitudes of the covalent radii of the donor atoms. The angles within the imidazole ring, N(1)-C(1)-N(2), 106.1(4)°, and N(3)-C(17)-N(4), 104.2(4)°, are within the known range 101° -106°. ¹⁴ Selected bond lengths and angles are presented in Table 3.3.

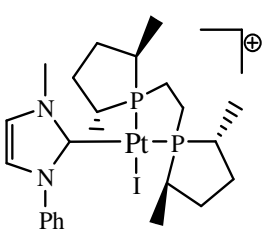
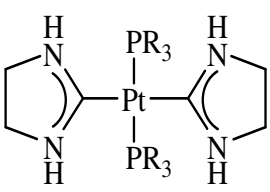
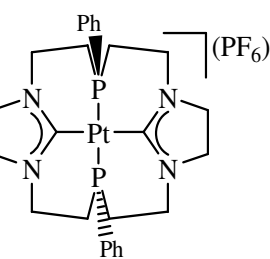
Table 3.3: Selected bond lengths (Å) and angles (°) for phosphorus-NHC Pt-complex, **3.6**.

Bond Lengths(Å)				Bond Angles (°)	
P(1)-Pt(1)	2.3187(12)	C(6)-P(1)	1.841(5)	C(1)-Pt(1)-P(1)	80.16(13)
P(2)-Pt(1)	2.3137(12)	C(11)-P(1)	1.833(5)	C(17)-Pt(1)-P(2)	84.82(13)
C(1)-Pt(1)	2.033(5)	C(14)-P(1)	1.852(5)	C(1)-Pt(1)-P(2)	97.65(13)
C(17)-Pt(1)	2.026(4)	C(26)-P(2)	1.842(5)	C(17)-Pt(1)-P(1)	100.91(14)
C(1)-N(1)	1.341(6)	C(27)-P(2)	1.840(5)	C(1)-Pt(1)-C(17)	170.67(19)
C(1)-N(2)	1.352(6)	C(30)-P(2)	1.844(5)	P(1)-Pt(1)-P(2)	157.96(4)
C(17)-N(3)	1.367(6)			N(1)-C(1)-N(2)	106.1(4)
C(17)-N(4)	1.349(6)			N(3)-C(17)-N(4)	104.2(4)

Angles and bonds, Table 3.4, of complex **3.6** show close agreement with those of related structures of distorted square planar Pt-P-NHC complexes, such as the bis-trimethyl phosphine bis-carbene reported by Yong-Joo,¹⁶ Figure 3.11, and the bis-triethylphosphine chelating bis-carbene reported by Fryzuk¹¹ and others reported by Rourke,¹⁷ Marinetti^{18,19} and Hahn.²⁰ Metrical values are within normal ranges.

Table 3.4: Comparison of angles and lengths of complex **3.6** with other P-NHC Pt complexes

<div>Lengths (Å) & Angles(°)</div> <div>Complexes</div>	C-Pt-C (°)	P-Pt-P (°)	C-Pt-P (°)	C-Pt (Å)	P-Pt (Å)
Pt-complex, 3.6 	170.67(19)	157.96(4)	80.16(13) 84.82(13) 97.65(13) 100.91(14)	2.033 2.026	2.318 2.313
Yong-Joo¹⁶ (I) 	180.0(4)	180.00(8)	88.32(17) 88.32(17) 91.68(17) 91.68(17)	2.033(6)	2.3037(16)
Yong-Joo¹⁶ (II) 	178.82(16)	167.88(5)	88.02(13) 89.25(12) 90.82(12) 91.84(12)	2.033(5) 2.056(5)	2.303(1) 2.307(1)
Fryzuk¹¹ 	—	178.00(4)	89.86(12) 89.32(12)	2.008(4)	2.2484(12) 2.2474(13)
Rourke¹⁷ 	—	174.42(8)	88.6(2) 93.3(2)	2.013(7)	2.329(2) 2.336(2)

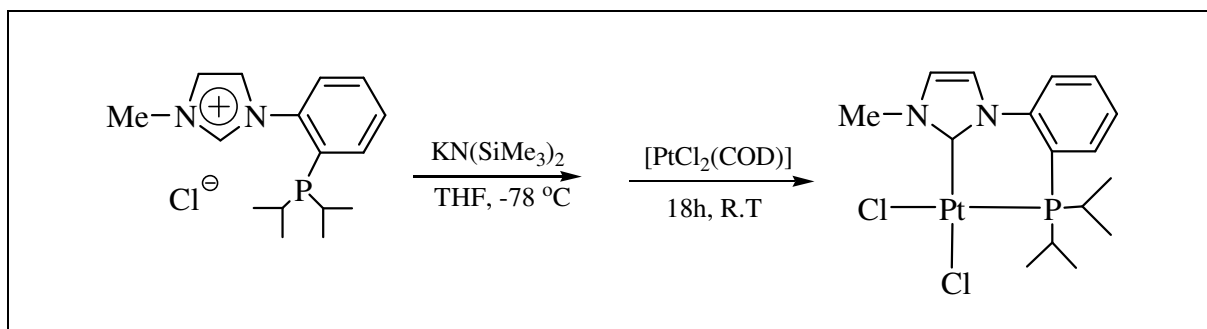
Marinetti ¹⁸ 	—	—	95.55(18)	2.051(6)	2.2886(18)
Hahn ²⁰ 	180.00(15)	180.00(15)	90.18(7) 90.18(7) 89.82(7) 89.82(7)	2.026(2) 2.026(2)	2.3070(6) 2.3070(6)
Hahn ²⁰ 	180.0(2)	180.00(6)	90.10(9) 90.10(9) 89.90(9) 89.90(9)	2.023(3) 2.023(3)	2.3005(8) 2.3005(8)

3.3.3.2: Mono-(phosphine-NHC) Pt(II) complex, **3.7**

The mono-(phosphine-NHC) Pt(II) complex, **3.7**, could be prepared either directly from the free carbene, or *via* transmetallation with the Ag-carbene complex.

A. *Via* Free Carbene:

Following the same synthetic procedure described above, the mono-(phosphine-NHC) platinum(II) complex, **3.7** was obtained from the stoichiometric reaction of the Pt(II) precursor, [PtCl₂(COD)], with the phosphine-carbene formed from the imidazolium salt, **2.6**, by action of a base; the product mono-(phosphine-NHC) Pt(II) complex was isolated as a pale brown solid, Scheme 3.9.

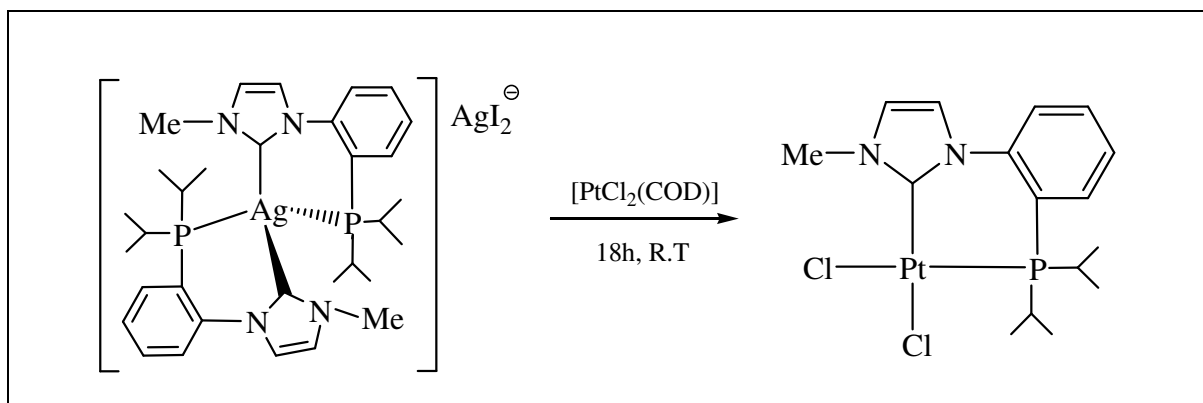


Scheme 3.9: Formation of Pt-complex, **3.7**, *via* free carbene

B. *Via* Transmetallation:

The synthesis of the phosphine-NHC platinum(II) complex, **3.7**, was also achieved *via* transmetallation from the corresponding Ag(I) complex **3.2** when half a molar quantity of complex **3.2** was reacted with the Pt(II) precursor, [PtCl₂(COD)]. The reaction was deemed to be complete when no more silver chloride precipitated from the reaction mixture. Again, the Pt(II) product complex was isolated as a pale brown solid, Scheme 3.10; crystals suitable for X-ray crystallography could not be obtained.

The product, Pt(II) complex **3.7**, was characterised by ¹H, ¹³C, ³¹P-NMR and high resolution mass spectroscopies. The ¹H-NMR spectrum of **3.7**, in CDCl₃, gave broad peaks in the aliphatic region but clearly shows the coordination of the carbene to the platinum by the absence of the distinctive protonated carbene proton, ^{im}C₁-H, Figure 3.11.



Scheme 3.10: Formation of Pt-complex, **3.7**, *via* transmetallation

A characteristic singlet was observed in the ³¹P{¹H}-NMR spectrum at 16 ppm, in CDCl₃, Figure 3.11, indicating that only one product was formed from this reaction and that the ligand chelates the metal. Two platinum satellites are also observed as would be expected

($^1J_{\text{Pt-P}} = 4449 \text{ Hz}$). The Pt-P coupling in the bis(P-NHC)Pt complex, **3.6**, (2790 Hz) is substantially smaller than the coupling observed in the mono (P-NHC)Pt complex, **3.7**, (4449 Hz); a difference of about 1660 Hz. The geometrical distribution of P *cis* or *trans* to halide in mixed ligand complexes has previously been inferred from the magnitude of $J_{\text{P-Pt}}$ coupling constants. It is known^{21,22} that typical $J_{\text{P-Pt}}$ values lie in a range around 2500 Hz and less for P *cis* to a halide or around 3500 Hz and above for P *trans* to a halide. These observations have been validated in a number of complexes reported by Rourke,¹⁷ Marinetti,^{18,19} Huynh²³ and Hahn.²⁴ For complex **3.7**, the coordinated P atom is *trans* to chloride which go in parallel with the above mentioned observation. The bis-chelate complex, **3.6**, has a lower $^1J_{\text{Pt-P}}$ value. The *trans* phosphine arrangement weakens (or reduces the sigma character) the Pt-P bond due to the larger trans influence of P donors over chloride.

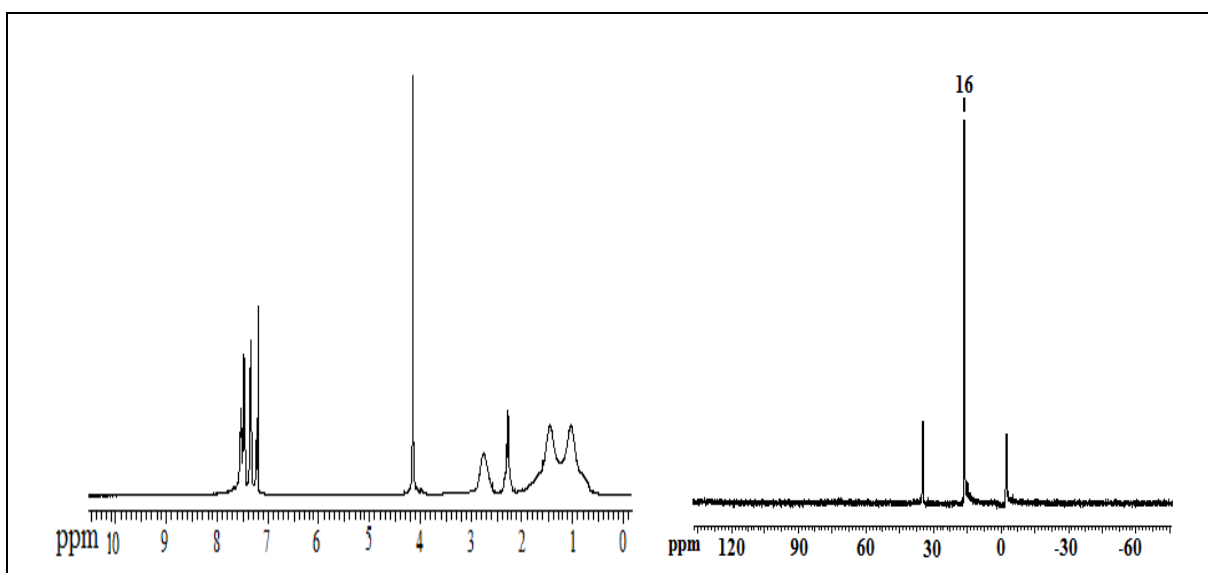
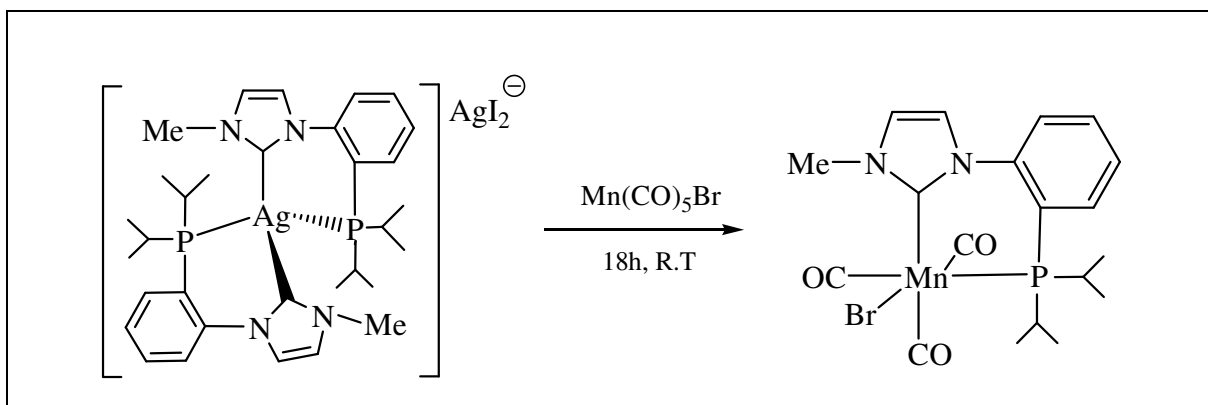


Figure 3.11: ^1H -NMR and $^{31}\text{P}\{^1\text{H}\}$ -NMR spectra of Pt-complex **3.7**, in CDCl_3 .

3.4: Results and discussion of NHC-phosphine complexes of Mn

Via Transmetallation:

The synthesis of phosphorus-NHC manganese(I) complex **3.8** was achieved *via* transmetallation from the corresponding Ag(I) complex **3.2**. Reaction of half a molar quantity of the Ag(I) complex, **3.2**, with the Mn(I) precursor, $\text{Mn}(\text{CO})_5\text{Br}$ gives a yellow solid identified as the mono-(phosphine-NHC)Mn(I) bromotricarbonyl complex, **3.8**, Scheme 3.11.



Scheme 3.11: Synthesis of Mn-complex, **3.8**, via transmetalation

The product was fully characterised by ^1H , ^{13}C , ^{31}P -NMR and high resolution mass spectroscopies, and by an X-ray crystallographic determination. The ^1H -NMR spectrum of **3.8**, in CDCl_3 , shows the coordination of the carbene to the manganese metal centre by the absence of $\text{imC}_2\text{-H}$, Figure 3.12. The spectrum shows broad peaks in the aliphatic region presumably due to quadrupolar broadening from the Mn nucleus, which is commonly observed. A singlet was observed in the $^{31}\text{P}\{^1\text{H}\}$ -NMR spectrum, in CDCl_3 , at 48.4 ppm due to the Mn-coordinated phosphine exhibiting a substantial coordination chemical shift of (*ca.*) 55 ppm, Figure 3.12. The molecular ion was observed in the mass spectrum.

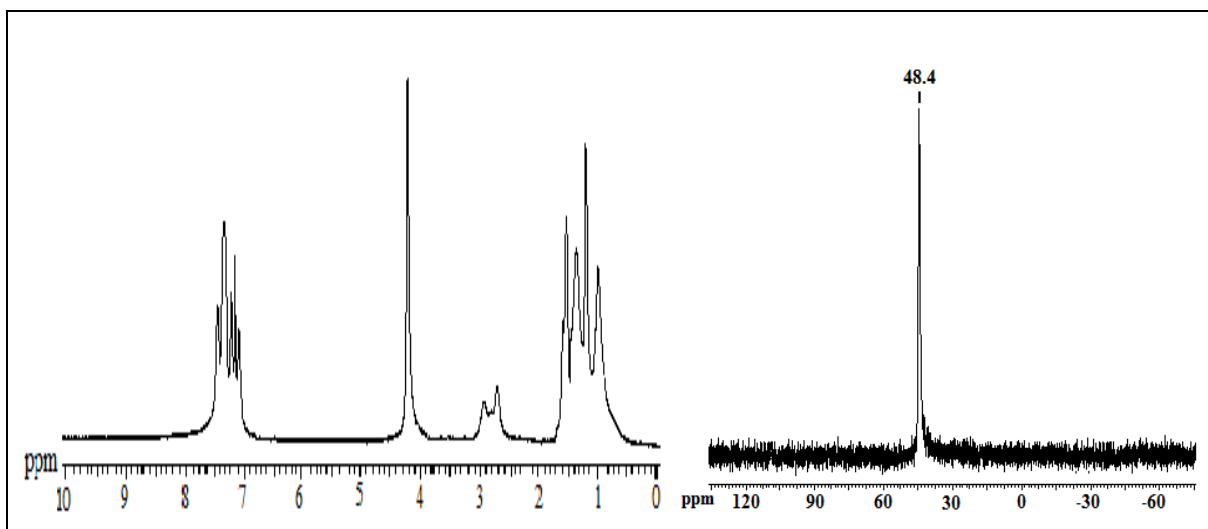


Figure 3.12: ^1H -NMR and $^{31}\text{P}\{^1\text{H}\}$ -NMR spectra of Mn-complex, **3.8**, in CDCl_3

Crystals suitable for a single crystal X-ray crystallographic determination were obtained by cooling a saturated solution of **3.8** (in MeOH at 5 $^\circ\text{C}$). The crystal structure and

labelling Scheme for **3.8** is shown in Figure 3.13. The structure of complex **3.8** is constituted of a single ligand unit bound to a manganese bromo-tricarbonyl fragment in a distorted octahedral geometry around the manganese metal centre. The bromine occupies a *cis*-position to both chelating arms of the carbene and the phosphine atoms; thus the P and C donors both appear to prefer coordination *trans* to the higher *trans* effect (carbonyls) than the low *trans* effect (bromine). Distortions from idealised octahedral parameters are confirmed by the deviation of the C₁-Mn-C₁₈ (178.05°) and the C₁₇-Mn-P angles (171.8°) from the ideal 180°. These angles are similar to the data reported by Edwards and Hahn *et al.* for similar chelating carbene-phosphine ligands.²⁵ Like the nickel complex, the C₁-Ni-C₁₈ angle is closer to linearity than is the P₁-Ni-P₂ angle.

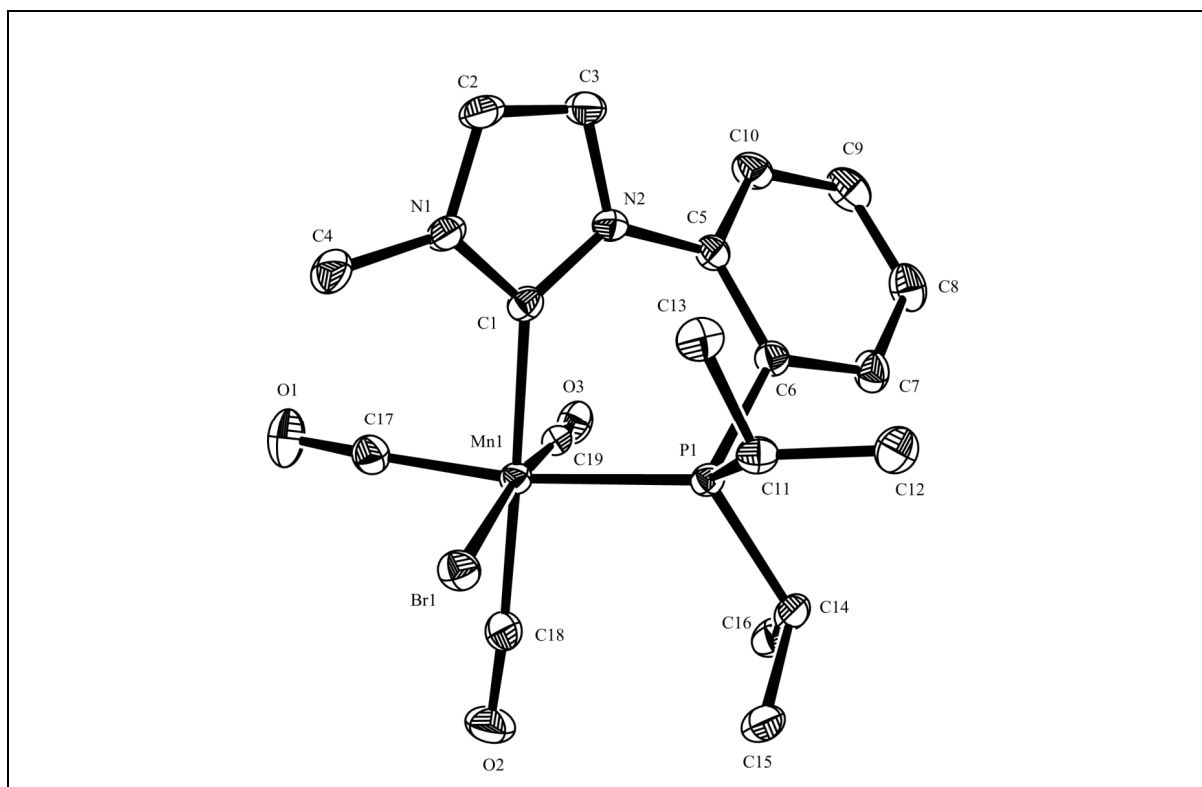


Figure 3.13: Molecular structure of Mn-complex (ORTEP projection of compound **3.8**, in CD₃OD, 40% probability ellipsoids, hydrogen atoms are omitted for clarity, Appendix: Data Set 5)

The six-membered ring formed by the two chelating donors to the metal centre is twisted and the ligand bite angle (for the chelating unit) is 82.5°. This bite angle is close to that of related manganese(I) phosphine-NHC complexes (e.g. 81.6°).²² The Mn-C(1) bond

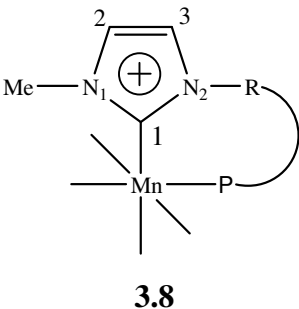
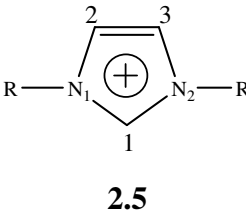
length in **3.8** is in the normal range, 2.047(3) Å, and again is similar to values in related complexes although the Mn-P(1) bond length, 2.3171(8) Å, is longer than in previously reported analogues.²⁵ Angles within the imidazole ring, N(1)-C(1)-N(2), 103.6(2)° are within the expected range 101° -106°.¹⁴ Selected bond lengths and angles are collected in Table 3.5.

Table 3.5: Some selected bond lengths and angles for P-NHC manganese complex, **3.8**.

Bond Lengths(Å)				Bond Angles (°)	
P(1)-Mn(1)	2.317(1)	C(6)-P(1)	1.835(3)	C(1)-Mn(1)-P(1)	82.5(0)
Br(1)-Mn(1)	2.593(7)	C(11)-P(1)	1.861(3)	C(1)-Mn(1)-Br(2)	96.3(8)
C(1)-Mn(1)	2.047(3)	C(14)-P(1)	1.856(3)	C(1)-Mn(1)-C(17)	89.6(9)
C(17)-Mn(1)	1.824(3)			C(1)-Mn(1)-C(18)	178.0(5)
C(1)-N(1)	1.359(4)			C(1)-Mn(1)-C(19)	91.2(9)
C(1)-N(2)	1.370(4)			P(1)-Mn(1)-Br(1)	88.0(4)
C(18)-Mn(1)	1.815(3)			N(1)-C(1)-N(2)	103.6(2)
C(19)-Mn(1)	1.823(4)				

In Mn-complex, **3.8**, bond length of C₂-C₃ and N₁-C₄ are 1.337(5) and 1.463(4) which nearly match the bond length of the same position in the free ligand **2.5**, 1.334(8) and 1.460(7) respectively. However, the ¹H-NMR spectrum show multiplet peaks of these two imidazolinium protons, C₂-H and C₃-H, due to the paramagnetic behaviour of Mn. C₁-N₁ (1.359(4) Å) and C₁-N₂ (1.370(4) Å) get longer than their analogous bonds in the ligand **2.5**, (1.313(7) and 1.34(7) Å), Table 3.6. It may due to the σ- donation from the carbene to the metal and negligible back bonding from the metal to the vacant carbene orbitals. The Mn-C(carbonyl) bond lengths are 1.815 (3), 1.823(4) and 1.824(3) which are in the average range. However, the observed shortest bond length of the carbonyl (CO) is the one (C₁₉- O₃) being *trans* to bromine due to the oxygen back bonding to the carbon, Table 3.6.

Table 3.6: Comparison of selected bond lengths (Å) for phosphorus-NHC manganese complex, **3.8**

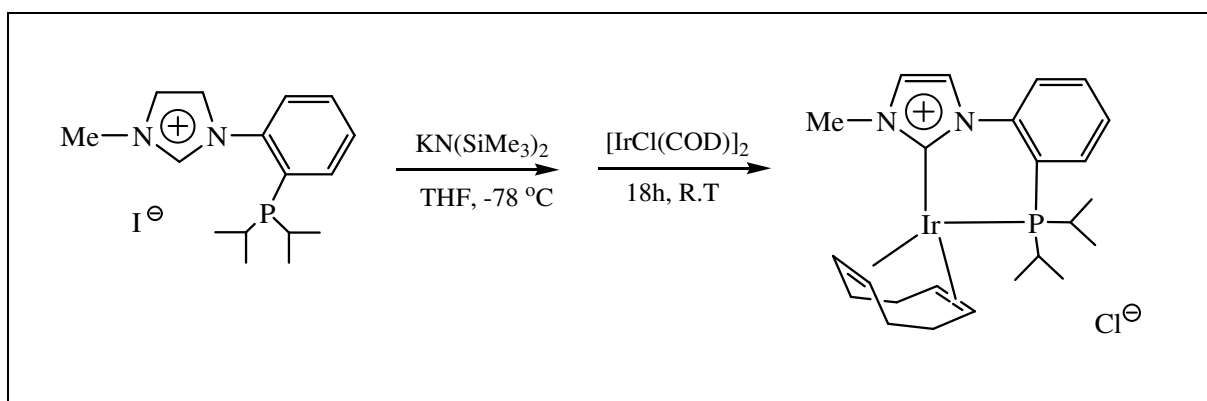
Bond Compound	C ₁ -N ₁	C ₁ -N ₂	C ₄ -N ₁	Mn-C ₁₇ Mn-C ₁₈ Mn-C ₁₉	C ₁₇ -O ₁ C ₁₈ -O ₁ C ₁₉ -O ₃
 3.8	1.359(4)	1.370(4)	1.463(4)	1.824(3) 1.815(3) 1.823(4)	1.141(4) 1.152(4) 1.057(4)
 2.5	1.313(7)	1.341(7)	1.460(7)	—	—

3.5: Results and discussion of NHC-phosphine complexes of Ir

Via Free Carbene:

The same work-up methodology as previously reported for complexes synthesised by the formation of free carbene was followed. When phosphine-imidazolium salt **2.5** was reacted with one equivalent of base of $\text{KN}(\text{SiMe}_3)_2$ in THF at -78°C , the imidazolium salt was rapidly deprotonated by the base to form the carbene, Scheme 3.12. The deprotonation was complete in about 15 minutes and the solution was added *via* a cannula into a second Schlenk containing one equivalent of the Ir(I) precursor, $[\text{IrCl}(\text{COD})]_2$. The mixture was left stirring at this temperature for another ten minutes and then allowed to reach ambient temperature and stirred for 18 hours. After the reaction, THF was evaporated, and DCM was added to extract the crude product. DCM was removed under vacuum and the addition of

Et₂O led to the isolation of a red/brown solid, as mono-(phosphine-NHC) Ir(I) complex, **3.9**, Scheme 3.12.



Scheme 3.12: Attempted synthesis of Ir-complex, **3.9**, *via* free carbene

Although there was no $_{\text{im}}\text{C}_2\text{-H}$ proton in the ^1H -NMR, Figure 3.14, broad peaks were present in the aliphatic region of the spectra and made it difficult to interpret clearly. Attempts to isolate complex **3.9** as a pure compound *via* recrystallization failed. The ^{31}P -NMR spectrum, in CDCl_3 , showed no sign of the free phosphine, but a single peak at 0.4 ppm indicated the formation of a new Ir(I) complex, Figure 3.14. The mass spectrometry data showed one highest fragment peak at 573.2 amu corresponding to the molecular mass of the mono-(phosphine-NHC) iridium(I) complex minus one proton, $[\text{M-H}]$.

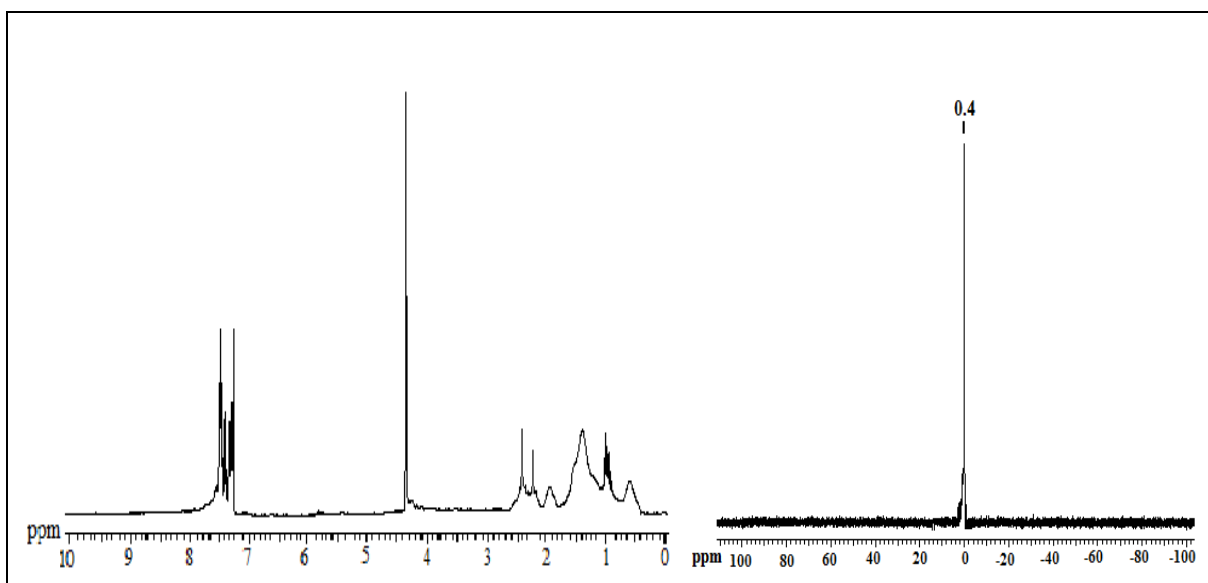


Figure 3.14: ^1H -NMR and $^{31}\text{P}\{^1\text{H}\}$ -NMR spectra of Ir-complex, **3.9**, in CDCl_3

3.6: Conclusion:

New manganese, iridium, group 10, and group 11 metal phosphine-NHC complexes have been prepared and characterised by spectroscopic means, including ^1H , ^{13}C and ^{31}P -NMR and mass spectrometry and in some cases by elemental analysis. These complexes are synthesised *via* known methods such as formation of free carbene or by transmetallation. Complexes of Au (**3.1**), Cu (**3.3**), Ni (**3.4**), Pd (**3.5**), Pt-bis (**3.6**), Pt-mono (**3.7**) and Ir (**3.9**) metals were solely synthesised *via* the formation of free carbene, while complexes of Pd (**3.5**) and Pt-mono (**3.7**) metals were synthesised by both free carbene and by transmetallation from the corresponding silver(I) complex **3.2**. The Mn complex (**3.8**) was prepared by transmetallation. Solid state structures of complexes **3.4**, **3.6** and **3.8** have been obtained by crystallographic measurements, showing some information and properties in depth of these chelating ligands. Some metal complexes have mono chelating unit and others are bis chelating unit, where each unit is a bi-dentate stems of carbene and phosphine groups.

The complexes formed clearly demonstrate that this carbene-phosphine ligand forms robust chelate complexes. In examples where two carbene-phosphine ligands coordinate the same central metal ion, a *trans* orientation of phosphines (P *trans* to P) and carbenes is observed.

3.7: Experimental

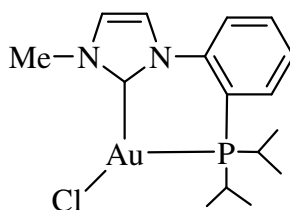
3.7.1: General Comments and Materials:

Acetonitrile (MeCN) was dried over 3Å molecular sieves and calcium hydride. Petrol was initially dried over sodium wire and distilled under nitrogen and over sodium wire. NMR deuterated solvents (MeOD and CD₃CN) were purchased from Aldrich or Across Fisher. KN(SiMe₃)₂ was purchased from its commercial supplier and kept inside a glove box and used as it's. Metal precursors such as NiCl₂.DME^{26,27}, PdCl₂(COD), PtCl₂(COD),^{28,29} [Cu(MeCN)₄]BF₄,³⁰ and [IrCl(COD)]₂^{31,32} were prepared by known procedures. However, the metal precursors of MnCO₅Br, K₂PtCl₄, Pd(OAc)₂, Ag₂O and (Me₂S)AuCl were purchased from commercial suppliers.

The other relevant general comments and materials are detailed in the experimental section in chapter 2, (2.4.1).

3.7.2 Preparation of Complexes

Synthesis of mono-(phosphine-carbene) Au(I) complex (3.1):

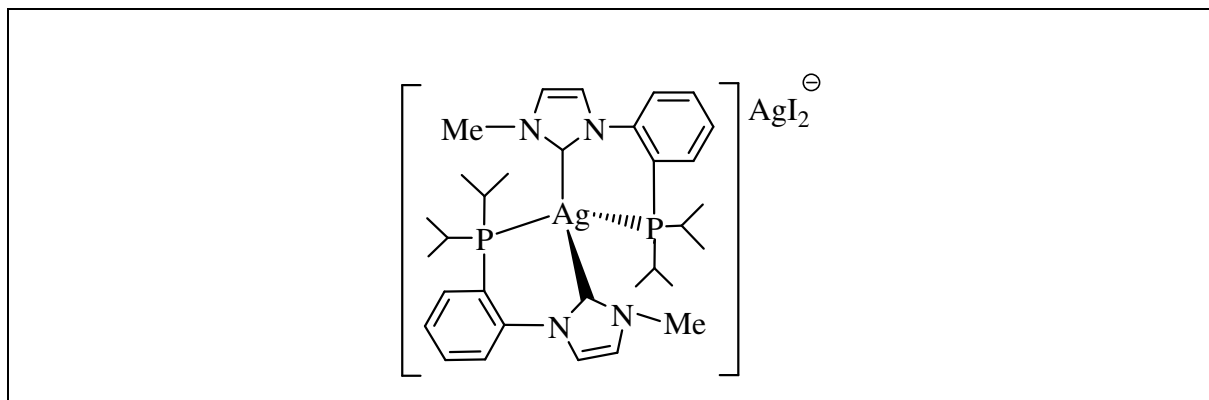


(Via Free Carbene):

To a mixture of phosphine-imidazolium salt (**2.5**) (0.10 g, 0.248 mmol) (1 equiv.) and KN(SiMe₃)₂ (0.054 g, 0.273 mmol) (1.1 equiv.) was added pre-cooled THF (50 ml at -78 °C). The resulting mixture was stirred at this temperature for 10 min., then added *via* a cannula to a pre-cooled gold precursor (Me₂S)AuCl (0.073 g, 0.248 mmol) (1 equiv.) in THF (30 ml). The mixture was left stirring at this temperature for another 10 min. and then allowed to reach ambient temperature, and stirred for 18 h. No precipitate was formed. The solvent was removed under vacuum to give a brown solid which was dissolved in DCM and Et₂O was

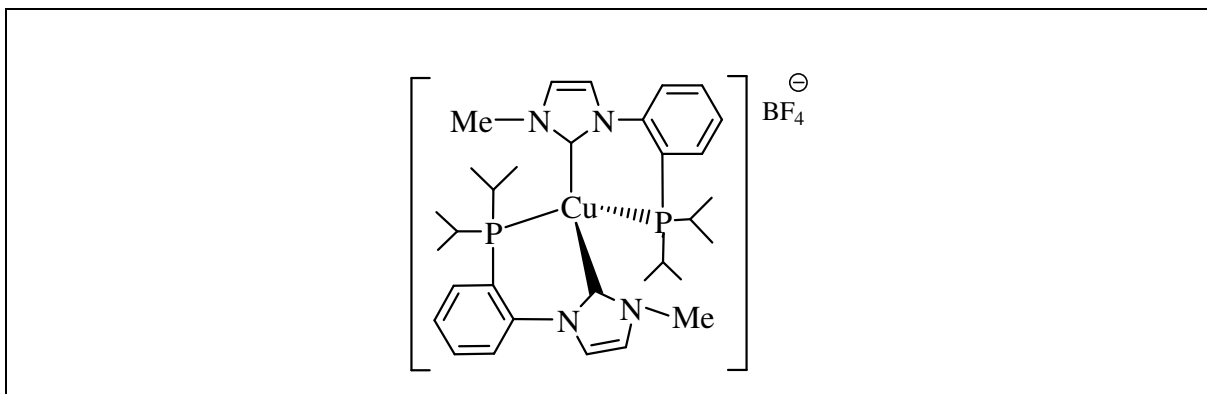
added (3x30 ml) to precipitate the light brown product complex in 20% yield. ^1H NMR (500 MHz, CDCl_3 , δ): 7.64 (s, 1H, $\text{imH}_{2/3}$), 7.52 (m, 2H, H_{Ar}), 7.47 (s, 1H, $\text{imH}_{2/3}$), 7.45 (m, 2H, H_{Ar}), 4.0 (s, 3H, Me), 1.28 (m, 1H, $\text{CH}_{11/14}$), 1.25 (m, 1H, $\text{CH}_{11/14}$), 0.85 (m, 12H, CH_3). ^{31}P NMR (202.5 MHz, CDCl_3 , δ): 47.8 ppm. MS (ES⁺): M/z (%); 745.2831 [M]

Synthesis of bis-(phosphine-carbene) Ag(I) complex (3.2):



To a mixture of phosphine-imidazolium salt (**2.5**) (0.1 g, 0.248 mmol) (2 equiv.) and Ag_2O (0.043, 0.186 mmol) (1 equiv.) dried and degassed 4Å molecular sieves was added DCM (50 ml at ambient temperature). The resulting mixture was stirred in the dark at this temperature for 18 h. The solvent was filtered three times into another Schlenk and the precipitate was washed once with DCM. The combined solvents were removed under vacuum to give a light grey solid. The solid was washed twice with Et_2O (2x20 ml) and then extracted into DCM (2x20 ml), filtered and dried *in vacuo*; yield is (80%). ^1H NMR (400 MHz, CDCl_3 , δ): 7.50 (m, 6H, H_{Ar}), 7.20 (s, 2H, H_{Ar}), 7.10 (s, 2H, $\text{imH}_{2/3}$), 6.95 (s, 2H, $\text{imH}_{2/3}$), 3.77 (s, 6H, Me), 2.25 (m, 4H, $\text{CH}_{11,14/27,30}$), 1.10 (dd, J= 6.9, 17.8, 12H, CH_3), 0.95 (dd, J= 6.9, 14.5, 12H, CH_3) ppm. ^{13}C NMR (125.75 MHz, CDCl_3 , δ): 181.4 (s, C), 145.3 (d, J=13.75, C), 133.5 (s, CH), 131.5 (s, CH), 129.4 (d, J= 32.5, CH), 128.7 (s, CH), 123.8 (d, J=35, CH), 122.8 (s, CH), 116.7 (d, J= 20, CH), 39.9 (s, CH_3), 24.9 (s, CH), 19.9 (d, J= 13.75 CH_3), 19.1 (d, J= 31.25, CH_3) ppm. ^{31}P NMR (202.5 MHz, CDCl_3 , δ): 5.43 ppm. MS (ES⁺): M/z; 655.2 $[\text{M}-\text{H}]^+$, 671.2 $[\text{M}+\text{Me}]^+$. MS (ES⁻): M/z; 360.6 $[\text{M}-\text{H}]$.

Synthesis of bis-(phosphine-carbene) Cu (I) complex (3.3):



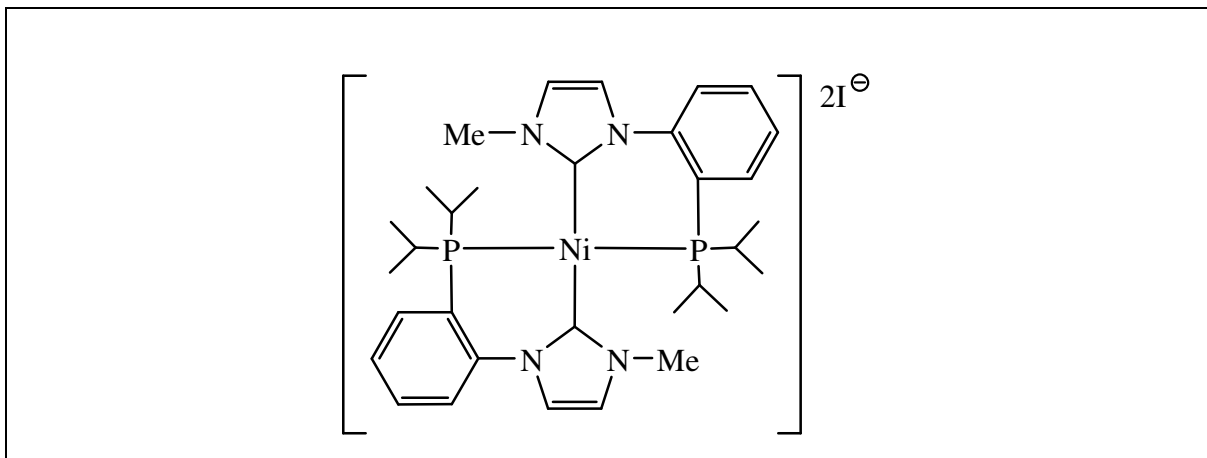
(Via Free Carbene):

To a mixture of phosphine-imidazolium salt (**2.5**) (0.15 g, 0.373 mmol) (1 equiv.) and $\text{KN}(\text{SiMe}_3)_2$ (0.082 g, 0.41 mmol) (1.1 equiv.) was added pre-cooled THF (50 ml at -78°C). The resulting mixture was stirred at this temperature for 10 min., then added *via* a cannula to a pre-cooled copper precursor $[\text{Cu}(\text{MeCN})_4]\text{BF}_4$ (0.058 g, 0.186 mmol) (0.5 equiv.) in THF (30 ml). The mixture was left stirring at this temperature for another 10 min. and then allowed to reach r.t. and stirred for 18 h. The precipitated solid was filtered and washed with THF (2x20 ml) and then Et_2O (2x20 ml) and then extracted into DCM (2x20 ml). The DCM was removed under vacuum to give an off-white solid.

(Via transmetallation):

To a mixture of $[\text{Cu}(\text{MeCN})_4]\text{BF}_4$ (0.015 g, 0.098 mmol) and the silver adduct of the carbene-phosphine complex, **3.2**, (0.05 g, 0.049 mmol) was added DCM (0 ml) and the mixture left to stir at r.t. for 18 h. The solution was filtered. DCM was removed under vacuum and the resulting solid was washed twice with Et_2O (20x2). The resulting pale brown solid was re-crystallised from DCM/ Et_2O to give the product which was then dried under vacuum. Yield is (25%). ^1H NMR (500 MHz, CDCl_3 , δ): 7.47 (m, 2H, H_{Ar}), 7.32 (m, 6H, H_{Ar}), 7.24 (s, 4H, $\text{imH}_{2,3}$), 3.45 (s, 6H, Me), 2.14 (m, 4H, $\text{CH}_{11,14/27,30}$), 0.87 (br, 12H, CH_3), 0.60 (br, 6H, CH_3), 0.38 (dd, $J=17.5, 7.5$, 6H, CH_3) ppm. ^{13}C NMR (125.75 MHz, CDCl_3 , δ): 189.1 (s, C), 144.2 (d, $J=10$, C), 132.8 (s, CH), 130.9 (s, CH), 126.7 (s, CH), 124.6 (d, $J=3.75$, CH), 123.7 (d, $J=7.5$, CH), 123.1 (s, CH), 121.0 (s, CH), 38.2 (s, CH_3), 22.7 (s, CH), 22.2 (s, CH), 18.7 (s, CH_3), 17.8 (s, CH_3), 17.1 (s, CH_3) ppm. ^{31}P NMR (121.7 MHz, CDCl_3 , δ): 3.8 ppm. MS (ES⁺): M/z ; 611.1 $[\text{M}-\text{H}]^+$. Anal.: Calc. For $\text{C}_{32}\text{H}_{46}\text{N}_4\text{P}_2\text{CuBF}_4$: C, 54.98; H, 6.63; N, 8.01%. Found: C, 50.31; H, 6.03; N, 7.13%.

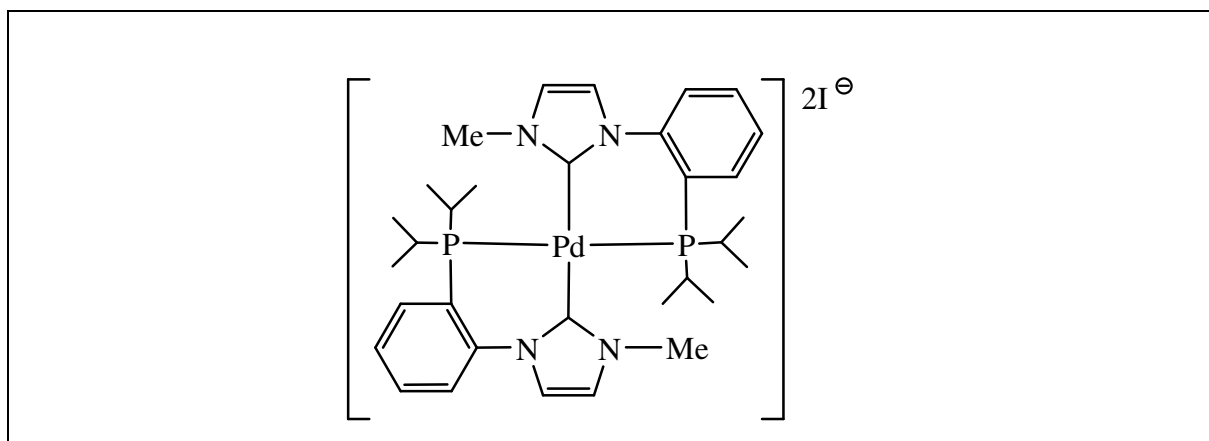
Synthesis of bis-(phosphine-carbene) Ni(II) complex (3.4):



(Via Free Carbene)

To a mixture of phosphine-imidazolium salt (**2.5**) (0.10 g, 0.25 mmol) (1 equiv.) and $\text{KN}(\text{SiMe}_3)_2$ (0.055 g, 0.276 mmol) (1.1 equiv.) was added pre-cooled THF (50 ml at -78°C). The resulting mixture was stirred at this temperature for 10 min., then added *via* a cannula to a pre-cooled nickel precursor $\text{NiCl}_2\cdot\text{DME}$ (0.055 g, 0.25 mmol) (1 equiv.) in THF (30 ml). The mixture was left stirring at this temperature for another 10 min. and then allowed to reach room temperature, and stirred for 18 h after which time the reaction had ceased and a precipitate formed. The supernatant was decanted and the solid washed twice with THF and extracted into DCM. The solution was left to settle for about 2h whereupon a yellow precipitate formed. The solid was re-crystallised from EtOH. Yield (0.13g, 32%). ^1H NMR (500 MHz, CD_3CN , δ): 7.75–7.4 (m, 12H, H_{Ar}), 4.20 (s, 6H, Me), 2.58 (m, 2H, $\text{H}_{11/14}$), 2.34 (m, 2H, $\text{H}_{27/30}$), 0.82 (dd, $J = 14.2, 7.0$, 3H, CH_3), 0.55 (dd, $J = 14.9, 7.4$, 3H, CH_3), 0.42 (m, 18H, 6 CH_3) ppm. ^{13}C NMR (125.75 MHz, CD_3CN , δ): 134.1 (d, $J = 17.5$, CH), 129.2 (d, $J = 37.5$, CH), 123.5 (d, $J = 47.5$, CH), 38.5 (s, CH_3), 27.4 (d, $J = 11.25$, CH), 20.3 (d, $J = 26.25$, CH), 17.0 (d, $J = 7.5$, CH_3), 16.5 (s, CH_3), 13.9 (s, CH_3) ppm. ^{31}P NMR (202.5 MHz, CD_3CN , δ): 36.9 ppm. MS (ES+): M/z (%); 303.13 (100) $[\text{M}/2]$, 734 (67) $[\text{M}+\text{I}]^+$, 648.3 (20) $[\text{M}+\text{CH}_3\text{CN}]^+$. X-Ray: Single crystals of the nickel complex **3.4** were obtained from a saturated solution in ethanol (EtOH) at 5°C .

Synthesis of bis-(phosphine-carbene) Pd(II) complex, using [PdCl₂COD] (3.5):



Method # 1 (Via Free Carbene):

Using (2.5):

To a mixture of phosphine-imidazolium salt (**2.5**) (0.1 g, 0.248 mmol) (1 equiv.) and KN(SiMe₃)₂ (0.05 g, 0.273 mmol) (1.1 equiv.) was added pre-cooled THF (30 ml at -78 °C). The resulting mixture was stirred at this temperature for 10 min. and then added *via* a cannula to a stirred solution of pre-cooled palladium precursor PdCl₂(COD) (0.071 g, 0.248 mmol) (1 equiv.) in THF (30 ml at -78 °C). The mixture was left stirring at this temperature for another 10 min and then allowed to reach ambient temperature and stirred for 18 h. THF was removed under vacuum and the solid washed twice with Et₂O (2x20ml). The solid was extracted into EtOH, filtered and the solvent removed *in vacuo* to give the product as a light brown solid.

Using (2.6):

Reacting the palladium precursor mentioned above with the chloride adduct precursor (**2.6**) by following the same reaction steps as using the iodide (**2.5**) gave the same Pd-complex.

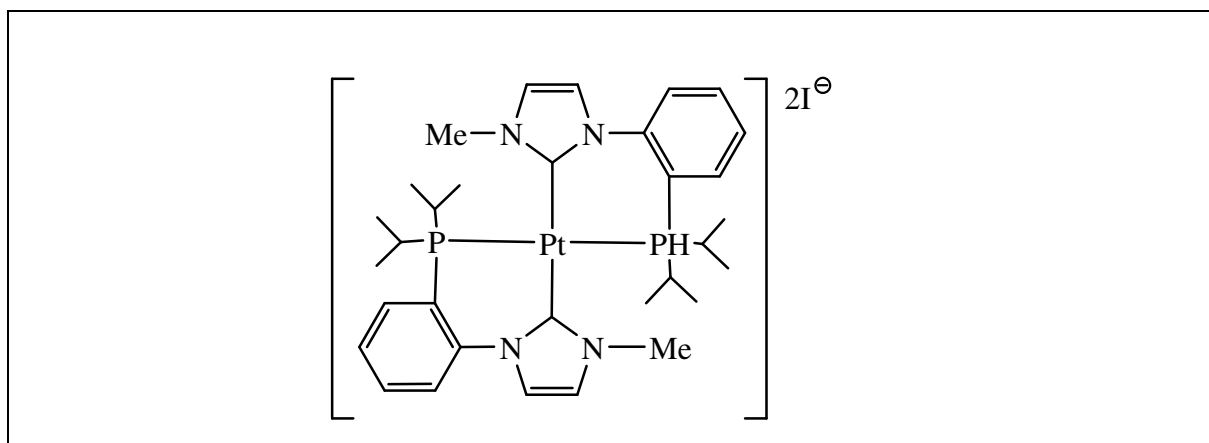
Method # 2 (Via Transmetallation):

To a mixture of PdCl₂(COD) (0.084 g, 0.295 mmol) and the silver adduct of the carbene-phosphine complex, **3.2**, (0.15 g, 0.147 mmol) was added DCM (80 ml) and the mixture left to stir in at ambient temperature for 18 h in the dark. The solution was filtered and DCM was removed under vacuum. The residue was washed twice with Et₂O (20x2) and the resulting pale brown solid was re-crystallised from DCM/Et₂O to give the product which was then dried under vacuum.

Synthesis of bis-(phosphine-carbene) Pd(II) complex using Pd(OAc)₂, Via Free Carbene (3.5):

Following the method described above (method # 1) with the ligand **2.6** gave the product as a pale brown solid by extraction of the solid reaction residue (following evaporation of solvent *in vacuo*) into acetonitrile, filtration and evaporation *in vacuo*. Yield was (25%). ¹H NMR (400 MHz, CDCl₃, δ): 7.60 (m, 2H, H_{Ar}), 7.52 (m, 4H, H_{Ar}), 7.42 (m, 4H, H_{Ar}), 7.32 (s, 2H, H_{Ar}), 3.95 (s, 6H, Me); (400 MHz, CD₃CN, δ): 2.85 (m, 2H, CH_{11/14}), 2.27 (m, 2H, CH_{27/30}), 0.90 (dd, J=7.7, 15.53 Hz, 6H, CH₃), 0.73 (m, 6H, CH₃), 0.52 (m, 12H, CH₃) ppm. ¹³C NMR (125.75 MHz, CDCl₃, δ): 153.8 (d, J=8.75, C), 141.9 (d, J=7.5, C), 132.2 (s, CH), 130.5 (s, CH), 127.1 (d, J=6.25, CH), 126.5 (s, CH), 121.6 (d, J=6.25, CH), 120.06 (s, CH), 117.6 (d, J= 42.5, CH), 39.4 (s, Me), 27.0 (s, CH), 20.51 (s, CH), 18.2 (d, J=32.5, 2CH₃), 16.81 (s, CH₃), 15.0 (s, CH₃) ppm. ³¹P NMR (121.7 MHz, CD₃CN, δ): 37.54 ppm. MS (ES+): M/z; 696.25 [M+CH₃CN], 653.24 [M-2H], 327.1 [M/2].

Synthesis of bis-(phosphine-carbene) Pt(II) complex (3.6):

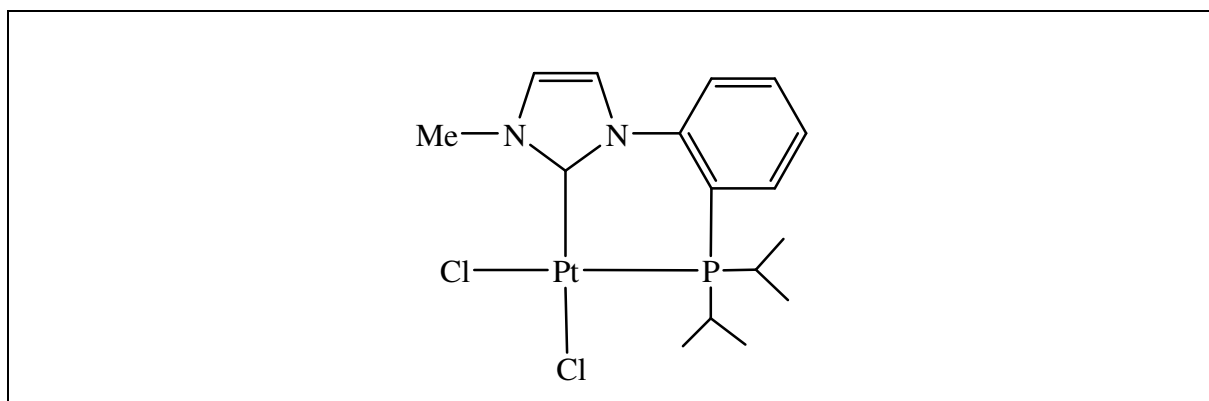


(Via Free Carbene):

To a mixture of phosphine-imidazolium iodide (**2.5**) (0.1 g, 0.25 mmol) (1 equiv.) and KN(SiMe₃)₂ (0.055 g, 0.276 mmol) (1.1 equiv.) was added pre-cooled THF (30 ml at -78 °C). The resulting mixture was stirred at this temperature for 10 min., and then added *via* a cannula to a pre-cooled solution of the platinum precursor PtCl₂(COD) (0.093 g, 0.25 mmol) (1 equiv.) in THF (30 ml). The mixture was left stirring at this temperature for another 10 min. and then was allowed to reach ambient temperature and stirred for 18 h. The solvent was filtered and the light brown precipitate was washed with THF (2x20 ml) and then Et₂O (2x20

ml) before extraction into DCM. The solid was then dried under vacuum to give the product as a yellow to brown solid. It was recrystallised from MeOH at 5 °C. Yield (0.08 g, 40%). ¹H NMR (400.13 MHz, CD₃OD, δ): 8.0-7.5 (m, 12H, H_{Ar}), 4.10 (s, 6H, Me), 2.93 (m, 2H, CH_{11,14}), 2.45 (m, 2H, CH_{11,14}), 1.68 (dd, J= 6.9, 14 Hz, 6H, CH₃), 1.58 (dd, J = 7.5, 17.5 Hz, 6H, CH₃), 0.98 (dd, J = 7.8, 19 Hz, 6H, CH₃), 0.85-0.60 (m, 6H, CH₃) ppm. ¹³C NMR (125.75 MHz, CDCl₃, δ): 143.1 (d, J=5, C), 142.3 (d, J=12.5, C), 133.1 (s, CH), 131.0 (s, CH), 127.6 (d, J=7.5, CH), 126.6 (s, CH), 122.6 (d, J=5, CH), 120.3 (s, CH), 117.8 (d, J=50, CH), 39.7 (s, CH₃), 18.0 (d, J=13.75, CH₃), 17.8 (d, J=20, CH₃) ppm. ³¹P NMR (121.7 MHz, CD₃OD, δ): 29.68 (¹J_{Pt-P} = 2790 Hz) ppm. MS (ES+): M/z (%); 870.1 (13) [M+I]⁺, 371.7 (100) [M/2]. X-Ray: Single crystals of platinum complex **3.6** were obtained from a saturated solution in methanol (MeOH) at 5 °C.

Synthesis of mono-(phosphine-carbene) Pt(II) complex (**3.7**):



Two methods were applied to get the mono-(phosphine-NHC) platinum complex, **3.7**.

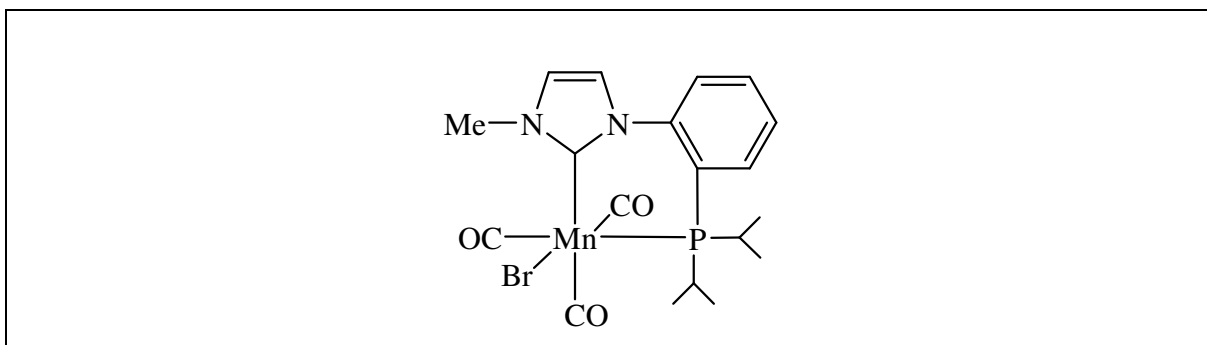
Method # 1 (Via Free Carbene):

To a mixture of phosphine-imidazolium salt (**2.6**) (0.1 g, 0.32 mmol) (1 equiv.) and KN(SiMe₃)₂ (0.0635 g, 0.354 mmol) (1.1 equiv.) was added pre-cooled THF (30 ml at -78 °C). The resulting mixture was stirred at this temperature for 10 min., then added *via* a cannula to a pre-cooled solution of platinum precursor PtCl₂(COD) (0.12 g, 0.32 mmol) (1 equiv.) in THF (30 ml). The mixture was left stirring at this temperature for another 10 min. and then was allowed to reach ambient temperature and stirred for 18 h. The reaction ceased and a supernatant layer was formed. This solution was filtered; the solid residue washed once with THF (10 ml) and the combined solution and washings was then dried under vacuum. The residue was washed twice with Et₂O (2x20ml) to give the product as a light brown solid.

Method # 2 (Via Transmetallation):

To a mixture of $\text{PtCl}_2(\text{COD})$ (0.037 g, 0.098 mmol) and the silver adduct of the carbene-phosphine complex, **3.2**, (0.05 g, 0.049 mmol) was added DCM (60 ml) and the solution stirred at room temperature for 18 h. The solution was then filtered. The volume of DCM was reduced under vacuum and the resulting solid was washed with Et_2O . The resulting pale brown solid was re-crystallised from a minimum volume of DCM to give the product which was then dried under vacuum. ^1H NMR (500 MHz, CDCl_3 , δ): 7.7-7.2 (m, 6H, H_{Ar}), 4.15 (s, 3H, Me), 2.65 (br, 1H, $\text{CH}_{11/14}$), 2.3 (m, 1H, $\text{CH}_{11/14}$), 1.6-0.70 (br, 12H, CH_3) ppm. ^{13}C NMR (125.75 MHz, CDCl_3 , δ): 143.2 (d, $J=5$, C), 142.5 (d, $J=13.75$, C), 133.1 (s, CH), 131.0 (s, CH), 128.6 (s, CH), 127.6 (d, $J=7.5$, CH), 126.5 (s, CH), 122.6 (d, $J=5$, CH), 120.2 (s, CH), 39.7 (s, Me), 21.5 (br, CH), 18.0 (br, CH_3), 17.7 (br, CH_3) ppm. ^{31}P NMR (121.7 MHz, CDCl_3 , δ): 15.88 ($^1J_{\text{Pt-P}} = 4449$ Hz) ppm. MS (ES+): m/z ; 650.15 [$\text{M}+\text{COD}$], 546.1 [$\text{M}-\text{Cl}+\text{CH}_3\text{CN}$], 558.1 [$\text{M}+\text{NH}_4^+$], 505.1 [$\text{M}-\text{Cl}$].

Synthesis of mono-(phosphine-carbene) Mn (I) complex (3.8):

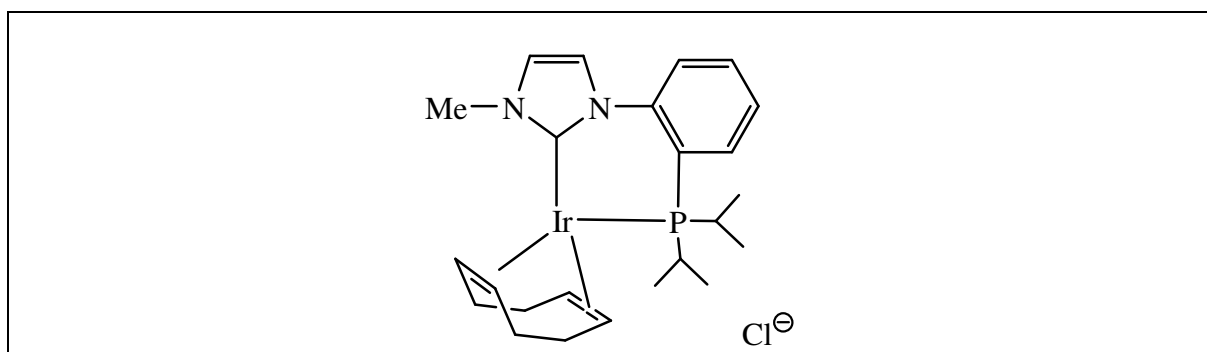


(Via Transmetallation):

To a mixture of MnCO_5Br (0.027 g, 0.098 mmol) (1 equiv) and the silver adduct of the carbene-phosphine complex, **3.2**, (0.05 g, 0.049 mmol) (1/2 equiv) was added DCM (80 ml) and the mixture stirred at ambient temperature for 18 h. The solution was then filtered and the DCM was removed under vacuum. The resulting solid was washed with petrol and Et_2O (alternatively, toluene may be substituted successfully) was added (2x30 ml) to extract the desired complex. The Et_2O was removed under vacuum to give a yellow solid in 70% yield. It was recrystallised from MeOH at 5 °C. ^1H NMR (400 MHz, CDCl_3 , δ): 7.50 (br, 1H, $\text{imH}_{2/3}$), 7.40 (br, 2H, $\text{imH}_{2/3}$), 7.20 (br, 1H, H_{Ar}), 7.16 (br, 1H, H_{Ar}), 7.10 (br, 1H, H_{Ar}), 4.30 (s, 3H, Me), 2.9 (br, 1H, $\text{CH}_{11/14}$), 2.65 (br, 1H, $\text{CH}_{11/14}$), 1.40-1.20 (br, 6H, CH_3), 1.10 (br, 3H, CH_3),

0.90 (br, 3H, CH₃) ppm. ¹³C NMR (75.57 MHz, CDCl₃, δ): 187.0 (d, J=37.5, C), 144.0 (s, C), 131.0 (s, CH), 130. (s, CH), 125.5 (s, CH), 124.5 (s, CH), 122.0 (s, CH), 121.6 (s, CH), 39.4 (s, Me), 22.0 (d, J=15, CH), 21.0 (br, CH₃), 16.5 (s, CH₃), 15.8 (s, CH₃), 14.5 (br, CH₃), 13.9 (s, CH₃) ppm. ³¹P NMR (121.7 MHz, CDCl₃, δ): 48.4 ppm. MS (ES⁺): M/z; 512 [M+NH₄⁺], 411.2 [M-2H-Br]. X-Ray: Single crystals of magnesium complex **3.8** were obtained from a saturated solution in methanol (MeOH) at 5 °C.

Synthesis of mono-(phosphine-carbene) Ir complex (**3.9**):



(Via Free Carbene):

To a mixture of phosphine-imidazolium salt (**2.5**) (0.1 g, 0.248 mmol) (1 equiv.) and KN(SiMe₃)₂ (0.055 g, 0.273 mmol) (1.1 equiv.) was added pre-cooled THF (50 ml at -78 °C). The resulting mixture was stirred at this temperature for 10 min. and then added *via* a cannula to a pre-cooled solution of the iridium precursor [IrCl(COD)]₂ (0.083 g, 0.124 mmol) (0.5 equiv.) in THF (30 ml). The mixture was left stirring at this temperature for another 10 min. and then allowed to reach ambient temperature and stirred for 18 h. The solvent was removed *in vacuo* and the solid was extracted with DCM. The DCM was removed *in vacuo* and the crude complex was extracted twice with Et₂O (2x30 ml). Et₂O was then removed under vacuum to give a red-brown solid. ¹H NMR (400 MHz, CDCl₃, δ): 7.4 (m, 2H, H_{Ar}), 7.30 (m, 2H, imH_{2,3}), 7.20 (m, 2H, H_{Ar}), 4.35 (s, 3H, Me), 2.40 (s, 1H, CH_{11/14}), 2.25 (s, 1H, CH_{11/14}), 2.05-1.80 (br, COD, CH₂), 1.70-1.05 (br, 6H, CH₃), 0.90 (m, 3H, CH₃), 0.60-0.40 (br, 3H, CH₃) ppm. ¹³C NMR (100 MHz, CDCl₃, δ): 167.8 (s, C), 144.0 (d, J=10.2, C), 129.5 (s, CH), 128.8 (d, J=27.8, CH), 128.4 (s, CH), 126.2 (d, J=3.9, CH), 124.1 (s, CH), 122.4 (d, J=4.9, CH), 119.9 (s, CH), 43.4 (s, CH₂), 38.7 (s, CH₃), 28.0 (s, CH), 18.7 (br, CH₃), 16.5 (br, CH₃), 14.0 (s, CH), 11.0 (s, CH) ppm. ³¹P NMR (121.7 MHz, CDCl₃, δ): 0.4 ppm. MS (ES⁺): M/z; 573.2 [M-H].

References

- [1] C. Bohler, D. Stein, N. Donati, H. Grutzmacher, *New J. Chem.*, **2002**, 26, 1291
- [2] M. V. Baker, P. J. Barnard, S. J. Berners-Price, S. K. Brayshaw, J. L. Hickey, B. W. Skelton, A. H. White, *J. Organomet. Chem.*, **2005**, 690, 5625.
- [3] H. M. J. Wang, B. J. I. Lin, *Organometallics*, **1998**, 17, 972.
- [4] R. J. Lane, Thesis, Cardiff University, **2006**
- [5] E. Lappert, G. Helmchen, *Syn. Lett.*, **2004**, 10, 1789.
- [6] (a) F. Chen, R. E. Wasylshen, *Magn Reson Chem.*, **2010**, 48,4, 270.
(b) K. Zangger and I. M. Armitage, *Met. Based Drugs* **1999**, 6, 4, 239.
- [7] (a) U. Letinois-Halbes, P. Pale, S. Berger, *Magn. Reson. Chem.* **2004**, 42, 831
(b) R. J. Goodfellow, *In Multinuclear NMR* (ed. J. Mason), Plenum Press: New York, **1987**, 563.
(c) P. M. Henrichs, *NMR of Newly Accessible Nuclei*, vol 2, Academic Press: new York, **1983**, 319
- [8] N. Tsoureas, A. A. Danopoulos, A. A. D. Tulloch, M. A. Light, *Organometallics*, **2003**, 22, 4750.
- [9] A. W. Waltman, R. H. Grubbs, *Organometallics*, **2004**, 23, 3105.
- [10] Ch. Ch. Lee, W. Ch. Ke, K. T. Chan, Ch. L. Lai, Ch. H. Hu, H. M. Lee, *Chem. Eur. J.*, **2007**, 13, 582.
- [11] S. Tobias, B. K. Shaw, J. Howard, O. P. Brian, M. D. Fryzuk, *Organometallics*, **2009**, 28, 2830.
- [12] K. Matsubara, K. Ueno, Y. Shibata, *Organometallics* **2006**, 25, 3422.
- [13] J. Wolf, A. Labande, J. C. Daran, R. Poli, *J. Organomet. Chem.*, 2006, 691, 433.
- [14] E. Teuma, C. L. Saunier, H. Gornitzka, G. Mignani, A. Baceiredo, G. Bertrand, *J. Organomet. Chem.*, **2005**, 690, 5541.
- [15] D. S. McGuinness, K. J. Cavell, *Organometallics*, **2000**, 19, 741
- [16] Y. J. Kim, Y. S. Kwak, Y. S. Joo, S. W. Lee, *J. Chem. Soc., Dalton Trans.*, **2002**, 144.
- [17] Ch. P. Newman, R. J. Deeth, G. J. Clarkson, J. P. Rourke, *Organometallics* **2007**, 26, 6225.
- [18] D. Brissy, M. Skander, P. Retailleau, A. Marinetti, *Organometallics*, **2007**, 26, 5782.

- [19] D. Brissy, M. Skander, P. Retailleau, G. Frison, A. Marinetti, *Organometallics*, **2009**, 28, 140.
- [20] A. F. Figueroa, T. Pape, K. O. Feldmann, F. E. Hahn, *Chem. Comm.*, **2010**, 46, 324.
- [21] C. Gallego, M. Martinez, V. S. Safont, *Organometallics*, **2007**, 26, 527.
- [22] M. Crespo, X. Solans, M. Font-Bardi'a, *J. Organomet. Chem.*, **1996**, 105.
- [23] H. V. Huynh, Y. Han, G. K. Tan, *Organometallics*, **2007**, 26, 4612.
- [24] F. E. Hahn, C. J. Mareike, T. Pape, *Organometallics*, **2006**, 25, 5927.
- [25] O. Kaufhold, A. Stasch, T. Pape, A. Hepp, P. G. Edwards, P. D. Newman, F. E. Hahn, *J. Am. Chem. Soc.*, **2009**, 131, 306.
- [26] R. J. Errington, *Advanced Practical Inorganic and Metalorganic Chemistry*, p. 246, CRC press, **1997**.
- [27] L. Kayser, R. Pattacini, G. Rogez, P. Braunstein, *Chem. Commun.*, **2010**, 46, 6461.
- [28] W. A. Hermann, A. Slazer, *Synthetic Methods of Organometallic and Inorganic Chemistry*, **1996**, 1, 168.
- [29] S. Komiya, *Synthesis of Organometallic Compounds" Apractical guid*, **1977**, 294
- [30] D. Knol, N. J. Koole, M. J. A. De Bie, *Org. Magn. Reson.*, **1976**, 8, 213.
- [31] G. Giordano, H. Crabtree, *Inorg. Chem.*, **2001**, 40, 2980.
- [32] R. H. Crabtree, G. E. Morris, *J. Organomet. Chem.*, **1977**, 135, 395.

Chapter 4

Other Attempted Complexations

4. Other attempted complexations

Attempted synthesis of NHC-phosphine complexes of Groups 4, 6, 7, 8, 9 and 10 metals:

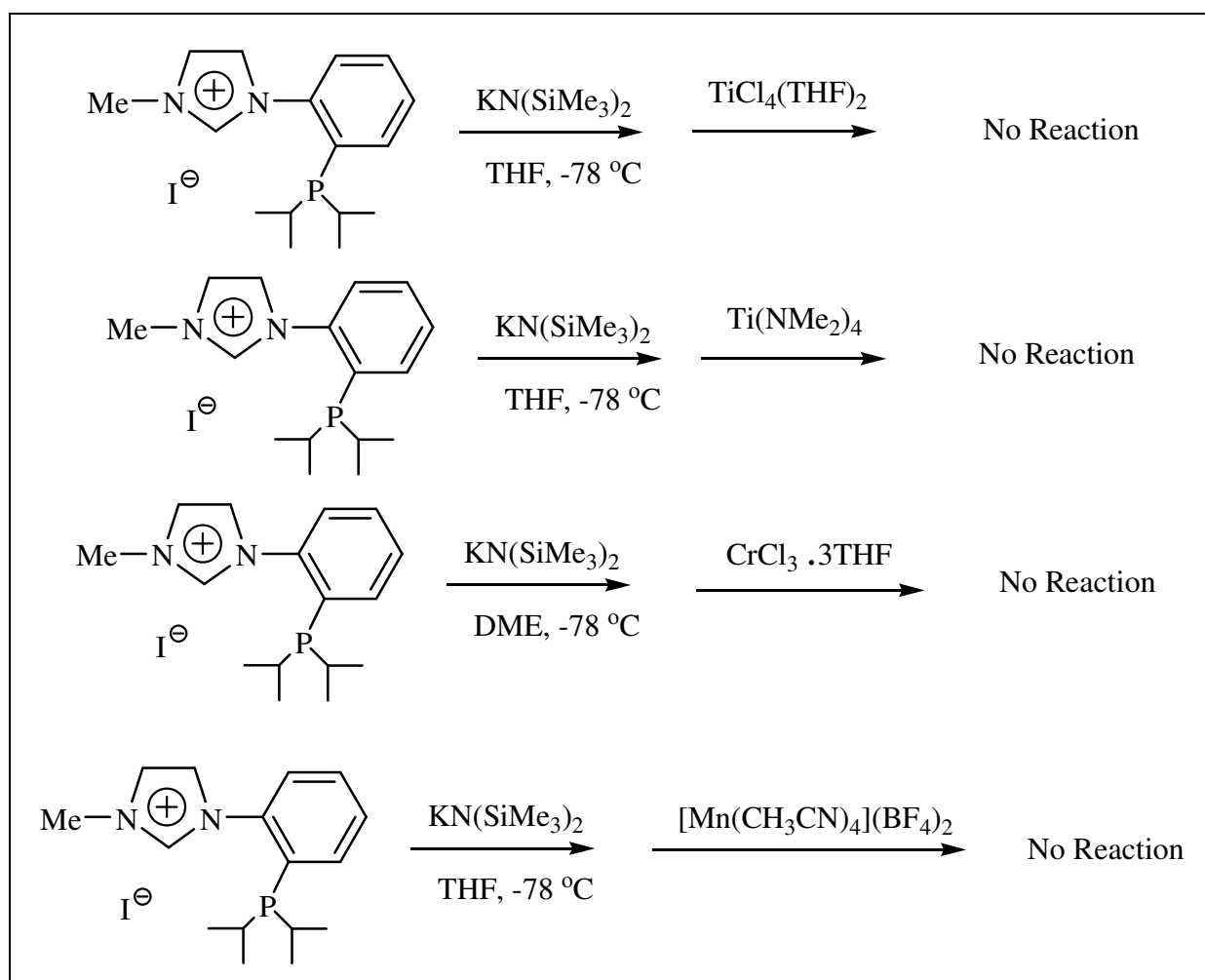
This chapter is concerned with attempted complexation of a series of the chelating carbene-phosphine ligand, **2.5**, with some metals of Groups 4, 6, 7, 8, 9 and 10: Ti(IV), Cr(3), Mn(II), Fe(II), Ru(II), Co(II), Rh(I), Ir(I), Pt(II), Pd(II). The reactions listed below are for the failed experiments. Ligand **2.5** was reacted with other metal precursors under the same conditions that were used to obtain the complexes presented and discussed in Chapter 3. General comments and materials are detailed in the experimental sections in Chapter 2 and 3.

The same work-up methodology as previously reported, in chapter 3, for complexes synthesised by the formation of free carbene (*via* free carbene) or *via* transmetallation was followed. Metal precursors, $\text{TiCl}_4(\text{THF})_2$, $\text{Ti}(\text{NMe}_2)_4$, $\text{CrCl}_3 \cdot 3\text{THF}$, $[\text{Mn}(\text{CH}_3\text{CN})_4](\text{BF}_4)_2$, $[\text{Fe}(\text{CH}_3\text{CN})_6](\text{BF}_4)_2$, $\text{Ru}(\text{DMSO})_4\text{Cl}_2$, $\text{RuCl}_2(\text{PPh}_3)_3$, $\text{RuCl}_2(\text{cymene})_4$, $[\text{Co}(\text{CH}_3\text{CN})_6](\text{BF}_4)_2$, $\text{Rh}_2\text{Cl}_2(\text{COD})_2$, $\text{Rh}_2\text{Cl}_2(\text{CO})_4$, and $\text{Ir}_2\text{Cl}_2(\text{COT})_4$, were reacted with the ligand, **2.5**, *via* the formation of free carbene. Rh and Ir precursors, $\text{Rh}_2\text{Cl}_2(\text{COD})_2$, $\text{Rh}_2\text{Cl}_2(\text{CO})_4$, $\text{Ir}_2\text{Cl}_2(\text{COD})_2$ and $\text{Ir}_2\text{Cl}_2(\text{COT})_4$, were also reacted with the ligand, **2.5**, by transmetallation from the corresponding Ag(I) complex **3.2**.

Via free carbene, a phosphine-imidazolium salt, **2.5**, was reacted with one equivalent of base of $\text{KN}(\text{SiMe}_3)_2$ in THF at -78°C . The imidazolium salt was deprotonated by the base to form the carbene. The deprotonation was complete in about 15 minutes and the solution was added into a second Schlenk containing one equivalent of the metal precursors. The mixture was stirred at this temperature for another ten minutes and then allowed to reach ambient temperature and stirred for 18 hours. In case the product was dissolved in the solution, THF was evaporated, and DCM was added to extract the crude product which was extracted by the addition of Et_2O . In case the product was solid, the precipitated solid was filtered and washed with THF and Et_2O and then extracted into DCM. The DCM was removed under vacuum to give the product. The isolated solids were investigated by $^{31}\text{P}\{\text{H}\}$ -NMR to check on their purity.

Via Transmetallation, to a mixture of a metal precursor and the silver adduct of the carbene-phosphine complex, **3.2**, was added DCM and the mixture left to stir at r.t. for 18 h. The solution was filtered. DCM was removed under vacuum and the resulting solid was washed with Et_2O . The resulting solid was recrystallised from DCM/ Et_2O to give a product which was then dried under vacuum.

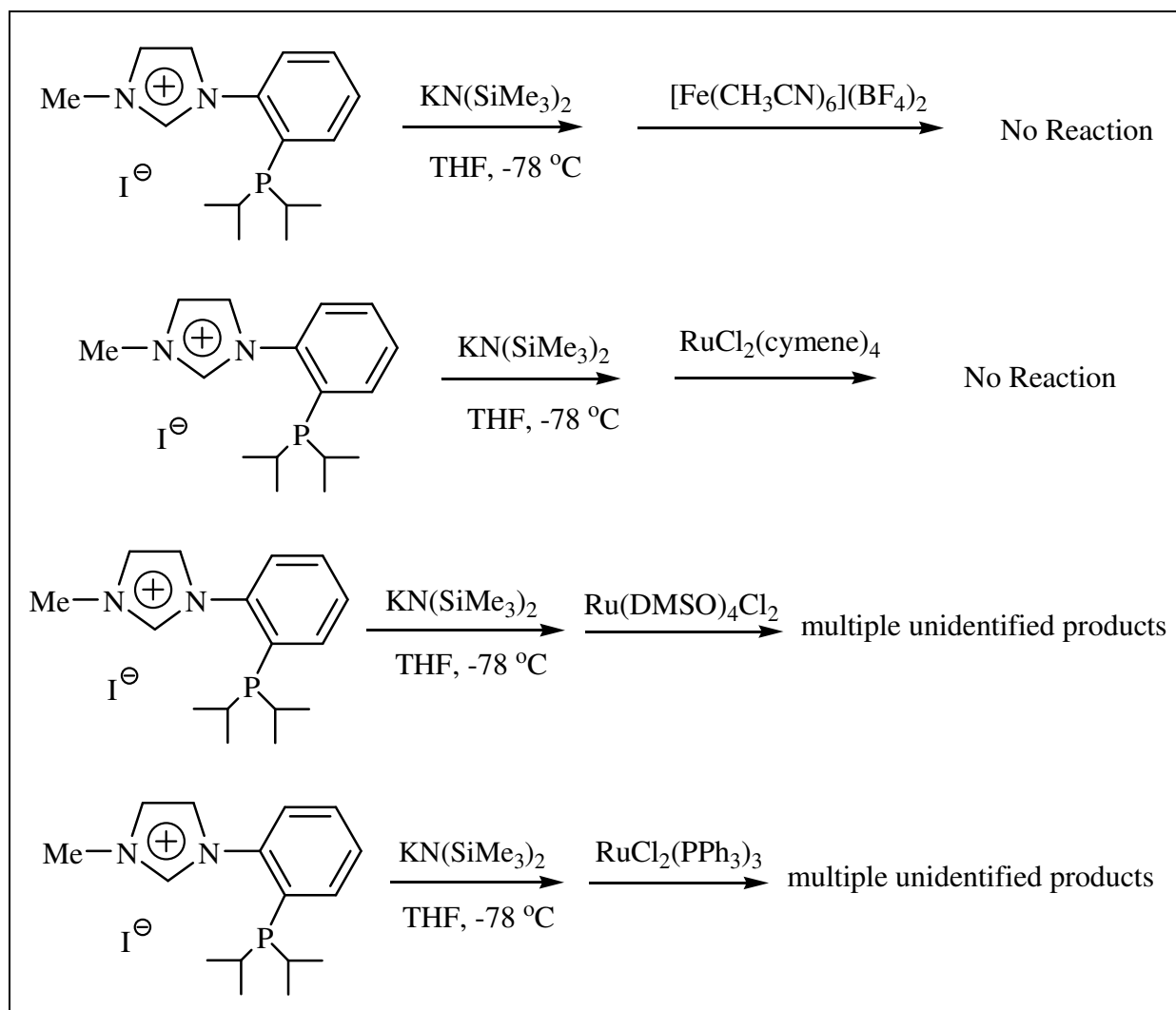
In all cases below, either no reaction occurred or multiple unidentified products were obtained and the reaction did not lead to isolable complexes or other tractable products. *Via* the formation of free carbene, metal precursors of Ti, Cr and Mn were added under the same conditions mentioned in Chapter 3. No meaningful results were obtained because of no reaction apparently occurred as shown in Scheme 4.1. The mixture was left under reflux overnight and no results were obtained. As for no reaction occurs which is given in schemes below, no characteristic changes were observed between reactants and products in all the ^1H , $^{13}\text{C}\{^1\text{H}\}$ and $^{31}\text{P}\{^1\text{H}\}$ spectroscopic techniques.



Scheme 4.1: Reaction of Ti, Cr and Mn precursors with the free ligand, **2.5**, *via* free carbene

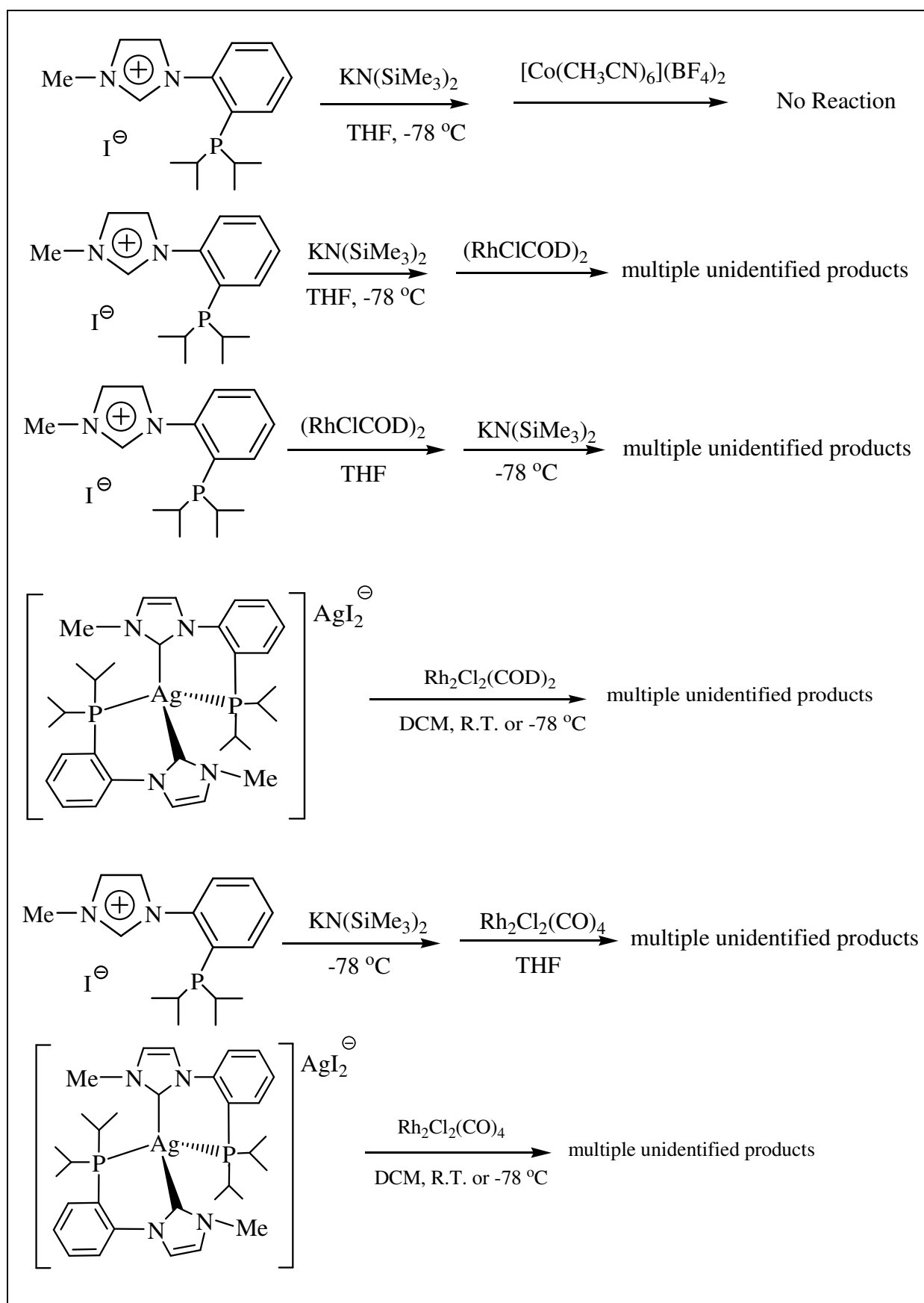
From Group 8, Fe and Ru precursors were reacted with the free ligand, **2.5**. The reaction was conducted *via* the formation of free carbene under the same conditions used in Chapter 3. In the case of $[\text{Fe}(\text{CH}_3\text{CN})_6](\text{BF}_4)_2$ and $\text{RuCl}_2(\text{cymene})_4$, no reaction occurred. However, products with $\text{Ru}(\text{DMSO})_4\text{Cl}_2$ and $\text{RuCl}_2(\text{PPh}_3)_3$ gave multiple unidentified products, from which it was impossible to obtain isolable products, Scheme 4.2. The products

were characterized by $^{31}\text{P}\{^1\text{H}\}$ -NMR, but gave multiple unidentified products' spectra. Thus, it was not possible to characterize with ^1H -NMR technique due to formation of the multiple products. Attempted recrystallization of the products with different combination of solvents proved futile.



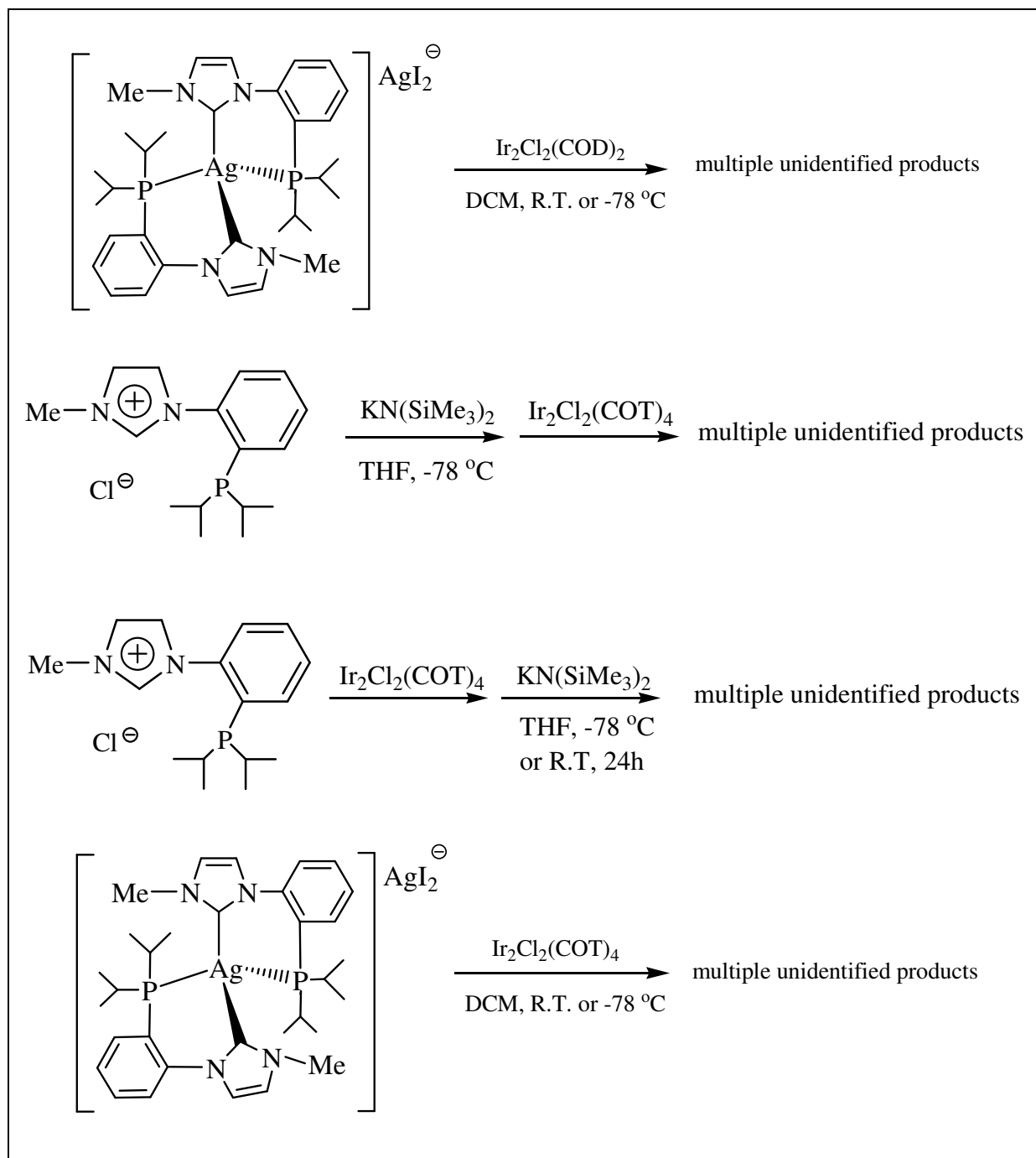
Scheme 4.2: Reaction of Fe and Ru precursors with the free ligand, **2.5**, via free carbene

From Group 9, metal precursors of Co, Rh and Ir, $[\text{Co}(\text{CH}_3\text{CN})_6](\text{BF}_4)_2$, $\text{Rh}_2\text{Cl}_2(\text{COD})_2$, $\text{Rh}_2\text{Cl}_2(\text{CO})_4$, $\text{Ir}_2\text{Cl}_2(\text{COD})_2$ and $\text{Ir}_2\text{Cl}_2(\text{COT})_4$, were used. With cobalt precursor, no complexation occurred with the free ligand, **2.5**, by the method of free carbene formation, Scheme 4.3. Both free carbene and transmetallation methods were applied to Rh precursors and resulted in mixtures having multiple unidentified products' spectra. An addition of the Rh precursors to the ligand before the addition of the base, $\text{KN}(\text{SiMe}_3)_2$, was not a successful trial to achieve complexation. All attempted trials failed to purify and isolate expected products, Scheme 4.3.



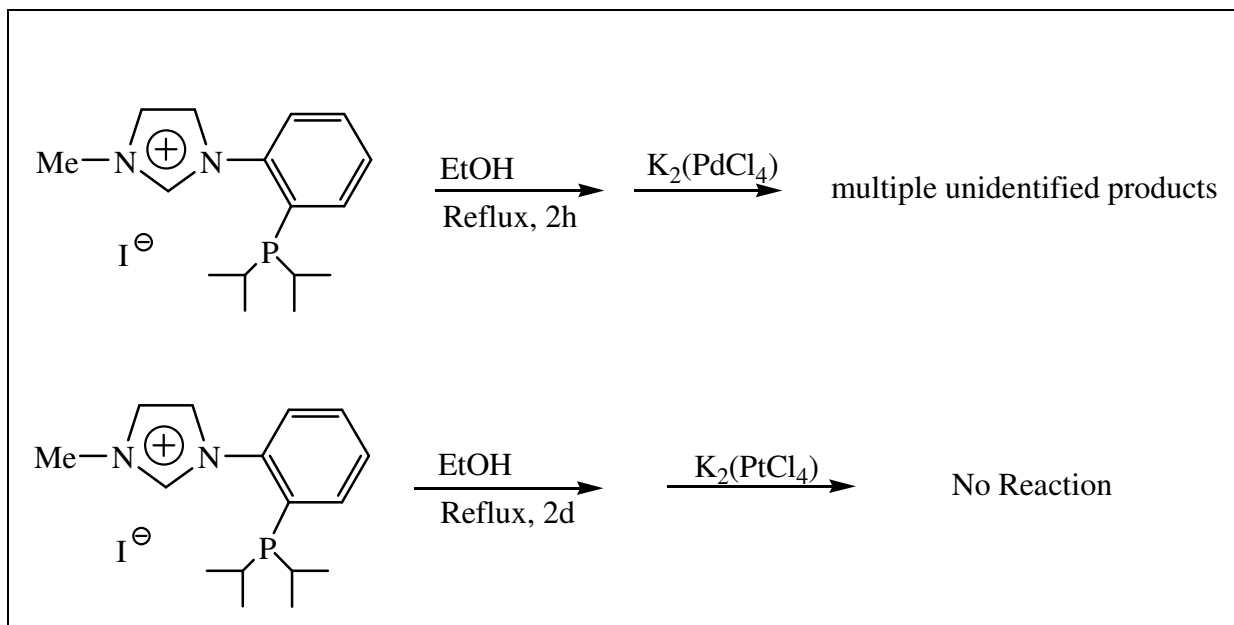
Scheme 4.3, Reaction of Co and Rh precursors with the free ligand, **2.5**, *via* free carbene and *via* transmetallation

Similarly, for Ir precursors, methods *via* free carbene and *via* transmetallation were used and resulted in having multiple unidentified products' spectra. Addition of the Ir precursors to the ligand before the addition of the base, $\text{KN}(\text{SiMe}_3)_2$, was not a successful trial to achieve purer complexation. Efforts failed to purify and isolate desired products, Scheme 4.4.



Scheme 4.4: Reaction of Ir precursors with the free ligand, **2.5**, *via* free carbene and *via* transmetallation

In absence of a base, reaction of the ligand, **2.5**, with $K_2(PdCl_4)$ and $K_2(PtCl_4)$ precursors showed no sign of reaction or multiple unidentified products' spectra. Attempts of purification did not lead to isolable complexes or other tractable products, Scheme 4.5.



Scheme 4.5: Reaction of Pd and Pt precursors with the free ligand, **2.5**, *via* free carbene and *via* transmetallation

Recommendation for future work

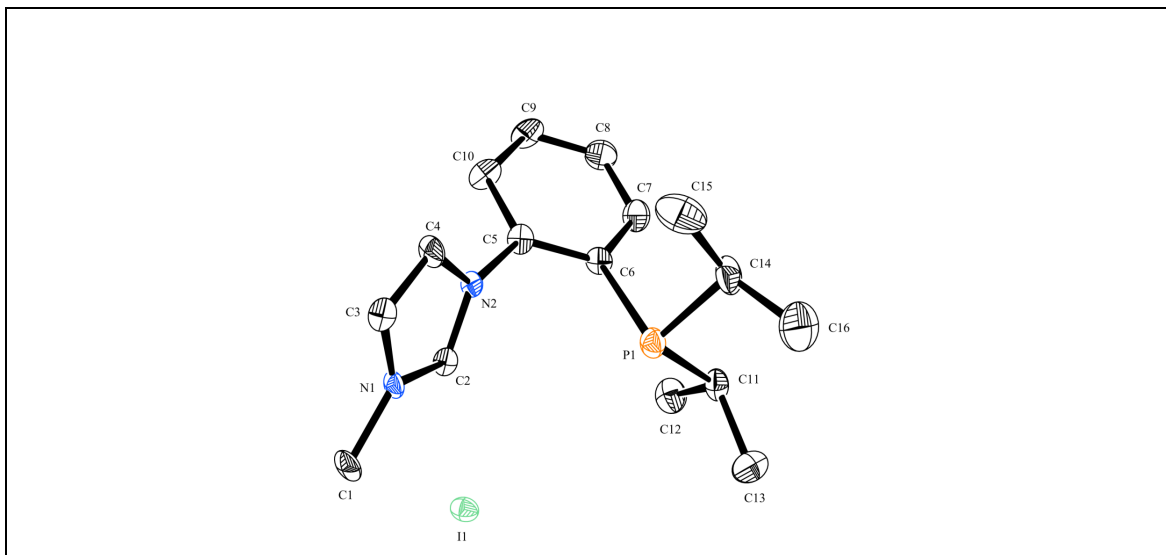
Future research should be focused on preparation of mono NHC-phosphine complexes, investigation of new synthetic methods for better yields, optimization for rapid and clean reactions with minimal waste and by-products, modification to the imidazolium ring substituents to alkyl or aryl groups, extending the coordination chemistry to include systems where only one of the donors, phosphine or carbene is bound, possibility of bimetallic systems where the NHC binds one metal and the P donor another, extending the coordination chemistry to other metals including main group compounds, modification to the imidazolium ring substituents at C₃ and C₄ positions, looking at synthetic routes to ligands with different linking groups between the imidazolium ring and the phosphine, having more bulky groups for phosphine substituents, and study of the catalytic behavior of these complexes.

N-heterocyclic carbenes-phosphine complexes have electronic and steric properties suitable for effective catalysis as both phosphines and NHCs have been very successful in this area. One application I had in mind was hydrogenation (addition of pair of hydrogen atoms to a molecule, generally an alkene). Hydrogenation plays an essential role in food, petrochemical, pharmaceutical, and agricultural industries. Other relevant possible applications in homogeneous catalysis are hydrosilylation, hydroamination, carbon-carbon bond forming reactions through cross-coupling and alkene metathesis (Grubbs' type) as well as their application in a range of other synthetically useful reactions. Further research is recommended in this area.

APPENDIX

Crystallographic Data

Data Set 1: Free ligand Crystal data and structure refinement, 2.5



Identification code	pge0707
Empirical formula	$\text{C}_{16}\text{H}_{24}\text{N}_2\text{PI}$
Formula weight	402.24
Temperature	150(2)
Crystal system	Orthorhombic
Space group	Pbca
$a/\text{\AA}$, $b/\text{\AA}$, $c/\text{\AA}$	9.0469(2), 12.8839(3), 31.5861(8)
$\alpha/^\circ$, $\beta/^\circ$, $\gamma/^\circ$	90.00, 90.00, 90.00
Volume/ \AA^3	3681.66(15)
Z	8
$\rho_{\text{calc}}/\text{mg}/\text{mm}^3$	1.451
m/mm^{-1}	1.821
F(000)	1616
Crystal size	$0.52 \times 0.40 \times 0.22$
Theta range for data collection	3.04 to 27.47°
Index ranges	$-10 \leq h \leq 11$, $-16 \leq k \leq 16$, $-38 \leq l \leq 40$
Reflections collected	13231

Independent reflections	4061[R(int) = 0.0959]
Data/restraints/parameters	4061/0/186
Goodness-of-fit on F^2	1.019
Final R indexes [$I > 2\sigma(I)$]	$R_1 = 0.0522$, $wR_2 = 0.1062$
Final R indexes [all data]	$R_1 = 0.1199$, $wR_2 = 0.1402$
Largest diff. peak/hole	0.971/-0.730

Table 2 Atomic Coordinates ($\text{\AA} \times 10^4$) and Equivalent Isotropic Displacement

Parameters ($\text{\AA}^2 \times 10^3$) . U_{eq} is defined as 1/3 of of the trace of the orthogonalised

U_{ij} tensor.

Atom	x	y	z	U(eq)
C1	7394(7)	3505(4)	2186(2)	28.8(16)
C2	6699(7)	1865(4)	1838.3(18)	20.2(14)
C3	4895(7)	2989(4)	1884.1(19)	23.9(15)
C4	4346(7)	2135(5)	1704(2)	29.1(16)
C5	5358(6)	385(5)	1518(2)	21.9(15)
C6	4384(7)	-254(5)	1735(2)	27(15)
C7	4227(7)	-1295(5)	1611(2)	33.3(17)
C8	5017(8)	-1656(6)	1272(2)	39.5(19)
C9	5948(7)	-998(5)	1054(2)	35(17)
C10	6148(7)	37(4)	1168(2)	22.3(15)
C11	8825(8)	128(5)	655(2)	29.6(16)
C12	9501(8)	-512(6)	1011(2)	41.7(19)
C13	10019(9)	857(6)	473(3)	52(2)
C14	6015(8)	963(6)	370(2)	39.7(18)
C15	4492(8)	1409(6)	493(3)	61(2)
C16	6673(10)	1569(7)	-3(2)	67(3)
N1	6384(5)	2812(4)	1962.5(15)	21(11)
N2	5496(5)	1429(4)	1665.2(16)	20.6(12)
P1	7253.9(19)	955.8(13)	841.4(5)	28.9(4)
I1	10605(4)	958.5(3)	2131.35(14)	27.62(17)

Table 3 Anisotropic Displacement Parameters ($\text{\AA}^2 \times 10^3$) . The Anisotropic displacement factor is defined as $2\pi^2[h^2a^{*2}U_{11}+...+2hka \times b \times U_{12}]$

Atom	U ₁₁	U ₂₂	U ₃₃	U ₂₃	U ₁₃	U ₁₂
C1	43(4)	14(3)	29(4)	-9(3)	-1(3)	-4(3)
C2	30(4)	9(3)	21(4)	5(3)	4(3)	2(3)
C3	39(4)	8(3)	25(4)	8(3)	7(3)	2(3)
C4	28(4)	25(3)	34(4)	-16(3)	0(3)	9(3)
C5	27(4)	15(3)	24(4)	5(3)	-2(3)	11(3)
C6	30(4)	15(3)	36(4)	15(3)	5(3)	7(3)
C7	39(4)	19(3)	42(5)	12(3)	12(4)	-6(3)
C8	45(4)	30(4)	44(5)	-2(4)	3(4)	-10(4)
C9	37(4)	31(4)	37(4)	-11(4)	6(3)	6(3)
C10	32(3)	8(3)	27(4)	2(3)	1(3)	0(3)
C11	43(4)	25(4)	21(4)	0(3)	2(3)	1(3)
C12	43(5)	39(4)	43(5)	-5(4)	0(4)	11(4)
C13	46(4)	58(5)	53(5)	-4(5)	13(4)	-14(4)
C14	47(4)	52(5)	20(4)	-2(4)	-5(3)	5(4)
C15	50(5)	55(5)	78(7)	0(5)	-24(5)	4(4)
C16	79(7)	85(7)	37(5)	21(5)	-9(5)	-2(5)
N1	29(3)	16(3)	19(3)	-7(2)	3(2)	-1(2)
N2	24(3)	12(2)	26(3)	-9(2)	6(3)	2(2)
P1	36.2(10)	24.7(9)	25.9(10)	-4.2(8)	3.4(8)	-1(8)
I1	25.6(2)	21.6(2)	35.7(3)	-2.8(2)	-2(2)	0.27(19)

Table 4 Bond Lengths:

Atom	Atom	Length/ \AA	Atom	Atom	Length/ \AA
C1	N1	1.460(7)	C7	C8	1.367(9)
C2	N1	1.313(7)	C8	C9	1.380(9)
C2	N2	1.341(7)	C9	C10	1.393(8)

C3	C4	1.334(8)	C10	P1	1.862(6)
C3	N1	1.388(8)	C11	C12	1.521(9)
C4	N2	1.387(7)	C11	C13	1.543(9)
C5	C6	1.389(8)	C11	P1	1.871(7)
C5	C10	1.390(8)	C14	C16	1.534(10)
C5	N2	1.428(7)	C14	C15	1.543(9)
C6	C7	1.404(9)	C14	P1	1.863(7)

Table 5 Bond Angles:

Atom	Atom	Atom	Angle/°	Atom	Atom	Atom	Angle/°
N1	C2	N2	109.6(5)	C12	C11	P1	112.5(5)
C4	C3	N1	107.6(5)	C13	C11	P1	107.6(4)
C3	C4	N2	107.4(6)	C16	C14	C15	110.5(6)
C6	C5	C10	121.8(6)	C16	C14	P1	112.5(5)
C6	C5	N2	117.0(5)	C15	C14	P1	109.8(5)
C10	C5	N2	121.2(5)	C2	N1	C3	108.0(5)
C5	C6	C7	119.5(6)	C2	N1	C1	125.3(5)
C8	C7	C6	119.4(6)	C3	N1	C1	126.4(5)
C7	C8	C9	120.1(7)	C2	N2	C4	107.3(5)
C8	C9	C10	122.5(6)	C2	N2	C5	126.7(5)
C5	C10	C9	116.6(6)	C4	N2	C5	125.5(5)
C5	C10	P1	120.8(4)	C10	P1	C14	97.1(3)
C9	C10	P1	122.3(5)	C10	P1	C11	102.7(3)
C12	C11	C13	108.9(6)	C14	P1	C11	102.1(3)

Table 6 Torsion Angles :

A	B	C	D	Angle/°
N1	C3	C4	N2	-0.7(7)
C10	C5	C6	C7	2.5(9)

N2	C5	C6	C7	-178.6(5)
C5	C6	C7	C8	-1.2(10)
C6	C7	C8	C9	-0.6(11)
C7	C8	C9	C10	1.2(11)
C6	C5	C10	C9	-1.9(9)
N2	C5	C10	C9	179.2(6)
C6	C5	C10	P1	171.9(5)
N2	C5	C10	P1	-7.0(8)
C8	C9	C10	C5	0.1(10)
C8	C9	C10	P1	-173.6(6)
N2	C2	N1	C3	2.6(7)
N2	C2	N1	C1	176.4(5)
C4	C3	N1	C2	-1.1(7)
C4	C3	N1	C1	-174.8(6)
N1	C2	N2	C4	-3.1(7)
N1	C2	N2	C5	-175.5(5)
C3	C4	N2	C2	2.3(7)
C3	C4	N2	C5	174.9(5)
C6	C5	N2	C2	114.0(7)
C10	C5	N2	C2	-67.0(8)
C6	C5	N2	C4	-57.1(8)
C10	C5	N2	C4	121.8(7)
C5	C10	P1	C14	-107.8(5)
C9	C10	P1	C14	65.6(6)
C5	C10	P1	C11	148.1(5)
C9	C10	P1	C11	-38.5(6)
C16	C14	P1	C10	-173.5(5)
C15	C14	P1	C10	63.0(5)
C16	C14	P1	C11	-68.8(6)
C15	C14	P1	C11	167.6(5)
C12	C11	P1	C10	-46.4(6)

C13	C11	P1	C10	-166.3(5)
C12	C11	P1	C14	-146.6(5)
C13	C11	P1	C14	93.5(5)

Table 7 Hydrogen Atom Coordinates ($\text{\AA} \times 10^4$) and Isotropic

Displacement Parameters ($\text{\AA}^2 \times 10^3$) :

Atom	<i>x</i>	<i>y</i>	<i>z</i>	U(eq)
H1A	7090	3562	2483	43
H1B	7370	4193	2054	43
H1C	8400	3226	2172	43
H2	7635	1539	1867	24
H3	4364	3605	1947	29
H4	3351	2029	1619	35
H6	3828	9	1967	32
H7	3578	-1743	1760	40
H8	4925	-2360	1188	47
H9	6473	-1261	817	42
H11	8467	-347	427	36
H12A	10393	-860	907	62
H12B	8785	-1032	1106	62
H12C	9759	-55	1247	62
H13A	10468	1257	704	78
H13B	9566	1333	269	78
H13C	10782	444	331	78
H14	5869	228	278	48
H15A	4611	2123	595	91
H15B	4056	983	718	91
H15C	3841	1405	245	91
H16A	5963	1580	-237	101
H16B	7588	1232	-96	101
H16C	6889	2282	86	101

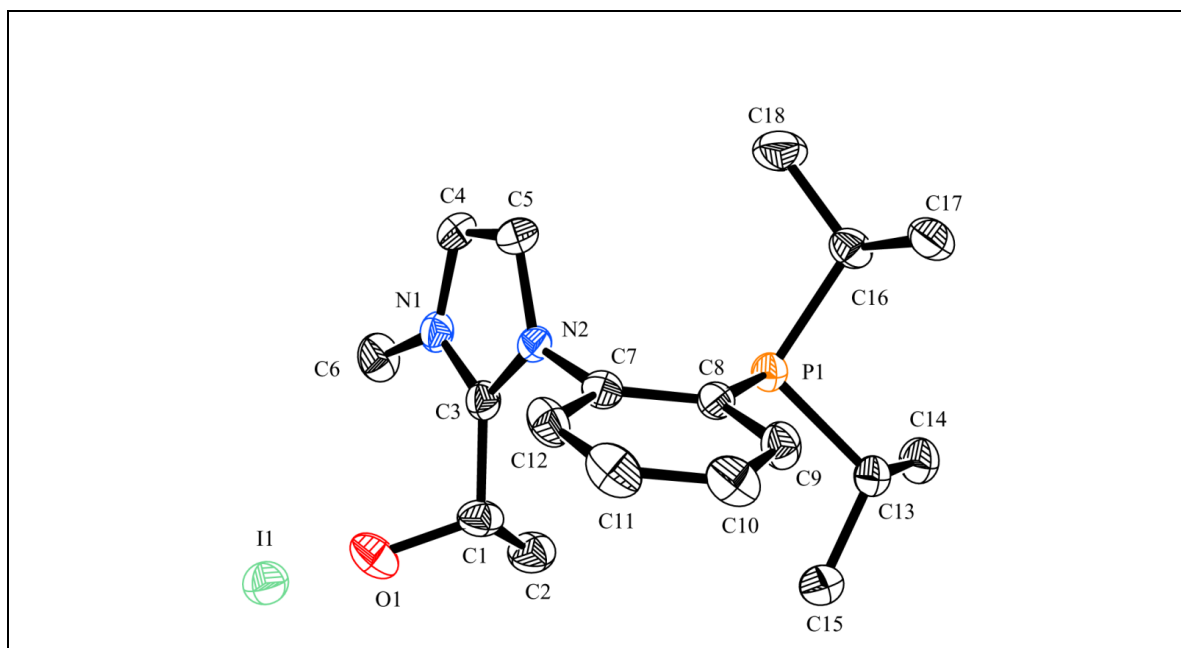
Experimental

Single crystals of $\text{C}_{16}\text{H}_{24}\text{N}_2\text{PI}$ were recrystallised from dichloromethane (DCM) mounted in inert oil and transferred to the cold gas stream of the diffractometer.

Crystal structure determination of

Crystal Data. $\text{C}_{16}\text{H}_{24}\text{N}_2\text{PI}$, $M = 402.24$, Orthorhombic, $a = 9.0469(2) \text{ \AA}$, $b = 12.8839(3) \text{ \AA}$, $c = 31.5861(8) \text{ \AA}$, $U = 3681.66(15) \text{ \AA}^3$, $T = 150(2)$, space group Pbca (no. 61), $Z = 8$, $\mu(\text{Mo-K}\alpha) = 1.821$, 13231 reflections measured, 4061 unique ($R_{\text{int}} = 0.0959$) which were used in all calculations. The final $wR(F_2)$ was 0.1402 (all data).

Data Set 2: Ligand-hydroxyethyl derivative crystal data and structure refinement, 2.7



Identification code	P21N
Empirical formula	$C_{18}H_{28}N_2IPO$
Formula weight	446.29
Temperature	150(2)
Crystal system	Monoclinic
Space group	$P2_1/n$
$a/\text{\AA}$, $b/\text{\AA}$, $c/\text{\AA}$	10.062(5), 9.235(5), 21.923(5)
$\alpha/^\circ$, $\beta/^\circ$, $\gamma/^\circ$,	90.000(5), 98.366(5), 90.000(5)
Volume/ \AA^3	2015.5(16)
Z	4
$\rho_{\text{calc}}/\text{mg/mm}^3$	1.471
m/mm^{-1}	1.674
F(000)	904
Crystal size	$0.12 \times 0.10 \times 0.08$
Theta range for data collection	3.01 to 25.00°
Index ranges	$-11 \leq h \leq 11$, $-10 \leq k \leq 10$, $-26 \leq l \leq 25$
Reflections collected	6548

Independent reflections 3527[R(int) = 0.0298]
 Data/restraints/parameters 3527/0/218
 Goodness-of-fit on F^2 1.026
 Final R indexes [$I > 2\sigma(I)$] $R_1 = 0.0309$, $wR_2 = 0.0606$
 Final R indexes [all data] $R_1 = 0.0441$, $wR_2 = 0.0653$
 Largest diff. peak/hole 0.691/-0.454

Table 2 Atomic Coordinates ($\text{\AA} \times 10^4$) and Equivalent Isotropic Displacement

Parameters ($\text{\AA}^2 \times 10^3$). U_{eq} is defined as 1/3 of the trace of the orthogonalised U_{IJ} tensor.

Atom	x	y	z	U(eq)
I1	2771.4(2)	-3660(3)	4120.8(10)	35.9(9)
P1	8486.4(9)	651.5(10)	3370.6(4)	28.6(2)
O1	3137(3)	-931(3)	3046.4(12)	45.4(7)
N1	4392(3)	1813(3)	3650.1(13)	32.2(7)
C1	4506(4)	-531(4)	3046.9(15)	37(9)
N2	5975(3)	326(3)	4010.9(11)	27.6(6)
C2	4663(4)	82(4)	2419.2(16)	45.4(10)
C3	4947(3)	527(4)	3554.9(14)	30.4(8)
C4	5081(4)	2433(4)	4172.2(16)	37.5(9)
C5	6060(4)	1509(4)	4398.9(16)	38.3(9)
C6	3249(4)	2488(4)	3258.1(18)	45.5(10)
C7	6865(3)	-922(4)	4081.4(14)	29.5(8)
C8	8083(3)	-883(4)	3845.6(14)	27.6(8)
C9	8883(3)	-2132(4)	3952.2(16)	35.3(8)
C10	8481(4)	-3323(4)	4257.9(17)	42.2(10)
C11	7269(4)	-3325(4)	4473.2(17)	43.4(10)
C12	6450(4)	-2112(4)	4389.5(15)	37.8(9)
C13	9361(3)	-266(4)	2784.8(15)	33.6(8)
C14	9787(4)	876(4)	2350.8(16)	43.4(10)

C15	8407(4)	-1326(4)	2411(17)	46.6(10)
C16	9896(4)	1596(4)	3863.2(16)	35.3(9)
C17	11023(4)	666(4)	4190.3(16)	41.7(9)
C18	9352(4)	2617(4)	4309(19)	57(12)

Table 3 Anisotropic Displacement Parameters ($\text{\AA}^2 \times 10^3$). The Anisotropic

displacement factor exponent takes the form: $-2\pi^2[h^2a^{*2}U_{11}+...+2hka \times b \times U_{12}]$

Atom	U ₁₁	U ₂₂	U ₃₃	U ₂₃	U ₁₃	U ₁₂
II	36.06(15)	37.61(15)	33.8(15)	-3.48(11)	4.33(10)	0.74(11)
P1	28(5)	26.8(5)	31.2(5)	2.2(4)	5.1(4)	1.6(4)
O1	37(16)	44.9(17)	49.7(16)	2.3(14)	-9.6(12)	-6.7(13)
N1	25.3(16)	34(17)	38.2(17)	-0.8(14)	7.1(13)	4.1(13)
C1	38(2)	34(2)	36(2)	-6(17)	-6.1(16)	4.6(17)
N2	24.9(16)	34.1(17)	24.3(14)	-3.6(12)	5.3(12)	0.7(13)
C2	47(3)	50(3)	37(2)	-5.7(18)	-3(17)	3(2)
C3	24(19)	35(2)	32.2(19)	-0.4(16)	3.6(15)	2.8(16)
C4	37(2)	37(2)	41(2)	-11.6(17)	12.4(17)	2.4(18)
C5	39(2)	47(2)	29.7(19)	-11.4(17)	7.3(16)	-2.8(19)
C6	33(2)	37(2)	64(3)	4.6(19)	2(19)	11(18)
C7	29.5(19)	35(2)	22(17)	0.2(15)	-1.6(14)	0.7(16)
C8	24.5(18)	32(2)	24.9(17)	-1(14)	-1.3(14)	3(15)
C9	28(2)	32(2)	46(2)	3.2(17)	4.3(16)	3.5(16)
C10	42(2)	31(2)	50(2)	6.4(18)	-5.3(19)	-0.4(18)
C11	49(3)	37(2)	42(2)	15.1(18)	0(18)	-10.6(19)
C12	32(2)	48(2)	33(2)	7.1(18)	2.9(16)	-10.7(18)
C13	30(2)	37(2)	34.8(19)	-0.8(16)	8.2(15)	-1.8(16)
C14	39(2)	49(2)	44(2)	1.2(19)	13.5(18)	-4.5(19)
C15	45(2)	50(3)	46(2)	-14.5(19)	12(18)	-6(2)
C16	36(2)	28(2)	41(2)	0.5(16)	2(16)	-5.6(16)
C17	36(2)	41(2)	45(2)	-4.6(18)	-4(17)	-4.4(18)
C18	54(3)	47(3)	65(3)	-24(2)	-8(2)	9(2)

Table 4 Bond Lengths.

Atom	Atom	Length/Å	Atom	Atom	Length/Å
P1	C8	1.839(3)	C4	C5	1.343(5)
P1	C13	1.863(3)	C7	C12	1.386(5)
P1	C16	1.869(4)	C7	C8	1.398(5)
O1	C1	1.426(4)	C8	C9	1.406(5)
N1	C3	1.342(4)	C9	C10	1.379(5)
N1	C4	1.374(4)	C10	C11	1.370(5)
N1	C6	1.470(4)	C11	C12	1.388(5)
C1	C3	1.499(5)	C13	C14	1.523(5)
C1	C2	1.517(5)	C13	C15	1.524(5)
N2	C3	1.343(4)	C16	C18	1.516(5)
N2	C5	1.380(4)	C16	C17	1.518(5)
N2	C7	1.454(4)			

Table 5 Bond Angles.

Atom	Atom	Atom	Angle/°	Atom	Atom	Atom	Angle/°
C8	P1	C13	101.84(16)	C12	C7	C8	122.9(3)
C8	P1	C16	104.13(15)	C12	C7	N2	117.1(3)
C13	P1	C16	102.47(16)	C8	C7	N2	120.0(3)
C3	N1	C4	109.1(3)	C7	C8	C9	115.4(3)
C3	N1	C6	126.3(3)	C7	C8	P1	120.5(2)
C4	N1	C6	124.6(3)	C9	C8	P1	123.9(3)
O1	C1	C3	110.6(3)	C10	C9	C8	122.2(3)
O1	C1	C2	108.9(3)	C11	C10	C9	120.5(4)
C3	C1	C2	111.8(3)	C10	C11	C12	119.6(3)
C3	N2	C5	108.7(3)	C7	C12	C11	119.3(3)
C3	N2	C7	125.8(3)	C14	C13	C15	108.7(3)
C5	N2	C7	125.5(3)	C14	C13	P1	108.7(2)
N1	C3	N2	107.5(3)	C15	C13	P1	109.8(2)

N1	C3	C1	127.4(3)	C18	C16	C17	111.3(3)
N2	C3	C1	125.1(3)	C18	C16	P1	110.4(3)
C5	C4	N1	107.3(3)	C17	C16	P1	117.4(3)
C4	C5	N2	107.4(3)				

Table 6 Hydrogen Atom Coordinates ($\text{\AA} \times 10^4$) and Isotropic Displacement

Parameters ($\text{\AA}^2 \times 10^3$).

Atom	<i>x</i>	<i>y</i>	<i>z</i>	U(eq)
H1	5074	-1420	3119	44
H1A	3100(6)	-1710(7)	3370(3)	140(2)
H2A	4530	-691	2110	68
H2B	5566	489	2433	68
H2C	3993	844	2309	68
H4	4899	3347	4341	45
H5	6694	1645	4760	46
H6A	3572	3004	2918	68
H6B	2804	3172	3504	68
H6C	2610	1737	3092	68
H9	9729	-2156	3809	42
H10	9049	-4148	4320	51
H11	6991	-4153	4679	52
H12	5613	-2097	4542	45
H13	10169	-794	2994	40
H14A	10258	408	2043	65
H14B	10387	1576	2588	65
H14C	8990	1378	2143	65
H15A	7618	-803	2208	70
H15B	8124	-2065	2686	70
H15C	8868	-1792	2099	70

H16	10322	2230	3577	42
H17A	11745	1290	4391	63
H17B	11373	40	3890	63
H17C	10679	66	4502	63
H18A	9019	2055	4634	86
H18B	8616	3190	4087	86
H18C	10070	3267	4493	86

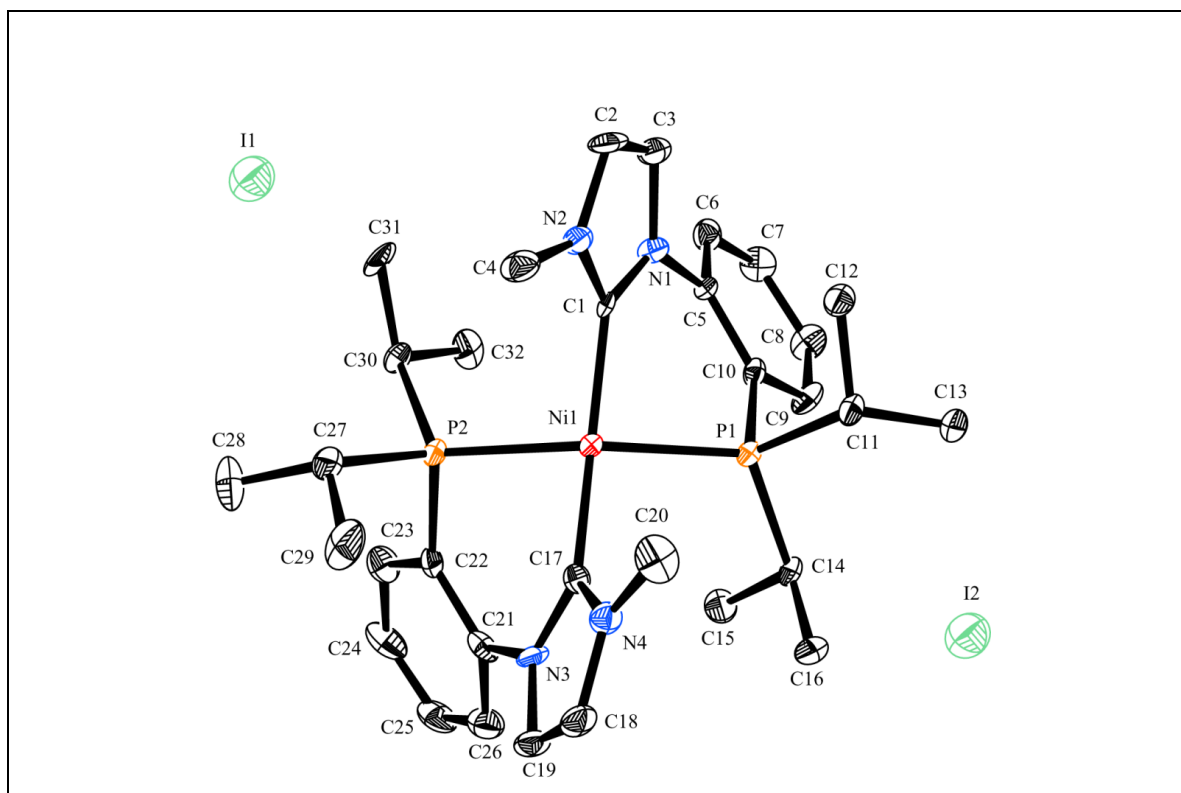
Experimental

Single crystals of $C_{18}H_{28}N_2IPO$ were recrystallised from tetrahydrofuran (THF) mounted in inert oil and transferred to the cold gas stream of the diffractometer.

Crystal structure determination

Crystal Data. $C_{18}H_{28}N_2IPO$, $M = 446.29$, Monoclinic, $a = 10.062(5) \text{ \AA}$, $b = 9.235(5) \text{ \AA}$, $c = 21.923(5) \text{ \AA}$, $\beta = 98.366(5)^\circ$, $U = 2015.5(16) \text{ \AA}^3$, $T = 150(2)$, space group $P2_1/n$ (no. 14), $Z = 4$, $\mu(\text{Mo-K}\alpha) = 1.674$, 6548 reflections measured, 3527 unique ($R_{\text{int}} = 0.0298$) which were used in all calculations. The final $wR(F_2)$ was 0.0653 (all data).

Data Set 3: Nickel complex crystal data and structure refinement, 3.4



Identification code	Ni-pge0822
Empirical formula	C ₃₂ H ₄₆ I ₂ P ₂ NiN ₄
Formula weight	897.21
Temperature	150(2)
Crystal system	Monoclinic
Space group	P2 ₁ /c
a/Å, b/Å, c/Å	8.7370(2), 39.0870(7), 10.9220(2)
α/°, β/°, γ/°	90.00, 100.4400(10), 90.00
Volume/Å ³	3668.15(13)
Z	4
ρ _{calc} /mg/mm ³	1.625
m/mm ⁻¹	2.333
F(000)	1800
Crystal size	0.24 × 0.22 × 0.04
Theta range for data collection	1.97 to 27.49°

Index ranges	$-11 \leq h \leq 11, -46 \leq k \leq 50, -14 \leq l \leq 11$
Reflections collected	19169
Independent reflections	7864[R(int) = 0.0736]
Data/restraints/parameters	7864/6/410
Goodness-of-fit on F^2	1.038
Final R indexes [$I > 2\sigma(I)$]	$R_1 = 0.0659, wR_2 = 0.1588$
Final R indexes [all data]	$R_1 = 0.1147, wR_2 = 0.1816$
Largest diff. peak/hole	1.384/-1.558

Table 2 Atomic Coordinates ($\text{\AA} \times 10^4$) and Equivalent Isotropic Displacement

Parameters ($\text{\AA}^2 \times 10^3$). U_{eq} is defined as 1/3 of the trace of the orthogonalised U_{IJ} tensor.

Atom	<i>x</i>	<i>y</i>	<i>z</i>	U_{eq}
C1	1060(7)	982.5(19)	4981(6)	19.4(15)
C2	2868(8)	654(2)	6166(7)	28.8(17)
C3	1708(8)	693(2)	6795(7)	27.7(17)
C4	3479(8)	862(2)	4150(7)	36(2)
C5	-769(7)	1032(2)	6453(6)	22.3(16)
C6	-1567(9)	823(2)	7158(7)	31.9(19)
C7	-2815(9)	955(3)	7612(7)	36(2)
C8	-3233(9)	1286(3)	7401(7)	40(2)
C9	-2475(8)	1493(2)	6681(7)	30.9(18)
C10	-1196(8)	1372.3(19)	6168(6)	21.1(15)
C11	1355(8)	1857(2)	6182(7)	28(17)
C12	2679(10)	1611(2)	6689(9)	49(3)
C13	816(10)	2052(3)	7248(8)	46(2)
C14	-1702(8)	1981(2)	4625(7)	25.9(16)
C15	-3212(8)	1840(2)	3863(7)	31.7(19)
C16	-1016(9)	2263(2)	3910(8)	31(18)
C17	-158(8)	1581(18)	2304(6)	17.8(14)

C18	457(9)	1964(2)	933(7)	28.6(17)
C19	-978(8)	1848(2)	480(7)	26.6(17)
C20	2464(8)	1856(2)	2848(7)	29.8(18)
C21	-2661(7)	1384.2(18)	1098(6)	17.3(14)
C22	-2510(7)	1044.6(18)	1424(6)	17.8(14)
C23	-3841(8)	835(2)	1074(7)	27.4(17)
C24	-5221(8)	971(2)	436(7)	31.5(18)
C25	-5325(8)	1315(2)	172(7)	30.2(18)
C26	-4069(8)	1522(2)	490(6)	26.4(17)
C27	415(8)	736.8(19)	1091(6)	21.4(15)
C28	-398(9)	443(2)	262(7)	30.4(18)
C29	731(8)	1033.5(19)	292(7)	24.3(16)
C30	-1311(8)	458.4(18)	2949(6)	22.5(15)
C31	49(9)	232(2)	3508(7)	29.8(17)
C32	-2412(9)	526(2)	3876(7)	32.5(19)
N1	596(6)	895.1(15)	6058(5)	21.7(13)
N2	2486(6)	830.7(16)	5066(5)	23.8(13)
N3	-1337(6)	1607.8(16)	1332(5)	21.6(13)
N4	956(6)	1798.2(16)	2059(5)	20.5(13)
P1	-267.5(19)	1636.8(5)	5145.4(15)	18.8(4)
P2	-699.9(19)	863.9(5)	2304.6(15)	17.7(4)
Ni1	142.2(9)	1271.9(2)	3678.3(7)	15.7(2)
I1	3911.3(6)	1.19(16)	2218.6(5)	42.23(19)
I2	4263.3(7)	2457.89(16)	419.6(6)	43.7(2)
O1	7136(7)	-225.1(18)	925(6)	44.9(15)
O2	6084(7)	2882.9(18)	3120(7)	54.8(18)

Table 3 Anisotropic Displacement Parameters ($\text{\AA}^2 \times 10^3$). The Anisotropic**displacement factor exponent takes the form: $-2\pi^2[h^2a^{*2}U_{11}+...+2hka \times b \times U_{12}]$**

Atom	U_{11}	U_{22}	U_{33}	U_{23}	U_{13}	U_{12}
C1	18(3)	20(4)	17(3)	-2(3)	-5(3)	-4(3)
C2	30(4)	20(5)	33(4)	3(3)	-3(3)	9(3)
C3	30(4)	20(5)	28(4)	7(3)	-6(3)	3(3)
C4	19(4)	51(6)	40(5)	-4(4)	8(3)	6(4)
C5	19(3)	35(5)	13(3)	0(3)	1(3)	-7(3)
C6	34(4)	34(5)	27(4)	6(3)	4(3)	-5(4)
C7	38(4)	49(6)	22(4)	9(4)	7(3)	-16(4)
C8	35(4)	65(7)	21(4)	5(4)	9(3)	-1(4)
C9	28(4)	39(6)	27(4)	-4(3)	7(3)	2(3)
C10	27(4)	21(4)	16(3)	-6(3)	6(3)	0(3)
C11	33(4)	21(5)	28(4)	-1(3)	0(3)	-7(3)
C12	38(5)	32(6)	63(6)	-10(5)	-26(4)	-2(4)
C13	48(5)	50(7)	40(5)	-26(4)	8(4)	-11(4)
C14	36(4)	14(4)	28(4)	-2(3)	7(3)	11(3)
C15	27(4)	36(5)	32(4)	-8(4)	3(3)	20(4)
C16	41(4)	7(4)	45(5)	-1(3)	6(4)	8(3)
C17	29(4)	7(4)	17(3)	-4(3)	4(3)	-3(3)
C18	38(4)	19(5)	30(4)	14(3)	10(3)	-1(3)
C19	33(4)	19(5)	26(4)	5(3)	2(3)	-3(3)
C20	31(4)	23(5)	33(4)	6(3)	-1(3)	-10(3)
C21	23(3)	11(4)	17(3)	0(3)	4(3)	-3(3)
C22	19(3)	15(4)	20(3)	-5(3)	4(3)	-4(3)
C23	28(4)	14(4)	41(4)	-1(3)	8(3)	-6(3)
C24	21(4)	30(5)	42(4)	-1(4)	1(3)	-6(3)
C25	18(4)	36(6)	35(4)	2(4)	1(3)	4(3)
C26	29(4)	25(5)	27(4)	-4(3)	11(3)	0(3)
C27	26(4)	15(4)	24(3)	-4(3)	5(3)	2(3)

C28	46(5)	19(5)	27(4)	-3(3)	12(3)	6(3)
C29	28(4)	20(4)	28(4)	-1(3)	13(3)	-2(3)
C30	33(4)	11(4)	23(3)	-4(3)	2(3)	-5(3)
C31	43(4)	17(5)	28(4)	4(3)	3(3)	-1(3)
C32	45(4)	28(5)	28(4)	-1(3)	15(3)	-17(4)
N1	28(3)	12(3)	24(3)	7(2)	2(2)	2(2)
N2	23(3)	22(4)	25(3)	0(3)	1(2)	3(3)
N3	23(3)	17(4)	24(3)	4(2)	4(2)	-1(2)
N4	23(3)	16(4)	23(3)	1(2)	3(2)	-1(2)
P1	23.4(9)	13.1(10)	19.1(8)	-2.6(7)	2.1(7)	0.7(7)
P2	21.7(9)	12.9(10)	18.4(8)	-0.7(7)	3(7)	-0.9(7)
Ni1	19.7(4)	11.8(5)	15.4(4)	0.1(3)	2.6(3)	0.3(3)
I1	42.4(3)	36.9(4)	46(3)	-0.5(3)	4.4(2)	2.2(3)
I2	53.9(4)	33.9(4)	45.6(3)	8.1(3)	15.1(3)	8.3(3)
O1	45(3)	44(5)	44(3)	8(3)	0(3)	0(3)
O2	52(4)	42(5)	68(4)	4(4)	4(3)	-1(3)

Table 4 Bond Lengths :

Atom	Atom	Length/Å	Atom	Atom	Length/Å
C1	N1	1.356(9)	C17	N4	1.354(9)
C1	N2	1.368(9)	C17	Ni1	1.908(7)
C1	Ni1	1.880(7)	C18	C19	1.341(10)
C2	C3	1.333(11)	C18	N4	1.387(9)
C2	N2	1.374(9)	C19	N3	1.396(9)
C3	N1	1.390(9)	C20	N4	1.455(9)
C4	N2	1.444(9)	C21	C22	1.374(10)
C5	C6	1.391(10)	C21	C26	1.397(10)
C5	C10	1.402(11)	C21	N3	1.435(9)
C5	N1	1.442(9)	C22	C23	1.417(10)
C6	C7	1.378(12)	C22	P2	1.837(7)

C7	C8	1.350(13)	C23	C24	1.383(11)
C8	C9	1.379(11)	C24	C25	1.377(12)
C9	C10	1.419(10)	C25	C26	1.358(11)
C10	P1	1.817(7)	C27	C29	1.507(10)
C11	C12	1.527(11)	C27	C28	1.552(10)
C11	C13	1.536(11)	C27	P2	1.849(7)
C11	P1	1.857(7)	C30	C31	1.519(10)
C14	C15	1.529(10)	C30	C32	1.541(10)
C14	C16	1.534(11)	C30	P2	1.852(7)
C14	P1	1.856(7)	P1	Ni1	2.2220(19)
C17	N3	1.343(8)	P2	Ni1	2.2216(19)

Table 5 Bond Angles :

Atom	Atom	Atom	Angle/°	Atom	Atom	Atom	Angle/°
N1	C1	N2	104.1(6)	C29	C27	C28	110.1(6)
N1	C1	Ni1	130.9(5)	C29	C27	P2	112.6(5)
N2	C1	Ni1	124.8(5)	C28	C27	P2	111.9(5)
C3	C2	N2	107.8(6)	C31	C30	C32	111.9(6)
C2	C3	N1	106.5(6)	C31	C30	P2	113.1(5)
C6	C5	C10	122.6(7)	C32	C30	P2	111.1(5)
C6	C5	N1	118.2(7)	C1	N1	C3	111.0(6)
C10	C5	N1	119.1(6)	C1	N1	C5	124.1(6)
C7	C6	C5	119.3(8)	C3	N1	C5	124.5(6)
C8	C7	C6	120.2(8)	C1	N2	C2	110.6(6)
C7	C8	C9	121.1(8)	C1	N2	C4	124.8(6)
C8	C9	C10	121.6(8)	C2	N2	C4	124.6(6)
C5	C10	C9	115.1(7)	C17	N3	C19	110.3(6)
C5	C10	P1	123.1(5)	C17	N3	C21	124.8(6)
C9	C10	P1	121.7(6)	C19	N3	C21	124.2(5)
C12	C11	C13	110.7(7)	C17	N4	C18	110.2(6)

C12	C11	P1	112.0(6)	C17	N4	C20	125.9(6)
C13	C11	P1	112.8(5)	C18	N4	C20	123.9(6)
C15	C14	C16	111.1(6)	C10	P1	C14	104.4(3)
C15	C14	P1	111.9(5)	C10	P1	C11	105.4(3)
C16	C14	P1	111.9(5)	C14	P1	C11	104.5(3)
N3	C17	N4	105.7(6)	C10	P1	Ni1	103.1(2)
N3	C17	Ni1	130.4(5)	C14	P1	Ni1	115.6(2)
N4	C17	Ni1	123.5(5)	C11	P1	Ni1	122.1(3)
C19	C18	N4	107.0(6)	C22	P2	C27	104.1(3)
C18	C19	N3	106.8(6)	C22	P2	C30	104.3(3)
C22	C21	C26	122.1(6)	C27	P2	C30	105.6(3)
C22	C21	N3	120.4(6)	C22	P2	Ni1	103.1(2)
C26	C21	N3	117.4(6)	C27	P2	Ni1	121.6(2)
C21	C22	C23	116.9(6)	C30	P2	Ni1	116.2(2)
C21	C22	P2	122.7(5)	C1	Ni1	C17	162.9(3)
C23	C22	P2	120.4(6)	C1	Ni1	P2	97.1(2)
C24	C23	C22	120.9(7)	C17	Ni1	P2	86.7(2)
C25	C24	C23	119.9(7)	C1	Ni1	P1	86.7(2)
C26	C25	C24	120.7(7)	C17	Ni1	P1	98.3(2)
C25	C26	C21	119.5(7)	P2	Ni1	P1	150.56(7)

Table 6 Hydrogen Atom Coordinates ($\text{\AA} \times 10^4$) and Isotropic Displacement

Parameters ($\text{\AA}^2 \times 10^3$) :

Atom	<i>x</i>	<i>y</i>	<i>z</i>	U(eq)
H2	3795	526	6430	35
H3	1651	600	7590	33
H4A	2970	1007	3463	54
H4B	3672	635	3829	54
H4C	4471	966	4536	54
H6	-1254	593	7324	38

H7	-3384	813	8076	43
H8	-4062	1377	7755	48
H9	-2818	1722	6525	37
H11	1787	2030	5662	34
H12A	3587	1742	7095	73
H12B	2956	1477	6002	73
H12C	2344	1456	7295	73
H13A	374	1890	7776	69
H13B	24	2220	6902	69
H13C	1707	2170	7747	69
H14	-1971	2088	5390	31
H15A	-3930	2029	3593	48
H15B	-3693	1681	4377	48
H15C	-2982	1719	3132	48
H16A	-906	2177	3088	47
H16B	7	2330	4374	47
H16C	-1711	2462	3813	47
H18	1025	2128	555	34
H19	-1626	1916	-276	32
H20A	2547	1717	3604	45
H20B	2568	2099	3076	45
H20C	3292	1792	2396	45
H23	-3786	599	1279	33
H24	-6094	826	181	38
H25	-6286	1409	-237	36
H26	-4148	1760	300	32
H27	1444	648	1526	26
H28A	-1409	523	-187	46
H28B	-551	247	786	46
H28C	254	374	-338	46
H29A	1269	951	-364	36

H29B	1386	1202	808	36
H29C	-256	1141	-86	36
H30	-1926	329	2235	27
H31A	549	325	4315	45
H31B	806	224	2946	45
H31C	-328	0	3622	45
H32A	-2674	309	4237	49
H32B	-3366	636	3441	49
H32C	-1897	677	4542	49
H1O	6870(8)	-380(2)	240(6)	66
H2O	6140(4)	-160(2)	1090(8)	66
H3O	5730(10)	2780(2))	2330(3)	66
H4O	5560(10)	2760(2)	3670(5)	66

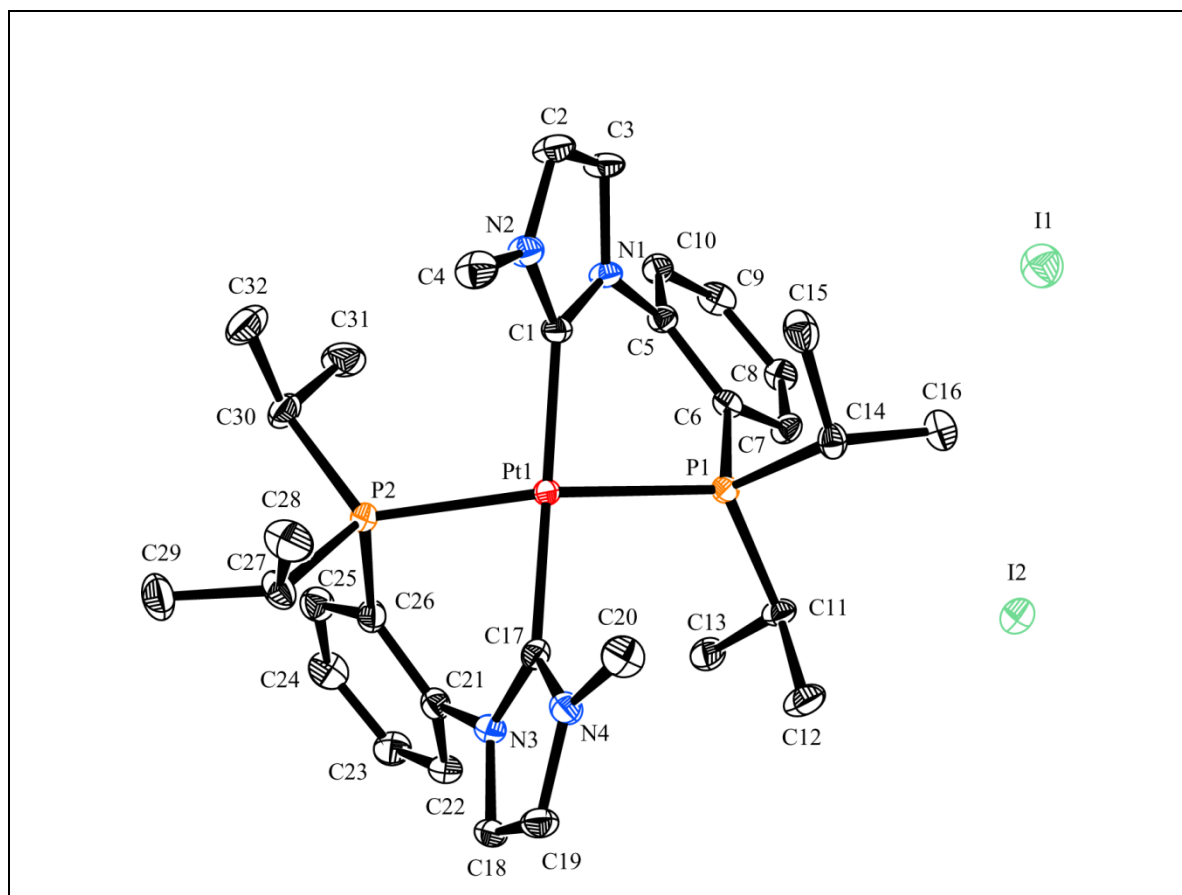
Experimental

Single crystals of $\text{C}_{32}\text{H}_{46}\text{I}_2\text{P}_2\text{NiN}_4$ were recrystallised from ethanol (EtOH) mounted in inert oil and transferred to the cold gas stream of the diffractometer.

Crystal structure determination]

Crystal Data. $\text{C}_{32}\text{H}_{46}\text{I}_2\text{P}_2\text{NiN}_4$, $M = 897.21$, Monoclinic, $a = 8.7370(2) \text{ \AA}$, $b = 39.0870(7) \text{ \AA}$, $c = 10.9220(2) \text{ \AA}$, $\beta = 100.4400(10)^\circ$, $U = 3668.15(13) \text{ \AA}^3$, $T = 150(2)$, space group $\text{P2}_1/\text{c}$ (no. 14), $Z = 4$, $\mu(\text{Mo-K}\alpha) = 2.333$, 19169 reflections measured, 7864 unique ($R_{\text{int}} = 0.0736$) which were used in all calculations. The final $wR(F_2)$ was 0.1816 (all data).

Data Set 4: Platinum complex crystal data and structure refinement, 3.6



Identification code	pge0704
Empirical formula	$\text{C}_{32}\text{H}_{44}\text{I}_2\text{P}_2\text{PtN}_4$
Formula weight	995.54
Temperature	150(2)
Crystal system	Monoclinic
Space group	$\text{P2}_1/\text{c}$
$a/\text{\AA}$, $b/\text{\AA}$, $c/\text{\AA}$	15.5350(2), 13.7400(2), 19.6770(3)
$\alpha/^\circ$, $\beta/^\circ$, $\gamma/^\circ$,	90.00, 91.070(1), 90.00
Volume/ \AA^3	4199.34(10)
Z	4
$\rho_{\text{calc}}/\text{mg}/\text{mm}^3$	1.575
m/mm^{-1}	4.911
$F(000)$	1912
Crystal size	$0.25 \times 0.13 \times 0.10$

Theta range for data collection	2.97 to 30.09°
Index ranges	$-21 \leq h \leq 21$, $-19 \leq k \leq 19$, $-27 \leq l \leq 27$
Reflections collected	71044
Independent reflections	12250[R(int) = 0.1104]
Data/restraints/parameters	12250/0/380
Goodness-of-fit on F^2	1.026
Final R indexes [$I > 2\sigma(I)$]	$R_1 = 0.0440$, $wR_2 = 0.1002$
Final R indexes [all data]	$R_1 = 0.0565$, $wR_2 = 0.1050$
Largest diff. peak/hole	1.890/-3.427

Table 2 Atomic Coordinates ($\text{\AA} \times 10^4$) and Equivalent Isotropic Displacement

Parameters ($\text{\AA}^2 \times 10^3$) . U_{eq} is defined as 1/3 of the trace of the orthogonalised U_{ij} tensor:

Atom	<i>x</i>	<i>y</i>	<i>z</i>	$U(\text{eq})$
C1	2274(3)	3380(3)	3399(2)	17.7(9)
C2	2137(3)	5004(4)	3435(3)	23.4(10)
C3	2841(3)	4815(3)	3073(3)	21.8(9)
C4	1039(3)	4011(4)	4058(3)	27.8(11)
C5	3652(3)	3287(4)	2807(2)	20.4(9)
C6	4025(3)	2544(4)	3206(2)	21.5(9)
C7	4790(3)	2133(4)	2977(3)	27.1(11)
C8	5149(4)	2417(4)	2363(3)	31.6(12)
C9	4740(4)	3115(4)	1970(3)	28.7(11)
C10	3995(3)	3573(4)	2199(3)	24.6(10)
C11	4142(3)	1074(4)	4269(3)	26(10)
C12	4031(4)	209(4)	3777(3)	37(13)
C13	3922(4)	763(5)	4997(3)	36.9(14)
C14	3746(3)	3153(4)	4579(3)	25.2(10)
C15	3140(4)	3192(4)	5190(3)	34.2(13)
C16	4695(4)	3159(5)	4804(3)	38.4(14)

C17	1843(3)	579(3)	3929(2)	18.7(9)
C18	1458(4)	-661(4)	4603(3)	27.5(11)
C19	1440(4)	-1007(4)	3974(3)	25.2(10)
C20	1662(4)	962(4)	5167(2)	26.3(11)
C21	1615(3)	-293(3)	2829(2)	18.3(9)
C22	1880(3)	-1152(4)	2525(3)	22.5(10)
C23	1732(4)	-1296(4)	1834(3)	26.7(11)
C24	1314(3)	-584(4)	1452(2)	23.3(10)
C25	1077(3)	283(4)	1750(2)	21.6(9)
C26	1218(3)	462(3)	2448(2)	18(9)
C27	-124(3)	1636(4)	3119(2)	19.7(9)
C28	-217(3)	1029(4)	3766(3)	28.1(11)
C29	-756(3)	1305(4)	2564(3)	26.8(11)
C30	941(3)	2462(4)	2068(2)	20.9(9)
C31	1816(3)	2513(4)	1711(3)	27.1(11)
C32	614(4)	3489(4)	2225(3)	30.3(12)
N1	2915(3)	3799(3)	3058(2)	18.8(8)
N2	1796(3)	4116(3)	3648(2)	21.8(8)
N3	1678(3)	-238(3)	3552.9(19)	18.5(8)
N4	1686(3)	306(3)	4574(2)	21.7(8)
P1	3509.7(8)	2132.1(9)	3990.1(6)	18.1(2)
P2	991.5(8)	1663.1(8)	2821.1(6)	15.6(2)
Pt1	2104.7(11)	1940.34(12)	3594.42(8)	14.35(5)
I1	-378.2(2)	1799.7(2)	415.01(17)	26.73(8)
I2	-3058.1(2)	1124.1(3)	3696.5(17)	29.27(9)

Table 3 Anisotropic Displacement Parameters ($\text{\AA}^2 \times 10^3$) . The Anisotropic

displacement factor exponent takes the form: $-2\pi^2[\mathbf{h}^2\mathbf{a}^{*2}\mathbf{U}_{11}+\dots+2\mathbf{h}\mathbf{k}\mathbf{a}\times\mathbf{b}\times\mathbf{U}_{12}]$

Atom	\mathbf{U}_{11}	\mathbf{U}_{22}	\mathbf{U}_{33}	\mathbf{U}_{23}	\mathbf{U}_{13}	\mathbf{U}_{12}
C1	17(2)	20(2)	16(2)	1.9(17)	-0.7(17)	1.3(17)

C2	28(2)	15(2)	27(2)	1.7(18)	0(2)	0.7(19)
C3	19(2)	15(2)	31(3)	2.7(18)	-0.1(19)	-1.8(17)
C4	27(3)	26(3)	31(3)	-4(2)	6(2)	3(2)
C5	19(2)	24(2)	19(2)	0.4(17)	0.3(18)	-3.3(18)
C6	20(2)	25(2)	20(2)	0.6(18)	-2.2(18)	-1.9(19)
C7	25(2)	26(3)	31(3)	-1(2)	1(2)	0(2)
C8	29(3)	34(3)	33(3)	-4(2)	11(2)	-1(2)
C9	31(3)	34(3)	22(2)	6(2)	7(2)	-3(2)
C10	26(2)	21(2)	26(2)	4.3(19)	1(2)	-3(2)
C11	22(2)	28(3)	29(3)	7(2)	-3(2)	6(2)
C12	38(3)	21(3)	52(4)	4(2)	2(3)	4(2)
C13	30(3)	43(3)	38(3)	18(3)	-1(2)	9(3)
C14	27(2)	27(3)	22(2)	-6(19)	-2(2)	-8(2)
C15	48(4)	34(3)	20(2)	-4(2)	5(2)	-12(3)
C16	34(3)	49(4)	31(3)	1(3)	-11(3)	-15(3)
C17	22(2)	17(2)	17(2)	2.9(16)	-1.5(18)	-3.7(17)
C18	39(3)	18(2)	26(2)	7(19)	0(2)	0(2)
C19	37(3)	13(2)	25(2)	4.5(18)	2(2)	-2(2)
C20	38(3)	26(3)	15(2)	-1.5(18)	1(2)	-1(2)
C21	21(2)	16(2)	19(2)	-0.8(16)	-0.1(18)	-0.2(17)
C22	22(2)	20(2)	25(2)	-0.4(18)	0(2)	0.6(18)
C23	32(3)	20(2)	29(3)	-7.9(19)	8(2)	0(2)
C24	29(3)	24(2)	17(2)	-4.4(18)	0.3(19)	-3(2)
C25	27(2)	21(2)	17(2)	-0.1(17)	-3.4(19)	1.7(19)
C26	18(2)	17(2)	19(2)	-0.8(16)	2.9(17)	-2.5(17)
C27	16(2)	21(2)	22(2)	-4.5(18)	-0.6(18)	2(17)
C28	21(2)	41(3)	22(2)	0(2)	3(2)	-5(2)
C29	20(2)	32(3)	29(3)	-3(2)	0(2)	-2(2)
C30	28(2)	18(2)	16(2)	4.1(17)	-0.9(19)	0(19)
C31	30(3)	31(3)	21(2)	7(2)	0(2)	-1(2)
C32	43(3)	22(3)	25(3)	6(2)	-6(2)	4(2)

N1	19.7(19)	17.7(19)	18.9(18)	0.9(14)	1.9(16)	-1.8(15)
N2	18(18)	18.3(19)	29(2)	0.1(16)	-0.2(16)	-0.5(15)
N3	26(2)	15(18)	14.7(17)	1.7(14)	0.6(15)	-1.1(15)
N4	27(2)	19.5(19)	18.8(19)	1.1(15)	0.3(16)	-1(17)
P1	18(5)	19.4(6)	16.7(5)	1.8(4)	-3.1(4)	-1.2(4)
P2	16.5(5)	14.7(5)	15.7(5)	-0.8(4)	-0.6(4)	-0.3(4)
Pt1	15.71(8)	13.41(8)	13.91(8)	0.4(6)	-0.48(6)	-0.41(6)
I1	30.34(17)	26.19(17)	23.57(16)	-3.32(12)	-1.76(13)	5.29(13)
I2	29.26(17)	32.24(19)	26.28(17)	-1.01(13)	-0.84(14)	-1.53(14)

Table 4 Bond Lengths:

Atom	Atom	Length/Å	Atom	Atom	Length/Å
C1	N1	1.341(6)	C17	N3	1.367(6)
C1	N2	1.352(6)	C17	Pt1	2.026(4)
C1	Pt1	2.033(5)	C18	C19	1.326(7)
C2	C3	1.342(7)	C18	N4	1.378(6)
C2	N2	1.398(6)	C19	N3	1.396(6)
C3	N1	1.401(6)	C20	N4	1.475(6)
C4	N2	1.445(7)	C21	C22	1.389(6)
C5	C10	1.377(7)	C21	C26	1.414(6)
C5	C6	1.406(7)	C21	N3	1.428(6)
C5	N1	1.439(6)	C22	C23	1.389(7)
C6	C7	1.397(7)	C23	C24	1.386(7)
C6	P1	1.841(5)	C24	C25	1.381(7)
C7	C8	1.396(8)	C25	C26	1.409(6)
C8	C9	1.379(8)	C26	P2	1.842(5)
C9	C10	1.400(8)	C27	C29	1.525(7)
C11	C13	1.538(8)	C27	C28	1.531(7)
C11	C12	1.541(8)	C27	P2	1.840(5)
C11	P1	1.833(5)	C30	C32	1.533(7)

C14	C16	1.531(8)	C30	C31	1.544(7)
C14	C15	1.541(8)	C30	P2	1.844(5)
C14	P1	1.852(5)	P1	Pt1	2.3187(12)
C17	N4	1.349(6)	P2	Pt1	2.3137(12)

Table 5 Bond Angles :

Atom	Atom	Atom	Angle/°	Atom	Atom	Atom	Angle/°
N1	C1	N2	106.1(4)	C29	C27	C28	111.3(4)
N1	C1	Pt1	127.8(3)	C29	C27	P2	112.1(3)
N2	C1	Pt1	125.8(3)	C28	C27	P2	112.3(3)
C3	C2	N2	107.9(4)	C32	C30	C31	110.3(4)
C2	C3	N1	105.8(4)	C32	C30	P2	113.3(3)
C10	C5	C6	122.0(5)	C31	C30	P2	111.6(3)
C10	C5	N1	118.8(4)	C1	N1	C3	110.8(4)
C6	C5	N1	119.1(4)	C1	N1	C5	124.4(4)
C7	C6	C5	117.3(5)	C3	N1	C5	124.1(4)
C7	C6	P1	122.1(4)	C1	N2	C2	109.3(4)
C5	C6	P1	120.6(4)	C1	N2	C4	125.8(4)
C8	C7	C6	121.4(5)	C2	N2	C4	124.9(4)
C9	C8	C7	119.6(5)	C17	N3	C19	110.5(4)
C8	C9	C10	120.4(5)	C17	N3	C21	126.3(4)
C5	C10	C9	119.2(5)	C19	N3	C21	122.6(4)
C13	C11	C12	110.3(5)	C17	N4	C18	111.0(4)
C13	C11	P1	111.8(4)	C17	N4	C20	125.5(4)
C12	C11	P1	111.8(4)	C18	N4	C20	123.1(4)
C16	C14	C15	111.9(5)	C11	P1	C6	104.8(2)
C16	C14	P1	111.3(4)	C11	P1	C14	108.3(3)
C15	C14	P1	113.4(4)	C6	P1	C14	102.0(2)
N4	C17	N3	104.2(4)	C11	P1	Pt1	120.42(18)
N4	C17	Pt1	127.1(3)	C6	P1	Pt1	100.08(16)

N3	C17	Pt1	128.3(3)	C14	P1	Pt1	118.08(18)
C19	C18	N4	107.9(4)	C27	P2	C26	107.3(2)
C18	C19	N3	106.4(4)	C27	P2	C30	104.0(2)
C22	C21	C26	121.7(4)	C26	P2	C30	102.6(2)
C22	C21	N3	117.3(4)	C27	P2	Pt1	119.40(16)
C26	C21	N3	120.7(4)	C26	P2	Pt1	105.27(15)
C21	C22	C23	119.9(5)	C30	P2	Pt1	116.77(16)
C24	C23	C22	119.8(5)	C17	Pt1	C1	170.67(19)
C25	C24	C23	120.4(5)	C17	Pt1	P2	84.82(13)
C24	C25	C26	121.7(4)	C1	Pt1	P2	97.65(13)
C25	C26	C21	116.5(4)	C17	Pt1	P1	100.91(14)
C25	C26	P2	121.2(4)	C1	Pt1	P1	80.16(13)
C21	C26	P2	122.0(3)	P2	Pt1	P1	157.96(4)

Table 6 Torsion Angles:

A	B	C	D	Angle/°
N2	C2	C3	N1	1.0(5)
C10	C5	C6	C7	3.0(7)
N1	C5	C6	C7	-173.7(4)
C10	C5	C6	P1	-176.3(4)
N1	C5	C6	P1	7.0(6)
C5	C6	C7	C8	-2.8(8)
P1	C6	C7	C8	176.6(4)
C6	C7	C8	C9	-0.3(8)
C7	C8	C9	C10	3.3(9)
C6	C5	C10	C9	-0.2(8)
N1	C5	C10	C9	176.5(5)
C8	C9	C10	C5	-3.1(8)
N4	C18	C19	N3	1.1(6)
C26	C21	C22	C23	-2.0(7)

N3	C21	C22	C23	171.6(5)
C21	C22	C23	C24	-0.4(8)
C22	C23	C24	C25	2.6(8)
C23	C24	C25	C26	-2.3(8)
C24	C25	C26	C21	0.0(7)
C24	C25	C26	P2	174.2(4)
C22	C21	C26	C25	2.2(7)
N3	C21	C26	C25	-171.2(4)
C22	C21	C26	P2	-171.9(4)
N3	C21	C26	P2	14.6(6)
N2	C1	N1	C3	-1.4(5)
Pt1	C1	N1	C3	-175.6(3)
N2	C1	N1	C5	169.3(4)
Pt1	C1	N1	C5	-5.0(7)
C2	C3	N1	C1	0.2(5)
C2	C3	N1	C5	-170.4(4)
C10	C5	N1	C1	144.5(5)
C6	C5	N1	C1	-38.7(7)
C10	C5	N1	C3	-46.1(7)
C6	C5	N1	C3	130.8(5)
N1	C1	N2	C2	2.0(5)
Pt1	C1	N2	C2	176.4(3)
N1	C1	N2	C4	-179.3(4)
Pt1	C1	N2	C4	-4.9(7)
C3	C2	N2	C1	-1.9(6)
C3	C2	N2	C4	179.3(5)
N4	C17	N3	C19	-1.3(5)
Pt1	C17	N3	C19	-173.8(4)
N4	C17	N3	C21	169.4(4)
Pt1	C17	N3	C21	-3.2(7)
C18	C19	N3	C17	0.1(6)

C18	C19	N3	C21	-170.9(5)
C22	C21	N3	C17	147.8(5)
C26	C21	N3	C17	-38.5(7)
C22	C21	N3	C19	-42.6(7)
C26	C21	N3	C19	131.1(5)
N3	C17	N4	C18	2.0(6)
Pt1	C17	N4	C18	174.6(4)
N3	C17	N4	C20	-171.7(5)
Pt1	C17	N4	C20	1.0(7)
C19	C18	N4	C17	-2.0(6)
C19	C18	N4	C20	171.8(5)
C13	C11	P1	C6	168.0(4)
C12	C11	P1	C6	-67.8(4)
C13	C11	P1	C14	59.7(5)
C12	C11	P1	C14	-176.0(4)
C13	C11	P1	Pt1	-80.6(4)
C12	C11	P1	Pt1	43.6(4)
C7	C6	P1	C11	-6.2(5)
C5	C6	P1	C11	173.1(4)
C7	C6	P1	C14	106.7(5)
C5	C6	P1	C14	-74.0(4)
C7	C6	P1	Pt1	-131.6(4)
C5	C6	P1	Pt1	47.7(4)
C16	C14	P1	C11	37.2(4)
C15	C14	P1	C11	-90.0(4)
C16	C14	P1	C6	-73.0(4)
C15	C14	P1	C6	159.8(4)
C16	C14	P1	Pt1	178.6(3)
C15	C14	P1	Pt1	51.3(5)
C29	C27	P2	C26	-52.5(4)
C28	C27	P2	C26	73.7(4)

C29	C27	P2	C30	55.8(4)
C28	C27	P2	C30	-178.0(4)
C29	C27	P2	Pt1	-171.9(3)
C28	C27	P2	Pt1	-45.7(4)
C25	C26	P2	C27	91.6(4)
C21	C26	P2	C27	-94.5(4)
C25	C26	P2	C30	-17.6(4)
C21	C26	P2	C30	156.3(4)
C25	C26	P2	Pt1	-140.3(4)
C21	C26	P2	Pt1	33.6(4)
C32	C30	P2	C27	59.1(4)
C31	C30	P2	C27	-175.7(4)
C32	C30	P2	C26	170.7(4)
C31	C30	P2	C26	-64.0(4)
C32	C30	P2	Pt1	-74.7(4)
C31	C30	P2	Pt1	50.6(4)
N4	C17	Pt1	C1	-21.5(14)
N3	C17	Pt1	C1	149.5(10)
N4	C17	Pt1	P2	-127.3(4)
N3	C17	Pt1	P2	43.7(4)
N4	C17	Pt1	P1	74.2(4)
N3	C17	Pt1	P1	-114.8(4)
N1	C1	Pt1	C17	149.4(10)
N2	C1	Pt1	C17	-23.8(14)
N1	C1	Pt1	P2	-105.8(4)
N2	C1	Pt1	P2	81.0(4)
N1	C1	Pt1	P1	52.0(4)
N2	C1	Pt1	P1	-121.2(4)
C27	P2	Pt1	C17	71.6(2)
C26	P2	Pt1	C17	-48.8(2)
C30	P2	Pt1	C17	-161.9(2)

C27	P2	Pt1	C1	-99.3(2)
C26	P2	Pt1	C1	140.2(2)
C30	P2	Pt1	C1	27.1(2)
C27	P2	Pt1	P1	178.0(2)
C26	P2	Pt1	P1	57.55(19)
C30	P2	Pt1	P1	-55.5(2)
C11	P1	Pt1	C17	15.7(2)
C6	P1	Pt1	C17	129.6(2)
C14	P1	Pt1	C17	-120.9(2)
C11	P1	Pt1	C1	-173.8(2)
C6	P1	Pt1	C1	-59.8(2)
C14	P1	Pt1	C1	49.6(2)
C11	P1	Pt1	P2	-87.7(2)
C6	P1	Pt1	P2	26.2(2)
C14	P1	Pt1	P2	135.7(2)

Table 7 Hydrogen Atom Coordinates ($\text{\AA} \times 10^4$) and Isotropic Displacement

Parameters ($\text{\AA}^2 \times 10^3$) :

Atom	<i>x</i>	<i>y</i>	<i>z</i>	U(eq)
H2	1911	5631	3530	28
H3	3212	5275	2868	26
H4A	550	4335	3832	42
H4B	1145	4308	4504	42
H4C	909	3318	4115	42
H7	5072	1649	3245	32
H8	5671	2132	2217	38
H9	4966	3286	1540	34
H10	3730	4076	1938	29
H11	4763	1267	4270	31
H12A	4459	-292	3889	55

H12B	4113	433	3309	55
H12C	3452	-63	3819	55
H13A	3318	559	5010	55
H13B	4015	1313	5307	55
H13C	4294	220	5136	55
H15A	3219	2604	5466	51
H15B	2542	3229	5025	51
H15C	3275	3767	5466	51
H16A	4824	3765	5048	58
H16B	5059	3113	4404	58
H16C	4810	2603	5104	58
H18	1335	-1018	5004	33
H19	1294	-1650	3837	30
H20A	2013	1539	5079	40
H20B	1890	622	5569	40
H20C	1066	1161	5246	40
H22	2162	-1639	2789	27
H23	1915	-1881	1623	32
H24	1191	-694	984	28
H25	811	772	1477	26
H27	-281	2320	3237	24
H28A	-822	1025	3900	42
H28B	138	1313	4132	42
H28C	-28	361	3680	42
H29A	-615	639	2425	40
H29B	-717	1741	2171	40
H29C	-1343	1322	2738	40
H31A	1781	2986	1339	41
H31B	1959	1870	1529	41
H31C	2264	2715	2039	41
H32A	1038	3828	2514	45

H32B	66	3445	2462	45
H32C	529	3850	1800	45

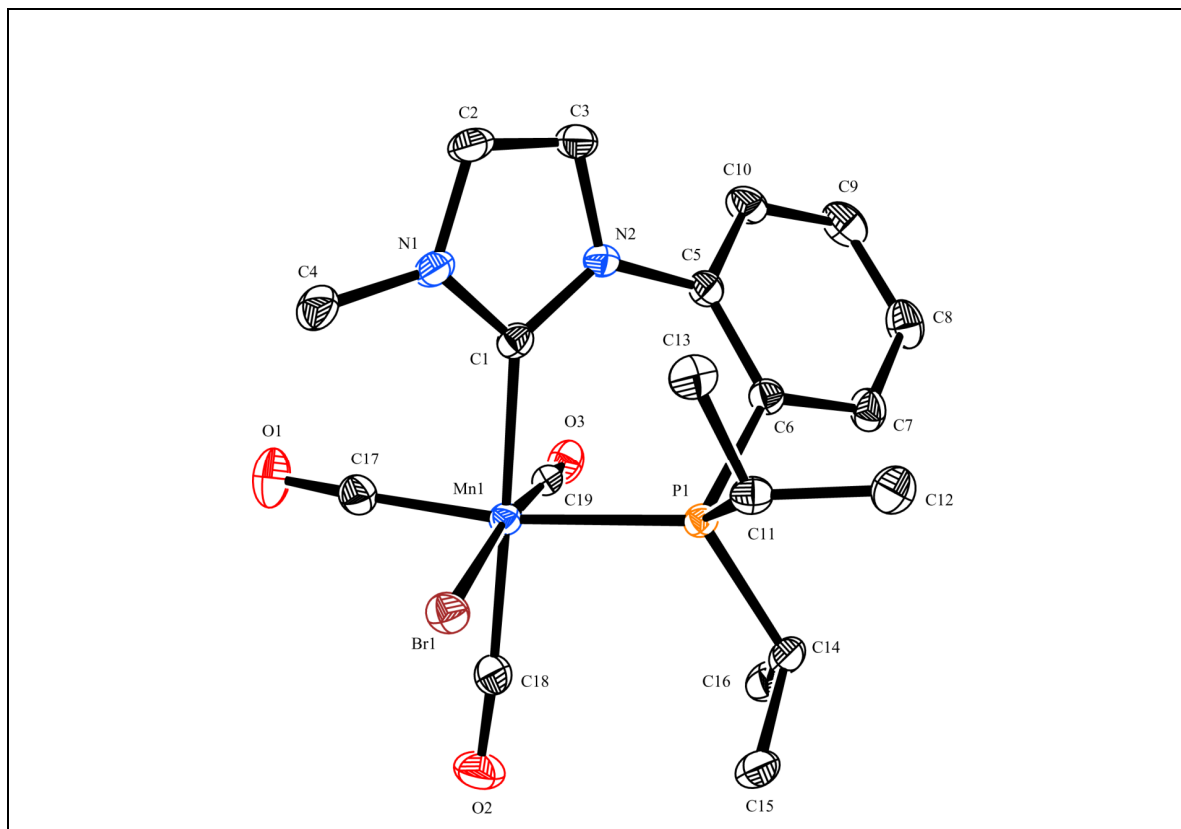
Experimental

Single crystals of $\text{C}_{32}\text{H}_{44}\text{I}_2\text{P}_2\text{PtN}_4$ were recrystallised from methanol (MeOH) mounted in inert oil and transferred to the cold gas stream of the diffractometer.

Crystal structure determination

Crystal Data. $\text{C}_{32}\text{H}_{44}\text{I}_2\text{P}_2\text{PtN}_4$, $M = 995.54$, Monoclinic, $a = 15.5350(2) \text{ \AA}$, $b = 13.7400(2) \text{ \AA}$, $c = 19.6770(3) \text{ \AA}$, $\beta = 91.070(1)^\circ$, $U = 4199.34(10) \text{ \AA}^3$, $T = 150(2)$, space group $\text{P2}_1/\text{c}$ (no. 14), $Z = 4$, $\mu(\text{Mo-K}\alpha) = 4.911$, 71044 reflections measured, 12250 unique ($R_{\text{int}} = 0.1104$) which were used in all calculations. The final $wR(F_2)$ was 0.1050 (all data).

Data set 5: Manganese complex crystal data and structure refinement, 3.8



Identification code	pge0811
Empirical formula	$\text{C}_{19}\text{H}_{23}\text{PO}_3\text{BrMnN}_2$
Formula weight	535.68
Temperature	150(2)
Crystal system	Monoclinic
Space group	$C2/c$
$a/\text{\AA}$, $b/\text{\AA}$, $c/\text{\AA}$	27.4450(6), 8.7250(2), 18.6360(4)
$\alpha/^\circ$, $\beta/^\circ$, $\gamma/^\circ$,	90.00, 100.840(2), 90.00
Volume/ \AA^3	4382.90(17)
Z	8
$\rho_{\text{calc}}/\text{mg}/\text{mm}^3$	1.624
m/mm^{-1}	2.644
$F(000)$	2168
Crystal size	$0.30 \times 0.26 \times 0.12$
Theta range for data collection	3.30 to 27.47°

Index ranges	$-35 \leq h \leq 35, -11 \leq k \leq 10, -24 \leq l \leq 24$
Reflections collected	8358
Independent reflections	5010[R(int) = 0.0346]
Data/restraints/parameters	5010/3/276
Goodness-of-fit on F^2	1.027
Final R indexes [$I > 2\sigma(I)$]	$R_1 = 0.0389, wR_2 = 0.0840$
Final R indexes [all data]	$R_1 = 0.0521, wR_2 = 0.0898$
Largest diff. peak/hole	0.760/-0.659

Table 2 Atomic Coordinates ($\text{\AA} \times 10^4$) and Equivalent Isotropic Displacement

Parameters ($\text{\AA}^2 \times 10^3$). U_{eq} is defined as 1/3 of the trace of the orthogonalised

U_{IJ} tensor:

Atom	<i>x</i>	<i>y</i>	<i>z</i>	U(eq)
C1	1561.1(10)	4633(3)	7141.6(14)	20.4(6)
C2	1645.4(12)	6217(4)	8121.8(16)	29.9(7)
C3	1450.4(11)	4911(4)	8315.9(15)	27.5(7)
C4	1916.3(13)	7279(4)	7026.8(17)	32.6(7)
C5	1181.3(10)	2450(3)	7720.1(14)	20.7(6)
C6	868.1(10)	1842(3)	7099(14)	21.1(6)
C7	642.7(11)	436(4)	7171.4(16)	27.1(6)
C8	731.2(12)	-370(4)	7826.3(17)	32.2(7)
C9	1049.5(12)	222(4)	8423.9(17)	32.8(7)
C10	1272(11)	1632(4)	8372.9(15)	27.5(7)
C11	298.4(10)	4206(3)	6203.6(15)	22.4(6)
C12	-182.6(11)	3417(4)	6306(17)	31.1(7)
C13	421.9(11)	5521(4)	6745.6(16)	28.7(7)
C14	534.6(11)	1376(3)	5532.5(15)	24.2(6)
C15	375.3(12)	2151(4)	4783.4(15)	29.2(7)
C16	883.4(12)	21(4)	5492.3(17)	30.4(7)
C17	2239.5(12)	4393(4)	6244.3(16)	27.7(7)

C18	1650.2(11)	2890(4)	5265.8(16)	26.2(6)
C19	1875.5(11)	1927(4)	6596.3(15)	26.5(7)
N1	1709.6(9)	6042(3)	7407.4(13)	25.5(5)
N2	1400.4(9)	3937(3)	7713.8(12)	21(5)
O1	2648.8(9)	4722(3)	6330.7(14)	45.1(6)
O2	1704.9(10)	2418(3)	4709.3(12)	41.5(6)
O3	2048.9(8)	921(3)	6837.6(12)	30(5)
Br1	1198.81(11)	5937.3(3)	5357.23(15)	25.87(9)
Mn1	1606.66(15)	3675(5)	6153.6(2)	18.4(11)
P1	816.2(3)	2822.4(8)	6216.5(4)	18.46(15)
Cl1	2524.3(10)	1431(3)	10509.2(14)	62.7(7)
Cl2	2793.4(12)	4145(4)	9773.1(16)	84.8(8)
C20	2338(3)	2730(10)	9777(5)	80(4)

Table 3 Anisotropic Displacement Parameters ($\text{\AA}^2 \times 10^3$). The Anisotropic

displacement factor exponent takes the form: $-2\pi^2[\mathbf{h}^2\mathbf{a}^{*2}\mathbf{U}_{11}+\dots+2\mathbf{h}\mathbf{k}\mathbf{a}\times\mathbf{b}\times\mathbf{U}_{12}]$

Atom	\mathbf{U}_{11}	\mathbf{U}_{22}	\mathbf{U}_{33}	\mathbf{U}_{23}	\mathbf{U}_{13}	\mathbf{U}_{12}
C1	21(14)	19.8(14)	18.9(13)	1.1(11)	-0.6(10)	0.7(11)
C2	31.4(17)	35.6(19)	21.3(14)	-10.4(13)	1.3(12)	-2(14)
C3	27.5(15)	36.7(19)	18.3(13)	-4.4(12)	3.9(11)	-1(14)
C4	43.8(19)	22.2(17)	30.1(16)	-0.5(13)	2.6(14)	-9.3(14)
C5	21.4(14)	20.8(15)	20(13)	2.2(11)	4(10)	1.4(11)
C6	20.5(14)	23.2(15)	19(13)	2.9(11)	2.3(10)	1(12)
C7	28(16)	24.4(16)	29.2(15)	5.2(13)	5.7(12)	-2.9(13)
C8	35.2(18)	26.2(17)	36.7(17)	12.2(14)	10.5(14)	-1.5(14)
C9	39(19)	32.7(19)	27.3(15)	15.4(14)	8.2(13)	8.5(15)
C10	29.9(16)	33.2(18)	18.7(13)	7.3(12)	3(11)	3.3(14)
C11	22.7(14)	23.8(15)	19(13)	2.4(11)	-0.2(10)	4.8(12)
C12	22.3(15)	37.7(19)	31.4(16)	1.6(14)	0.3(12)	3.3(14)

C13	27.2(16)	29.7(17)	28.2(15)	-2.5(13)	2.6(12)	6.3(13)
C14	24.7(15)	23.3(15)	22.6(14)	-0.9(12)	-1.1(11)	-4.5(12)
C15	33.7(17)	28.6(17)	22.3(14)	-1.8(12)	-2.8(12)	-3.7(14)
C16	37(18)	21.9(16)	30.4(16)	-5.3(13)	1.4(13)	-1.6(14)
C17	32.4(18)	25.7(17)	25.7(15)	1.6(12)	6.8(12)	-2.2(14)
C18	28.9(16)	23.6(16)	25.6(15)	2.1(12)	4.2(12)	-1.9(13)
C19	26.4(15)	35.6(19)	17.9(14)	-6.2(13)	5.4(11)	-13.6(14)
N1	29.6(14)	23.8(14)	21.4(12)	-4.6(10)	0.7(10)	-4.4(11)
N2	23.2(12)	23.5(13)	15.5(11)	0(9)	2(9)	-1(10)
O1	25.8(13)	47.2(16)	62.5(16)	1.6(13)	9.2(11)	-9.3(12)
O2	59.6(16)	43.1(15)	24.7(12)	-7.5(11)	15(11)	-4.8(13)
O3	22.4(11)	28.4(13)	38.7(12)	-3.8(10)	4.4(9)	-0.3(10)
Br1	32.05(17)	22.08(16)	22.45(15)	4.48(11)	2.51(11)	1.49(12)
Mn1	21.3(2)	17.4(2)	16(2)	0.82(16)	2.46(15)	-1.2(17)
P1	20.4(3)	17.1(4)	16.7(3)	1.1(3)	0.6(2)	-0.4(3)
Cl1	48.6(14)	77.1(18)	64.4(14)	-23.2(13)	15.9(11)	-23.6(12)
Cl2	86(2)	101(2)	69.7(16)	22.3(16)	20.7(15)	-5.6(18)
C20	38(6)	109(10)	89(8)	-50(8)	0(5)	9(6)

Table 4 Bond Lengths:

Atom	Atom	Length/Å	Atom	Atom	Length/Å
C1	N1	1.359(4)	C14	C16	1.531(4)
C1	N2	1.370(4)	C14	C15	1.539(4)
C1	Mn1	2.047(3)	C14	P1	1.856(3)
C2	C3	1.337(5)	C17	O1	1.141(4)
C2	N1	1.384(4)	C17	Mn1	1.824(3)
C3	N2	1.394(4)	C18	O2	1.152(4)
C4	N1	1.463(4)	C18	Mn1	1.815(3)
C5	C10	1.392(4)	C19	O3	1.057(4)
C5	C6	1.409(4)	C19	Mn1	1.823(4)

C5	N2	1.431(4)	Br1	Mn1	2.5937(5)
C6	C7	1.392(4)	Mn1	P1	2.3171(8)
C6	P1	1.835(3)	Cl1	C20	1.020(8)
C7	C8	1.390(4)	Cl1	Cl2	1.057(4)
C8	C9	1.380(5)	Cl1	C20	1.774(8)
C9	C10	1.384(5)	Cl2	Cl1	1.057(4)
C11	C13	1.524(4)	Cl2	C20	1.758(8)
C11	C12	1.533(4)	Cl2	C20	1.904(9)
C11	P1	1.861(3)			

Table 5 Bond Angles:

Atom	Atom	Atom	Angle/°	Atom	Atom	Atom	Angle/°
N1	C1	N2	103.6(2)	C3	N2	C5	121.6(2)
N1	C1	Mn1	129.2(2)	C18	Mn1	C19	90.37(13)
N2	C1	Mn1	127.0(2)	C18	Mn1	C17	89.39(13)
C3	C2	N1	107.2(3)	C19	Mn1	C17	87.02(14)
C2	C3	N2	106.6(3)	C18	Mn1	C1	178.05(13)
C10	C5	C6	120.4(3)	C19	Mn1	C1	91.29(12)
C10	C5	N2	117.8(3)	C17	Mn1	C1	89.69(12)
C6	C5	N2	121.8(2)	C18	Mn1	P1	98.49(10)
C7	C6	C5	117.8(3)	C19	Mn1	P1	90.67(9)
C7	C6	P1	122.5(2)	C17	Mn1	P1	171.81(9)
C5	C6	P1	119.5(2)	C1	Mn1	P1	82.50(8)
C8	C7	C6	121.6(3)	C18	Mn1	Br1	82.00(10)
C9	C8	C7	119.9(3)	C19	Mn1	Br1	171.98(9)
C8	C9	C10	119.8(3)	C17	Mn1	Br1	95.32(10)
C9	C10	C5	120.5(3)	C1	Mn1	Br1	96.38(8)
C13	C11	C12	110.2(2)	P1	Mn1	Br1	88.04(2)
C13	C11	P1	113.9(2)	C6	P1	C14	104.51(13)
C12	C11	P1	112.4(2)	C6	P1	C11	104.14(13)

C16	C14	C15	111.6(3)	C14	P1	C11	102.35(13)
C16	C14	P1	112.0(2)	C6	P1	Mn1	106.22(9)
C15	C14	P1	109.6(2)	C14	P1	Mn1	117.16(10)
O1	C17	Mn1	173.9(3)	C11	P1	Mn1	120.73(10)
O2	C18	Mn1	176.2(3)	C20	Cl1	Cl2	115.7(6)
O3	C19	Mn1	176.7(3)	C20	Cl1	C20	38.7(7)
C1	N1	C2	111.5(3)	Cl2	Cl1	C20	80.2(3)
C1	N1	C4	127.4(2)	Cl1	Cl2	C20	31.5(3)
C2	N1	C4	121.1(3)	Cl1	Cl2	C20	66.7(3)
C1	N2	C3	111.0(2)	C20	Cl2	C20	36.9(5)
C1	N2	C5	127.3(2)	Cl2	C20	Cl1	110.5(4)

Table 6 Hydrogen Atom Coordinates ($\text{\AA} \times 10^4$) and Isotropic Displacement

Parameters ($\text{\AA}^2 \times 10^3$) :

Atom	<i>x</i>	<i>y</i>	<i>z</i>	U(eq)
H2	1725	7100	8419	36
H3	1363	4690	8775	33
H4A	2279	7204	7125	49
H4B	1817	8270	7201	49
H4C	1791	7191	6500	49
H7	423	17	6763	33
H8	573	-1328	7862	39
H9	1116	-337	8869	39
H10	1488	2043	8786	33
H11	231	4676	5705	27
H12A	-130	2908	6783	47
H12B	-279	2654	5919	47
H12C	-446	4183	6281	47
H13A	138	6221	6696	43
H13B	712	6077	6645	43

H13C	495	5111	7244	43
H14	229	971	5687	29
H15A	655	2734	4664	44
H15B	97	2847	4800	44
H15C	272	1367	4409	44
H16A	708	-768	5169	46
H16B	992	-408	5982	46
H16C	1173	373	5300	46
H20A	2284	2165	9308	96
H20B	2021	3221	9827	96

Experimental

Single crystals of $\text{C}_{19}\text{H}_{23}\text{PO}_3\text{BrMnN}_2$ were recrystallised from methanol (MeOH) mounted in inert oil and transferred to the cold gas stream of the diffractometer.

Crystal structure determination

Crystal Data. $\text{C}_{19}\text{H}_{23}\text{PO}_3\text{BrMnN}_2$, $M = 535.68$, Monoclinic, $a = 27.4450(6) \text{ \AA}$, $b = 8.7250(2) \text{ \AA}$, $c = 18.6360(4) \text{ \AA}$, $\beta = 100.840(2)^\circ$, $U = 4382.90(17) \text{ \AA}^3$, $T = 150(2)$, space group C2/c (no. 15), $Z = 8$, $\mu(\text{Mo-K}\alpha) = 2.644$, 8358 reflections measured, 5010 unique ($R_{\text{int}} = 0.0346$) which were used in all calculations. The final $wR(F_2)$ was 0.0898 (all data).